University of Kentucky Doctoral Dissertations   Graduate School

2009

REGENERATION OF DAMAGED GROWTH PLATE USING IGF-I PLASMID-RELEASING POROUS PLGA SCAFFOLDS

Nirmal Ravi

University of Kentucky, nirmal.ravi@uky.edu

ABSTRACT OF DISSERTATION

Nirmal Ravi

The Graduate School
University of Kentucky

2009

REGENERATION OF DAMAGED GROWTH PLATE USING IGF-I PLASMID-
RELEASING POROUS PLGA SCAFFOLDS

_____

ABSTRACT OF DISSERTATION
_____

A dissertation submitted in partial fulfillment of the
requirements for the degree of Doctor of Philosophy in the
Graduate School at the University of Kentucky

By

Nirmal Ravi
Lexington, Kentucky

Director: Dr. David A. Puleo
Professor of Biomedical Engineering
Lexington, Kentucky

2009
Copyright © Nirmal Ravi 2009

ABSTRACT OF DISSERTATION

REGENERATION OF DAMAGED GROWTH PLATE USING IGF-I PLASMID-
RELEASING POROUS PLGA SCAFFOLDS

Growth plate injuries account for 15-30% of long bone fractures in children. About 10% of these result in significant growth disturbances due to formation of a boney bar. If not treated correctly, this can lead to life-lasting consequences of limb length inequalities and angular deformities. Current treatments for growth plate injuries include removal of boney bar and insertion of fat, silicone, bone cement, etc.. This treatment y is inadequate, leaving almost half of these patients with continued deformities. This dissertation reports characterization of a DNA–containing porous poly(lactic-co-glycolic acid) (PLGA) scaffold system, chondrogenesis using insulin-like growth factor I (IGF-I) plasmid-releasing scaffolds *in vitro*, and *in vivo* testing of IGF-I plasmid-releasing scaffolds to regenerate growth plate . Controlled release of naked and DNA complexed with polyethylenimine (PEI) was achieved from porous PLGA scaffolds. PEI affected release of complexes from PLGA scaffolds, as PEI:DNA complexes were released at a lower rate compared to naked DNA encapsulated in low molecular weight (LMW) and high molecular weight PLGA scaffolds, as well as hydrophilic and hydrophobic PLGA scaffolds. Hydrophilicity and molecular weight of PLGA affected the release profiles of both naked DNA and PEI:DNA complexes from the scaffolds, as evidenced by later peak DNA and PEI:DNA release with increasing hydrophilicity and molecular weight. LMW hydrophilic PLGA scaffolds supported growth and chondrogenic differentiation of mesenchymal multipotent D1 cells, chondrocytes, and bone marrow cells (BMCs) *in vitro*. Culturing BMCs on IGF-I plasmid-encapsulated scaffolds resulted in elevated expression of IGF-I compared to blank scaffolds. Removal of boney bar and implantation of IGF-I plasmid-releasing LMW PLGA scaffolds in a rabbit model of growth plate injury resulted in some improvement of leg angular deformity compared to no scaffold implantation. Histological analysis of the newly developed cartilage showed growth plate-like columnar arrangement of chondrocytes in a defect that received IGF-I plasmid

encapsulated scaffold, although the level of organization of newly formed cartilage was inferior to that of native growth plate. This appears to be the first report of the regeneration of growth plate-like structure without the use of stem cells in an animal model of physeal injury.

Nirmal Ravi

May 12, 2009

REGENERATION OF DAMAGED GROWTH PLATE USING IGF-I PLASMID-
RELEASING POROUS PLGA SCAFFOLDS

By

Nirmal Ravi

David A Puleo
Director of Dissertation

Abhijit Patwardhan
Director of Graduate Studies

May 12, 2009

RULES FOR THE USE OF DISSERTATIONS

Unpublished dissertations submitted for the Doctor's degree and deposited in the Univerity of Kentucky Library are as a rule open for inspection, but are to be used only with due regard to the rights of the authors. Bibliographical references may be noted, but quotations and or summaries of parts may be published only with the permission of the author, and with the usual scholarly acknowledgments.

Extensive copying or publication of the dissertation in whole or in part also requires the consent of the Dean of the Graduate School of the University of Kentucky.

A library that borrows this dissertation for use by its patrons is expected to secure the signature of each user.

<u>Name</u>   <u>Date</u>

_____
_____
_____
_____
_____
_____
_____
_____
_____
_____
_____
_____
_____
_____
_____
_____
_____
_____
_____

DISSERTATION

Nirmal Ravi

The Graduate School

University of Kentucky

2009

REGENERATION OF DAMAGED GROWTH PLATE USING IGF-I PLASMID-
RELEASING POROUS PLGA SCAFFOLDS

_____

DISSERTATION
_____

A dissertation submitted in partial fulfillment of the
requirements for the degree of Doctor of Philosophy in the
Graduate School at the University of Kentucky

By

Nirmal Ravi

Lexington, Kentucky

Director: Dr. David A. Puleo

Professor of Biomedical Engineering

Lexington, Kentucky
2009

ACKNOWLEDGMENTS

TABLE OF CONTENTS

LIST OF TABLES

LIST OF FIGURES

ix

xiv

LIST OF FILES

1. INTRODUCTION

Growth plate injuries account for approximately 15% to 30% of all fractures of long bones in children (Mizuta, 1987). About 10% of these will result in significant growth disturbances due to the formation of a boney bar (Salter, 1994). This boney bar can act as a tether, attaching the epiphyseal bone to the diaphyses, and limiting the continued normal growth of the limb. If not treated correctly, this can lead to life lasting consequences of limb length inequalities and angular deformities. Current treatments for growth plate injuries include removal of boney bar, and insertion of fat, silicone, bone cement etc to replace the growth plate. These treatment modalities are inadequate, leaving almost half of these patients with continued deformities.

The current main strategy to regenerate tissue employs biodegradable scaffolds with or without progenitor cells and delivery of growth factors that promote the growth and differentiation of the target tissue. Different polymer scaffolds made of poly(lactic-co-glycolic acid) (PLGA) (Munirah, 2008b), hydrogels (Choi, 2007), and chitin (Li 2004), as well as growth factors as varied as transforming growth factor-β (TGF-β) (Choi, 2007), insulin like growth factor-I (IGF-I) (Lee, 2002), connective tissue growth factor (CTGF) (Shimo, 2004), and bone morphogenetic factor-2 (BMP-2) (Schmitt, 2003) have been used for regeneration of tissue. The polymer scaffolds serve as a framework for the growth of cells, and can be designed to have degradation rates that match the rate of new tissue formation. Delivery of appropriate growth factors from these scaffolds can help in recruiting progenitor cells to infiltrate the scaffold, differentiate to the right cell type and synthesize the extracellular matrix. Porous PLGA scaffolds have been used for controlled delivery of plasmid DNA encoding platelet derived growth factor (PDGF), which produced matrix deposition and angiogenesis in developing tissue in rats (Shea, 1999). Generating new tissue using a patient's own cells avoids problems with allografts or xenografts, and use of drug-eluting biodegradable scaffolds requires only a single surgery to implant the scaffold.

But delivery of growth factors from scaffolds comes with its own set of problems. The loading and release of the growth factors will have to be precisely controlled. The half-life of some growth factors is also extremely small. IGF-I had a half-life of 240 minutes after injection in rats, while TGF-β1 had a half-life of 60-163 minutes (Zapf, 1986; Zioncheck, 1994). This necessitates large initial loading of the delivery device with growth factors to last during the entire duration of the treatment.

Delivery of plasmids coding for the growth factors would be a more efficient form of therapy since the synthesis and expression of the factors would now be cell mediated. The biological amplification that happens in the DNA to protein synthesis pathway will reduce the amount of plasmid DNA that needs to be delivered. Inclusion of corresponding regulator genes for the different growth factors can bring their expression completely under the control of the cells producing them. This may result in optimal levels of growth factor concentrations. The transient transfection that happens after plasmid delivery also eliminates concerns of uncontrolled long-term production of growth factors. Controlled delivery of plasmids coding for growth factors and their regulators can give cell-regulated, short-term expression of therapeutic growth factors.

1

This dissertation reports the DNA release and degradation behavior of a porous PLGA scaffold system, chondrogenesis using these scaffolds in vitro, and in vivo testing of these scaffolds to regenerate growth plate in a rabbit model of physeal injury.

2

2. BACKGROUND AND SIGNIFICANCE

2.1 Growth plate cartilage: structure and function

The growth plate, or physis, is a narrow layer of cartilage interposed between the epiphysis and metaphysis. The epiphysis is the region at the end of long bones that forms the articular surface, and the metaphysis is a flared, contoured region of bone that tapers into the diaphysis, or shaft of long bones (Beaty). The physis serves to provide longitudinal growth for skeletally immature individuals (Ballock). Figure 2.1 illustrates the structure of growth plate.

The primary cell type found in all cartilage is called a chondrocyte. Chondrocytes are predominantly round cells located within spaces in cartilage called lacunae (Lin, 2006). They arise from pluripotent mesenchymal stem cells through a series of differentiation steps (Lin, 2006). Chondrocytes synthesize extracellular proteins, the most abundant being type II collagen, as well as chondroitin sulfate proteoglycans, such as aggrecan (Lin, 2006). The string-like collagen molecules give cartilage primarily its tensile strength, while aggrecan and the water molecules associated with it give cartilage its compressive strength (Knudson, 2001). Aggrecan monomers are made of a core protein and keratin sulfate glycosaminoglycan chains, and fill up the interstices among the collagen network by interacting with hyaluronic acid molecules and link proteins (Nagase, 2003).

Physeal cartilage has several anatomic layers. The resting zone lies closest to the epiphyseal region. It contains chondrocytes in a relatively quiescent state, and there is a high ratio of extracellular matrix (ECM) to cell volume. The ECM consists mostly of Type II collagen and proteoglycans with aggrecan being the most abundant. Chondrocytes in this layer store lipids, glycogen, and proteoglycans. The proliferative zone is the main site for longitudinal growth. As the chondrocytes proliferate they become flattened in appearance and stack into columns. There is increased proteoglycan and ECM synthesis, and this helps prohibit calcification. In the hypertrophic zone, cells increase fivefold to tenfold in size and begin to terminally differentiate. This zone is sometimes divided into three zones: maturation, degeneration, and provisional zone of calcification (Ballock).

The periphery of the physis contains two distinct elements. The groove of Ranvier is a wedge-shaped region of chondrocyte progenitor cells that contributes reserve zone cells. This contributes to lateral growth of the physis allowing growth in width as well as length. A peripheral ring of fibrocartilage surrounds and overlies the groove of Ranvier. Known as the perichondrial ring of LaCroix, this fibrous band merges with the periosteum and provides mechanical support and an anchoring membrane to the periphery of the physis (Beaty; Ballock).
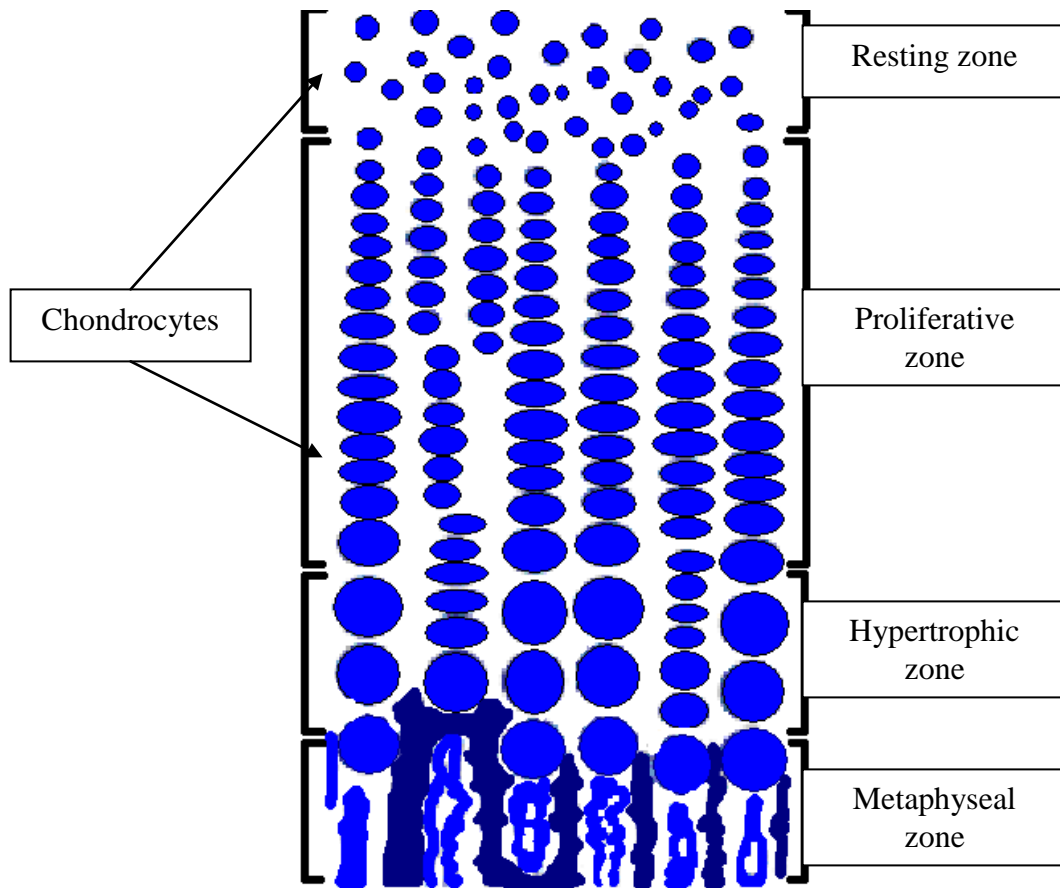
Figure 2.1 Illustration of growth plate

2.2 Cartilage development

Chondrogenesis is a multistep process that begins with the recruitment of mesenchymal progenitor cells. The recruitment, proliferation and condensation of mesenchymal cells are regulated by mesenchymal-epithelial cell interactions (Tuan, 2004; Hall, 2000). The aggregation of chondroprogenitor mesenchymal cells is one of the earliest events in chondrogenesis (Goldring, 2006). Limb buds form from the lateral plate mesoderm (Tickle, 2001). Genes than pattern mesenchymal condensation operate in a sequential manner to form limb buds (Tickle, 2003). TGF-β is one of the earliest of the growth factors that stimulate chondrogenic condensation (Goldring, 2006). Extracellular molecules in the matrix interact with cell adhesion molecules to convert the chondrogenic progenitors to fully committed chondrocytes (DeLise, 2000). BMPs are involved in the maturation of chondrocytes and terminal differentiation later into hypertrophic chondrocytes (Goldring, 2006). The differentiation of chondroprogenitors leads to further stages of skeletogenesis, and is marked by the production of Collagen II, IX and XI, and aggrecan (Goldring, 2006). Balance of signaling between BMPs and fibroblast growth factors (FGFs) determines the rate of proliferation, and thus differentiation of chondrocytes (Minima, 2002). Chondrocytes express a program driven by SOX9, Runx2 and other transcription factors (Kronenberg, 2003). SOX9, expressed by proliferating but not hypertrophic chondrocytes, is essential for every stage of chondrocytes differentiation, and stimulates transcription of multiple cartilage matrix genes such as

4

Col2a1, *Col11a2* and aggrecan (Kronenberg, 2003). Runx2 is a transcription factor important in the transformation of proliferative chondrocytes to hypertrophic chondrocytes (Kronenberg, 2003). The activities of different transcription factors, and their differential expression in different chondrocytes give an indication of the complex physiology in chondrocyte development.

2.3 Growth plate development

As described in section 2.1, growth plate has three regions: the resting zone, proliferative zone and hypertrophic zone. The chondroblasts in the resting zone are small in size and inactive. As they become active and differentiate, they move into the proliferative zone and start to synthesize matrix proteins (Van der Eerden, 2003). These chondrocytes then become hypertrophic and synthesize collagen X which allows mineralization of the extracellular matrix (Wit, 2003). At the growth plate-metaphyseal junction hypertrophic chondrocytes die by apoptosis, paving the way for invasion of blood vessels into the calcified zone (Chung, 2006). Proliferation of chondrocytes in the embryonic and post-natal growth plate is regulated by multiple FGFs that act on the cyclin D1 gene (Beier, 2005). Chondrocytes in the proliferative and prehypertrophic zone are controlled by a negative feedback loop involving parathyroid hormone-related protein (PTHrP) and Indian hedgehog (Goldring, 2006). Indian hedgehog, which is synthesized by chondrocytes, regulates bone development by coordinating chondrocyte differentiation (Kronenberg, 2003). PTHrP is synthesized by perichondrial cells and acts on proliferative chondrocytes to keep them in the proliferative pool (Kronenberg, 2003). Extracellular matrix proteins such as osteocalcin and osteopontin are thought to be involved in endochondral ossification (Goldring, 2006). Upregulation of the Cadherin-11 gene has been shown to be one of the factors involved in the process of growth plate calcification (Matsusaki, 2006). Extracellular matrix remodeling might be the rate limiting factor in the chain of events that occurs during endochondral ossification (Ortega, 2004). The angiogenic factor vascular endothelial growth factor (VEGF) promotes the invasion of blood vessels into cartilage, which is essential for the replacement of cartilage by bone (Colnot, 2001; Colnot, 2005). VEGF is released from the matrix by matrix metalloproteases expressed by endothelial cells (Goldring, 2006). These blood vessels bring osteoblasts and osteoclasts, which remodel the calcified cartilage into metaphyseal trabecular bone (Chung, 2006).

It has been postulated that a gradient of BMPs across the growth plate might be responsible for maintaining different phenotypes of chondrocytes in different zones of the growth plate (Nilsson, 2007). It was found that BMP-2 and BMP-6 were upregulated in the hypertrophic zone, while growth and differentiation factor-10 (GDF-10) and BMP-7 were upregulated in the proliferative zone (Nilsson, 2007). Chondrocytes in the resting zone and proliferative zone respond differently to BMP-2, with resting zone chondrocytes increasing DNA synthesis and higher alkaline phosphatase activity in response to BMP-2 (Erickson, 1997). Differential expression of genes in different zones of the growth plate has been reported. Genes *Fmod*, *Prelp*, *Ldha* and *Eno1* were expressed more in the proliferative zone, while MMP13 and Col1a1 were expressed more in the hypertrophic zone (Wang, 2004). Of the 40 genes that were differentially expressed in the proliferative zone of rat growth plate, 8% had cell cycle regulatory functions, while this was 0% among the 52 genes that were differentially expressed in the hypertrophic zone (Wang,

5

2004). This shows that chondrocytes in different zones of growth plate respond differently to growth factors and express different proteins according to their physiological role in the growth plate.

In addition to the autocrine and paracrine regulation of growth plate by growth factors, hormones play an endocrine role in growth plate physiology. It has been shown that decreasing levels of thyroid hormone or growth hormone as well as increasing levels of glucocorticoids can act on growth plate, resulting in slower growth rate (Nilsson, 2005). The dual effector hypothesis on growth hormone states that growth hormone acts directly at the growth plate to recruit resting chondrocytes into proliferation as well as stimulation of IGF-I production, which in turn leads to proliferation of proliferative zone chondrocytes (Ohlsson, 1992; Isaksson, 1987). Glucocorticoid receptors are expressed by growth plate chondrocytes (Silvestrini, 2000). In fetal mouse tibia, thyroid hormone promotes longitudinal growth by stimulating the hypertrophic zone (Miura, 2002). It has been shown that resting zone chondrocytes respond primarily to the $24,25\text{-}(OH)_2D_3$ metabolite of Vitamin D, while growth zone chondrocytes respond primarily to the $1,25\text{-}(OH)_2D_3$ metabolite (Boyan, 1988). Indirect evidence has suggested that epiphyseal fusion occurs when the proliferative capacity of the growth plate chondrocytes are exhausted, and that estrogen can hasten the onset of this event (Weise, 2001). Aromatase is expressed in the human growth plate cartilage, thus allowing androgens to influence growth by its conversion to estrogen (Oz, 2001).

2.4 Growth plate injuries

The physis is a unique component of skeletally immature bone. This thin layer of cartilage is susceptible to fracture under mechanical stress or loads that may result in metaphyseal or articular fractures in adults. The physis can be damaged by trauma as well as due to infection, tumors, or vascular insults (Beaty). As the region responsible for longitudinal growth in long bones, damage to the physis may result in growth abnormalities.

Fractures resulting in physeal injury are relatively common. The incidence varies in studies from 14.5% to 27.6%. Combining the results of multiple studies revealed 1,404 physeal injuries in 6,479 fractures for an overall average incidence of 21.7% (Beaty). There are several classification systems for fractures involving the physis. The most well known and commonly used is the Salter-Harris classification (Salter, 1963) (Figure 2.2). This classification involves five types. Type I is a fracture through the physis that is limited to or contained within the physis. Type II fractures extend from the physis into the metaphysis. In type III fractures, the fracture extends from the physis into the epiphysis and most frequently involves the articular surface. Type IV fractures involve extension of the fracture line through the metaphysis as well as the epiphysis and the articular surface. Type V fractures are defined as a crush injury to the physis. By definition, on initial presentation there is no radiographic abnormality, but these patients will experience premature physeal closure at the region of injury.
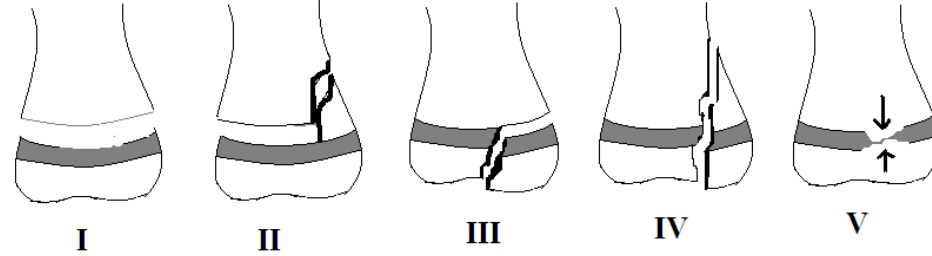
Figure 2.2 The Salter-Harris classification of physeal fractures

One of the unique complications of physeal fractures is partial growth arrest that results from the formation of a boney bar or bridge that connects the epiphysis to the metaphysis creating a tether. This tethering may result in uneven growth at the physis and subsequent angular limb deformity, leg length discrepancy, and joint abnormalities. Partial growth arrest is not very common, with significant growth disturbances occurring in approximately 10% of physeal injuries (Salter, 1994). It is found to occur most often in Salter-Harris types III and IV fractures. These fractures significantly disrupt the resting and proliferative zones of the physis, and this is suspected to increase the chance of boney bar formation. Salter-Harris type IV fractures are often significantly displaced allowing the metaphysis and epiphysis to come in contact and further increasing the risk of formation of a boney bridge tether. The physes of the distal femur and proximal tibia are those most at risk for this phenomenon (Beaty).

2.5 Chondrogenic growth factors

The majority of studies on cartilage regeneration have focused on regenerating damaged articular cartilage. Various growth factors such as IGF-1, TGF-β, FGF-2, BMPs and CTGF have been studied by different investigators for their chondrogenic potential.

Connective tissue growth factor belongs to a family of genes called *ctgf/cyr61/nov* (CCN) (Moussad, 2000). CTGF, a growth factor specific to hypertrophic growth plate chondrocytes, has been shown to enhance proliferation, maturation and hypertrophy of growth plate chondrocytes (Nakanishi, 2000). It also increased cell proliferation and production of aggrecan and collagen X when administered to chondrocytic cells (Nakanishi, 2000b). Treatment of auricular chondrocytes with rhCTGF significantly increased elastin and collagen-II mRNA, while also increasing the expression of matrix gla protein (MGP), an inhibitor of mineralization (Fujisawa, 2008). When micromass cultures were stimulated with CTGF, it resulted in chondrogenic differentiation (Shimo, 2004).

Adult canine chondrocytes cultured on a collagen scaffold with the addition of FGF-2 were shown to have a significant increase of GAG content (Veilleux, 2005). Interestingly, the combination of IGF-1 and FGF-2 led to an even higher GAG content compared to groups that received either growth factor alone (Veilleux, 2005). FGF-2 has also been shown to increase chondrocyte proliferation, but decrease the anabolic effect of IGF-1 and osteogenic protein 1 (OP-1) on articular chondrocytes cultured in alginate beads (Loeser, 2005). In a monolayer culture of human nasal septal chondrocytes, FGF-2,

7

along with TGF-β, was found to have the greatest effect on cell proliferation, but these cells took a fibroblast-like morphology (Richmon, 2005).

Growth and differentiation factor-5 (GDF-5) is a member of the TGF-β superfamily. It has been shown to increase chondrogenesis in vitro in a dose dependent manner, and increase the size of early cartilage condensation and skeletal elements in vivo (Francis-West, 1999). Addition of GDF-5 to mouse mesenchymal cells increased cell proliferation, mesenchymal condensations and cartilage nodule formation in vitro (Hatakeyama, 2004). This also led to increased expression of Col2a1, probably mediated through Sox9 (Hatakeyama, 2004).

Ectopic bone formation after demineralized bone matrix was injected into muscle compartments led to the discovery of the potent growth factor BMP (Urist, 1965). BMPs can induce osteogenic or chondrogenic differentiation of mesenchymal stem cells depending on the BMP isoform, dosage and origin of the cells (Mehlhorn, 2007). BMP-2 has been shown to induce an osteogenic phenotype in periosteum-derived progenitor cells (Iwasaki, 1994), while inducing chondrogenic phenotype in adult human mesenchymal stem cells (Schmitt, 2003). Low concentration of BMPs have been shown to induce differentiation of embryonic and mesenchymal cells to adipocytes, while high concentration induces differentiation into osteoblasts (Granjeiro, 2005). Alginate culture of human adipose-derived stem cells resulted in significantly higher GAG production and Col2a1and cartilage oligomeric matrix protein (COMP) mRNA production when treated with a combination of BMP-2 and TGF-β (Mehlhorn, 2007). BMP-4 and GDF-5 are closely related proteins and even share some receptors (Hatakeyama, 2004). Addition of BMP-4 to mesenchymal cell micromass culture has been shown to induce cartilage formation and maturation (Hatakeyama, 2004). Sekiya et al compared the effect of BMP-2, -4 and -6 on in vitro cartilage formation of adult human bone marrow stromal cells. BMP-2 was found to be the most effective, producing most cartilage matrix compared to BMP-4 and -6 (Sekiya, 2005).

IGFs are single chain polypeptide growth factors, and are expressed in a wide variety of cell types where they act as cellular growth factors (Kleffens, 1998). IGF-I and IGF-II both exert their effects through type-I IGF receptor (Kleffens, 1998). IGFs are bound in the extracellular compartment and in circulation by IGF binding proteins, which have comparable affinities for IGFs as their receptors (Kleffens, 1998). IGF binding proteins are thought to modulate the function of IGF by increasing or decreasing the availability of IGF (Jones, 1995). IGF-I can induce the formation of limb buds from prospective limb regions (Dealy, 1996). IGF-I has been shown to be expressed in regions undergoing precartilage condensation from mesoderm in mouse limb development (Kleffens, 1998). Combination of IGF-I and osteogenic protein 1/ (BMP-7) treatment produced significantly higher cell survival and matrix synthesis in osteoarthritic and normal human articular chondrocytes cultured in alginate beads (Loeser, 2003). Histological analysis of repair tissue after delivery of IGF-I gene using adenoviral vector to full thickness chondral defects was shown to increase aggrecan and collagen-II content in horses (Morisset, 2007). Transplantation of chondrocytes genetically altered to produce IGF-1 into an equine cartilage defect repair model resulted in significantly higher collagen-II content and gross filling of defects compared to untreated defects (Goodrich, 2007). Culturing human mesenchymal stem cells on IGF-1 loaded silk fibroin scaffolds have been shown to produce significantly higher GAG deposition compared to

8

unloaded silk fibroin scaffolds (Uebersax, 2008). Delivery of IGF-1 from a degradable hydrogel scaffold resulted in some cartilage regeneration in a rabbit osteochondral defect model (Holland, 2007). Interestingly, combination of IGF-1 and TGF-β did not result in any improvement over IGF-1 delivery alone, and delivery of TGF-β alone showed excessive tissue growth (Holland, 2007). IGF-1 was useful in maintaining the round morphology of humans nasal septal chondrocytes when grown as monolayer culture, and increased their proliferation (Richmon, 2005). Treatment of full thickness cartilage defects in horses with IGF-1 laden fibrin clots resulted in better tissue filling, more columnar cellular organization, and significantly higher collagen II content compared to untreated defects (Nixon, 1999). Similar results were seen when IGF-I laden chondrocyte-fibrin suspension, compared to chondrocytes-fibrin suspension was used to treat full thickness defects in horses (Fortier, 2002). Transplantation of alginate encapsulated chondrocytes overexpressing IGF-1 improved articular cartilage repair in a lapine model of osteochondral defect (Madry, 2005).

2.6 Gene delivery

A medical intervention designed to treat human diseases by correcting genetic deficiencies or by producing therapeutic proteins is called somatic cell gene therapy (Kupfer). The targeted organ becomes an "in situ factory" for the release of a therapeutic agent as the host cell uses its own regulatory machinery to control production and secretion of recombinant protein, (Kupfer). The first report of mammalian gene transfer appeared in 1980, when methotrexate-susceptible murine bone marrow cells were transformed into drug-resistant cells by the introduction of the gene for dihydrofolate reductase, a protein capable of metabolizing methotrexate (Cline, 1980).

Gene therapy involves five consecutive steps: delivery of DNA to target cells, cellular internalization, nuclear translocation, transcription and translation, and protein processing (Kupfer). Cellular uptake and nuclear translocation of naked DNA are difficult because of the large size of naked DNA. Plasmid DNA exhibits low transfection efficiency in vivo because of enzymatic degradation, chemical instability, and macrophage uptake (Mahato, 1999). Carrier molecules increase the transfection efficiency by efficiently delivering DNA to the interior of cells.

2.6.1 Carriers for gene therapy

Liposomes: Liposomes are small, non-toxic, biodegradable vesicles composed of a phospholipid bilayer (Wightman). A cationic lipid is a positively charged molecule with a hydrophilic head and a hydrophobic tail that self-associates in aqueous solution to form either micelles or bilayer liposomes (Wightman). Liposome-mediated gene delivery is based on the concept that the phospholipid composition would facilitate delivery of macromolecules by promoting membrane fusion. Preparation of liposomes is time consuming and employs organic solvents. Encapsulation efficiency using liposomes is variable and dependent on lipid composition and the method of preparation (Kupfer). Liposomes are also unstable in aqueous solutions and can have membrane-induced leakage.

Retrovirus: These viruses are exclusively of murine origin, and have been used as vectors in human gene therapy. Their ability to integrate and permanently alter the host genome carries the risk of producing cancer or mutations (Kupfer).

Adenovirus: Human adenovirus is not associated with malignant transformations in humans, as they have no mechanism for inserting their DNA into the host cell chromosome. They have high transfection efficiency and can be easily propagated (Kupfer). The greatest limitations to adenovirus mediated gene transfer are the immunogenic response to viral proteins and the transient nature of recombinant gene expression.

Immune response to the viral particles and their proteins, and safety concerns have limited the acceptability of viral vectors for gene delivery.

Chemical vectors: Chemical vectors are attractive to the pharmaceutical industry as alternatives to viral vectors because of compound stability and easy chemical modification (Wightman). Better biosafety, consistency of production, and low cost of these chemicals make them attractive candidates for gene delivery. Several polymeric molecules have been developed that can interact with the negatively charged phosphate groups in naked DNA, condense it into compact particles, protect it from degradation, and enhance the uptake of DNA into the cell resulting in efficient transgene expression (Wightman).

2.6.1.1 Polyethylenimine (PEI)

Polyethylenimines are positively charged polymers that are available in molecular weights ranging from 200 to 800,000 Da and in linear or branched form (Bieber, 2002). They are positively charged due to the large number of amine groups, which makes them suitable to condense the negatively charged DNA and facilitate their entry into cells (Bieber, 2002; Clamme, 2003). PEI has proved to be a highly effective non-viral vector for delivering plasmid DNA (Boussif, 1995). PEI interacts electrostatically with the phosphate groups of DNA via its protonated amine groups, creating a condensed particle called a polyplex (Wightman). The condensation of the PEI around the DNA protects it from nuclease activity within the cell. It also enhances cellular uptake of the condensed DNA by interacting with the negatively charged cell surface proteoglycans.

The extent of condensation between PEI and DNA will depend on the ratio of nitrogen atoms in PEI to phosphorus in DNA. PEI has been shown to efficiently condense and deliver large DNA up to 2.3 Mbp (Baker, 1997). PEI-DNA complexes are taken up by the cell, and the endosome is acidified, where the PEI acts as a proton sponge (Wightman). It is thought that the interaction of PEI amines with protons triggers osmotic swelling of the complex, causing the endosome to rupture and thus release the complexes into the cytoplasm (Wightman). Systemically delivered PEI-DNA complexes resulted in high gene expression in the lungs of mice (Goula, 1998).

The branched form of PEI is produced by cationic polymerization of aziridine monomers, while the linear form is produced by cationic polymerization of 2-substituted 2-oxazoline monomer (Godbey, 1999). Figure 2.3 shows the structure of branched PEI. The basic unit of branched PEI has a backbone of two carbons followed by a nitrogen atom. The branched form of PEI has 1°, 2°, 3° amines which can be protonated under physiological conditions.

10
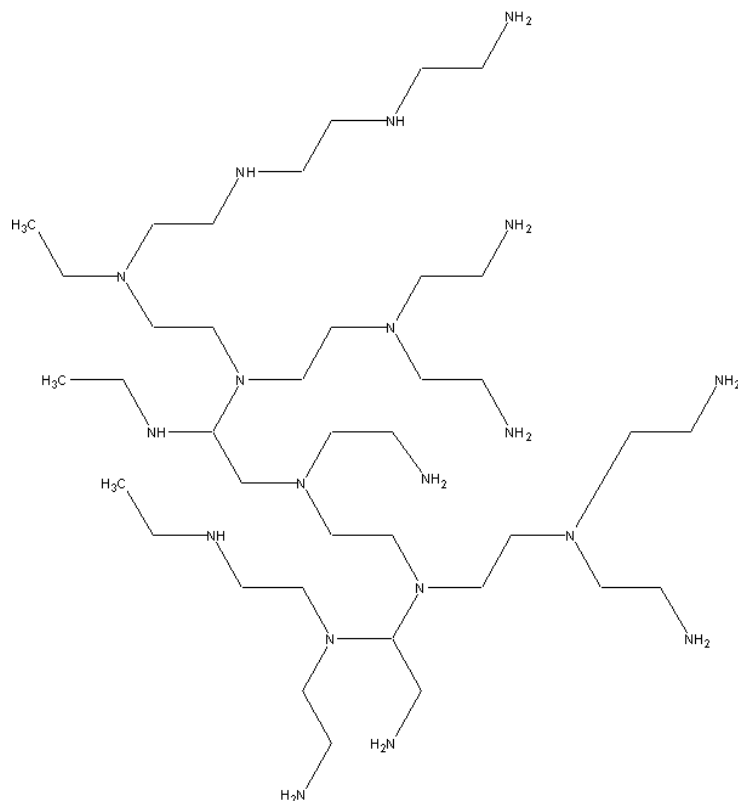
Figure 2.3 Structure of branched PEI (Adapted from Godbey, 1999)

In sufficient amounts, PEI can condense DNA by electrostatic interaction. The shape of the PEI:DNA condensate can take various forms and may be more a function of the kinetics behind the condensation than the particular form of PEI used (Godbey, 1999). The size of the PEI:DNA complex was found to be between 20nm and 40nm using atomic force microscopy (Dunlap, 1997), and between 90nm and 130 nm in solution using dynamic light scattering (Tang M, 1997).

2.7 Controlled delivery

Controlled delivery refers to the release of a substance in a predictable and precise manner from a carrier. Drug carriers can release their contents passively into their environment by two main methods: diffusion or degradation. The simpler of these two methods is a diffusive process where the drug is released from its carrier down its concentration gradient. Diffusion can be time independent or time dependent (Crank, 1968; Hopfenburg, 1969). When the carrier matrix reaches equilibrium with a solvent slower than the solvent reaching the solvent front during swelling, time independent diffusion occurs (Brannon-Peppas, 1989). On the other hand, if the carrier swells to equilibrium faster than the solvent reaching the solvent front, time dependent diffusion occurs (Brazel, 1999). In degradation controlled release, delivery of the drug is determined by the degradation kinetics of the carrier material (Langer, 1998). Degradation controlled release can also occur if the drug molecule is bound chemically or physically to the polymer molecule, and when the drug molecules are physically larger

11

than the pore size of the polymer carrier (Dihayat, 1993; Langer, 1998). Most controlled delivery devices have a combination of these processes occurring at the same time.

Release profiles usually have an initial "burst" immediately following the immersion of the delivery device in solvent. This is caused by release of drugs loosely bound or adsorbed onto the surface of the device (Hora, 1990). The initial burst release is followed by a diffusion controlled phase. Degradable devices then enter a third phase of degradation controlled release (Hora, 1990). During this phase, the device loses its mechanical integrity leading to release of drug into the solvent. These three phases together form a "triphasic release profile" (Hora, 1990).

2.7.1 DNA release from polymeric matrices

Various polymeric carriers have been investigated for the controlled release of naked DNA and PEI:DNA polyplexes. DNA-polycation nanospheres made by salt-induced coacervation of DNA and gelatin was used to transfect a variety of cell lines (Leong, 1998; Truong-Le, 1999). Plasmid genes were released from three-dimensional poly(lactic-co-glycolic) (PLGA) matrices with different degradation rates (Shea, 1999). The release rate from the PLGA polymeric matrix was controlled by changing the molecular weight of the polymer and diameter of the microspheres used to make the scaffolds (Jang, 2003). Amine derivatives of gelatin were used for release of plasmid genes to gastric mucosal cells in vitro (Hosseinkhani, 2002). Microspheres of PLGA were used to encapsulate polylysine-complexed DNA and successful transfection in vitro (Gebrekidan, 2000). Freeze-dried PEI:DNA complexes were mixed with granular PLGA and compression molded to create a DNA delivery device (Huang, 2003). An injectable in-situ formed gene delivery system using PLGA dissolved in glycofurol was successfully tested in rats (Eliaz, 2002).

2.8 Biodegradable polymers.

In this study, "biodegradable" refers to a polymer that can be converted to water-soluble material by a combination of physical and chemical processes. Although biodegradable materials are not designed to be permanently implanted in the body, they actually have to meet stringent conditions of biocompatibility because the degradation products of the material also have to be non-toxic and biocompatible with the host body. Very few polymers have found use as biodegradable polymer for implantation because of this restriction.

After exposure to the physiological environment a biodegradable polymer can degrade by surface erosion and bulk erosion. In bulk erosion, the degradation process takes place throughout the entire volume of the polymer after the intake of water. The rate at which water penetrates into the polymer matrix exceeds the rate at which the polymer transforms into water-soluble materials during bulk erosion (Heller, 1987). In surface erosion, degradation of the polymer is limited to the outer surface of the device (Heller, 1987). The rate at which water penetrates into the polymer matrix is slower than the rate at which the polymer is converted into water-soluble materials during bulk erosion (Heller, 1987). The device will therefore become thinner with time as the polymer is degraded from its surface. The polymer has to be hydrophobic to a certain extent in order for surface erosion to occur (Heller, 1987).

2.8.1 Types of Biodegradable polymers

Polyesters

Poly(lactic acid), poly(glycolic acid), and PLGA belong to a class of polymers called aliphatic polyesters (Agrawal, 2001). Nonspecific hydrolysis of ester linkages, which breaks polymer chains into shorter chains is the primary degradation mechanism of this type of polymers (Lewis, 1990). PLA-PGA materials have been widely used in musculoskeletal tissue engineering applications (Agrawal, 2001).

Polyanhydrides

The surface eroding property of polyanhydrides have made them attractive candidates for drug delivery applications (Agrawal, 2001). They are sensitive to hydrolysis and degrade rapidly (Agrawal, 2001). Aliphatic polyanhydrides degrade within days while aromatic anhydrides can take years to degrade, resulting in the development of copolymers with intermediate rate of degradation (Ratner). An example of polyanhydride is poly (sebacic acid-hexadecanoic acid anhydride).

Polyorthoesters

This surface eroding class of polymers also find applications in drug delivery (Agrawal, 2001). However, they have the disadvantage of mechanical weakness, limiting their applications in musculoskeletal applications (Agrawal, 2001). An example of polyorthoester polymer is 3,9-bis(ethylidene 2,4,8,10-tetraoxaspiro[5,5] undecane):trans-cyclohexane dimethanol:1,6-hexanediol (Ratner).

Polycaprolactones

These are also polyesters related to PLA and PGA, but with a slower degradation rate (Agrawal, 2001). They find applications as drug delivery devices as well as degradable staples for wound closure (Ratner). An example of this class of polymer is poly(ϵ-caprolactone) (Ratner).

Polycarbonates

Poly(bisphenol A-iminocarbonate) is a hydrolytically degradable polycarbonate that has good mechanical properties and biocompatibility (Agrawal, 2001). Poly(bisphenol A-iminocarbonate) are also called pseudo-poly(amino acids), and have the potential to be orthopedic biomaterials (Agrawal, 2001).

Polyfumarates

These are partially saturated linear polyesters with mechanical properties similar to that of trabecular bone (Agrawal, 2001). They have the ability to cure in vivo, making them ideal candidates for injectable scaffolds (Agrawal, 2001). An example of this class of polymer is poly(propylene fumarate).

2.8.2 Poly(lactic-co-glycolic Acid) PLGA

PLGA is a copolymer of lactic acid and glycolic acid. Its close analog PLA has found medical applications for over 30 years, mostly as an orthopedic biomaterial. PLGA has proven to be a versatile vehicle for drug delivery as PLGA devices have been used in hard tissue and soft tissue applications, and load bearing as well as non-load bearing applications (Athanasiou, 1996; An, 2000; Quereshy, 2000). PLGA has been fabricated into different physical forms such as thin films (Grizzi, 1995), microspheres (Witt, 2001; Park, 1998), foams (Lu, 2000), surface coatings (Price, 1996) and rods (Sendil, 2002). PLGA has been used to deliver hormones (Wei, 2004; Capan, 2003) as well as growth factors (Shea, 1999).

13

PLGA microspheres were used for controlled delivery of parathyroid hormone to osteosarcoma cells in vitro, and stimulated increased serum calcium levels in vivo (Wei, 2004). Porous PLGA scaffolds have been used for controlled delivery of plasmid DNA encoding PDGF, which produced matrix deposition and angiogenesis in developing tissue in rats (Shea, 1999). PLGA-surface adsorbed PEI:DNA complexes have been used for transfecting cells in-vitro, where similar transfection efficiency as bolus DNA delivery was seen with orders of magnitude less DNA (Jang, 2006). Porous PLGA scaffold with encapsulated PEI:DNA particles showed higher transfection in vivo, compared to bolus or plasmid delivery of DNA (Huang, 2005). This gene expression was seen up to 15 weeks, and at that time point the expression levels were nearly two orders of magnitude higher than controls (Huang, 2005). Delivery of PEI:DNA particles with DNA encoding BMP-4 from PLGA scaffolds resulted in significant bone regeneration in a rat cranial defect model (Huang, 2005b). PLGA microspheres have been used for intramuscular gene delivery, where the expression increased up to three months and continued until 6 months after microsphere injection (Jang, 2006b). Culturing human bone marrow stromal cells on PLGA sutures with the addition of TGF-β, and GDF-5 to a lesser extent, led to the production of collagenous tissue (Jenner, 2007). PLGA microspheres have also been used for controlled release of polylysine complexed DNA (Gebrekidan, 2000). Sustained release of BMP-2 from a PLGA device led to 75% healing of a rabbit calvarial defect, compared to 45% healing when the release was immediate (Woo, 2001). PLGA scaffolds can be made to release growth factors sequentially, a desirable feature since wound healing involves multiple growth factors acting in synchrony. Sequential delivery of TGF-β and IGF-I for 70 days have been achieved from PLGA scaffolds (Jaklenec, 2008). PLGA devices have also been used in combination with other polymers to enhance or alter the release profiles and cell response to these devices.

A hybrid scaffold using fibrin and PLGA scaffold has been shown to accelerate chondrogenesis using articular chondrocytes, as evidenced by GAG production, and intense safranin-O staining (Munirah, 2008). Implantation of similar scaffolds subcutaneously in mice resulted in cartilaginous tissue formation, with significantly higher GAG content compared to PLGA scaffolds at 2 weeks (Munirah, 2008b).

2.8.2.1 Mechanism of hydrolysis of PLGA

Hydrolysis is the cleavage of susceptible bonds by reacting with water. It can be catalyzed by acids, bases, salts or enzymes (Ratner). Hydrolysis is a single step process in which the rate of chain scission is directly proportional to the rate of initiation of the reaction (Schnabel, 1981). The rate of hydrolysis tends to increase with a high proportion of hydrolysable groups in the main or side chain, other polar groups that enhance hydrophilicity, low crystallinity, cross-link density, and a high ratio of exposed surface area to volume (Ratner). PLGA undergoes degradation by hydrolysis. The rate limiting step in the hydrolysis of PLGA is the nuclueophilic addition of water to the ester carbon by an SN_2 mechanism (Raiche *diss*). Chain scission occurs throughout the PLGA device until the oligomers formed are 8-10 monomers long, at which point they are soluble in water. Drug within the PLGA device is released in a diffusion controlled manner until the PLGA oligomers are of soluble length. Once the oligomers become soluble in water, the drug within PLGA is released by degradation (Raiche *diss*).

The bulk eroding property of PLGA means that device geometry is ineffective in controlling the release profile of the encapsulated drug. Two methods that can be employed to alter the release profiles are: changing the molecular weight of the polymer, and changing the hydrophilicity of the polymer molecule.

2.9 Current state-of-art and limitations

For all the positive results seen with the delivery of growth factors, this approach is also fraught with pitfalls. The effects of growth factors are highly dose dependent. TGF-β has shown negative effects with high doses (Fujimoto, 1999; Terell, 1993). The loading and release of the growth factors will thus have to be precisely controlled. The half- life of some of the growth factors is also extremely small. IGF-1 had a half-life of 240 minutes after injection in rats, while TGF-β1 had a half-life of 60-163 minutes (Zapf, 1986; Zioncheck, 1994). This necessitates large initial loading of the delivery device with growth factors to last during the entire duration of the treatment.

Delivery of plasmids coding for the growth factors would be a more efficient form of therapy since the synthesis and expression of the factors would now be cell mediated. Genes encoding FGF delivered from a gelatin-collagen admixture into muscle wounds resulted in tissue repair (Doukas, 2002). More importantly, recombinant human FGF delivered from the gelatin-collagen admixture failed to produce the same response (Doukas, 2002). Direct transfer of genes coding for BMP-4 and parathyroid hormone fragment from a collagen sponge resulted in new bone formation in adult rats (Fang, 1996).

The biological amplification that happens in the DNA to protein synthesis pathway will reduce the amount of plasmid DNA that needs to be delivered. Inclusion of corresponding regulator genes for the different growth factors will bring their expression completely under the control of the cells producing them. The transient transfection that happens after plasmid delivery also eliminates concerns of uncontrolled long-term production of growth factors. Controlled delivery of plasmids coding for growth factors and their regulators can give cell-regulated, short-term expression of therapeutic growth factors.

2.10 Objectives and hypotheses

The objectives of these studies were to develop a biodegradable polymer scaffold that could release a plasmid encoding a chondrogenic growth factor, in a controlled manner, and would be able to regenerate damaged growth plate in an animal model of growth plate injury. The hypotheses were that such scaffolds would be able to induce chondrocytic differentiation in vitro of mesenchymal precursor cells seeded on them, and would also regenerate growth plate-like structures when implanted in animals that had damaged growth plates. To test these hypotheses, we developed porous scaffold using PLGA polymer that released naked and PEI complexed plasmid DNA in a controlled manner. We tested the polymer scaffolds in vitro by culturing mesenchymal precursor cells on these scaffolds in the presence of a known chondrogenic factor, IGF-I, and analyzing their proliferation and cartilage matrix synthesis. Finally, we implanted blank and IGF-I plasmid releasing scaffolds in an animal model of growth plate injury and histologically and morphometrically analyzed the success in reversing the damaging effects of growth plate injury.

15

3. CONTROLLED RELEASE OF NAKED AND PEI-COMPLEXED DNA FROM POROUS PLGA SCAFFOLDS

3.1 INTRODUCTION

The ability to precisely control the delivery of single or multiple bioactive molecules is critical in tissue engineering, as tissue formation involves the interplay of multiple growth factors and signaling molecules. Biodegradable microspheres and porous scaffolds made of PLGA have been used extensively for the controlled release of therapeutics from proteins to DNA to small interfering RNAs (siRNAs). A copolymer of lactic acid and glycolic acid, PLGA is FDA approved for clinical use, and offers the possibility of tunable mechanical and degradation properties by varying its inherent viscosity/molecular weight, molar ratio of its constituents, and the presence of end caps.

The effects of growth factors are often highly dose dependent. TGF-β has shown inhibition of bone formation rate, and prolongation of mineralization lag time with high doses (Fujimoto, 1999). IGF-1 had a half-life of 240 minutes after intravenous injection in rats, while TGF-β1 had a half-life of 60-163 minutes (Zapf, 1986; Zioncheck, 1994). This necessitates large initial loading of the delivery device with growth factors to last during the entire duration of the treatment. Delivery of plasmids coding for the growth factors would be a more efficient form of therapy since the transfected cells themselves can control the synthesis and expression of the growth factors. Controlled delivery of plasmids coding for growth factors and their regulators can give cell-regulated, short-term expression of therapeutic growth factors. But naked DNA without a carrier system is highly susceptible to endonuclease degradation (Kawabata, 1995). Plasmid DNA injected intravenously is rapidly cleared from plasma (Yoshida, 1996). Several viral and chemical carriers are available for intracellular delivery of plasmid DNA. Although transfection efficiencies with viral carriers are quite high, it has the disadvantage of generating immune response in the host and the possibility of integrating plasmid DNA with the host genome. Plasmid DNA has limited issues of toxicity and immunogenicity compared to viral vectors (Winn, 2000). Polyethylenimines are positively charged polymers due to the large number of amine groups, making them suitable to condense the negatively charged DNA and to facilitate their entry into cells (Bieber, 2002; Clamme 2003). PEI-DNA complexes are taken up by the cell, and the endosome is acidified, where the PEI acts as a proton sponge (Wightman). It is thought that the interaction of PEI amines with protons triggers osmotic swelling of the complex, causing the endosome to rupture and thus release the complexes into the cytoplasm (Wightman). Freeze-dried PEI:DNA complexes were mixed with granular PLGA and compression molded to create a DNA delivery device (Huang, 2003). Controlled delivery of PEI complexed DNA encoding BMP-4 from PLGA scaffolds resulted in bone formation in a rat calvarial defect model (Huang, 2005b).

In an inductive approach to tissue engineering, a porous scaffold that provides space for tissue growth and differentiation is combined with local delivery of growth factors that can induce growth and differentiation of native precursor cells (Nof, 2002). This chapter of my dissertation presents our investigation of three types of PLGA for controlled release of naked and PEI-complexed DNA from porous PLGA scaffolds. Degradation profiles, mechanical properties and controlled release profiles of low

molecular weight hydrophilic PLGA, low molecular weight hydrophobic PLGA, and high molecular weight hydrophilic PLGA scaffolds were studied.

3.2 MATERIALS AND METHODS

3.2.1 Plasmid

Plasmids pEGFP-C1 and pDsRed2-C1 were obtained from Clontech. Figures 3.1 and 3.2 show the physical maps of the plasmids used. The plasmids were propagated using the procedure described below in DH-5α sub-clonal efficiency cells, obtained from Invitrogen. DH-5α cells were thawed in ice for about 10 minutes. One µl of 500ng/µl plasmid was added to 100 µl of DH-5α cells in a tube. The tube was kept in ice for about 30 minutes. The cells were then heat-shocked at 42ºC for 2 minutes. The cells were then put back in ice for 10 minutes. Nine hundred microlitres of SOC medium (Gibco) at 37ºC was added to the tube, and shaken at 37ºC, 225 rpm for 1 hour. The tube was centrifuged at 4000 rpm for about 20 seconds. 900 µl of supernatant was aspirated. The remaining medium and cells were resuspended. 80 µl of the transformed cells were plated on 100 mm Petri dishes containing 40g/L LB Agar-Miller (Fisher Scientific) with 30 µg/ml Kanamycin (50 mg/ml, Sigma) added to it. The dishes were incubated upside down at 37ºC overnight. They were then stored in the refrigerator until further use.
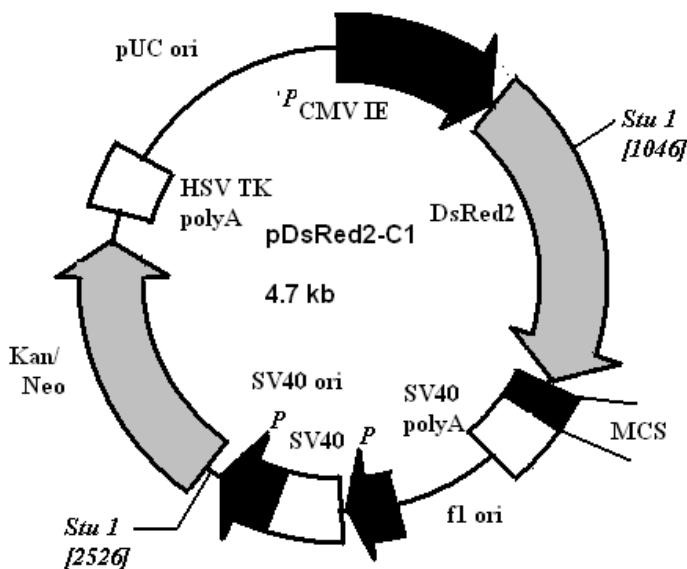
Figure 3.1 Physical map of pDsRed2-C1 plasmid
(http://www.clontech.com/images/pt/PT3603-5.pdf)

18
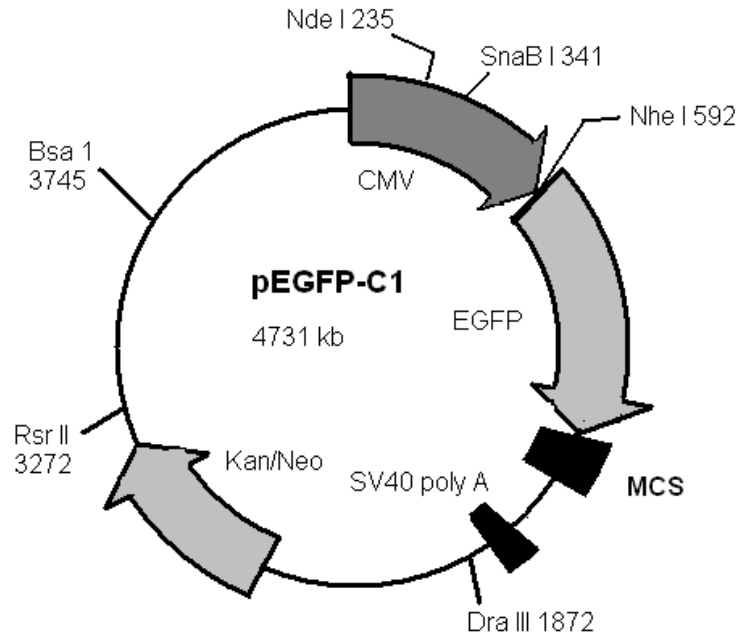
Figure 3.2 Physical map of pEGFP1-C1 plasmid
(http://www.biocenter.helsinki.fi/bi/peranen/Kotisivunlinkit/Vectors/EGFP-C1.htm)

3.2.1.1 Propogation and extraction of plasmid DNA

To extract DNA, a colony was picked from the dish and transferred to 1 ml of Terrific broth (Fisher Biotech) in a culture tube, and shaken vigorously for 8 hours at 37ºC. The Terrific broth had 0.06% v/v Kanamycin (50 mg/ml, Sigma) added to it. The starter culture was then added to 150 ml LB Broth in a 2L flask with 0.06% v/v Kanamycin and shaken overnight at 37ºC. The DNA from this culture was extracted using the GenElute HP Plasmid Maxiprep Kit (Sigma-Aldrich) following the manufacturer's instructions. Absorbance of the extracted DNA at 260 nm and 280 nm was measured using a UV spectrophotometer (Hitachi U 2000), and only DNA with an absorbance ratio greater than 1.8 was used in further experiments. Concentration of the extracted DNA was determined by measuring the absorbance at 260 nm using UV spectrophotometer (Hitachi U 2000).

3.2.2 Preparation of PEI:DNA complexes

Branched PEI 50% w/v aqueous solution Mn ~1,200 was obtained from Sigma. It was diluted to 10 mM solution for use in this study. PEI:DNA complexes were prepared according to previously published protocol (Boussif 1995). PEI:DNA complexes with an N/P ratio of 5 or 14 were prepared for our experiments. Briefly, appropriate amount of 10mM PEI was added drop wise to four milliliters of 500 µg/ml plasmid DNA with 1% sucrose. This PEI:DNA solution was quickly frozen to -80ºC and lyophilized for 3 days. Lyophilized PEI:DNA powder was resuspended in 700 µl of TE buffer. PEI was labeled with the amine-reactive probe Alexa488 (Molecular Probes/Invitrogen) using the manufacturer's protocol.

3.2.3 Preparation of PLGA microspheres

19

DNA-loaded microspheres were made using a W/O/W double emulsion method (Jain, 2000). In this study, 50:50 PLGA was obtained from Durect Corporation (Penham). 50:50 PLGA with an inherent viscosity of 0.15-0.25 dL/g and acid end group is called low molecular weight hydrophilic, 50:50 PLGA with an inherent viscosity of 0.15-0.25 dL/g and methyl ester end group is called low molecular weight hydrophobic PLGA, and 50:50 PLGA with an inherent viscosity of 0.55-0.75 dL/g and acid end group is called high molecular weight hydrophilic PLGA. Six hundred and eighty microliters of DNA alone or PEI:DNA solution were added to 10% w/v PLGA in methylene chloride. DNA solution was replaced with 680µl of TE buffer to create blank microspheres. This suspension was then vortexed for 30 seconds and added dropwise to rapidly spinning 1% polyvinyl alcohol (Sigma-Aldrich, MO) in deionized water to form the W/O/W emulsion. To create microspheres of high-molecular weight PLGA, a homogenizer was used to stir the suspension at 3500 rpm. Methylene chloride-DNA suspension was added drop wise to rapidly stirring PVA-water solution. The resulting suspension was homogenized using an Omni PDH (Omni International, GA) for 5 minutes. The emulsion was stirred overnight to evaporate methylene chloride, and the microspheres were collected using centrifugation. The collected microspheres were rinsed twice in deionized water and lyophilized for 48 hours before making discs.

3.2.4 Porous PLGA discs

To create porous PLGA discs for release experiments, 42 mg of PLGA microspheres were mixed by hand with 63 mg of 100-350 microns salt particles for 2 minutes, and compressed at 1.5 tons for 2 minutes in a 6 mm die using a Carver press. One hundred and twenty milligrams of PLGA microspheres were mixed with 180 mg of salt particles for 2 minutes, and compressed at 6 tons for 2 minutes in a 13 mm die to create discs for in vitro and in vivo experiments. The ratio of salt to microspheres was increased to 70 wt% for hydrophobic discs in order to maintain the porosity of all discs at 60%.

The discs were then sintered in an oven for 48 hours at the T_g for PLGA. For low-molecular weight PLGA, the sintering temperature was 42°C, while for high-molecular weight PLGA, the sintering temperature was 49°C. The sintered discs were then leached by stirring 6 discs/2L of deionized water overnight and dried in vacuum to create porous PLGA scaffolds.

To create discs with freeze-dried DNA on top, 40µl of 500 µg/ml DNA solution containing 1% sucrose was added to the surface of previously prepared scaffolds and then lyophilized overnight.

3.2.5 Mechanical testing of scaffolds

Six millimeter diameter scaffolds were tested to failure using a Bose Electroforce 3300. The rate of compression was set at 1 mm/minute (Leung, 2008), and scaffolds were compressed to 1.5mm. Load and displacement values were used to calculate stress and strain values. Stress-strain plots for different groups of scaffolds were generated using Excel, and ultimate stresses and compressive moduli were calculated.

3.2.6 Mass loss of scaffolds

20

Scaffolds were immersed in 2 ml of PBS in 12 well plates, and incubated at 37°C with continuous shaking. PBS was replaced every 2 days. Scaffolds were collected at various time points and lyophilized for 48 hours before measuring their final weights.

3.2.7 In vitro release and analysis

In vitro release was performed in 2 ml PBS with 2 mM EDTA, pH 7.4, at 37°C with continuous shaking. The supernatant was collected and replaced every 24 hours. The amount of DNA in the supernatant was determined using a fluorometric Picogreen® (Molecular Probes/Invitrogen) assay according to the manufacturer's instructions. For the Picogreen assay, the excitation/emission wavelengths were 480/520nm. Calf thymus DNA was used as a standard to calculate DNA mass from the fluorescence values. Alexa488 labeled PEI release from microspheres was measured at an excitation/emission wavelengths of 488/520 nm. The pH of released supernatant was measured using a pH microelectrode.

3.2.8 Statistical analysis

Statistical analysis was performed using SAS 9.1 NC software. A p-value of 0.05 was used for all statistical comparisons. The student's t-test and ANOVA were used for comparing results between different groups. Tukey-Kramer multiple comparison test was used post-hoc. All figures show mean value +/- standard deviation for measured variable. All samples were in triplicate. Mixed models with repeated measures were used, to compare various release profiles.

3.3 RESULTS

3.3.1 Mass loss of PLGA scaffolds

3.3.1.1 Low molecular weight hydrophilic scaffolds

Figure 3.3 shows the mass loss of low molecular weight hydrophilic scaffolds in PBS. Blank scaffolds had the highest slope, indicating the fastest mass loss, while PEI:DNA 5 encapsulated scaffolds had the lowest slope, indicating the slowest mass loss. Between days 5 and 15, PEI:DNA 5 encapsulated scaffolds lost their mass at an average rate of 4.6%/day. Naked DNA scaffolds had a mass loss rate of 5.3%/day during the same time period, while blank scaffolds lost mass at a rate of 6.2%/day. P-value for mixed-model analysis of mass loss rates for different scaffold groups was greater than 0.05. Blank and DNA encapsulated scaffolds had loss their mass completely by day 30, while PEI:DNA encapsulated scaffolds still had 20% of their mass left at day 30.
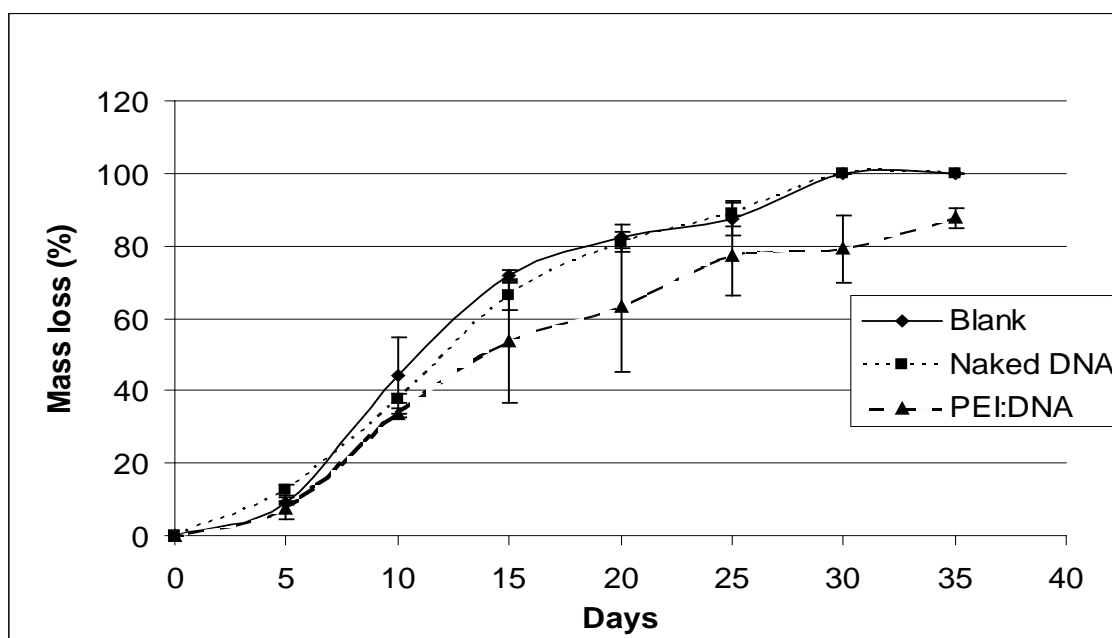
Figure 3.3 Mass loss of low molecular weight hydrophilic scaffolds in PBS

3.3.1.2 High molecular weight hydrophilic scaffolds

Figure 3.4 shows the mass loss of high molecular weight hydrophilic scaffolds in PBS. These scaffolds degraded slower compared to the scaffolds made from low molecular weight hydrophilic PLGA. By day 20, high molecular weight PLGA scaffolds had lost only about 10% of their mass, whereas low molecular weight scaffolds had lost more than 60% mass by that time point. The initial phase of mass loss from high molecular weight PLGA scaffolds lasted until day 20, when the average mass loss was 0.38%/day. P-value for mixed-model analysis of mass loss rates of blank scaffolds, naked DNA encapsulated scaffolds, and PEI:DNA encapsulated scaffolds was greater than 0.05. The second phase of mass loss was from day 20 to day 60. During this time, blank scaffolds lost mass at 2.05%/day, DNA encapsulated scaffolds last mass at 2.09%/day and PEI:DNA encapsulated scaffolds lost mass at 1.74%/day. P-value for mixed-model analysis of mass loss rates between days 20 and 60 for blank scaffolds, naked DNA

22

encapsulated scaffolds, and PEI:DNA encapsulated scaffolds was greater than 0.05. By day 60, blank scaffolds had lost 88% of their mass, while PEI:DNA encapsulated scaffolds had lost 77% of their mass. Mass loss for naked DNA encapsulated scaffolds was 93% at day 60. P-value for ANOVA of mass loss between different scaffold groups at day 60 was greater than 0.05. It appears that PEI:DNA encapsulated scaffolds had lost more mass at day 50 than at day 60. This is an experimental artifact, as one disc in the 60-day batch degraded less compared to the other discs in the same batch.
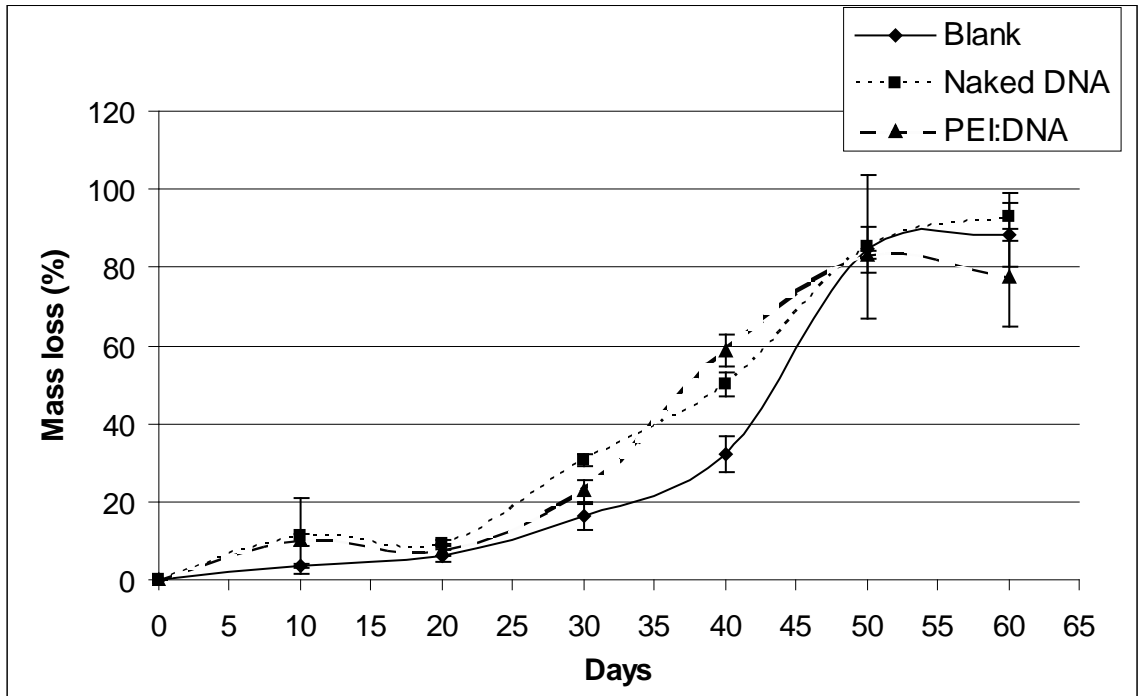
Figure 3.4 Mass loss of high molecular weight hydrophilic scaffolds in PBS

3.3.2 pH of release supernatant

In order to understand the degradation kinetics of the scaffolds, the pH of the supernatant was measured. Figure 3.5 shows the pH of supernatant from low molecular weight hydrophilic scaffolds. pH started dropping from the starting value of 7.4, reaching 4.7 for PEI:DNA 5 encapsulated scaffolds on day 8. It continued to rise after that time point until it reached 7.2 by day 30. pH of PEI:DNA encapsulated scaffolds were significantly higher compared to blank and DNA encapsulated scaffolds from day 4 until day 20 (p-value < 0.05), with the exception of day 8 when the difference was not statistically significant (p-value > 0.05). pH of the supernatant from blank and naked DNA encapsulated scaffolds showed values similar to each other throughout the experiment. They started around 7.4 and continued to decrease until day 16, reaching the lowest value of 3.5. Thereafter, they increased to the original value of 7.4 by day 30.

Figure 3.6 shows the pH of supernatant collected from low molecular weight hydrophobic scaffolds. The pH of supernatant from blank scaffolds was around 7.8 until day 23, when it started dropped sharply to around 3.2 on day 46. It started rising back towards 7 on day 50. The pH of supernatant from blank scaffolds were significantly higher than naked DNA and PEI:DNA encapsulated scaffolds until day 34, and

23

significantly lower from day 38 until day 66 (p-value < 0.05). Naked and PEI:DNA 5 encapsulated scaffolds started around pH 6.5, and steadily decreased to 4.8 by day 14, before rising gradually to reach 7 by day 55. There was no statistical difference in pH of naked and PEI:DNA encapsulated scaffolds (p-value > 0.05), except at day 10, when PEI:DNA encapsulated scaffolds had significantly higher pH compared to naked DNA scaffolds (p-value < 0.05). Blank hydrophobic scaffolds reached their lowest pH on day 46, compared to day 17 for blank hydrophilic scaffolds. Naked and PEI:DNA encapsulated hydrophobic scaffolds reached their lowest pH on day 14, compared to day 16 for naked DNA encapsulated hydrophilic scaffold and day 8 for PEI:DNA encapsulated hydrophilic scaffolds.
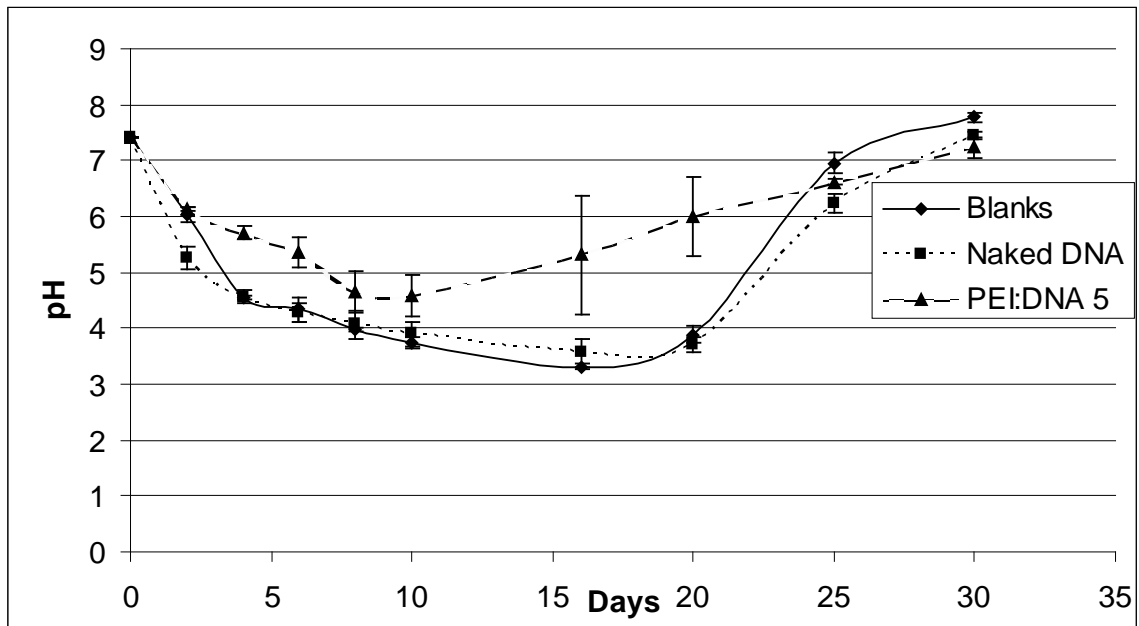
Figure 3.5 pH of supernatant from degrading low molecular weight hydrophilic scaffolds
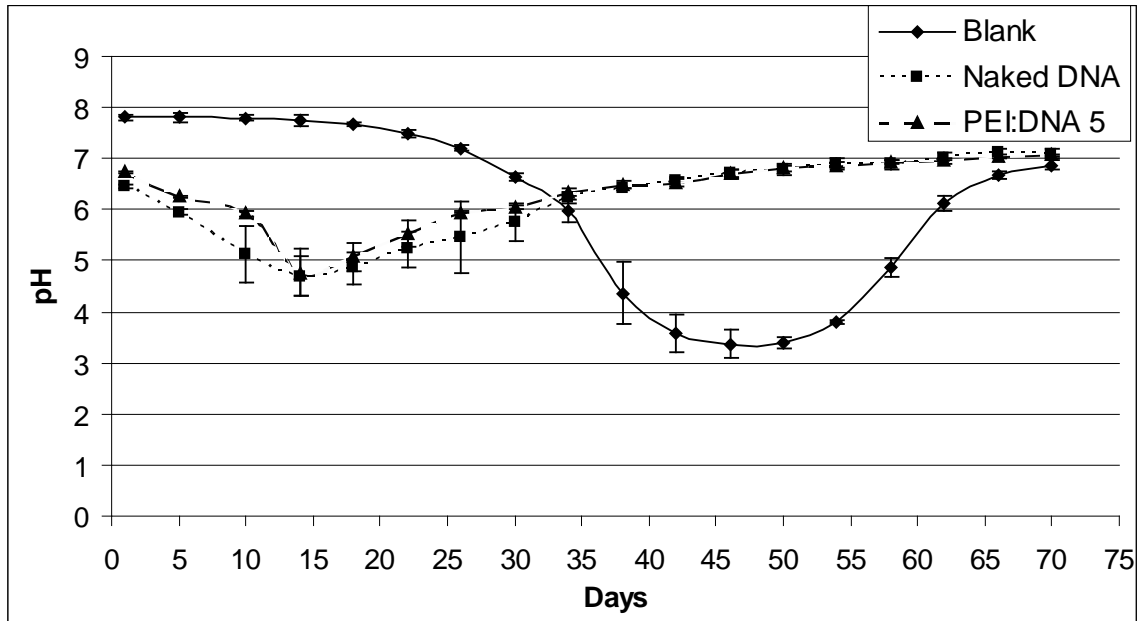
Figure 3.6 pH of supernatant from degrading low molecular weight hydrophobic
scaffolds

Figure 3.7 shows the pH from the high molecular weight hydrophilic scaffolds.
Naked DNA and PEI:DNA 5 encapsulated scaffolds, as well as blank scaffolds showed
similar values throughout the experiment. pH of the supernatant decreased from the
starting value of 7.4, reaching the lowest value of 4.3 around day 38. After that pH started
to rise, reaching a maximum of 6.8 by day 70. There were no statistical differences in the
pH values (p-value > 0.05). All high molecular weight hydrophilic scaffolds reached their
lowest pH around days 40-45, compared to days 8-16 for low molecular weight
hydrophilic scaffolds.

25
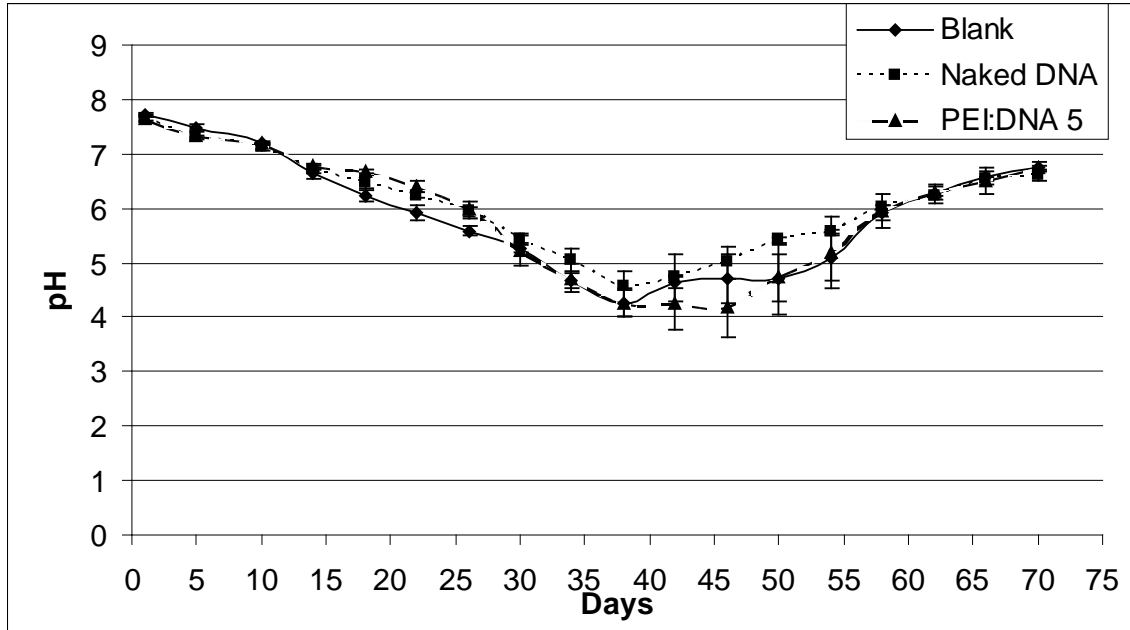
Figure 3.7 pH of supernatant from degrading high molecular weight hydrophilic scaffolds

3.3.3 Mechanical testing of PLGA scaffolds

Figures 3.8 is a representative stress-strain plot from the mechanical testing of low molecular weight PLGA scaffold. A brief toe region can be seen at the beginning of the plot. After that, stress increased linearly with strain, until the sample failed at around 1.45 MPa. Both the high molecular weight and low molecular weight PLGA scaffolds showed linear stress-strain relationships, but they differed in their ultimate compressive strengths as well as compressive moduli, as evident in Figures 3.9 and 3.10.

$$y = 25.936x + 0.055$$
$$R^2 = 0.9929$$
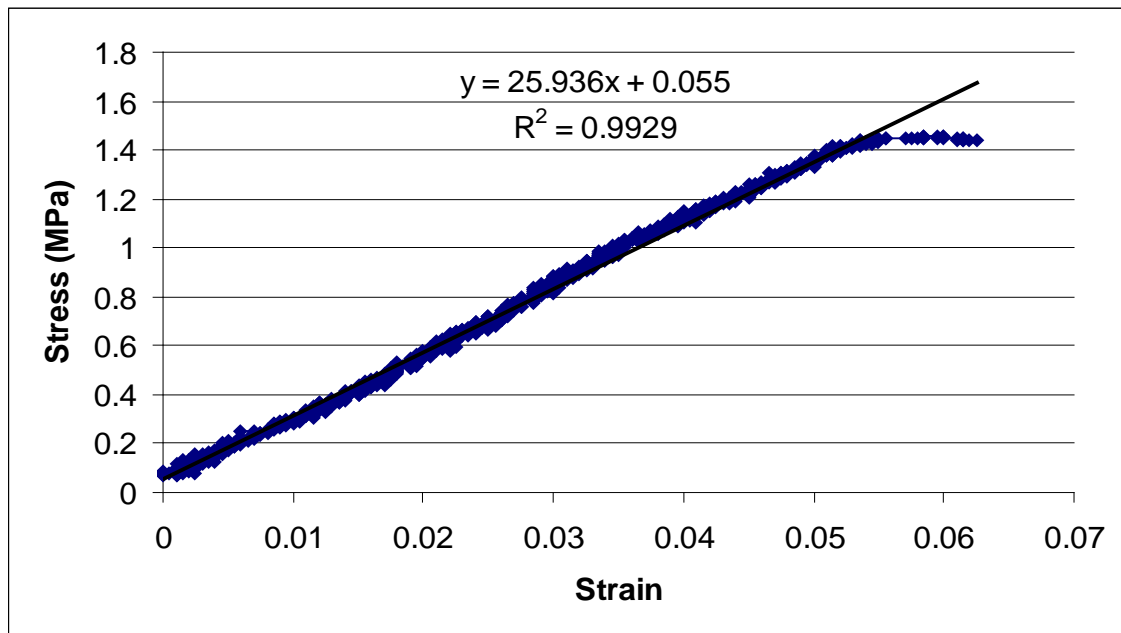
Figure 3.7 Representative stress-strain curve for low molecular weight hydrophilic scaffold

26

3.3.3.1 Effect of molecular weight on mechanical properties

Figures 3.9 and 3.10 show the effect of molecular weight of PLGA on compressive moduli and ultimate strength of scaffolds, respectively. Blank scaffolds made from low molecular weight PLGA had an average compressive modulus of 29.2 MPa, while blank scaffolds made from high molecular weight PLGA had an average compressive modulus of 78.46 MPa. The difference in compressive modulus between these two types of scaffolds was statistically significant, with a p-value < 0.05. PEI:DNA encapsulated scaffolds made from low molecular weight PLGA had an average compressive modulus of 25.51 MPa, while the average compressive modulus for high molecular weight PEI:DNA scaffolds was 81.13 MPa. The difference in compressive modulus between high and low molecular weight PEI:DNA 14 scaffolds was also statistically significant, with a p-value < 0.05.

Low molecular weight blank scaffolds had an average ultimate strength of 1.86 MPa, while their high molecular weight counterparts had a statistically significantly higher ultimate strength of 5.94 MPa (p-value < 0.05). Low molecular weight PEI:DNA 14 scaffolds had an average ultimate strength of 1 MPa, while their high molecular weight counterparts had a statistically significantly higher average ultimate strength of 7.2 MPa (p-value < 0.05).

3.3.3.2 Effect of PEI:DNA encapsulation on mechanical properties
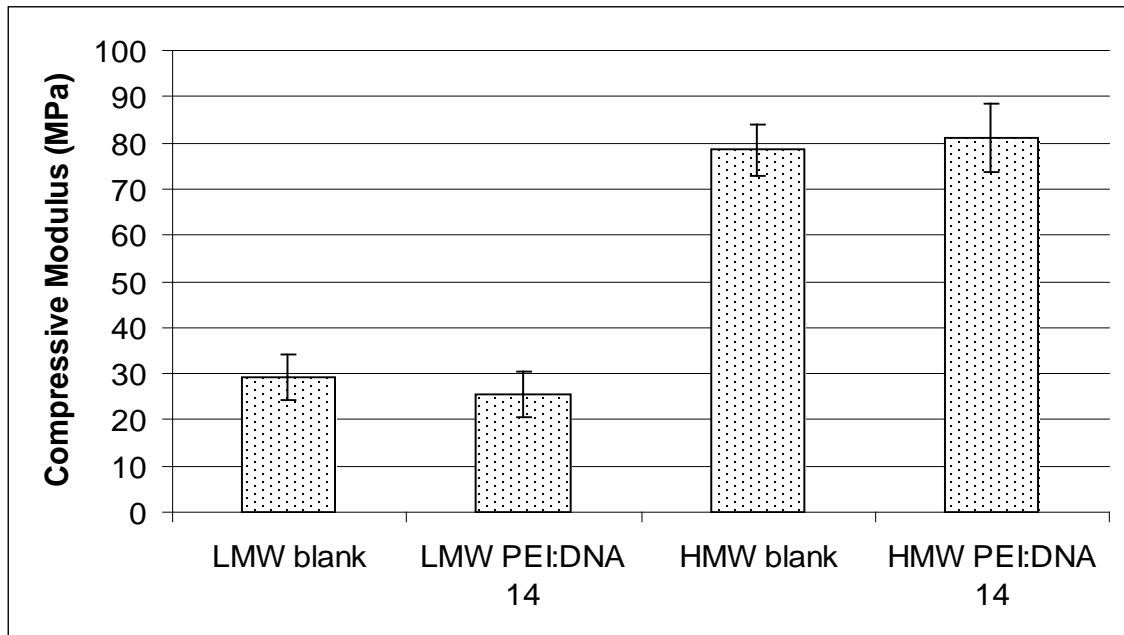
Figure 3.9 Compressive moduli of PLGA scaffolds

Figures 3.9 and 3.10 also show the effect of PEI on the mechanical properties of PEI:DNA encapsulated scaffolds compared to blank scaffolds. There was no significant difference between the compressive modulus of blank scaffolds and PEI:DNA encapsulated scaffolds for both low molecular or high molecular PLGA (p-value > 0.05).

27

This was not the case for ultimate strength. Ultimate strength for low molecular weight blank scaffolds was 1.86 MPa, while low molecular weight PEI:DNA encapsulated scaffolds had a statistically significantly lower ultimate strength of 1 MPa (p-value < 0.05). High molecular weight blank scaffolds had an average ultimate strength of 5.94 MPa, while high molecular weight PEI:DNA scaffolds had a higher average ultimate strength of 7.21 MPa. This difference was not statistically significant (p-value > 0.05).
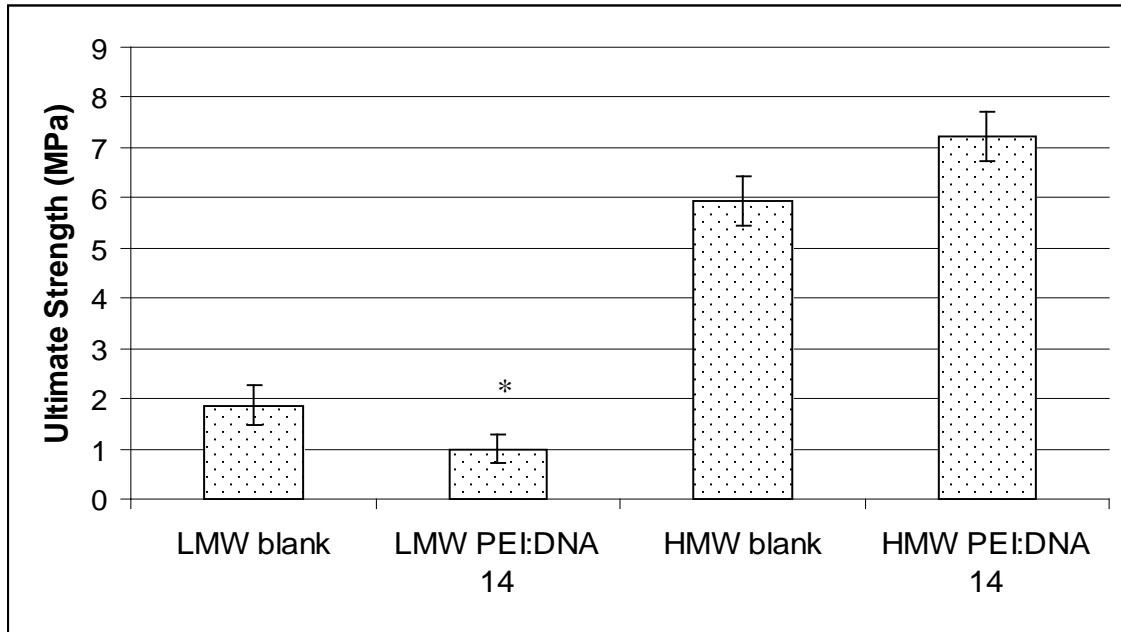
Figure 3.10 Ultimate strength of PLGA scaffolds. * denotes p-value < 0.05 between LMW blank and LMW PEI:DNA 14

3.3.4 DNA release from PLGA scaffolds

3.3.4.1 Low molecular weight hydrophilic PLGA

3.3.4.1.1 DNA release from microspheres alone
DNA release from low molecular weight hydrophilic PLGA microspheres that had naked DNA encapsulated is shown in Figure 3.11. DNA was detected in the supernatant from the first day of release. A peak release of 2.3 µg/ml was seen on the first day, followed by rapid decrease until day 18.
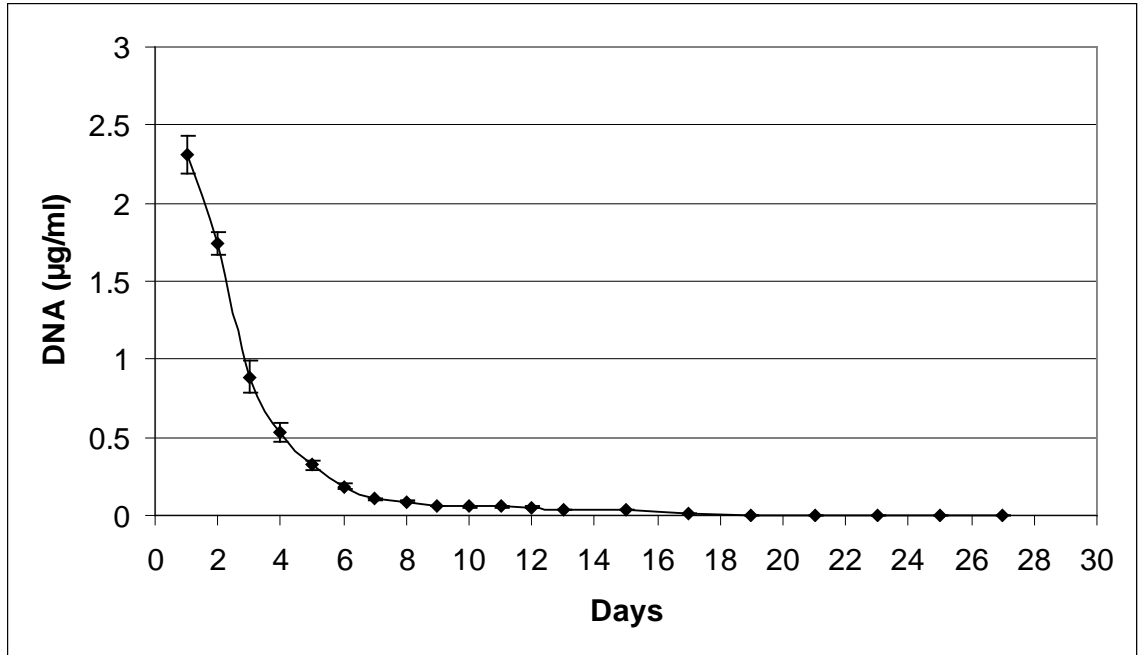
Figure 3.11 Naked DNA release profile for low molecular weight hydrophilic PLGA microspheres

3.3.4.1.2 DNA release from scaffolds

Figure 3.12 shows the release of encapsulated naked and PEI-complexed DNA from low molecular weight hydrophilic PLGA scaffolds. Naked and complexed DNA were detected in the supernatant from the first days of release. Both releases had biphasic profiles, with the first phase due to the release of surface bound naked and PEI:DNA polyplex, and the second phase from the swelling of scaffolds and release of naked and PEI:DNA polyplex from the interior of the scaffolds. Naked DNA release showed a peak around days 7-10 with 0.25 to 0.27 µg/ml of supernatant. The release of naked DNA was over by day 16. PEI:DNA 5 complexes showed a slightly different release profile compared to naked DNA particles. The initial phase of release lasted longer, ending by day 7, compared to day 4 for naked DNA particles. The concentration of PEI:DNA particles was also higher compared to naked DNA until day 5. The second peak of PEI:DNA release occurred on day 10, compared to days 7-10 for naked DNA. The release of PEI:DNA particles was complete by day 20.
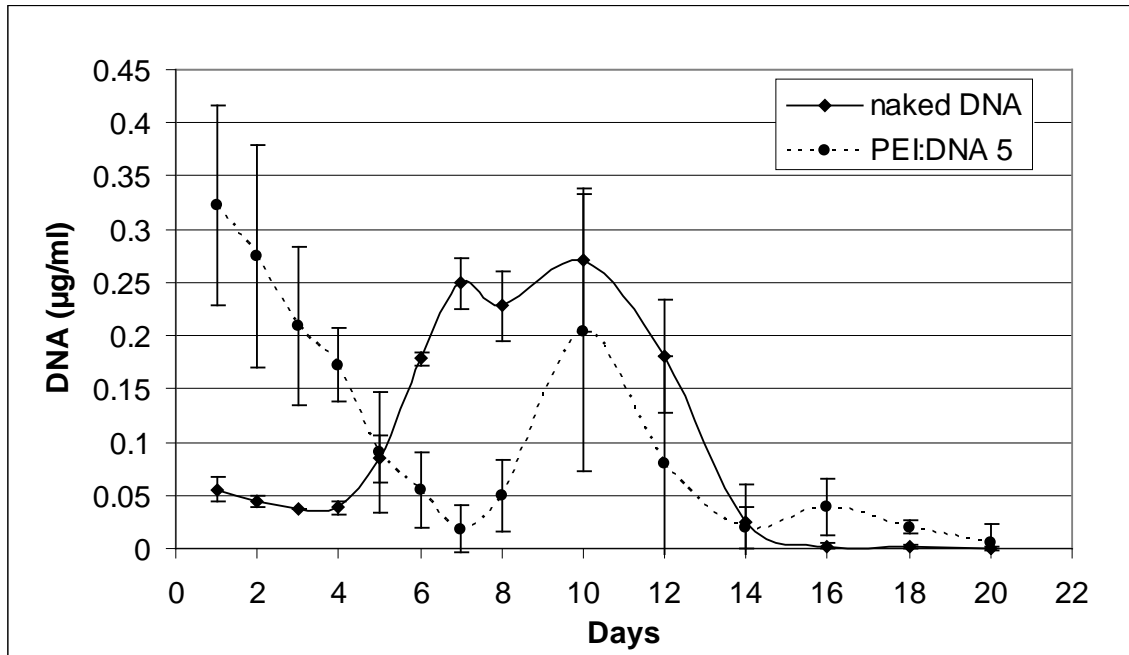
Figure 3.12 Naked and PEI complexed DNA release from low molecular weight hydrophilic PLGA scaffolds

The fractional cumulative release of naked and PEI complexed DNA particles from low molecular weight hydrophilic scaffolds can be seen in Figure 3.13. PEI:DNA encapsulated scaffolds released majority of their contents earlier than naked DNA encapsulated scaffolds although they had their second phase release later than naked DNA encapsulated scaffolds. This is evident by comparing the fraction of DNA released at day 6 for both types of scaffolds. By day 6, PEI:DNA encapsulated scaffolds had released 72% of their total content, while DNA encapsulated scaffolds had released only 31% of their total content. PEI:DNA encapsulated scaffolds, however, continued to release complexes for a longer duration. Naked DNA encapsulated scaffolds had an average release rate of 2.7%/day during the first phase, and 9.6%/day during the second phase of release, compared to 12.5%/day during the first phase, and 4.3%/day during the second phase for PEI:DNA encapsulated scaffolds. Mixed model analysis of the release rates during the first phase gave a p-value less than 0.05, while the p-value for the release rates during the second phase was greater than 0.05. PEI:DNA encapsulated scaffolds completed their release by day 20, compared to naked DNA encapsulated scaffolds that completed their release by day 16.

30
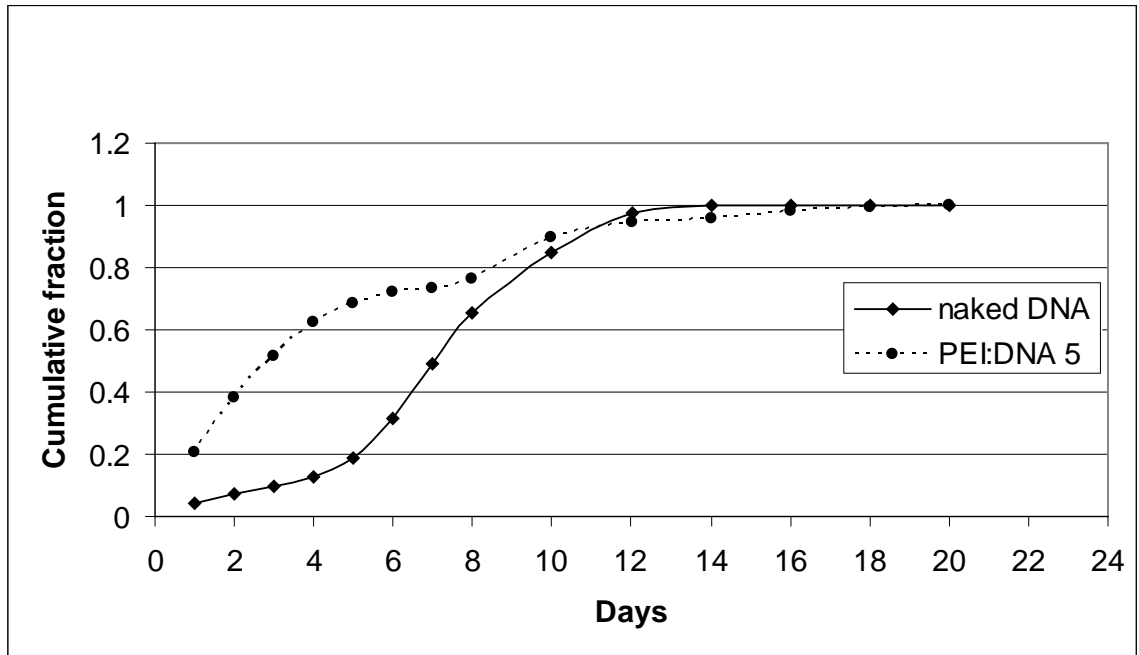
Figure 3.13 Cumulative fractional release of PEI:DNA 5 and DNA from low molecular weight hydrophilic PLGA scaffolds

3.3.4.1.3 Effect of additional freeze-dried layer on surface

An additional layer of naked DNA was freeze-dried onto the surface of scaffolds to increase the initial amount of DNA released. Figure 3.14 shows the combined release of freeze-dried and encapsulated DNA from PLGA scaffolds, while Figure 3.15 shows the release of encapsulated DNA alone from scaffolds. Superimposed release profiles from Figures 3.14 and 3.15 can be seen in Figure 3.16. The initial burst release of freeze-dried DNA was over by one week, after which the release profile of both types of scaffolds looked comparable. The initial amount of DNA released from scaffolds that had a freeze-dried layer of DNA was 87 fold higher than that from scaffolds with encapsulated DNA alone (2.6µg/ml as opposed to 0.03µg/ml). This difference was statistically significant with a p-value less than 0.05.

31
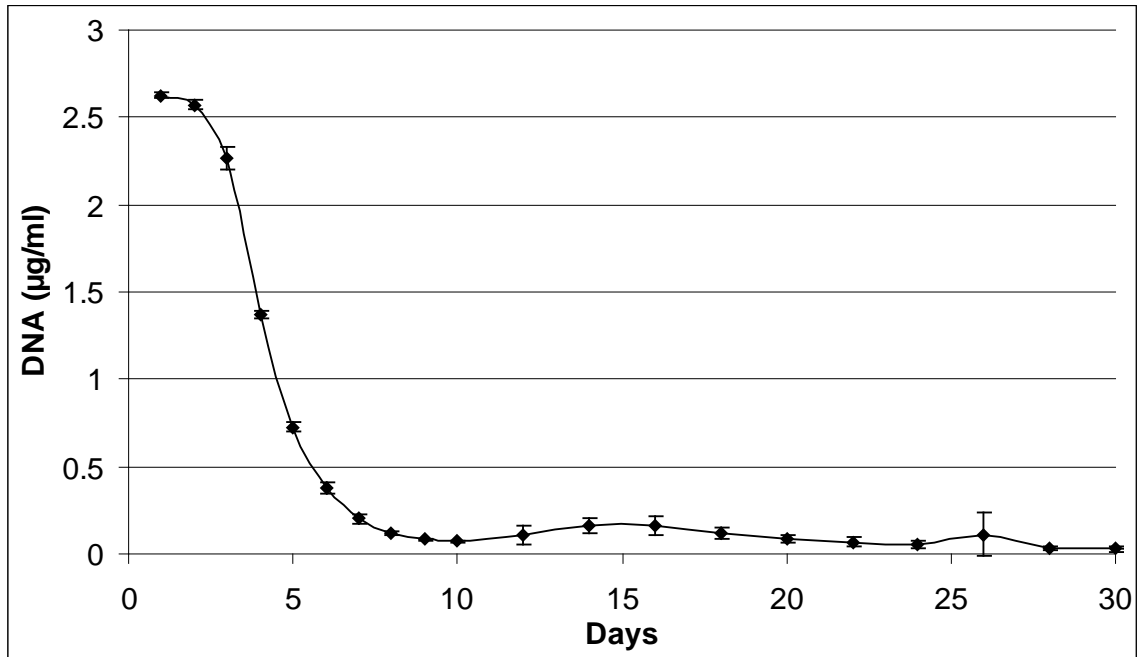
Figure 3.14 Release of freeze-dried and encapsulated naked DNA from low molecular weight hydrophilic PLGA scaffolds
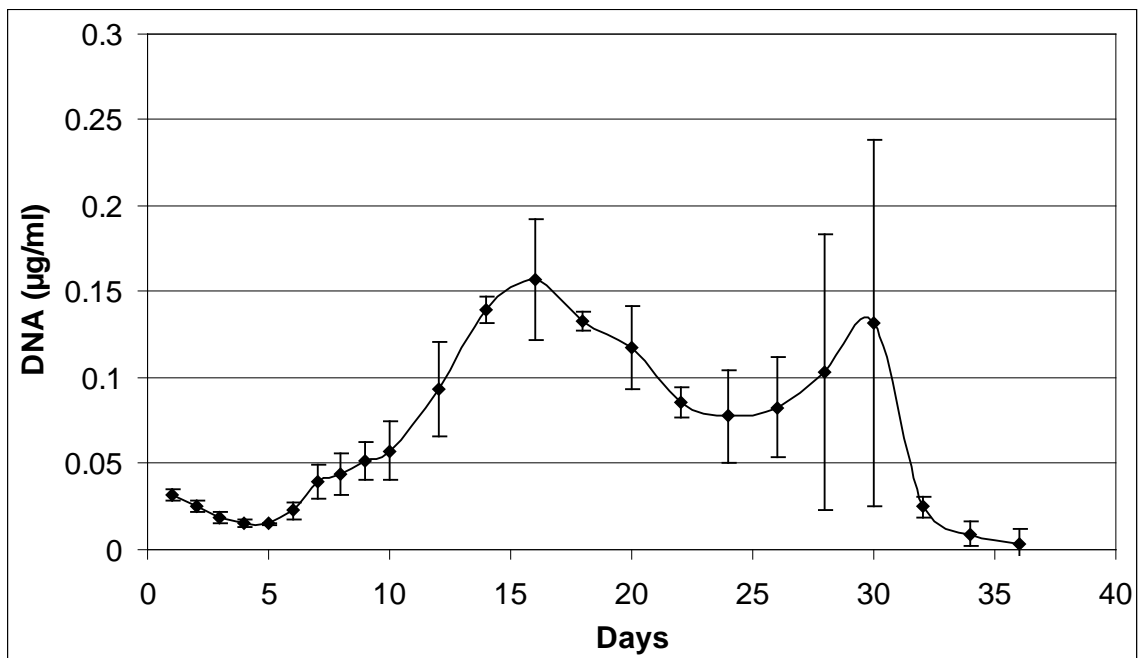
Figure 3.15 Release of encapsulated naked DNA from low molecular weight hydrophilic PLGA scaffolds

The peak release on day 16 was statistically significantly higher than the release values until day 12 (p-value < 0.05).
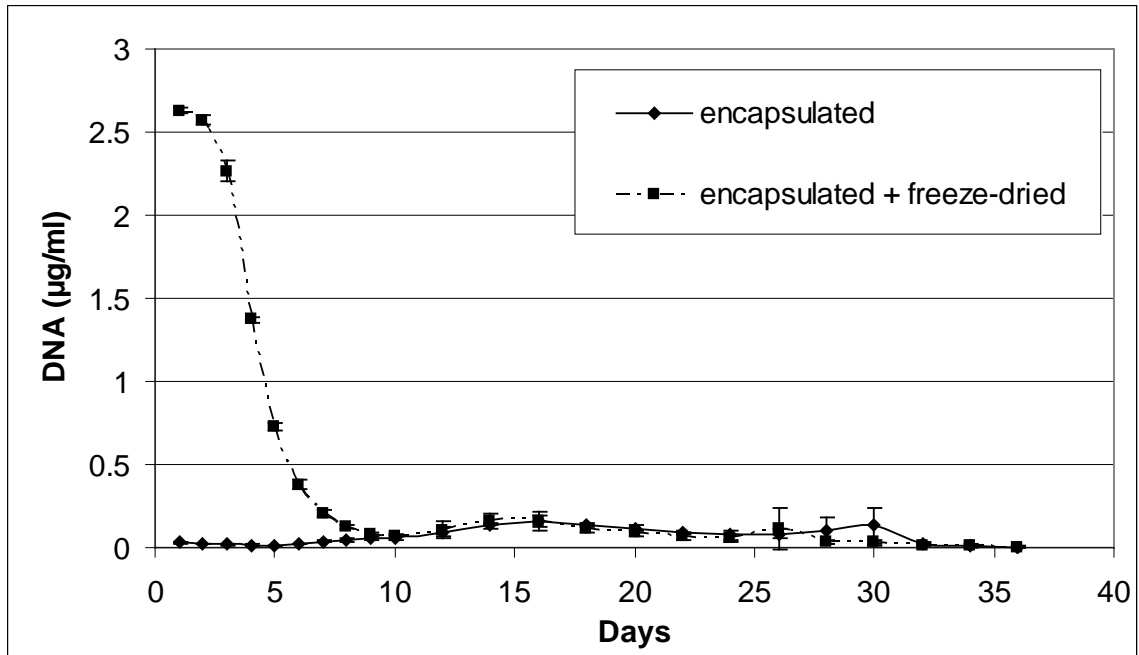
Figure 3.16 Superimposed release profiles of encapsulated and freeze-dried naked DNA
from low molecular weight hydrophilic PLGA scaffolds

3.3.4.1.4 Release of fluorescently labeled PEI

Complexation of DNA with PEI resulted in reduced detectablity of DNA using normal DNA assays. Therefore, PEI used for making PEI:DNA complexes was labeled using Alexa-480 to track its release from PLGA scaffolds. The results can be seen in Figure 3.17. PEI was detected in the supernatant from the first day of release. The release profile showed a typical biphasic pattern. The first phase of release for PEI:DNA 5 encapsulated scaffolds was over by day 7, while for scaffolds with PEI:DNA 14 complexes, the first phase continued until day 15. The second peak in release for PEI:DNA 5 encapsulated scaffolds lasted from day 27 to day 34, while for PEI:DNA 14 encapsulated scaffolds the second peak was from day 27 to 39. PEI:DNA 14 encapsulated scaffolds showed higher fluorescence values at all time points compared to scaffolds with PEI:DNA 5 complexes.

33
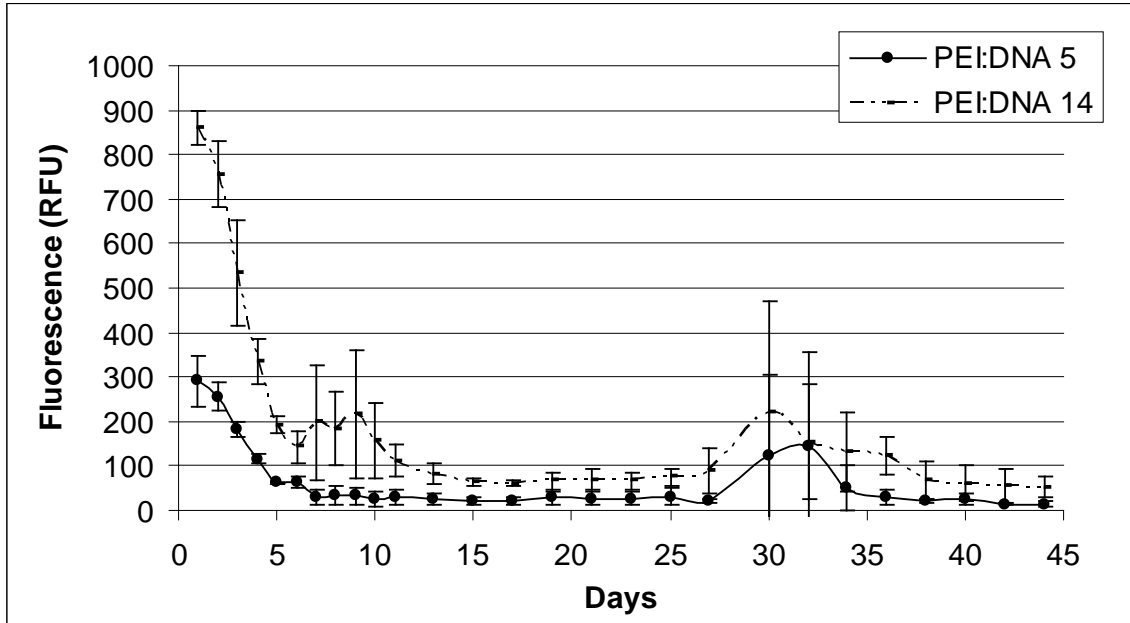
Figure 3.17 Release profile of fluorescently labeled PEI released from low molecular weight hydrophilic PLGA scaffolds

In addition to tracking fluorescently labeled PEI, DNA was also assayed from the same set of scaffolds. This afforded us the ability to simultaneously and independently track the release of both PEI and DNA. DNA release profile from the scaffolds can be seen in Figure 3.18. The first phase of PEI:DNA release started on day 1 and ended by day 5, whereas the second phase of release started on day 25 and ended by day 34. Figure 3.18 shows the excellent correlation between PEI and DNA release profiles. Variability between samples around day 30 was high as samples started disintegrating into smaller pieces.
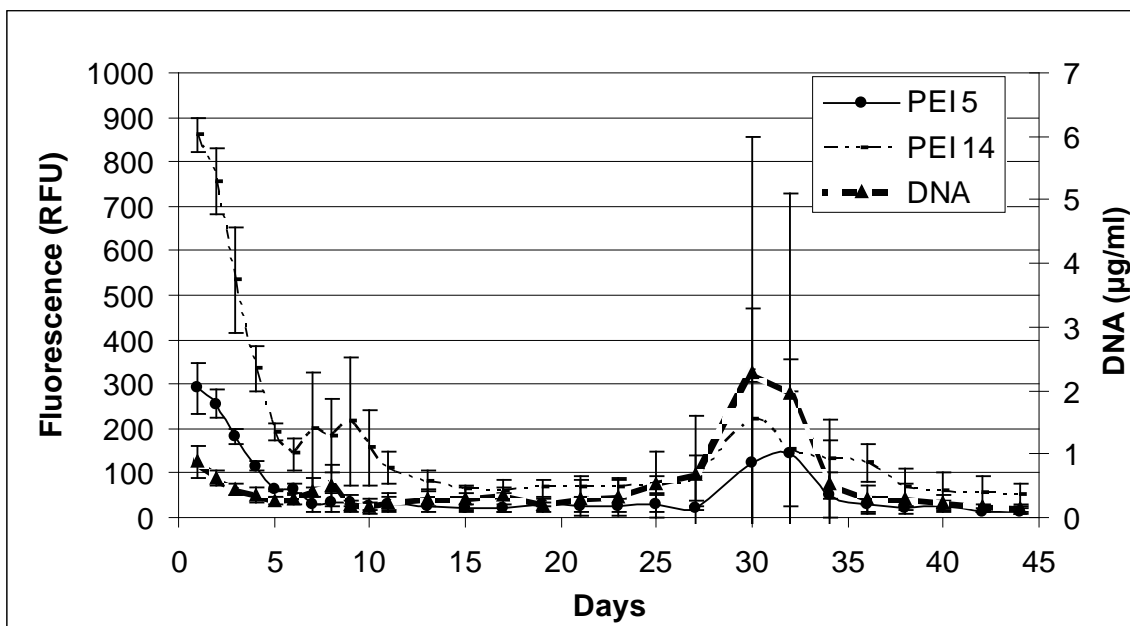
Figure 3.18 Superimposed release profiles of labeled PEI and DNA from low molecular weight hydrophilic PLGA scaffolds

3.3.4.2 Low molecular weight hydrophobic PLGA

Naked and PEI complexed DNA was encapsulated within methyl-terminated low molecular weight PLGA to study the effect of hydrophobicity on release behavior. Figure 3.19 shows the release profile of naked DNA from hydrophobic PLGA scaffolds. The release started on day 1 after incubation and continued until day 64. The first phase of release was over by day 3, after which the second phase of release started. The second phase of release peaked on day 9 and continued to decrease until day 35, after which there was almost constant release.
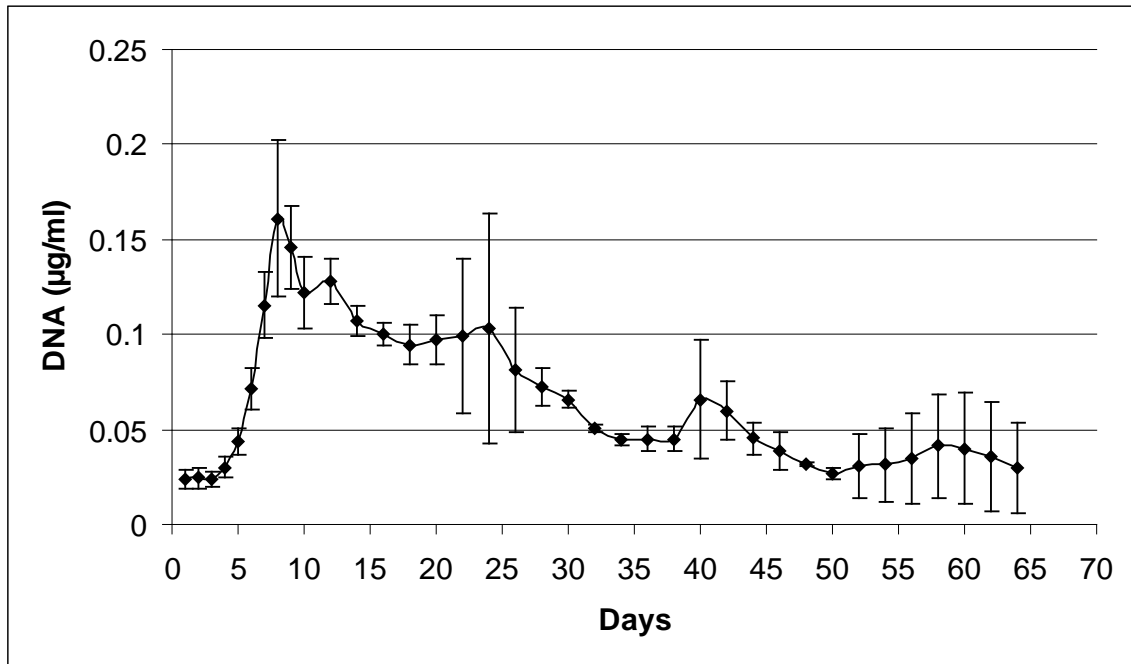
Figure 3.19 Release profile of naked DNA from low molecular weight hydrophobic PLGA scaffolds

Complexing of DNA with PEI resulted in a release profile shown in Figure 3.20. The first phase consisted of a sustained release of 0.35 µg/ml PEI:DNA complexes until day 10, after which the second phase of release started. The second phase of release peaked around day 15 and continued to decrease afterwards. PEI:DNA complexes were detected in the supernatant until day 65.
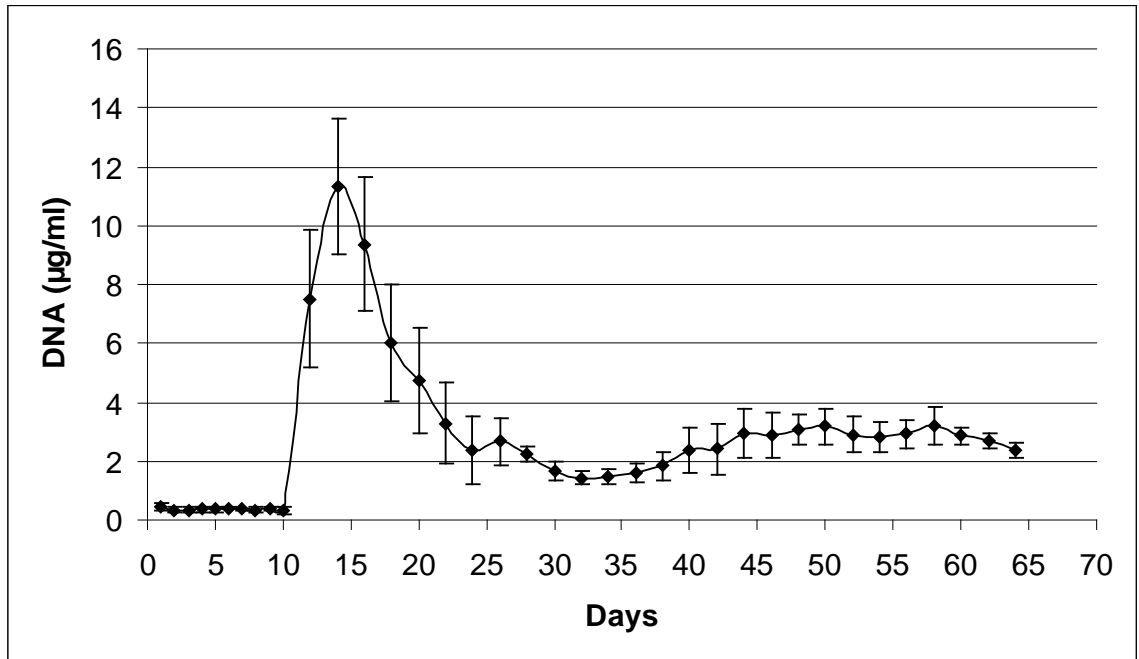
Figure 3.20 Release profile of PEI:DNA 5 complexes from low molecular weight
hydrophobic PLGA scaffolds

Figure 3.21 shows the fractional cumulative release of naked and PEI:DNA 5
complexes from low molecular weight hydrophobic PLGA scaffolds. Scaffolds with
encapsulated naked DNA had a faster release than scaffolds with encapsulated PEI:DNA
5 complexes. By day 30, naked DNA encapsulated scaffolds had released 68% of their
content, while PEI:DNA encapsulated scaffolds had released only 51% of their contents.
Both sets of scaffolds completed release by day 70. Naked DNA encapsulated scaffolds
had an average release rate of 1.2 %/day during the second phase of their release,
compared to 0.91%/day for PEI:DNA encapsulated scaffolds. Mixed model analysis of
this difference in release rates gave a p-value less than 0.05.
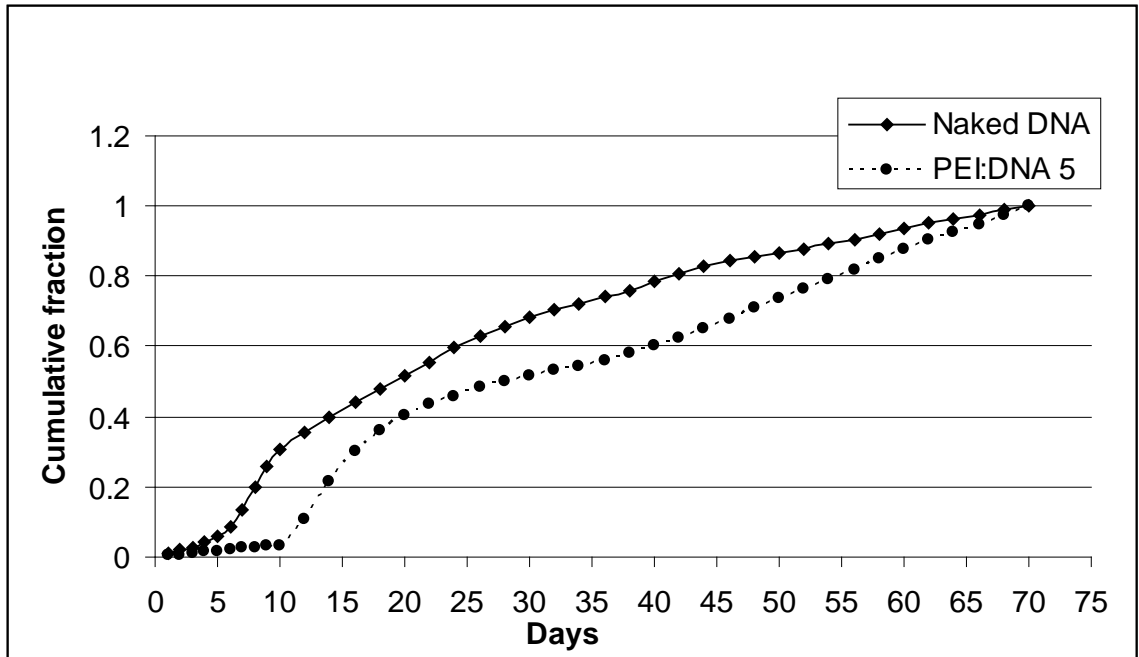
Figure 3.21 Fractional cumulative release of naked and PEI:DNA complexes from low molecular weight hydrophobic PLGA scaffolds

3.3.4.3 High molecular weight hydrophilic PLGA

Naked and PEI:DNA complexes were encapsulated in higher molecular weight hydrophilic PLGA scaffolds and their release characterized in order to study the effect of PLGA molecular weight on release profile. Figure 3.22 shows the release profile of naked DNA from high molecular weight (HMW) hydrophilic PLGA scaffolds. The first phase of release started on day 1 and was over by day 10. The second phase of release started on day 26 and peaked on day 36. The second phase of release ended by day 50. Complexation of DNA with PEI resulted in a later second phase of release as seen in Figure 3.23. The first phase of PEI:DNA release started on day 1 and continued until day 26. The second phase of release started on day 28, peaked around day 50, and continued until day 70. Variability between samples was high during peak release, as samples started disintegrating into smaller fragments.
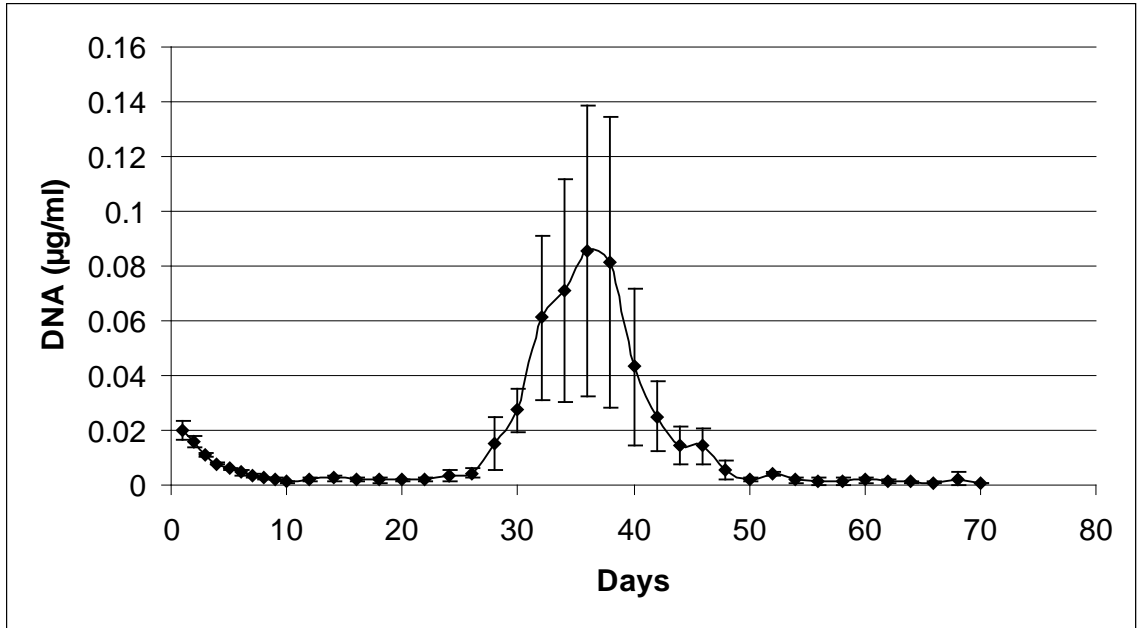
Figure 3.22 Release profile of naked DNA from high molecular weight hydrophilic PLGA scaffolds
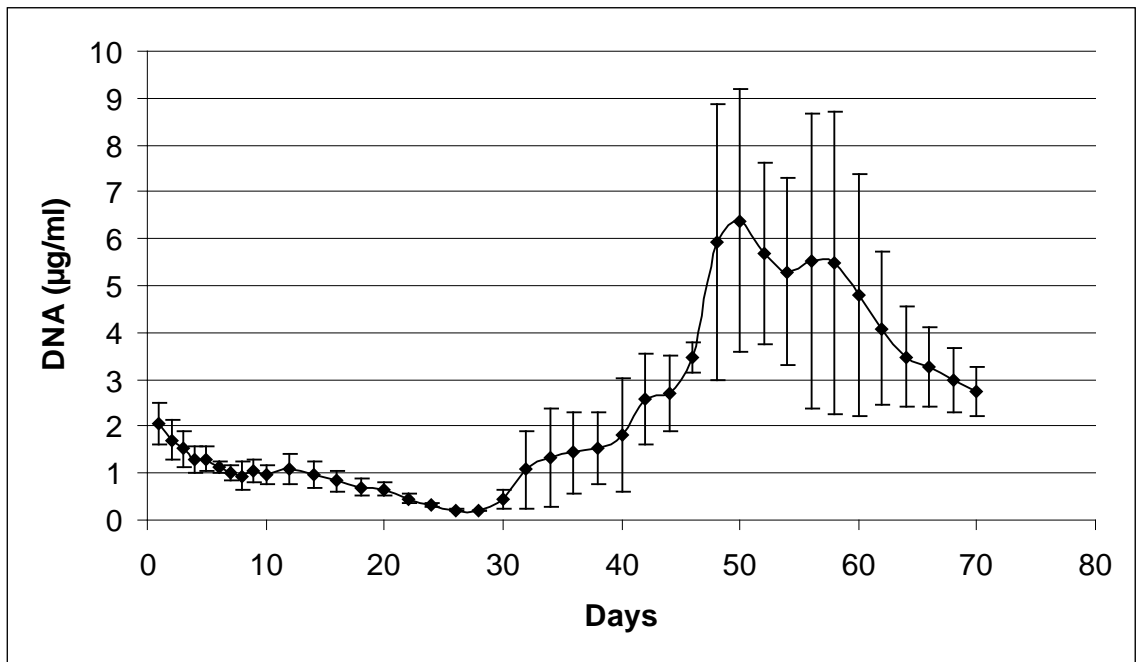
Figure 3.23 Release profile of PEI:DNA 5 complexes from high molecular weight hydrophilic PLGA scaffolds

Fractional cumulative release of naked and PEI complexed DNA from high molecular weight hydrophilic PLGA can be seen in Figure 3.24. Both kinds of scaffolds had similar release rates during the first phase of release. PEI:DNA encapsulated DNA had a slower release during the second phase, as evidenced by a lower slope in Figure 3.24. During the second phase of release DNA encapsulated scaffolds had an average

38

release rate of 7.1%/day compared to 3.05%/day for PEI:DNA encapsulated scaffolds. Mixed model analysis of this difference in release rates gave a p-value less than 0.05.
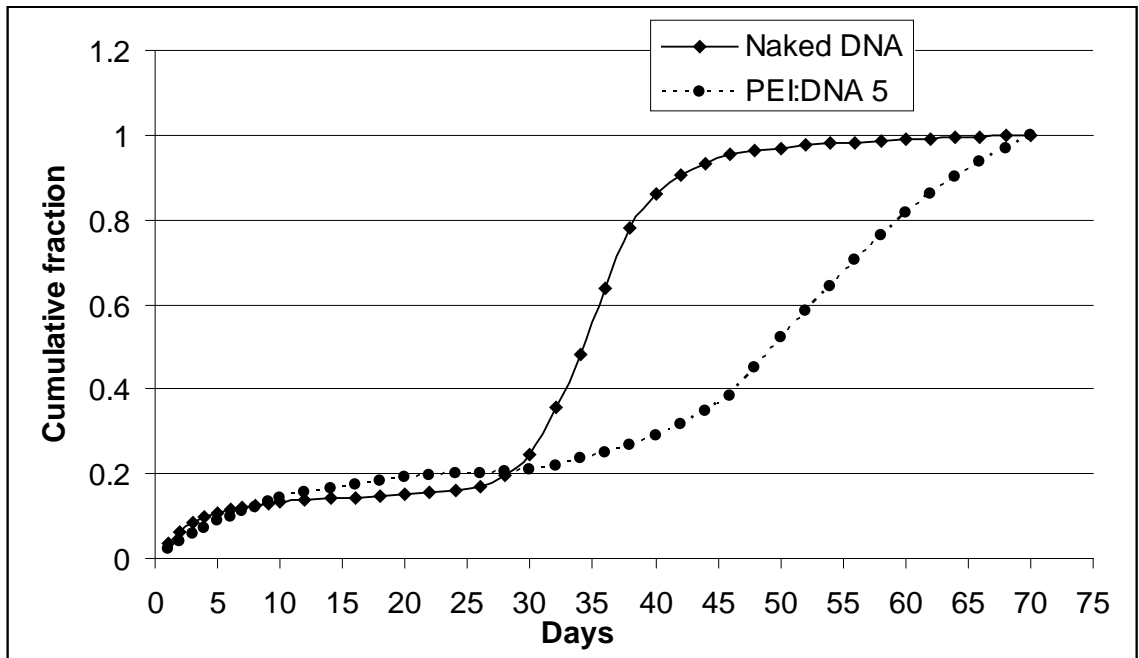
Figure 3.24 Fractional cumulative release of naked and PEI:DNA complexes from high molecular weight hydrophilic PLGA scaffolds

When comparing naked DNA and PEI:DNA encapsulated scaffolds, PEI:DNA encapsulated scaffolds consistently showed a delayed peak release irrespective of hydrophilicity or molecular weight of PLGA (Table 3.1). Molecular weight of the polymer used to make microspheres had an effect on the release profile of naked and PEI:DNA complexes. Table 1 shows that scaffolds made from higher molecular weight polymer had a later peak release of both naked and PEI:DNA complexes compared to lower molecular weight polymer. Hydrophilicity of the polymer also had an effect on release profile. Scaffolds made from hydrophilic polymer had a later peak release of both naked and PEI:DNA complexes compared to scaffolds made from hydrophobic polymer of similar molecular weight. Figures 3.25 and 3.26 illustrate how the release profiles of naked and PEI:DNA 5 complexes were altered depending on the hydrophilicity and molecular weight of PLGA.

Table 3.1 Day of peak release for different molecular weight and hydrophilicity of PLGA.

Day of peak release			
	LMW Hydrophilic	LMW Hydrophobic	HMW Hydrophilic
Naked DNA	Day 16	Day 8	Day 36
PEI:DNA 5	Day 30	Day 15	Day 50
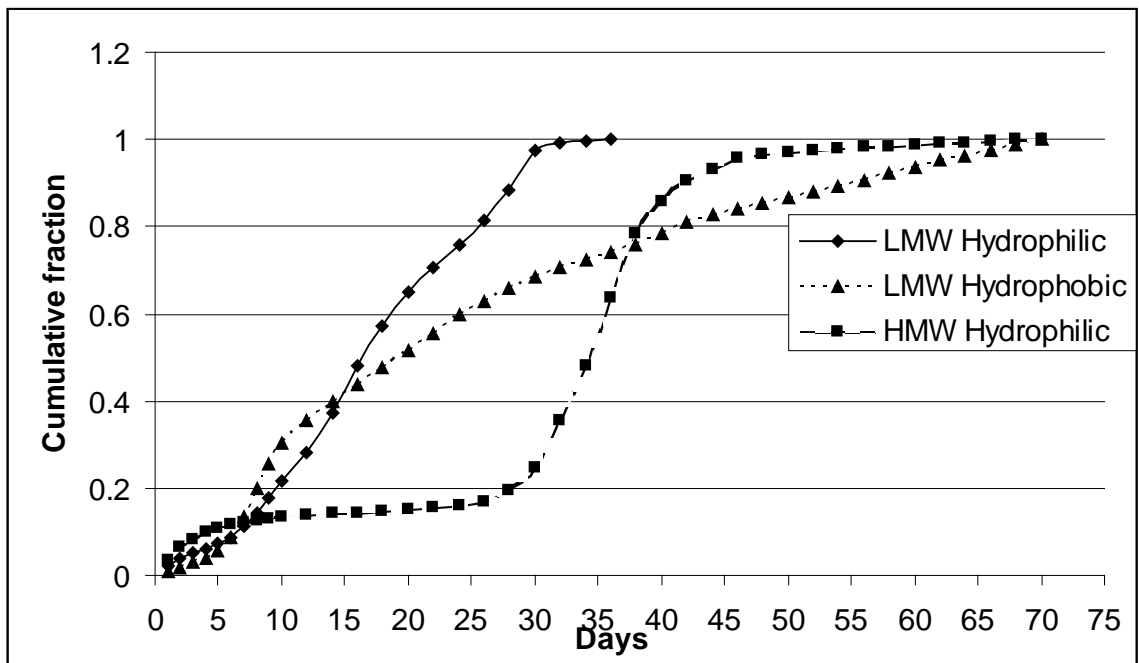
Figure 3.25 Fractional cumulative release of naked DNA from PLGA scaffolds
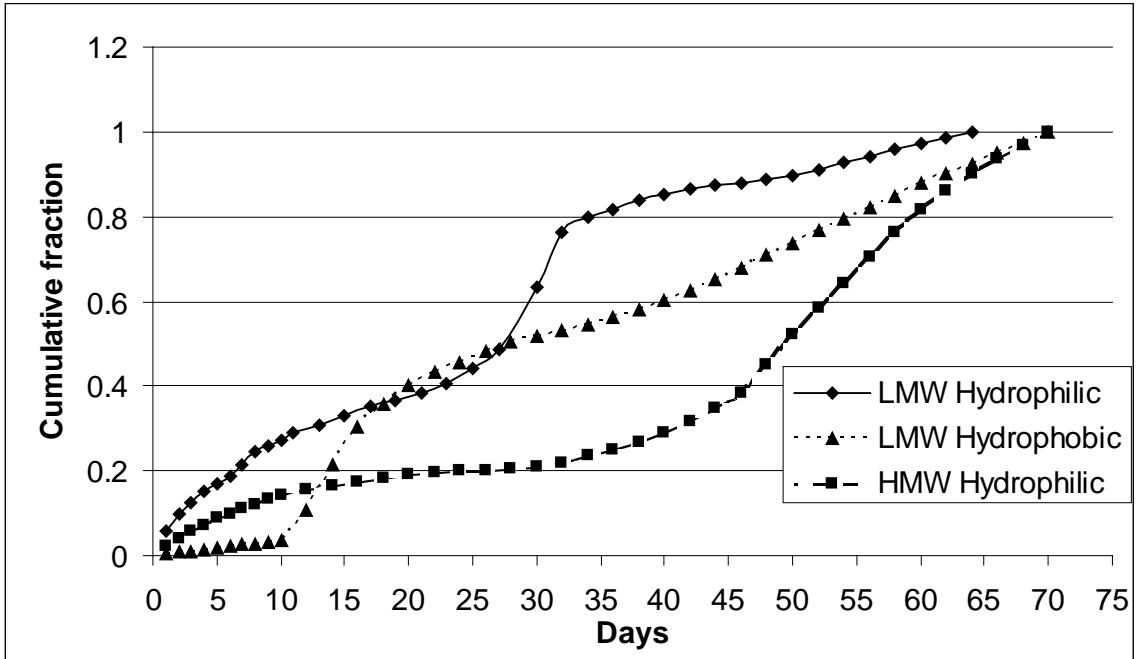
Figure 3.26 Fractional cumulative release of PEI:DNA 5 from PLGA scaffolds

3.4 DISCUSSION

3.4.1 Effect of PEI on mass loss

3.4.1.1 Low molecular weight PLGA scaffolds
We observed that PEI was effecting the rate of degradation of PEI:DNA encapsulated scaffolds. PEI:DNA encapsulated scaffolds degraded at a lower rate compared to naked DNA encapsulated scaffolds and blank scaffolds. At the end of 30 days of degradation experiment, PEI:DNA encapsulated scaffolds had lost only 80% of their mass, while naked DNA encapsulated scaffolds and blank scaffolds had degraded completely. It is possible that the branched PEI used in our study, with its structure and positive charge, was interacting with the negatively charged PLGA polymer molecules and slowing their degradation. The interaction between PEI and PLGA is in fact used for attaching PEI to PLGA microspheres using a technique called layer-by-layer deposition. PEI deposited on PLGA microspheres was used for coating TGF-β3 loaded nanoparticles for growth factor delivery (Park, 2008).

Comparison of the mass loss profile with naked and PEI:DNA 5 release from low molecular weight scaffolds shows that there is good correlation between the time points of peak degradation of scaffolds and peak DNA release. The second phase of naked DNA release was seen around days 5 to 15, while peak degradation occurred around days 5-20. The second phase of PEI:DNA 5 release from the scaffolds occurred between days 5-25, while peak degradation was observed around days 7 to 14. We observed a low concentration sustained release after the second phase release in most release experiments, probably from the release of any adsorbed DNA or PEI:DNA particles from the walls of the tubes in which the scaffolds were degrading.

3.4.1.2 High molecular weight PLGA scaffolds
PEI did not significantly effect the degradation rate of high molecular weight PLGA scaffolds, in contrast to the results from low molecular weight PLGA scaffolds. Although the mass loss rate for PEI:DNA encapsulated scaffolds was lower than that of blank and naked DNA encapsulated scaffolds, these differences were not statistically significant. It is possible that the electrostatic interaction between PEI and high molecular weight PLGA is not as strong as that with low molecular weight PLGA, as the longer chain lengths of high molecular weight PLGA means less negative charge per unit mass of polymer for interacting with positively charged PEI. It has been shown that higher molecular weight hydrophilic PLGA has a lower acid number, and less negative charge compared to lower molecular weight hydrophilic PLGA, leading to less interaction with positively charged BMP-2 molecules (Schrier, 1999).

There was good correlation between degradation and release profiles for both naked DNA and PEI:DNA encapsulated scaffolds. Naked DNA encapsulated scaffolds had the highest mass loss rate between 20 and 50 days. The peak naked DNA release was also observed between days 30 and 50. PEI:DNA encapsulated scaffolds had the highest mass loss rates between days 30 and 50, while PEI:DNA release from the scaffolds started increasing from day 30, reaching its peak around day 50.

3.4.2 pH of release supernatant

42

We set out to gain insight into the differences in degradation behavior of various PLGA scaffolds by measuring the pH of release supernatant. Our hypothesis was that a drop in pH would indicate increased degradation of scaffolds, and would allow us indirectly to observe the degradation profile of various kinds of PLGA scaffolds. However, this hypothesis was only partly proven to be true. In the case of hydrophobic scaffolds, there was significant differences in the pH profile between naked DNA and PEI:DNA 5 encapsulated scaffolds and blank scaffolds. Blank scaffolds showed a drop in pH almost 30 days later than naked DNA and PEI:DNA 5 encapsulated scaffolds. This was in contradiction to what we saw from the release experiments, which showed peak naked DNA release from hydrophobic scaffolds between 5 and 15 days, and peak PEI:DNA 5 release between 10 and 25 days. Mass loss studies using hydrophobic scaffolds in the future might help us explain the apparent difference in pH and release profiles.

For low molecular weight hydrophilic scaffolds, there was some agreement between the pH profile of supernatant, and release profile. Drop in pH occurred first for blank scaffolds and naked DNA scaffolds around day 5, while the first significant drop in pH for PEI:DNA 5 encapsulated scaffolds occurred around day 8. This correlated with the earlier second phase of release seen for naked DNA encapsulated scaffolds compared to PEI:DNA 5 encapsulated scaffolds. However, pH of release supernatant from naked DNA and blank scaffolds continued to drop until day 17, while pH from PEI:DNA 5 scaffold supernatant steadily recovered to baseline value after day 10. For scaffolds made from high molecular weight hydrophilic PLGA, pH of supernatant from blank scaffolds and naked DNA encapsulated scaffolds reached their lowest value on day 37, while the lowest point was reached on day 47 for PEI:DNA 5 encapsulated scaffolds. This correlated well with the second phase of release from these scaffolds, which peaked around day 35 and day 50, respectively.

Although pH of release supernatant provided an approximate indication of degradation of scaffolds, it proved to be an unreliable and imprecise indicator of degradation profile of PLGA scaffolds.

3.4.3 Mechanical properties of scaffolds

A biomaterial that is designed to replace or augment a tissue should ideally have mechanical properties that match that of the host tissue. This becomes an even greater challenge in the case of devices that are intended to replace complex tissues like cartilage, since the mechanical properties of cartilage depends on the zone within it. Compressive modulus of cartilage is provided in large part by the proteoglycans within the extracellular matrix of cartilage (Schinagl, 1997). Compressive modulus increases with increasing density of fixed charge (Grodzinsky, 1990), which in turn increases with depth into the cartilage (Maroudas, 1979). Compressive modulus of articular cartilage increased significantly with depth from 0.079 MPa in the superficial layer to 2.1 MPa in the deepest later (Schinagl, 1997). Similar depth dependent variation in mechanical properties was seen in growth plate cartilage also. Growth plates are designed for rapid interstitial growth, but should also withstand large mechanical forces (Radhakrishnan, 2004). Young's modulus for rabbit growth plate cartilage varied from 0.57 MPa in the reserve zone to 1.44 MPa in the mineralizing zone (Radhakrishnan, 2004).

43

Compressive modulus for our scaffolds varied from 25.51 MPa for low molecular weight PLGA, to 81.13 MPa for high molecular weight PLGA. Porous 50:50 PLGA scaffolds with a porosity of 85% had a compressive modulus of 1.7 MPa when loaded at 1 mm/minute (Leung, 2008). Higher porosity of these scaffolds compared to our samples might be the reason for the much lower compressive modulus. Although our compressive modulus values are an order of magnitude greater than the modulus for growth plate cartilage, we expect that these values will decrease significantly when the scaffolds become wet after insertion into the implant site.

3.4.4 DNA release from PLGA microspheres

PLGA microspheres have been used previously for delivery of plasmid DNA in vitro and in vivo. In addition to providing the ability to control the release of plasmid DNA, encapsulation protects the DNA from enzymatic degradation and enhances the retention its supercoiled structure (Gebrekidan, 2000). A single phase release profile similar to ours was seen with most of the release over in 2 weeks (Gebrekidan, 2000). PLGA microspheres with encapsulated DNA can be useful in applications such as DNA vaccines, but regenerating a complex tissue like growth plate would benefit from a biodegradable porous scaffold that can be inserted into a defect.

3.4.5 Release from PLGA scaffolds

PLGA scaffolds have been used for controlled release of both adsorbed and encapsulated plasmid DNA. Controlled release from a scaffold can provide sustained release of plasmid DNA, which is not possible with bolus injections. Porous matrices made of PLGA provided sustained release of encapsulated naked DNA for 10 to 30 days (Shea, 1999). Sustained release of naked plasmid DNA for 21 days was achieved from PLGA scaffolds manufactured using a thermally-induced phase-separation method (Chun, 2004).

Our scaffolds showed peak naked DNA release around days 7-10 with 0.25 to 0.27 µg/ml of supernatant. Release of naked DNA was over by day 16. Release profile of PEI:DNA 5 particles from our scaffolds differed in both time and concentration compared to the release profile of naked DNA. The initial phase of release lasted longer, ending by day 7, compared to day 4 for naked DNA particles. The concentration of PEI:DNA particles was also higher compared to naked DNA until day 5. The second peak of PEI:DNA release occurred on day 10, compared to days 7-10 for naked DNA. The release of PEI:DNA particles were complete by day 20. The slight delay in peak release as well as longer release duration might be from the interaction between PEI and PLGA. Electrostatic interaction between positively charged histones and negatively charged release substrates has been reported previously (Lee, 2006b). Less than 20% of PEI:DNA particles were released from PLGA scaffolds by 15 days, compared to 80% of naked DNA, suggesting interaction between PLGA and PEI (Huang, 2003). It was also proposed that excess PEI from the making of PEI:DNA particles might be interacting electrostatically with PLGA (Huang 2003). At N/P ratio of 6, approximately 86% of the PEI used to make PEI:DNA complexes remain in their free form (Clamme, 2003b). Surface adsorption of PEI:DNA particles on PLGA scaffolds resulted in an N/P ratio-dependent release of these particles (Jang, 2006). At the end of 4 days of release, 90% of adsorbed PEI:DNA 6 particles were released, while only 40% of PEI:DNA 18 particles

44

were released (Jang, 2006). Electrostatic and physical interaction between the positively charged PEI and PEI:DNA particles, and negatively charged PLGA molecules, can slow down the dissolution of PLGA scaffolds as well as release of PEI:DNA particles from PLGA scaffolds.

We consistently saw that the concentration of released PEI:DNA from scaffolds was higher than the concentration of naked DNA, even though both kinds of scaffolds were manufactured identically. Some of this effect can be explained by the technique employed to measure concentration of released DNA in the supernatant. Concentration of DNA from our release experiments was measured using the Picogreen® assay. Picogreen dye binds to double stranded DNA and fluoresces, allowing us to determine the concentration of DNA using a standard curve. The very property of PEI which enables us to condense DNA into toroidal particles, also limits our ability to detect DNA once it has been condensed. Picogreen® reagent binds less efficiently to PEI:DNA particles as the ratio of PEI to DNA increases, until it becomes impossible to detect DNA at high PEI:DNA ratios. This is the reason PEI:DNA ratio was kept at 5 in all our release experiments, so that we could use Picogreen® assay to detect DNA in the release supernatant. We calculated PEI:DNA 5 concentrations using PEI:DNA 5 calibration curves, but even a small amount of free DNA in the supernatant could have artificially increased the apparent concentration of PEI:DNA 5. Most researchers report PEI:DNA release as fractional cumulative release, which circumvents this problem. We are reporting both instantaneous and cumulative release of PEI:DNA 5 from our scaffolds, with a caveat that the instantaneous release profile should be used more as an indication of time profile rather than the absolute values of DNA concentration.

Addition of a freeze-dried layer of naked DNA on DNA encapsulated scaffolds can provide an initial burst release to "jump-start" the transfection of cells attaching to the scaffolds in vitro and in vivo. Our results show that this additional layer of DNA was bound only to the surface of the scaffolds. Surface adsorption of PEI:DNA 6 particles resulted in 90% of the particles being released within 4 days (Jang, 2006). We saw a similar quick release of freeze-dried DNA, that was over in 9 days, after which these scaffolds behaved similarly to DNA encapsulated scaffolds.

Fluorescent labeling of PEI enabled us to track its release simultaneously with DNA, and showed excellent correlation between these two releases. This also confirmed that the results from using Picogreen® to track PEI:DNA 5 release were not artifacts, and that Picogreen® was effective in detecting PEI:DNA 5 in supernatant.

3.4.5.1 Effect of hydrophobic PLGA on release

Naked and PEI complexed DNA was encapsulated within methyl-terminated (hydrophobic) low molecular weight PLGA to study the effect of hydrophobicity on release behavior. Scaffolds with encapsulated naked DNA had a faster release than scaffolds with encapsulated PEI:DNA 5 complexes, as seen with low molecular weight hydrophilic PLGA scaffolds. Eighty percentage of encapsulated naked DNA was released by day 42, while only 60% of encapsulated PEI:DNA 5 was released by the same time. When comparing the release of naked and PEI-complexed DNA from hydrophobic scaffolds with their hydrophilic scaffolds, we saw that peak releases from hydrophobic scaffolds occurred 1 to 2 weeks earlier than from the hydrophilic scaffolds. Peak release of naked DNA from hydrophilic scaffolds occurred around day 16 while it occurred

around day 8 from hydrophobic scaffolds. Similarly, peak PEI:DNA 5 release from hydrophilic scaffolds occurred around day 30, while it occurred around day 15 for hydrophobic scaffolds. This is counter-intuitive since we expected the hydrophobic scaffolds to degrade slower than the hydrophilic scaffolds. Similar results were seen when hydrophobic and hydrophilic PLGA microspheres were used for the released of encapsulated TGF-β. Microspheres made of hydrophobic PLGA released 100% of encapsulated TGF-β within the first four days, while microspheres made from hydrophilic PLGA did not show any significant release until after the first four days (Jaklenec, 2008). Hydrophilic PLGA, with its acid end groups, is thought to enhance protein-polymer interactions, and better internalize proteins within polymer microspheres (Jaklenec, 2008). Similar DNA-PLGA and PEI:DNA-PLGA interactions might be enhanced with acid-end groups in hydrophilic PLGA, leading to a delayed release profile compared to hydrophobic PLGA. We also observed a softening and collapse of the pore structure of hydrophobic PLGA scaffolds during an ethanol sterilization process. Hence, we discontinued the use of hydrophobic PLGA scaffolds in further studies.

3.4.5.2 Effect of molecular weight of PLGA on release

We encapsulated naked and PEI:DNA complexes in higher molecular weight hydrophilic PLGA scaffolds, and their release was characterized in order to study the effect of PLGA molecular weight on release profile. Complexation of DNA with PEI resulted in a later second phase of release compared to naked DNA, as seen in both low molecular weight hydrophilic scaffolds and low molecular weight hydrophobic scaffolds. Compared to scaffolds made from low molecular weight hydrophilic PLGA, peak release of both naked and PE:DNA complexes occurred at a later time for scaffolds made from high molecular weight PLGA. This was expected as polymer chains of higher molecular weight PLGA will take longer to be hydrolyzed into oligomers that are soluble in water. Porous scaffolds made from PLGA with an inherent viscosity of 0.6-0.8 dl/g (low molecular weight) released about 90% of their encapsulated naked DNA by 21 days, compared to 50% for scaffolds made from PLGA with an inherent viscosity of 0.16-0.24 dl/g (high molecular weight) (Jang, 2003). Microspheres made from PLGA with a molecular weight of 10,000 released 95% of their encapsulated poly(L-Lysine)-DNA complexes by 40 days, compared to 50% of encapsulated PLL-DNA complexes from microspheres made of PLGA with a molecular weight of 31,000 (Capan, 1999). We observed similar effects with 20% of naked and PEI:DNA complexes being released from high molecular weight PLGA scaffolds within 30 days, compared to 100% of encapsulated naked and PEI:DNA 5 complexes from low molecular weight PLGA scaffolds.

3.5 CONCLUSIONS

Controlled release of naked and PEI:DNA complexes was achieved from porous PLGA scaffolds. PEI effected the release of complexes from PLGA scaffolds, as PEI:DNA complexes were released at a lower rate compared to naked DNA from low molecular weight and high molecular weight PLGA scaffolds, as well as hydrophilic and hydrophobic PLGA scaffolds. Hydrophilicity and molecular weight of PLGA had effects on the release profiles of both naked DNA and PEI DNA complexes from the scaffolds, as evidenced by later peak naked DNA and PEI:DNA release with increasing hydrophilicity and molecular weight. Compressive modulus and ultimate strength for high molecular weight PLGA scaffolds were significantly higher than low molecular weight PLGA scaffolds. Although pH of release supernatant provided an approximate indication of degradation of scaffolds, it proved to be an unreliable and imprecise indicator of degradation profile of PLGA scaffolds. Porous scaffolds made of PLGA with the right hydrophobicity and molecular weight will allow us to tailor degradation profiles and mechanical properties of these scaffolds for controlled delivery of naked and condensed plasmid DNA in tissue engineering applications.

4. IN VITRO CHONDROGENESIS USING IGF-I AND POROUS PLGA SCAFFOLDS

4.1 INTRODUCTION

Cartilage is a major connective tissue in the body, serving as structural support, growth plates, and articulating surfaces at the ends of long bones. Because of its limited regeneration potential, there is tremendous interest in developing modalities to regenerate cartilage lost due to aging, disease and trauma. Using pulripotent cells in combination with a biodegradable scaffold is one approach that is being pursued towards regenerating cartilage, particularly articular cartilage. The biodegradable scaffolds are designed to give structural and mechanical support to the newly synthesized tissue as it develops, while the chondrogenic cells are intended to populate the scaffold and generate the cartilaginous tissue. A growth factor such as TGF-β or IGF-I, is often added to the recipe, being synthesized by the cells themselves or released by the matrix, to stimulate the cells to become chondrogenic (Choi, 2007; Capito, 2007).

Several cell types have been investigated for growing cartilaginous tissue on biodegradable scaffolds. Poly(glycolic acid) based scaffolds as well as agarose based hydrogels have been used to induce chondrogenesis from mesenchymal stem cells (Kafienah, 2007; Chen, 2003). Mesenchymal stem cells are multipotential cells that can differentiate into cells of mesenchymal lineage, such as chondrocytes, osteocytes and adipocytes, under appropriate culture conditions (Pittenger, 1999). Mesenchymal cells infected with AdIGF-I and suspended in fibrin glue have been used for successful repair of articular cartilage (Gelse, 2003). Bone marrow stromal cells (BMCs) have been shown to be particularly useful in tissue engineering because of their excellent proliferation and matrix production (Eijk, 2004). BMCs have been cultured in combination with TGF-β1 on PLGA scaffolds, which resulted in significant cell proliferation and chondrocytic differentiation (Jenner, 2007). They have also been seeded on silk scaffolds and grown in a rotating bioreactor with dexamethasone, TGF-β and insulin ,resulting in significantly higher DNA and GAG content compared to controls that did not receive the growth factors (Marolt, 2006). Previous studies have shown that ex vivo transfer of IGF-I DNA into chondrocytes can enhance chondrogenesis in vitro and in vivo (Madry, 2002; Madry, 2005). Significant chondrogenesis was reported with IGF-I plasmid-transfected chondrocytes cultured on collagen-GAG scaffolds (Xu, 2008).

Using a porous scaffold that can release the plasmid that codes for a chondrogenic growth factor eliminates the need to collect and expand progenitor cells, with its associated cost and morbidity, and meets the challenge of sustained local delivery of therapeutic doses of growth factors. This chapter of my dissertation presents our in vitro studies on chondrogenesis using mesenchymal multipotent D1 cells, bone marrow cells and articular chondrocytes on PLGA and PLGA-fibrin scaffolds, with the addition of exogenous rhIGF-I. Finally it presents our development of IGF-I plasmid releasing scaffolds, to be used for chondrogenesis by culturing bone marrow cells without the need for exogenous IGF-I addition. Chapter 5 presents our use of such IGF-I plasmid releasing scaffolds to regenerate growth plate cartilage in an animal model of growth plate injury.

4.2 MATERIALS AND METHODS

4.2.1 Plasmids

Recombinant hIGF-I plasmid SC119792 was obtained from OriGene. Figure 4.1 shows the physical map of the plasmid. DH-5α cells were transformed using plasmids as explained in section 3.2.1.
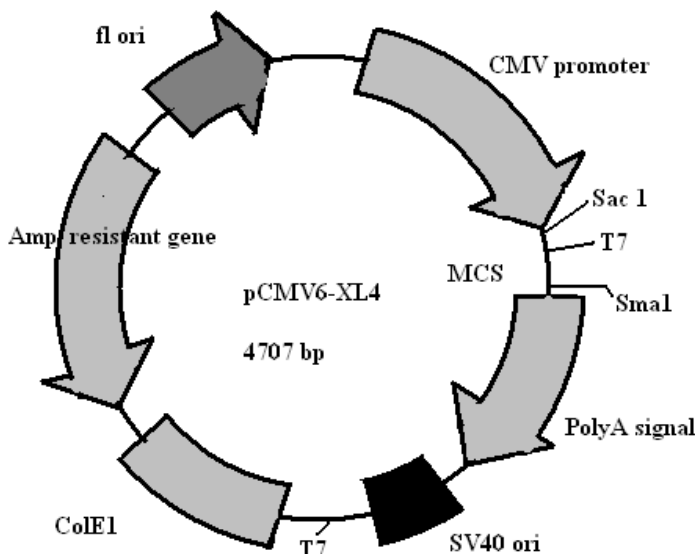
Figure 4.1 Physical map of rhIGF-I plasmid
(http://www.origene.com/assets/Documents/catalog_manual/AppGuideTrueclone10ug.pdf)

4.2.2 Propagation and extraction of plasmid DNA

Propagation and extraction of plasmid DNA was done as explained in section 3.2.1.1.

4.2.3 Preparation of PEI:DNA complexes

PEI:DNA complexes were prepared as explained in section 3.2.2.

4.2.4 Preparation of PLGA microspheres

PLGA microspheres were prepared as explained in section 3.2.3.

4.2.5 Porous PLGA discs

To create PLGA discs for in vitro experiments, 42mg of PLGA microspheres were mixed by hand with 63 mg of 100-350 µm salt particles for 2 minutes, and compressed at 1.5 tons for 2 minutes in a 6mm die using a Carver press. The discs were then sintered in an oven for 48 hours at the T_g for PLGA. For low-molecular weight PLGA, the sintering temperature was 42°C, while for high-molecular weight PLGA, the sintering temperature was 49°C. The sintered discs were then leached by stirring in 2

liters of deionized water/6 discs overnight and dried in vacuum to create porous PLGA scaffolds.

To create discs with freeze-dried PEI:DNA on top, 25μl of PEI:DNA solution containing 1% sucrose and 10μg DNA was created/disc (Boussif, 1995). This solution was then added to the surface of previously sterilized scaffolds, and lyophilized overnight to create scaffolds with freeze-dried PEI:DNA on the surface.

To create discs with adsorbed PEI:DNA on top, 25μl of PEI:DNA solution containing 1% sucrose and 10μg DNA was created/disc (Boussif, 1995). The scaffolds were incubated at 37°C in 10% FBS for 24 hours, and washed with PBS (Jang, 2006). PEI:DNA solution was then added to the surface of these scaffolds, and incubated for one hour at room temperature before seeding cells.

4.2.6 Cell culture on tissue culture plate
D1 cells (CRL-12424) were obtained from American Type Culture Collection. Cells were grown to confluence in T-75 flasks in DMEM/High Glucose medium with 10% fetal bovine serum (FBS) (HyClone laboratories). Cells were trypsinised and seeded in 6 well tissue culture plates at a density of 26,000 cells/ml and 1 ml/well. In order to create micromass cultures, 50μl of cell suspension at a density of 30 million cells/ml was added to the center of each well. Five ml of medium was added/well after incubating the plates in 5% CO_2 incubator for 2 hours to allow cells to adhere on the plate. Recombinant human IGF-I (R&D systems) was added to the medium at 100ng/ml for the treatment group, and the media was changed every 2 days. At the end of experiment, wells were washed twice with PBS, and the cells were sonicated in 1 ml PBS for 30 seconds using ultrasonic processor GE-50. The cell lysates were used for DNA and GAG analysis.

4.2.7 Preparation of agarose gels
D1 cells were grown to confluence in T-75 flasks in DMEM/High Glucose medium with 10% FBS. One percent w/v agarose was autoclaved and mixed with equal volume of DMEM to make 0.5% agarose/DMEM solution. Cells were trypsinised and were added to 0.5% agarose/DMEM solution to make a final cell density of 15 million cells/ml. Two milliliters of agarose/DMEM/cell solution were quickly plated/well in 6 well tissue culture plates and 5 ml DMEM was added/well. Recombinant human IGF-I was added to the medium at 100 ng/ml for the treatment group, and the media was changed every 3 days. At the end of experiment, agarose cultures were washed twice with PBS, and the gels were sonicated for 2 minutes using ultrasonic processor GE-50. The lysates were used for DNA and GAG analysis.

4.2.8 Seeding of D1 cells on porous PLGA scaffolds
D1 Cells were grown to confluence in T-75 flasks in DMEM/High Glucose medium with 10% FBS. One ml/well of 2% agarose was plated to the bottom of 6 well tissue culture plates to prevent cells from adhering to the plate surface. Porous PLGA scaffolds were sterilized using 70% ethanol and washed twice with PBS. Scaffolds were dried in a laminar flow hood overnight before seeding cells. Cells were trypsinised and centrifuged at 1710g in 15 ml tubes to create a cell pellet. The cell pellet was resuspended in 500μl of medium, and cell density was determined using a hemocytometer. Cell concentration was brought to 25 million cells/ml by adding additional medium. Twenty

five microliters of the cell suspension was added carefully to each scaffold, before keeping them in 5% CO_2 incubator for 2 hours to allow the cells to adhere on scaffold surface. To create PLGA-fibrin scaffolds, cells were resuspended in serum free medium containing 10 mg/ml sterile fibrinogen, after centrifugation. Fifteen microliters/scaffold of fibrinogen-cell suspension was added to each scaffold and placed in 5% CO_2 incubator for 30 minutes. At the end of this incubation, 15µl of 50 U/ml sterile thrombin containing 40mM $CaCl_2$ was added to the top of each scaffold to create fibrin clots. Scaffolds were then put back in the CO_2 incubator for another 30 minutes. Five milliliters of DMEM was then added/well. Recombinant human IGF-I was added to the medium at 200 ng/ml for the treatment group, and the media was changed every 2 days to remove acidic degradation products. Cells growing on scaffolds were labeled, if needed, using CellTracker Green CMFDA (Invitrogen/Molecular Probes) according to the manufacturer's protocol. Cells were then visualized using a Leica TCS-SP5 confocal microscope (Leica Microsystems). At the end of the study scaffolds were washed twice with PBS and transferred to 15 ml centrifuge tubes in 1ml PBS. Scaffolds were then sonicated for 30 seconds using an ultrasonic processor GE-50.

4.2.9 Seeding of rat bone marrow cells on porous PLGA scaffolds

Bone marrow cells were obtained from 4-6 weeks old naive Sprague-Dawley rats. Briefly, femurs were aseptically dissected from freshly euthanized animals. Intramedullary canals of femurs were then flushed with MEM Alpha modification medium with 10% FBS to collect bone marrow cells. Cells were transferred to T-75 flasks and grown to confluence using MEM Alpha modification medium with 10% FBS. The remainder of the procedure was the same as that for D1 cells described in section 4.2.8.

4.2.10 Seeding of pig chondrocytes on porous PLGA scaffolds

Chondrocytes were obtained by digesting cartilage from the knees of adult pig. Briefly, cartilage from femoral-patellar grooves of adult pig was dissected using aseptic techniques. The cartilage was then cut into 3mm^3 pieces and digested for 12 hours in sterile 0.3% type-I collagenase (Sigma). The cell suspension was then filtered using a 100 µm cell strainer (BD Falcon) to remove undigested material, and centrifuged at 1710g for 3 minutes. The cell pellet was resuspended in 500µl of serum free medium and cell density was determined using a hemocytometer. Cell concentration was brought to the required value by adding additional serum free medium. The remainder of the procedure was the same as that for D1 cells described in section 4.2.8.

4.2.11 Analysis of cell growth and cartilage matrix synthesis

Cell growth was determined by measuring the amount of DNA in the cell lysate using a fluorometric Picogreen® (Molecular Probes/Invitrogen) assay according to the manufacturer's protocol. Calf thymus DNA was used as a standard to calculate the concentration of DNA from the fluorescence values. The amount of glycosaminoglycan (GAG) was used as an indicator of cartilage matrix synthesized on tissue culture plates, agarose gel and PLGA scaffolds. The amount of GAG in cell/scaffold lysate was determined using Blyscan® (Biocolor, UK) reagent according to the manufacturer's

51

protocol. Chondroitin sulfate was used to create standards and calculate GAG concentration from absorbance values.

4.2.12 In vitro IGF-I secretion

Rat bone marrow cells were cultured for 4 weeks on PLGA scaffolds made from PEI:IGF-I plasmid encapsulated microspheres, and PLGA scaffolds that had freeze-dried PEI:IGF-I plasmid on the surface. Culture medium from this experiment was collected every 5 days and used for IGF-I ELISA. The amount of recombinant human IGF-I secreted by transfected cells was determined using RayBio® IGF-I ELISA kit (RayBiotech) according to the manufacturer's protocol. Specificity of the primary antibody in the kit towards human IGF-I was confirmed by testing against conditioned medium from rat cell cultures and FBS samples.

2.2.13 Statistical analysis

Statistical analysis was performed using SAS 9.1 NC software. A p-value of 0.05 was used for all statistical analysis. The student's t-test or ANOVA was used for comparing results between different groups. Tukey-Kramer multiple comparison test was used post-hoc. Sample size estimation with 80% power was done using nQuery Advisor software. All figures show mean value +/- standard deviation for measured variable. All samples were in triplicate.

4.3.1 D1 cells cultured on tissue culture plate

D1 cells were cultured on tissue culture plates (TCP), with the addition of recombinant human IGF-I in order to induce a chondrogenic phenotype in these cells. The results can be seen in Figures 4.2, 4.3 and 4.4. Figure 4.2 shows the amount of DNA at 4 days and 8 days in the IGF-I treated group and the control group, which did not have any IGF-I added to it. P-values for t-tests comparing the amount of DNA between control groups and IGF-I treated groups at either the 4 days time point or 8 days time point as greater than 0.05. After 5-6 days, we noticed that the cells were detaching from the surface of the plate after having reached confluence, especially in the IGF-I treated group (results not shown).
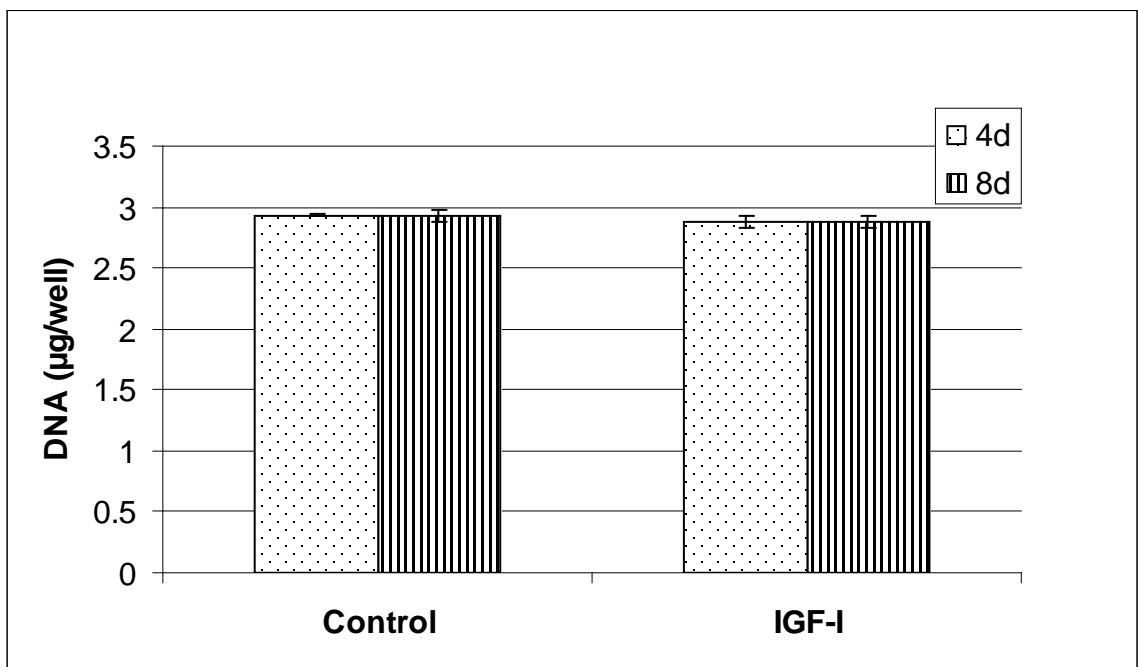
Figure 4.2 Amount of DNA at 4 and 8 days after seeding D1 cells on TCP

The amount of GAG synthesized by the cells can be seen in Figure 4.3. IGF-I treated cells created 4% more GAG content compared to untreated cells at 4 days. P-value for the t-test was greater than 0.05. At 8 days however, IGF-I treated group had 97% lower GAG content compared to the untreated group. This difference was statistically significant, with a p-value less than 0.05.
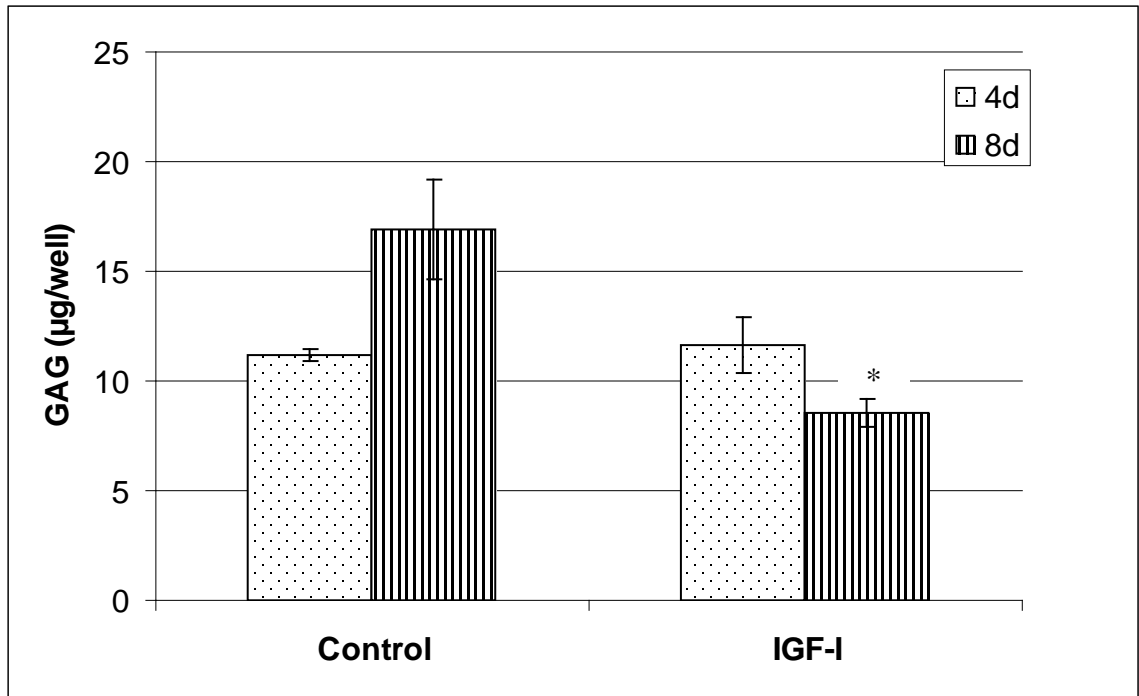
Figure 4.3 Amount of GAG synthesized by D1 cells growing on TCP for 4 and 8 days. *
denotes p-value < 0.05 for GAG content between control and IGF-I groups at 8 days

The amount of GAG synthesized by the control and IGF-I treated groups were
normalized to the amount of DNA in each group and plotted in Figure 4.4. The
normalized GAG content in the IGF-I treated group was 6% more compared to the
control group. This difference was not statistically significant, with a p-value > 0.05. At 8
days, normalized GAG content for the IGF-I treated group was 95% lower than the
untreated group. This difference was statistically significant, with a p-value less than
0.05.
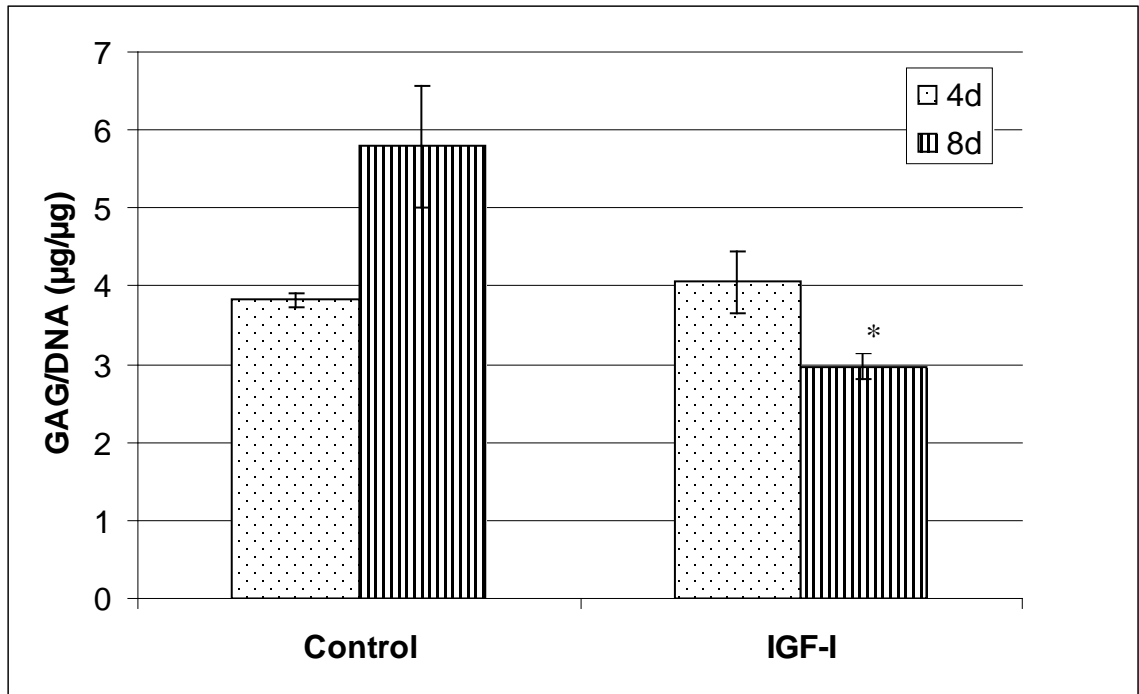
Figure 4.4 Normalized GAG content for D1 cells growing on TCP for 4 and 8 days. * denotes p-value < 0.05 for normalized GAG content between control and IGF-I treated groups at 8 days

4.3.2 Micromass culture of D1 cells

D1 cells were grown as micromass cultures to study the effect of high density cultures on their growth and differentiation. The results are shown in Figures 4.5, 4.6, and 4.7. Figure 4.5 shows the DNA content of D1 cells after growing for 7 and 14 days as micromass cultures. The DNA content for IGF-I treated and untreated groups were nearly identical at 7 days. At 14 days, the DNA content of IGF-I treated group was 0.9% lower compared to the untreated group. This difference however, was not significant with a p-value greater than 0.05. There was significant increase in the amount of DNA from 7 to 14 days for both the control and IGF-I treated groups (p-value < 0.05). We observed the detachment of IGF-I treated cells from the surface of the plate around 10-12 days.
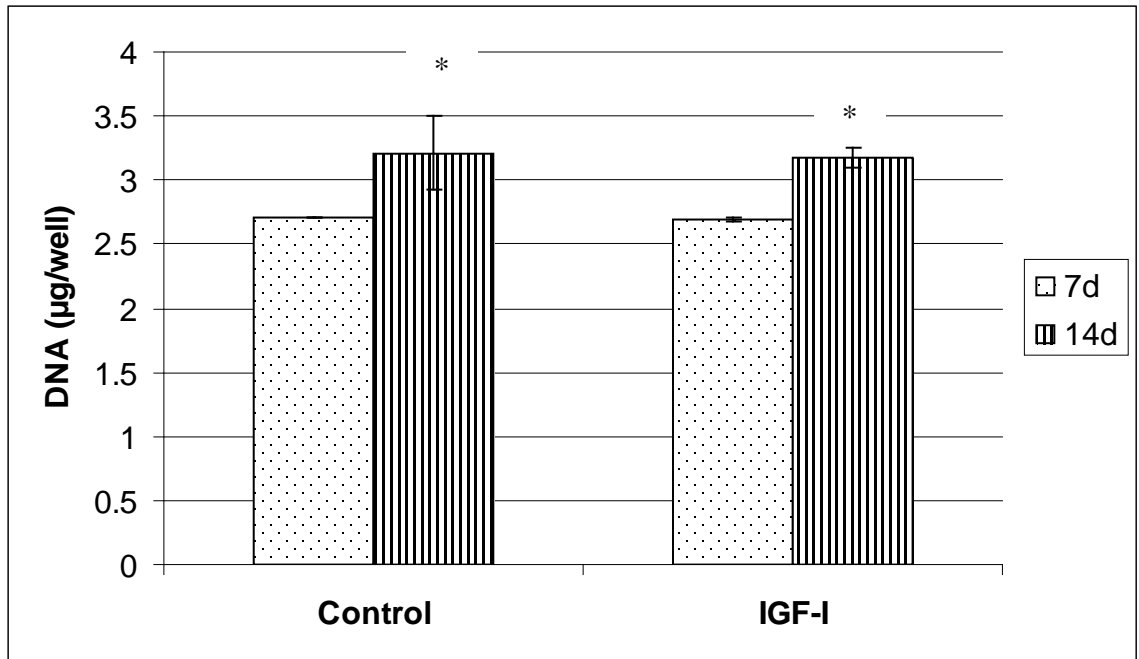
Figure 4.5 DNA content of D1 cell micromass culture at 7 and 14 days. * denotes p-value
< 0.05 for DNA between 7 days and 14 days for both control and IGF-I groups

Figure 4.6 shows the GAG content of IGF-I treated group and control group at 7
and 14 days. P-value for t-test comparing GAG content of IGF-I treated group and
control group after 7 days of culture was 0.055. GAG/DNA content for IGF-I treated
group was significantly higher than the control group at 7 days as shown in Figure 4.7 (p-
value < 0.05). At 14 days, the GAG content of IGF-I treated group was 30% lower
compared to the control group, although this difference was not statistically significant
(p-value > 0.05). After normalizing for the amount of DNA, GAG content for the IGF-I
treated group was 28% lower than the control group after 14 days, as shown in Figure
4.7. This difference was not statistically significant (p-value > 0.05).

56
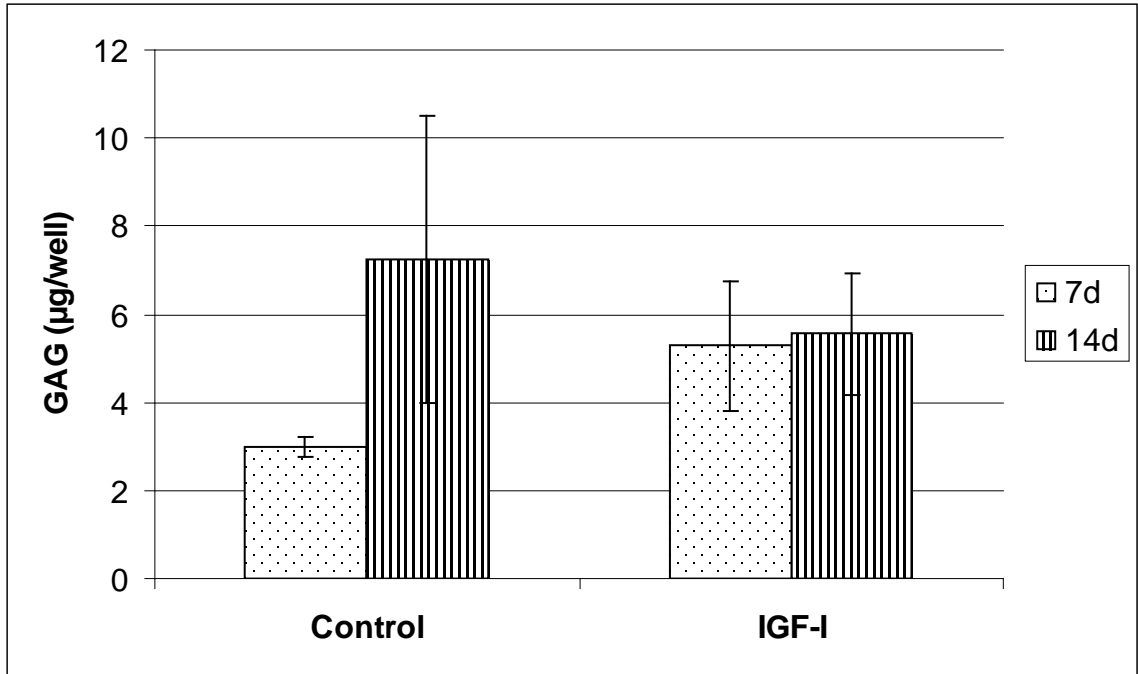
Figure 4.6 GAG content from micromass culture of D1 cells at 7 and 14 days
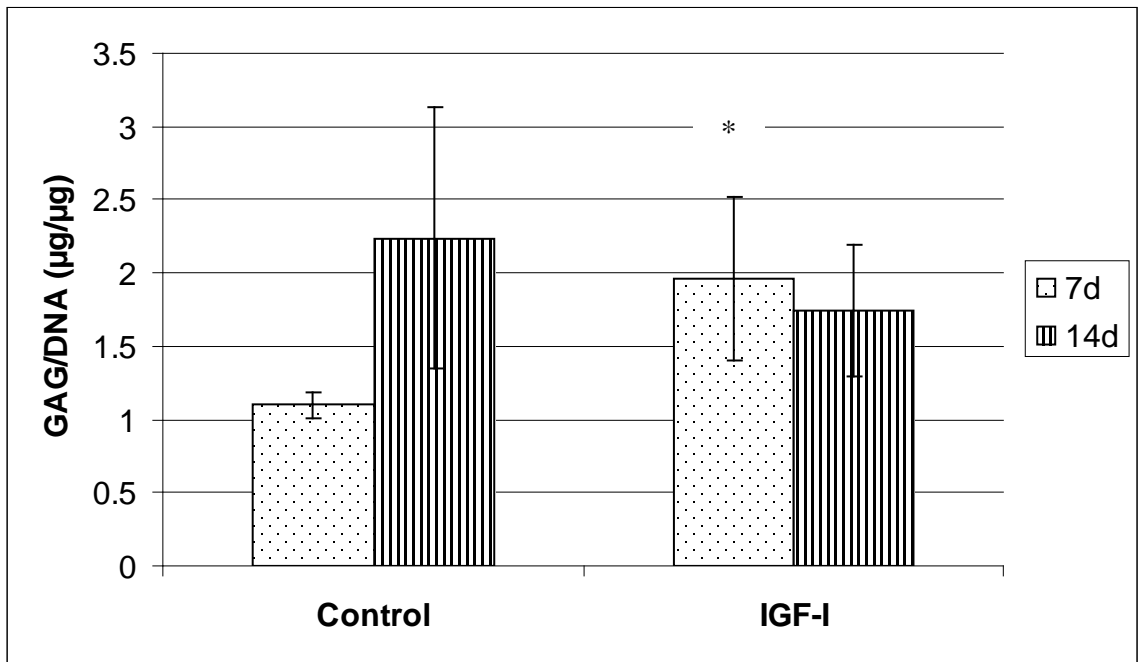
Figure 4.7 Normalized GAG content from micromass culture of D1 cells at 7 and 14
days.* denotes p-value < 0.05 for GAG/DNA between control and IGF-I group at 7 days

4.3.3 D1 cells cultured in 0.5% agarose gel

D1 cells were encapsulated and grown in 0.5% agarose to study the effect of
encapsulation on growth and differentiation. The results are shown in Figures 4.8, 4.9,
and 4.10. Figure 4.8 shows the DNA content of the control and IGF-I treated group at 1,

2 and 4 weeks of culture. DNA content for the IGF-I treated group was 5.7% and 0.5% higher than the control group at 1 and 2 weeks, respectively. But DNA content of IGF-I treated group was 14% lower than the control group at 4 weeks. These differences were not statistically significant (p-value > 0.05).
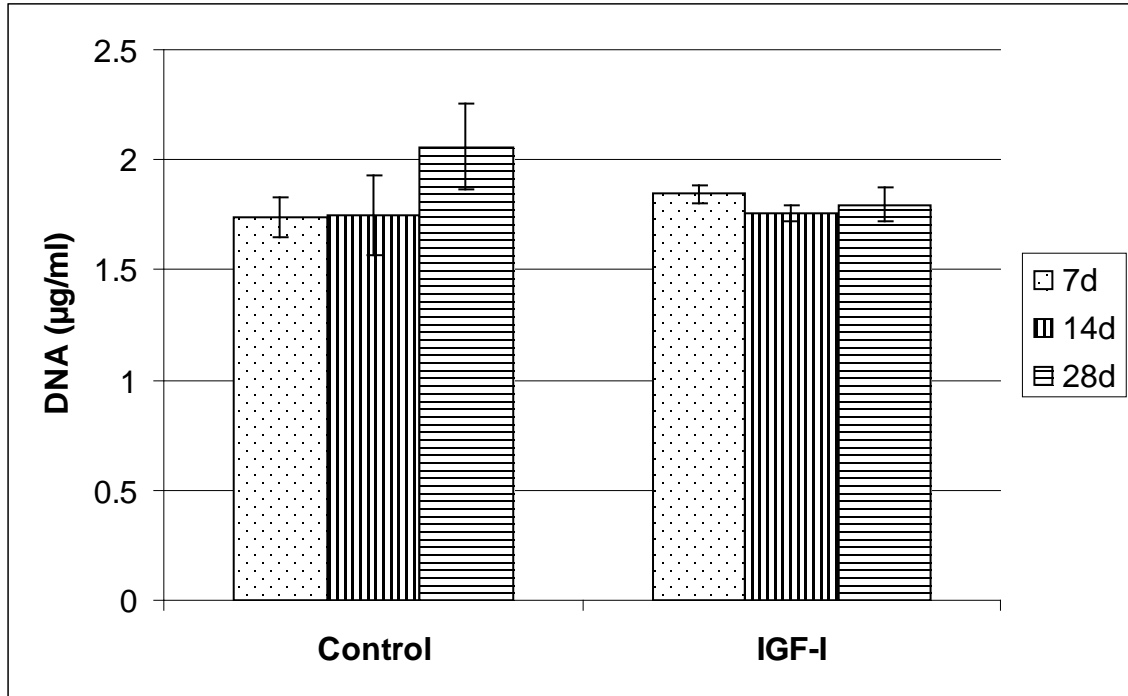
Figure 4.8 DNA content of 0.5% agarose encapsulated D1 cells at 1, 2, and 4 weeks of culture

Figure 4.9 shows the GAG content of 0.5% agarose encapsulated D1 cells after 1, 2 and 4 weeks of culture. IGF-I treated group had 29%, 40%, and 65% higher GAG content compared to the controls at 1, 2, and 4 weeks. The GAG content for the IGF-I treated group was significantly higher compared to the control groups at all three time points (p-value < 0.05). Figure 4.10 shows the normalized GAG content of the same cells. IGF-I treated group had 23%, 38%, and 68% higher GAG content compared to the controls at 1, 2, and 4 weeks. Normalized GAG content for the IGF-I treated group was significantly higher compared to the untreated group at all three time points (p-value < 0.05).

58

www.manaraa.com
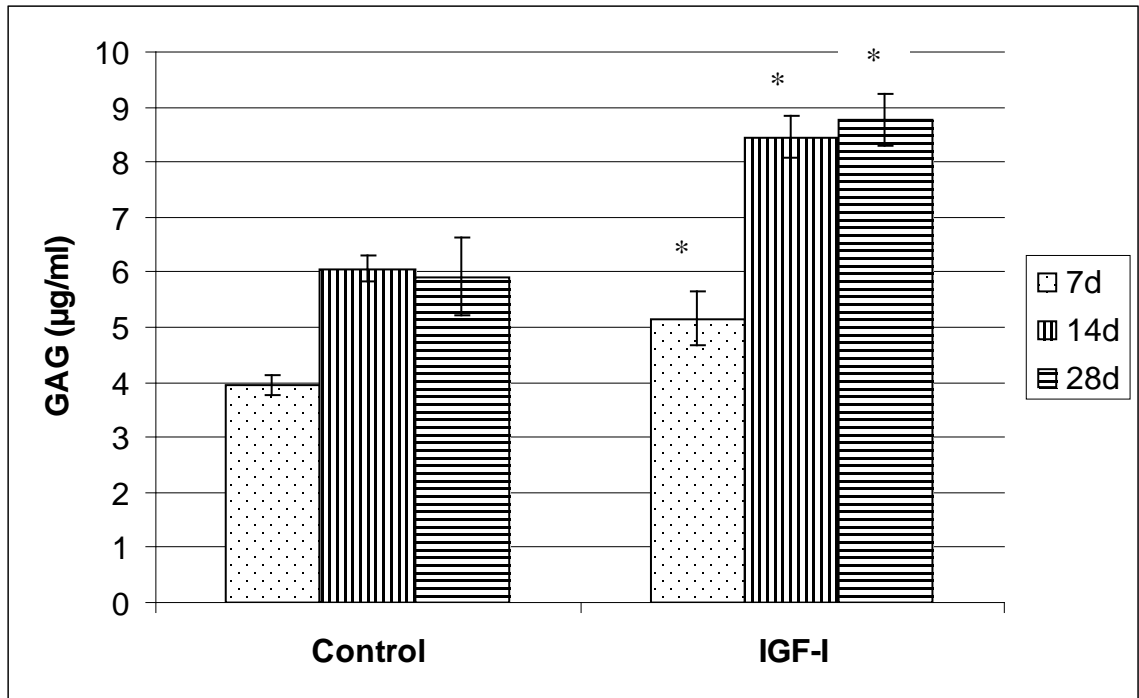
Figure 4.9 GAG content of 0.5% agarose encapsulated D1 cells at 1, 2, and 4 weeks. * denotes p-value < 0.05 for GAG between control and IGF-I group at each time point
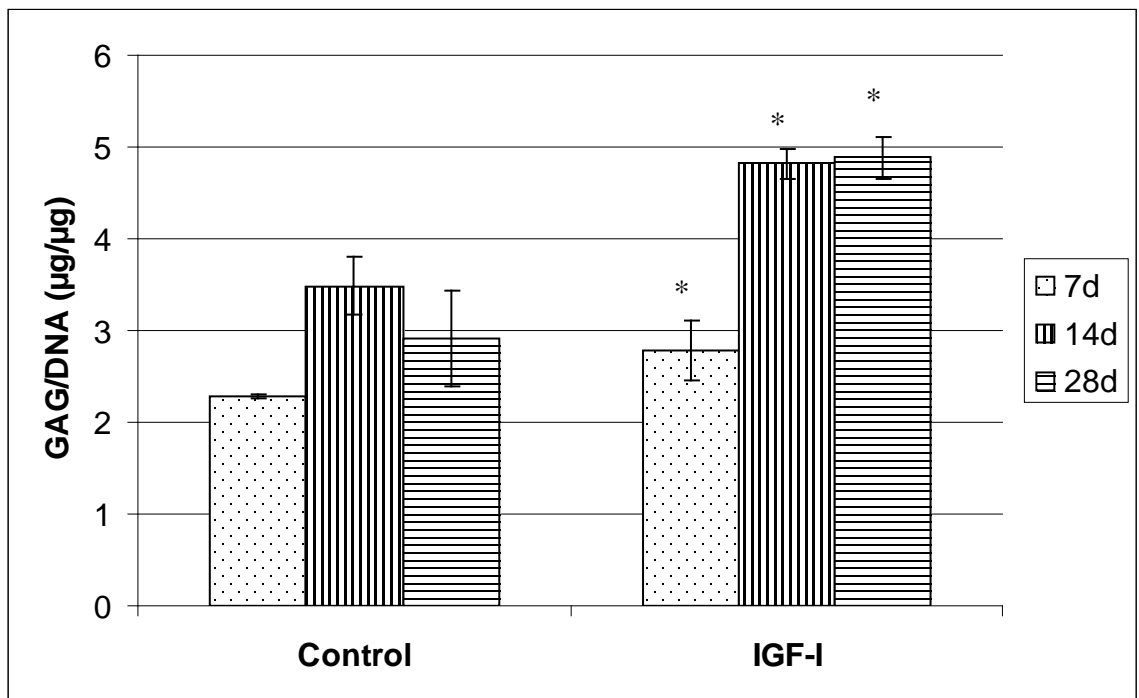
Figure 4.10 Normalized GAG content of 0.5% agarose encapsulated D1 cells at 1, 2, and 4 weeks. * denotes p-value < 0.05 for GAG/DNA between control and IGF-I group at each time point

4.3.4 D1 cells on PLGA scaffolds

59

Figure 4.11 shows CellTracker labeled D1 cells growing at day 3 on blank hydrophilic PLGA scaffolds that had 20µg dsRed plasmid:PEI complexes adsorbed on their surface. Transfected cells are seen as red, while non-transfected cells appear green. Figure 4.12 shows CellTracker labeled D1 cells growing at day 8 on blank hydrophilic scaffolds that had 20µg dsRed plasmid:PEI complexes freeze-dried on the surface. Transfected cell in the center appeared red from the expressed dsRed protein.
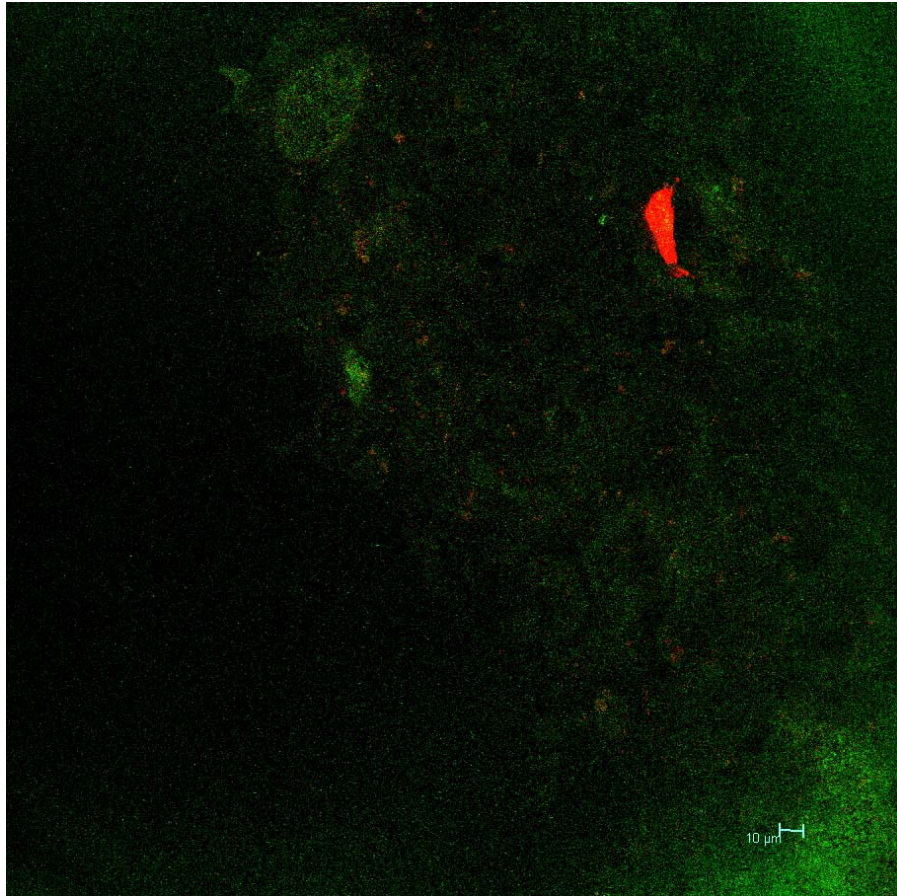
Figure 4.11 CellTracker labeled D1 cells growing on hydrophilic PLGA scaffolds that had 20µg dsRed plasmid:PEI complexes adsorbed on their surface. Transfected cells fluoresce red and non-transfected cells fluoresce green

60
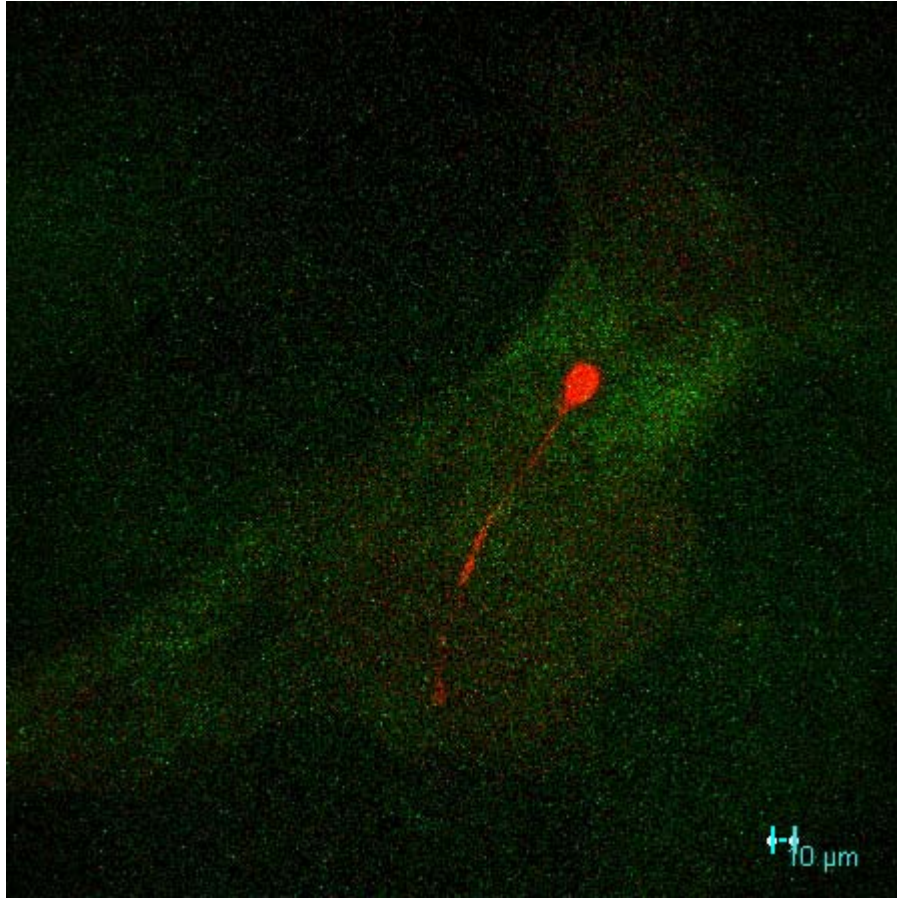
Figure 4.12 CellTracker labeled D1 cells growing on blank hydrophilic scaffolds that had 20µg dsRed plasmid:PEI complexes freeze-dried on the surface. Transfected cells appear red and non-transfected cells appear green

Figure 4.13 shows CellTracker labeled D1 cells growing on PEI:DNA encapsulated hydrophilic PLGA scaffold after 6 days of culture. Microspheres used to create these scaffolds contained encapsulated dsRed:PEI complexes. Transfected cells are seen as red.

61
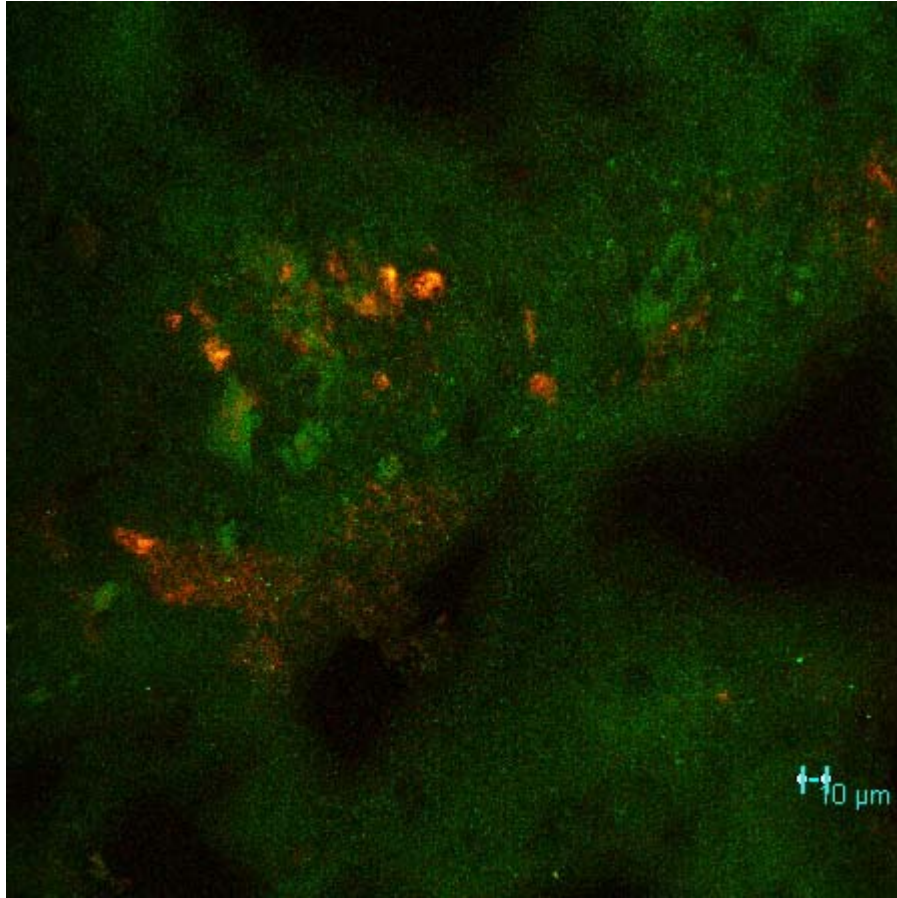
Figure 4.13 Celltracker labeled D1 cells growing on PEI:DNA encapsulated hydrophilic PLGA scaffold for 6 days. Scaffolds contained dsRed:PEI complexes. Transfected cells appear red and non-transfected cells appear green

D1 cells were seeded and grown directly on blank low molecular weight hydrophilic PLGA scaffolds for 28 days to study the effect of soluble IGF-I on growth and differentiation of mesenchymal stem cells on porous scaffolds. Figure 4.14 shows the amount of DNA on these scaffolds at multiple time points. A time-dependent significant increase in DNA content from 7 to 14 to 28 days for both the control and IGF-I treated groups can be seen (p-value < 0.05). DNA content in the control group increased by 120% from 7 to 14 days, and 50% from 14 to 28 days. For the IGF-I treated group these increases were 138% and 48%, respectively. There was, however, no significant difference in the DNA content between control and IGF-I treated scaffolds at any time point (p-value > 0.05).
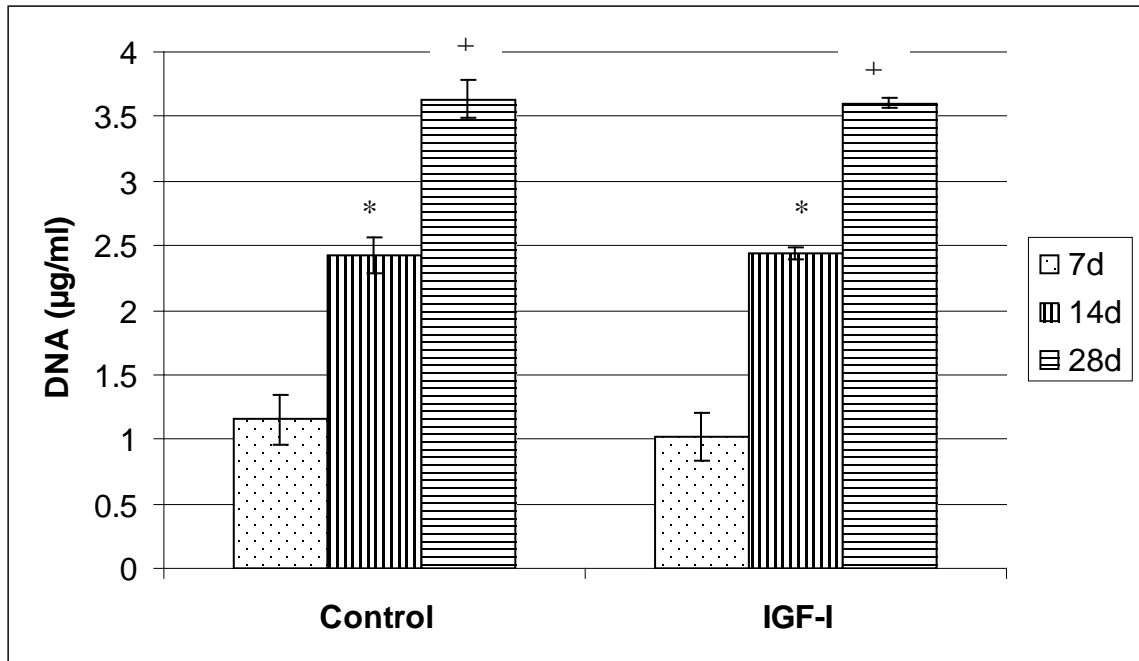
Figure 4.14 DNA content of D1 cells growing on PLGA scaffolds at 7, 14, and 28 days. * denotes p-value < 0.05 for DNA between 14 days and 7 days for both control and IGF-I groups. + denotes p-value < 0.05 for DNA between 28 days and 14 days for both control and IGF-I groups

Figure 4.15 shows the amount of GAG synthesized by D1 cells on PLGA scaffolds for up to 28 days. There was time-dependent increase in GAG content for both the control and IGF-I treated groups from 7 to 14 and 14 to 28 days, but these increases were not statistically significant (p-value > 0.05). Additionally, GAG content for IGF-I treated group was higher than the control group at every time point, but this difference was significant only for the 7 days time point (p-value < 0.05). GAG content in IGF-I treated group was 19% higher compared to the control group at 7 days.

المنارة للاستشارات

www.manaraa.com
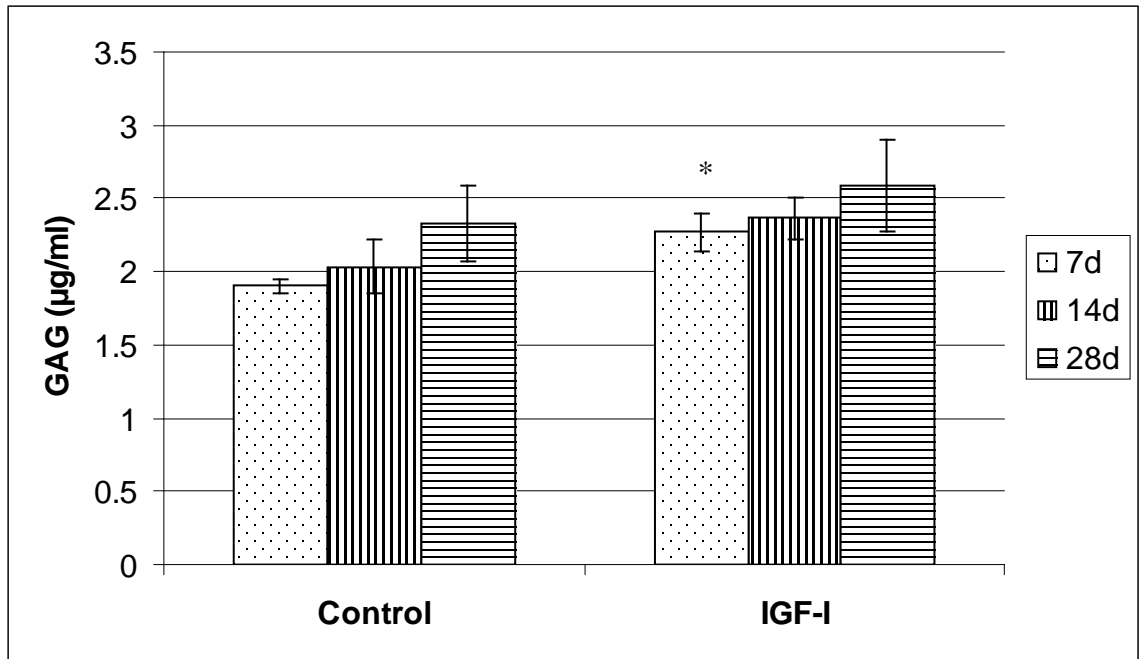
Figure 4.15 GAG content on PLGA scaffolds at 7, 14, and 28 days after seeding with D1 cells. * denotes p-value < 0.05 for GAG between control and IGF-I group at 7 days

We saw a time-dependent decrease in normalized GAG content for both the control and IGF-I treated group from 7 to 14 to 28 days, as shown in Figure 4.16. This decrease was statistically significant for both groups. At each time point, the normalized GAG content for the IGF-I treated group was higher compared to the control group. Normalized GAG content was 34%, 17%, and 13% higher for the IGF-I treated group compared to the control group, at 7, 14, and 28 days respectively. The difference at 14 days was statistically significant (p-value < 0.05).
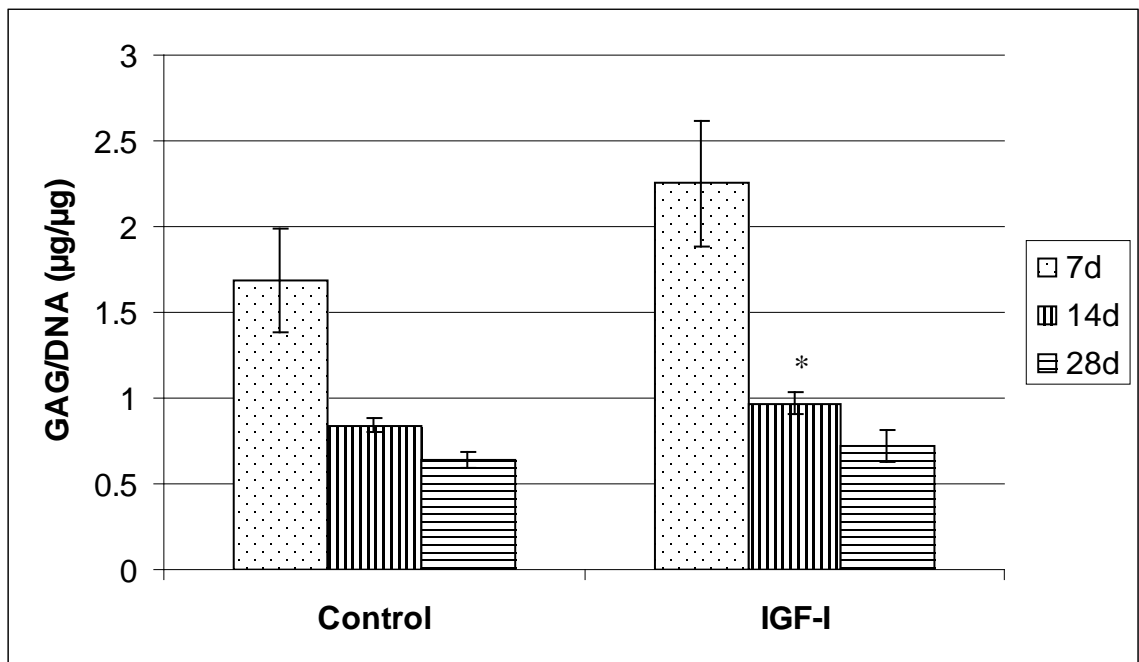
Figure 4.16 Normalized GAG content for D1 cells on PLGA scaffolds at 7, 14 and 28 days. * denotes p-value < 0.05 between control and IGF-I group at 14 days

4.3.5 BMCs on PLGA scaffolds

Rat bone marrow cells were cultured on blank hydrophilic low molecular weight scaffolds for 4 weeks with the addition of IGF-I to study its effect on growth and differentiation of these cells. Figure 4.17 shows CellTracker labeled rat BMCs growing on blank hydrophilic scaffold after 28 days of culture, while Figure 4.18 shows the cross section of a blank hydrophilic scaffold with cellTracker labeled rat BMCs growing across the entire cross section of the scaffold after 14 days of culture.
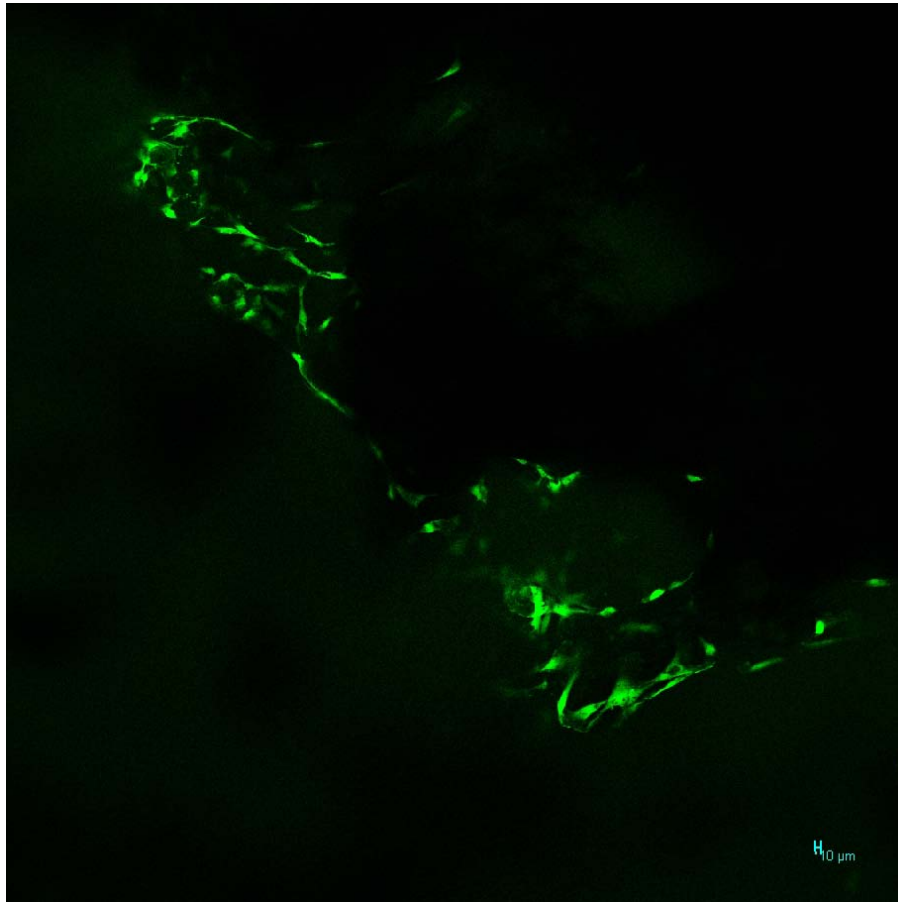
Figure 4.17 CellTracker labeled rat BMCs growing on blank hydrophilic scaffold after 28 days of culture
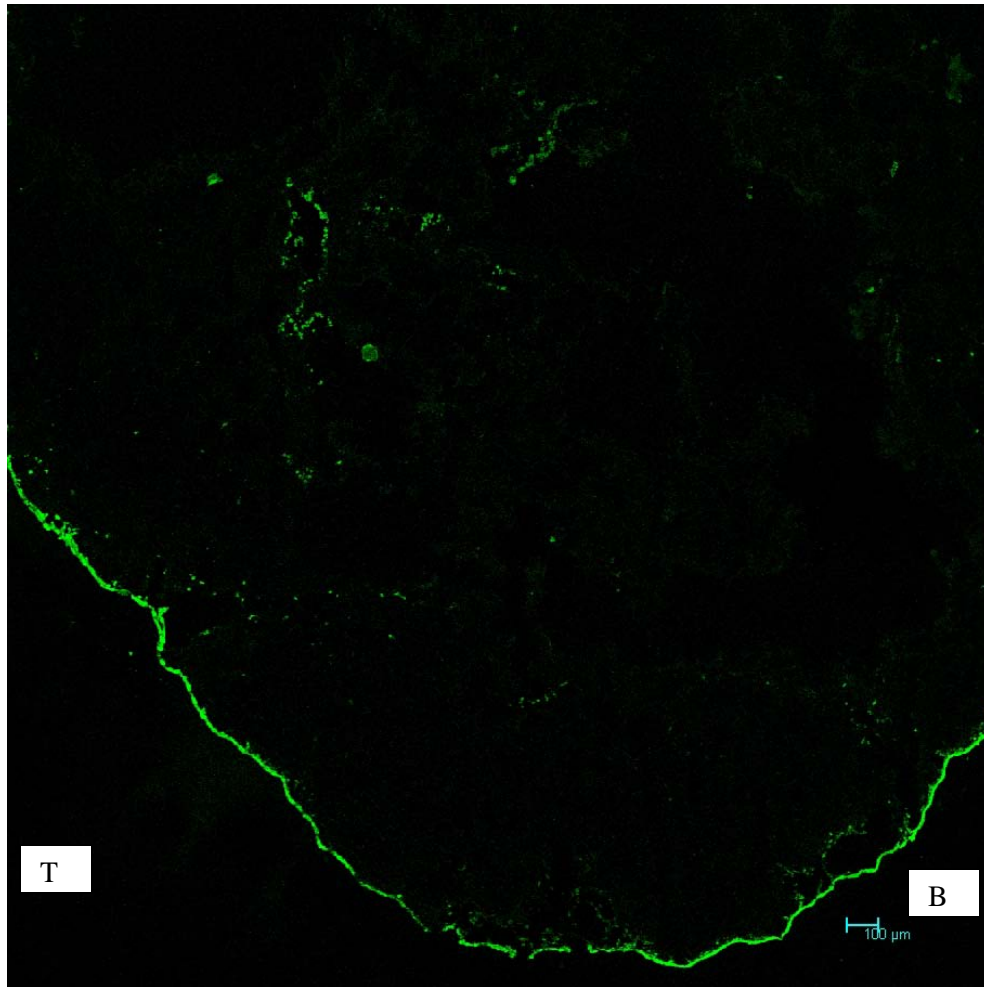
Figure 4.18 CellTracker labeled rat BMCs growing on blank hydrophilic scaffold after 14 days of culture. T and B denote top and bottom of a discoid scaffold

Figure 4.19 shows that the DNA content of IGF-I treated scaffolds was statistically significantly higher at 187% compared to the control group that did not receive IGF-I (p-value < 0.05). Similar results were seen when GAG content of these scaffolds were analyzed. The GAG content of IGF-I treated scaffolds were statistically significantly higher at 19% compared to the untreated scaffolds after 4 weeks of culture, as shown in Figure 4.20 (p-value < 0.05). Normalized GAG content for IGF-I treated scaffolds was, however, statistically significantly lower at 135% compared to the control scaffolds after 4 weeks of culture (p-value < 0.05). This is shown in Figure 4.21.

66
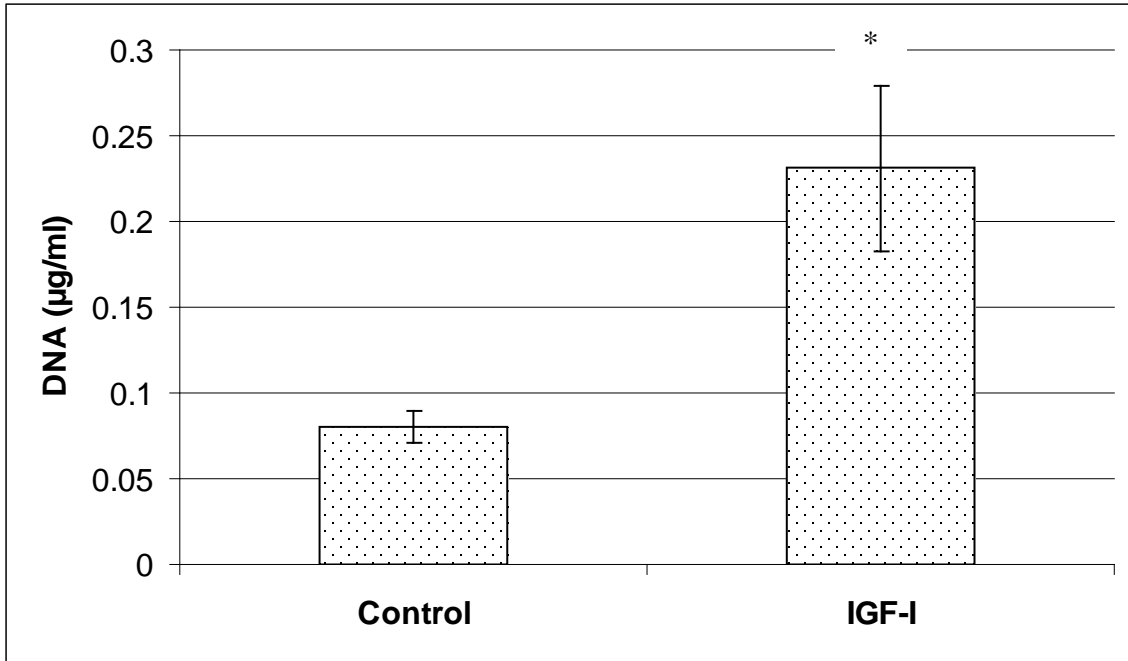
Figure 4.19 DNA content of BMCs growing on PLGA scaffold for 4 weeks. * denotes p < 0.05
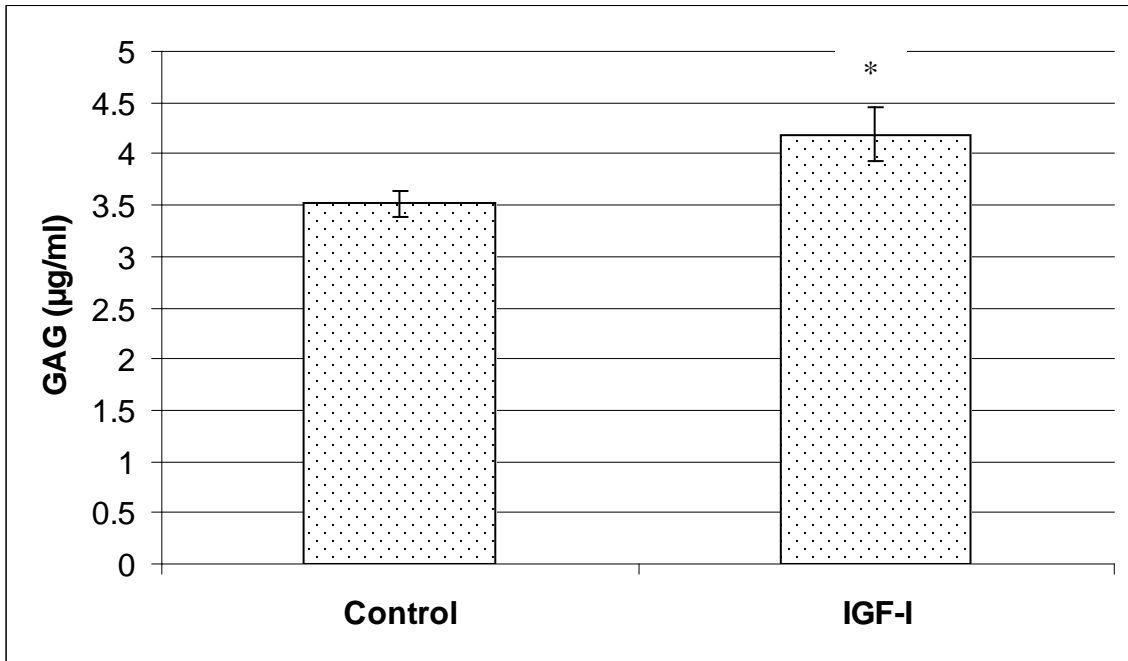
Figure 4.20 GAG content of BMCs growing on PLGA scaffolds for 4 weeks. * denotes p-value < 0.05
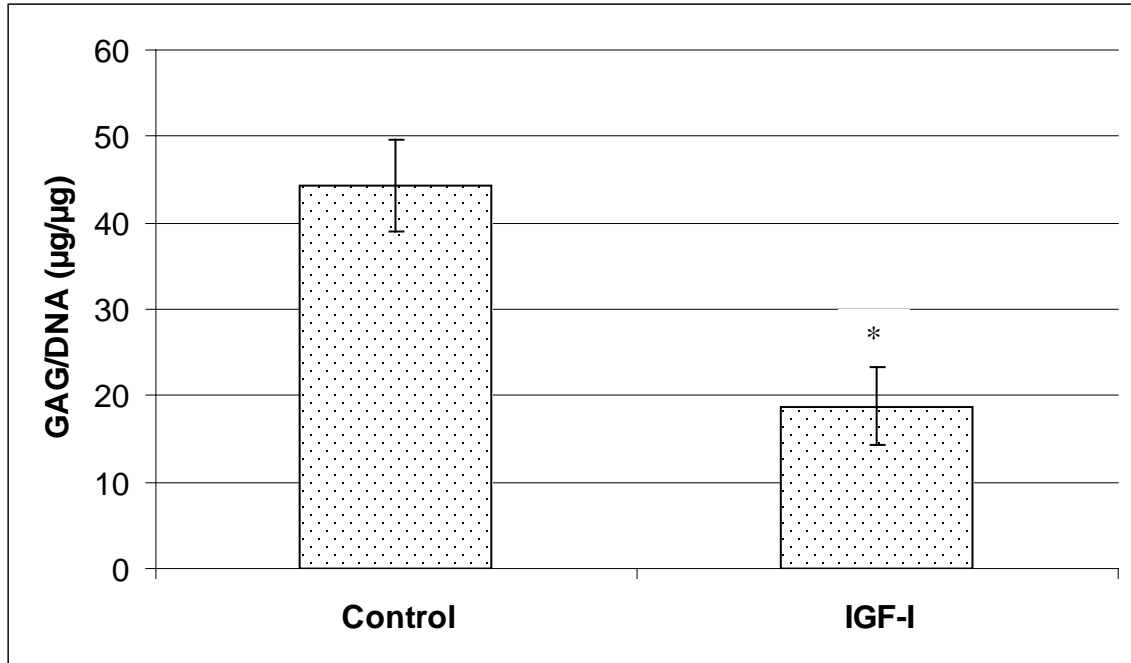
Figure 4.21 Normalized GAG content of BMCs growing on PLGA scaffolds for 4 weeks.
*denotes p-value < 0.05

4.3.6 D1 cells on PLGA scaffold with fibrin

D1 cells were seeded on blank hydrophilic low molecular weight PLGA scaffolds and then encapsulated in fibrin glue to investigate if the fibrin glue would enhance the chondrogenic potential of D1 cells. Figure 4.22 shows the DNA content of IGF-I treated and control scaffolds at 14 and 28 days of culture. IGF-I treated scaffolds had 6.4% higher DNA content compared to control scaffolds at 2 weeks, and 1.7% lower DNA content compared to control scaffolds at 4 weeks. These differences were not statistically significant (p-value > 0.05). Figure 4.23 shows the GAG content from the same experiment. IGF-I treated scaffolds had 52% higher GAG content compared to controls after 2 weeks of culture, while the difference was 10.2% at 4 weeks. The difference at 2 weeks, but not 4 weeks, was statistically significant (p-value < 0.05).
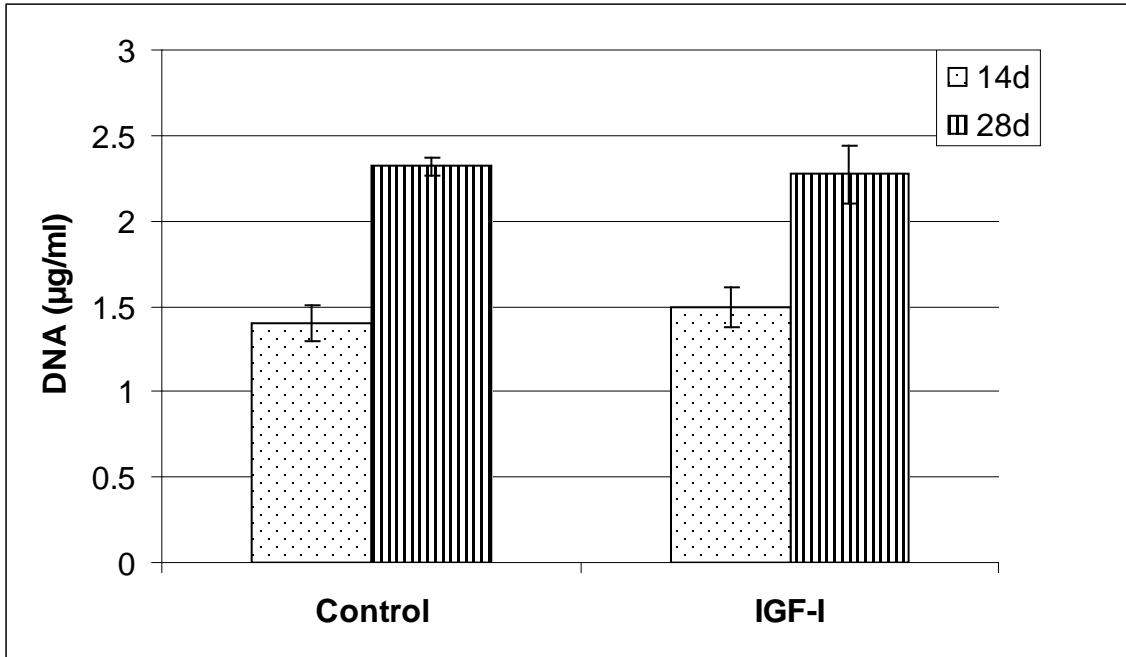
Figure 4.22 DNA content of D1 cells growing on PLGA-fibrin scaffolds for 2 and 4
weeks
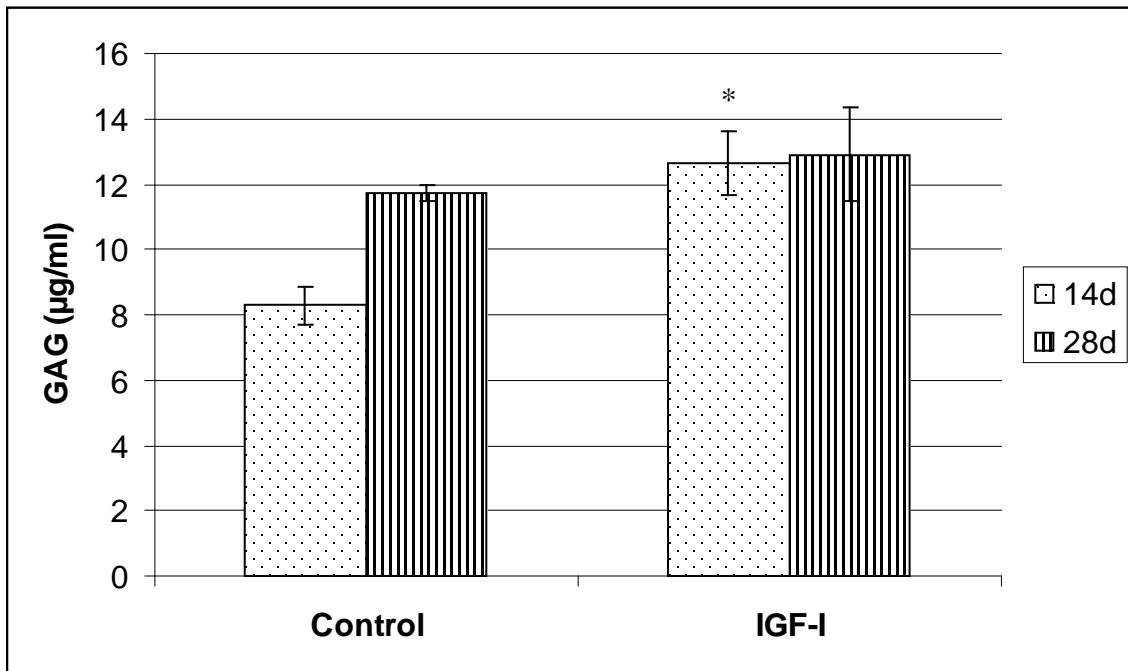
Figure 4.23 GAG content of D1 cells growing on PLGA-fibrin scaffolds for 2 and 4
weeks. *denotes p-value < 0.05 for GAG between control and IGF-I at 14 days

Figure 4.24 shows the normalized GAG content for IGF-I treated and control
PLGA-fibrin scaffolds after 2 and 4 weeks of culture. IGF-I treated scaffolds had 43%

and 12% higher amount of normalized GAG content compared to controls after 2 and 4 weeks of culture. Both of these differences were statistically significant (p-value < 0.05).
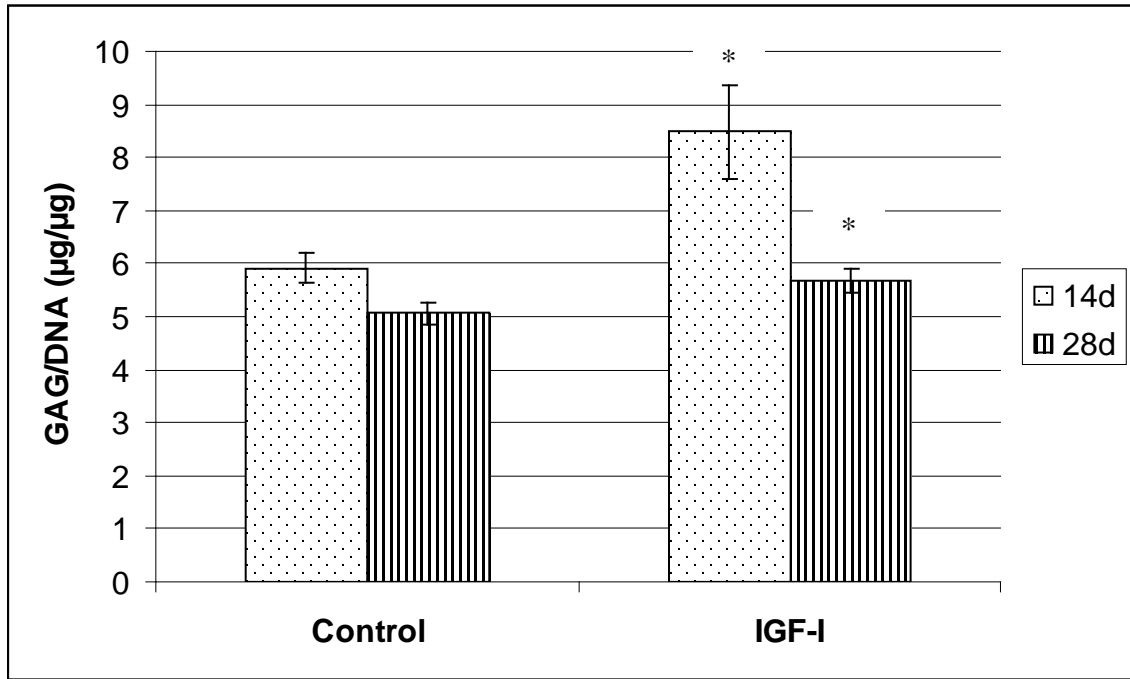
Figure 4.24 Normalized GAG content of D1 cells growing on PLGA-fibrin scaffolds for 2 and 4 weeks. * denotes p-value < 0.05 for GAG/DNA between control and IGF-I groups at both 14 and 28 days

4.3.7 BMCs on PLGA scaffold with fibrin

Rat bone marrow cells were seeded on blank hydrophilic low molecular weight PLGA scaffolds and then encapsulated in fibrin glue to investigate if the fibrin glue would enhance the chondrogenic potential of bone marrow cells. Figures 4.25, 4.26 and 4.27 show the results from this experiment. DNA content of IGF-I treated scaffolds were 22% higher compared to the control scaffolds, as seen in Figure 4.25. This difference was not statistically significant (p-value > 0.05). Figure 4.26 shows the GAG content of the IGF-I treated scaffolds and control scaffolds after 4 weeks of culture. GAG content of the IGF-I treated scaffolds were significantly higher compared to the control group, with a 167% difference.
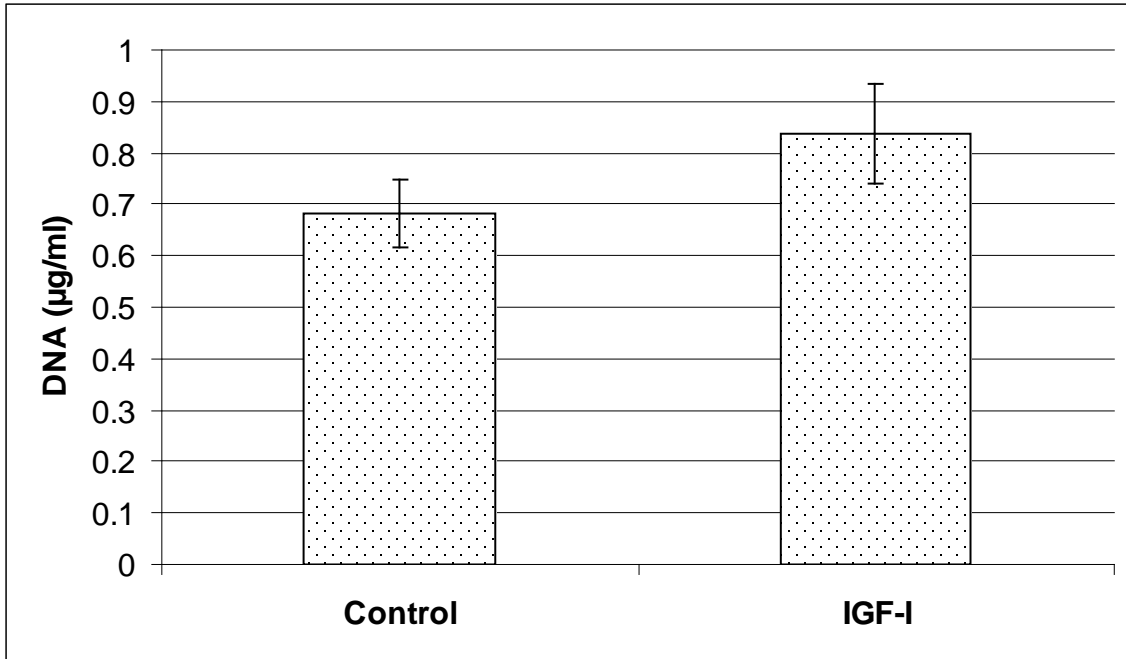
Figure 4.25 DNA content of BMCs growing on PLGA-fibrin scaffolds for 4 weeks
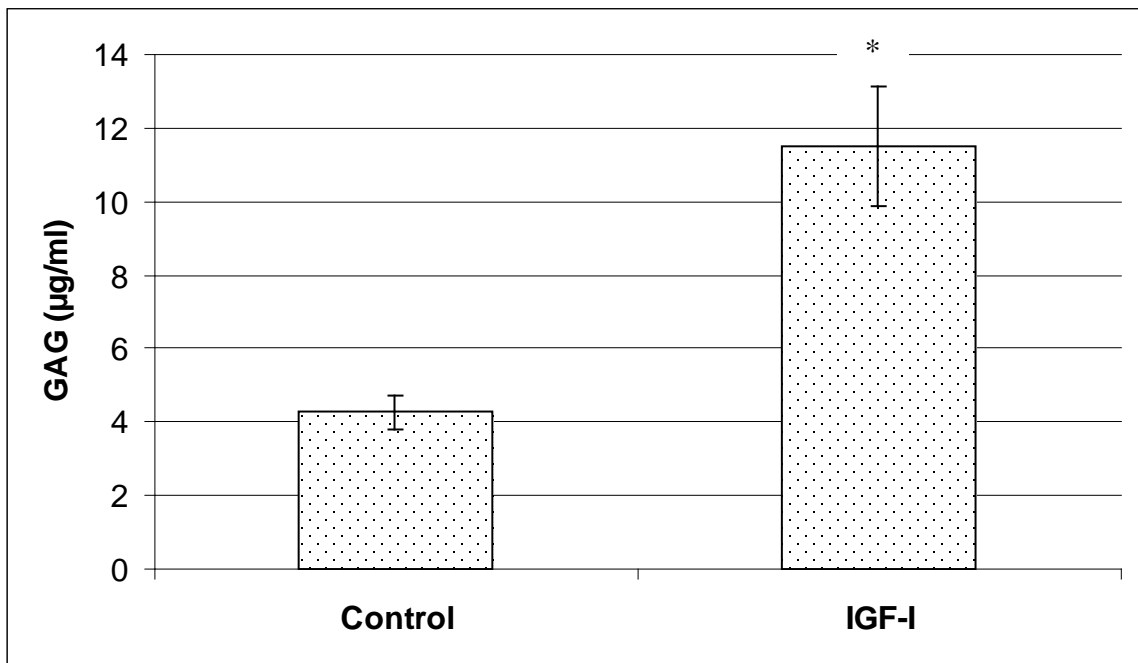
Figure 4.26 GAG content of BMCs growing on PLGA-fibrin scaffolds for 4 weeks. * denotes p-value < 0.05

Figure 4.27 shows the normalized GAG content from the same experiment. Normalized GAG content for the IGF-I treated scaffolds were significantly higher compared to the control scaffolds after 4 weeks of culture (p-value < 0.05). Normalized GAG content for the IGF-I treated scaffolds were 119% higher compared to the control scaffolds.

71
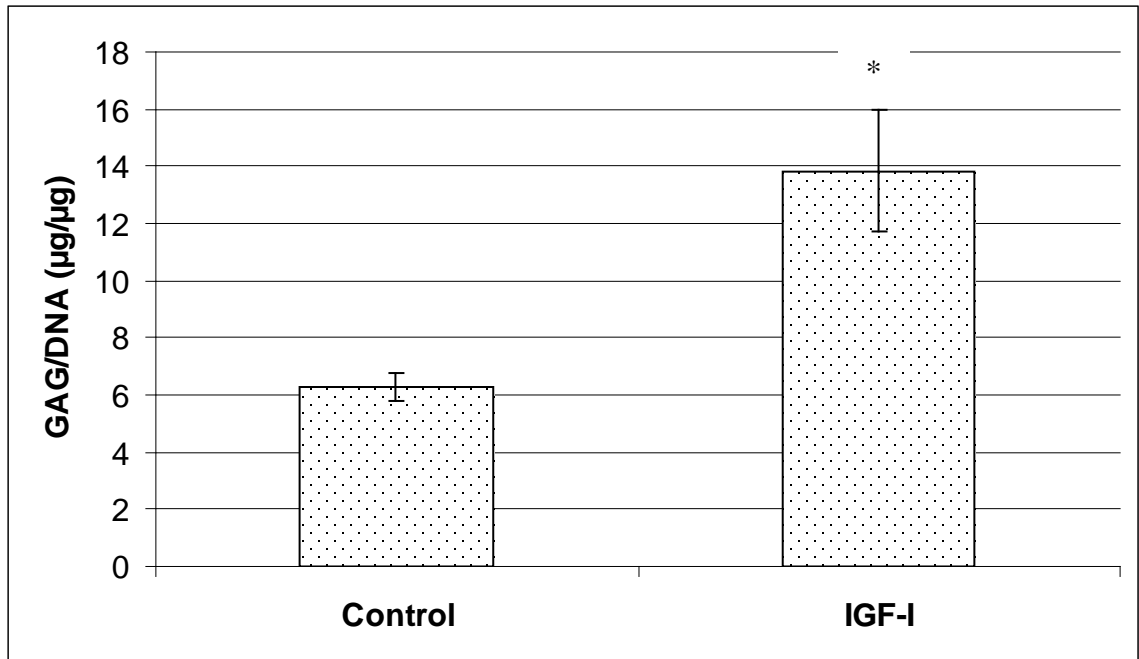
Figure 4.27 Normalized GAG content of BMCs growing on PLGA-fibrin scaffolds for 4 weeks. * denotes p-value < 0.05

4.3.8 Chondrocyte culture on PLGA scaffolds with fibrin

Pig articular chondrocytes were seeded on blank hydrophilic low molecular weight PLGA scaffolds and then encapsulated in fibrin glue to serve as a comparison of cartilage matrix synthesis by already differentiated chondrocytes. Figure 4.28 shows CellTracker labeled pig chondrocytes growing on blank hydrophilic scaffold after 7 days of culture.
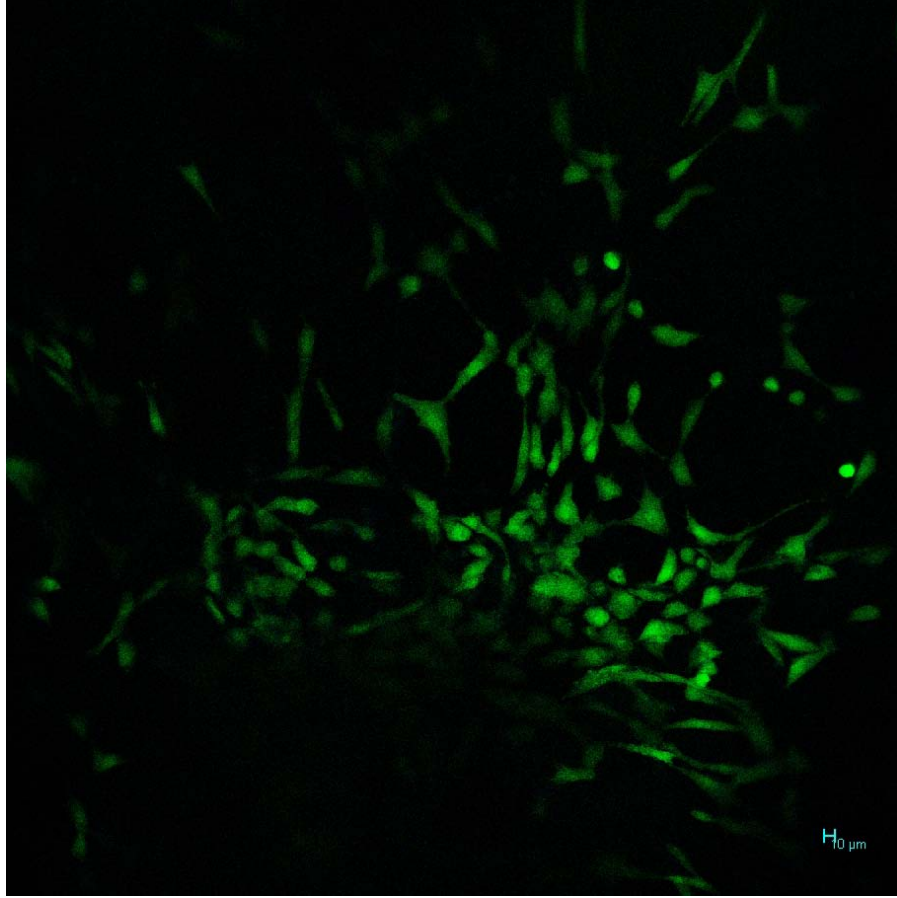
Figure 4.28 CellTracker labeled pig chondrocytes growing on blank hydrophilic scaffold after 7 days of culture

Figure 4.29 shows the DNA content of IGF-I treated and control scaffolds after 4 weeks of culture. DNA content of IGF-I treated scaffolds were 22% higher compared to control group, which was not statistically significant (p-value > 0.05).
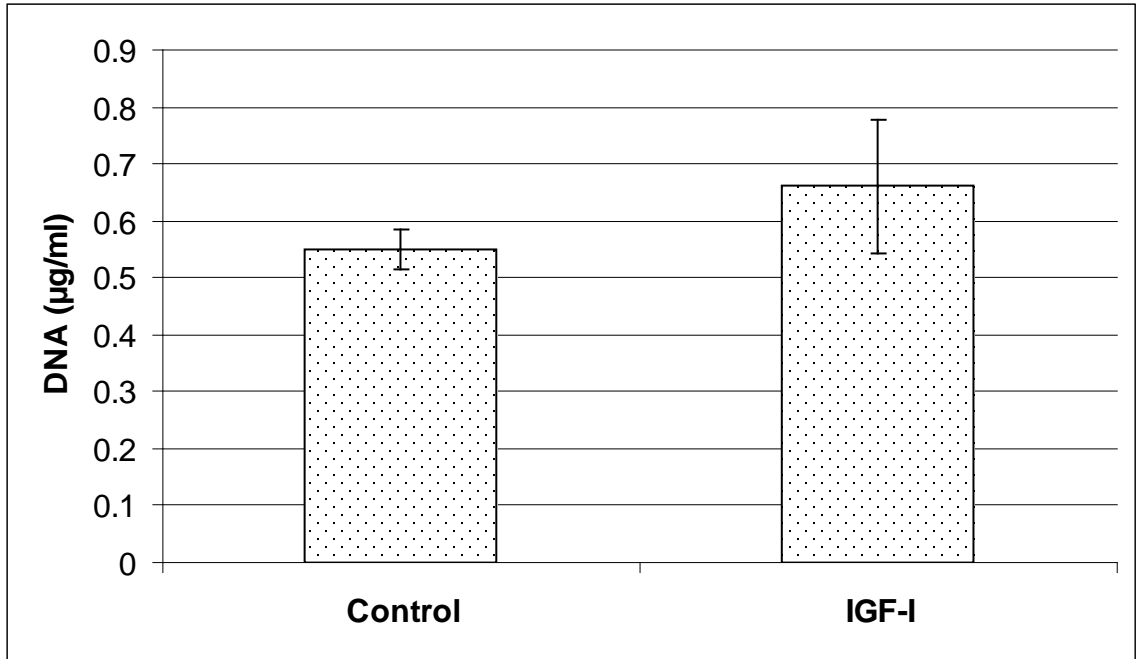
Figure 4.29 DNA content of pig articular chondrocytes growing on PLGA-fibrin scaffolds for 4 weeks
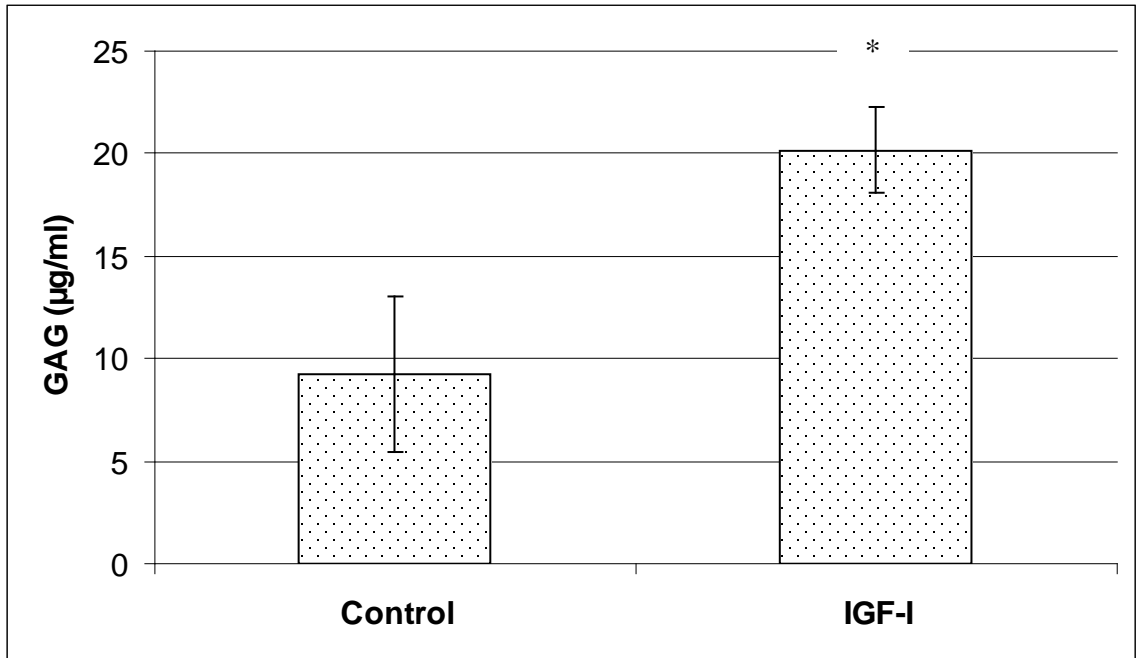
Figure 4.30 GAG content of pig articular chondrocytes growing on PLGA-fibrin scaffolds for 4 weeks. * denotes p-value < 0.05

GAG/DNA (µg/µg)

40
35
30
25
20
15
10
5
0

*
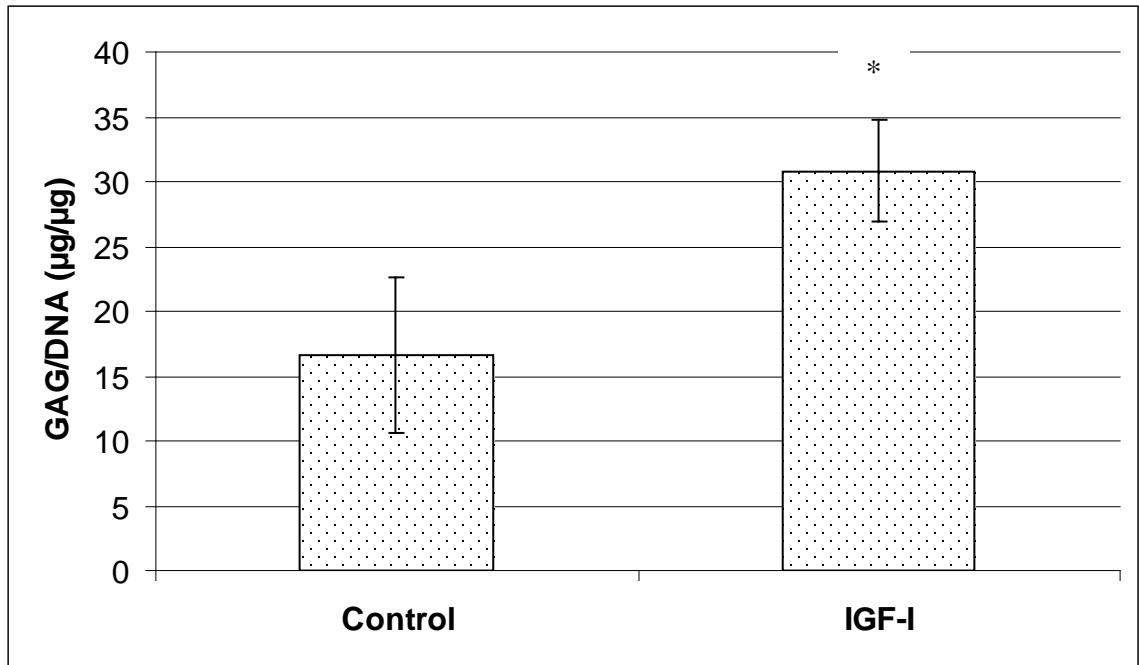
Control   IGF-I

Figure 4.31 Normalized GAG content of pig articular chondrocytes growing on PLGA-fibrin scaffolds for 4 weeks. * denotes p-value < 0.05

Figures 4.30 and 4.31 show the total GAG content and normalized GAG content of control and IGF-I treated scaffolds after 4 weeks of culture with pig chondrocytes. GAG content of IGF-I treated scaffolds were 117% higher compared to control group after 4 weeks of culture. This difference was statistically significant (p-value < 0.05). IGF-I treated scaffolds had 85.5% higher normalized GAG content compared to control group after 4 weeks of culture. This difference was also statistically significant (p-value < 0.05).

4.3.9 BMCs on plasmid-releasing scaffolds

Rat bone marrow cells were cultured on blank hydrophilic PLGA scaffold that had 20µg GFP plasmid:PEI complexes freeze-dried on the surface to investigate if the cells would be transfected from the released plasmid. The results can be seen in Figure 4.32. Outline of the scaffold can be seen in blue, while transfected cells are seen in green.
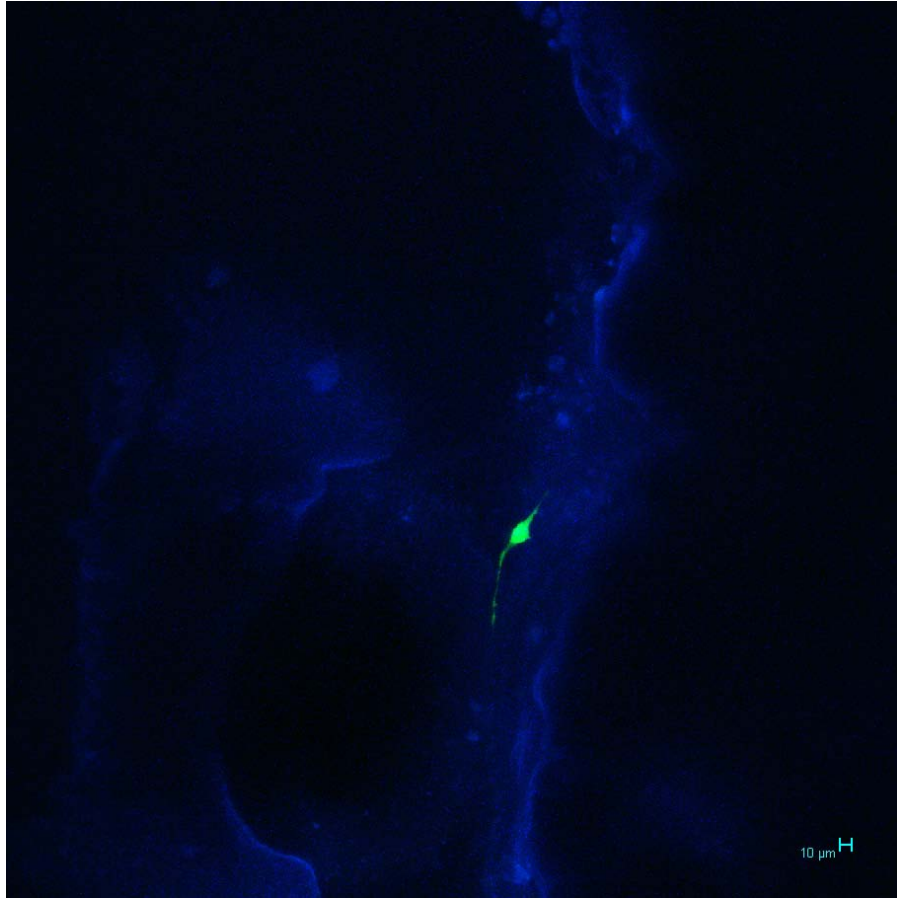
Figure 4.32 Rat bone marrow cells growing on blank hydrophilic PLGA scaffold that had 20µg GFP plasmid:PEI complexes freeze-dried on the surface. Outline of scaffold is blue while transfected cell is green

Rat bone marrow cells were then cultured on PEI:IGF-I plasmid-releasing scaffolds with fibrin to investigate if the cultured cells would get transfected by the released PEI complexed plasmid, express IGF-I protein and then differentiate towards a chondrocytic lineage. Three different types of plasmid releasing scaffolds were fabricated. Low molecular weight hydrophilic microspheres with encapsulated PEI:DNA complexes were used to make the scaffolds. In addition, blank scaffolds with freeze-dried plasmid on the surface, and scaffolds with both encapsulated and freeze-dried plasmid (dual) were also tested.

Figure 4.33 shows the secretion profile of rhIGF-I from different BMC seeded scaffolds up to 20 days of culture. IGF-I was detected in the supernatant from day 2 for all the groups. Highest concentration of 320pg/ml IGF-I was detected from PEI:IGF-I plasmid encapsulated scaffolds on days 9 and 14 after seeding the cells. Secreted IGF-I levels from encapsulated scaffolds were statistically significantly higher than freeze-dried and dual groups on days 9 and 14. Differences in secreted IGF-I concentration between PEI:IGF-I plasmid encapsulated scaffolds and blank scaffolds were not statistically significant at any time point, with a p-value of 0.07 on day 9. Sample size of four/group was needed to get $p-value < 0.05$ with 80% power. IGF-I levels started decreasing for all groups starting at day 14.
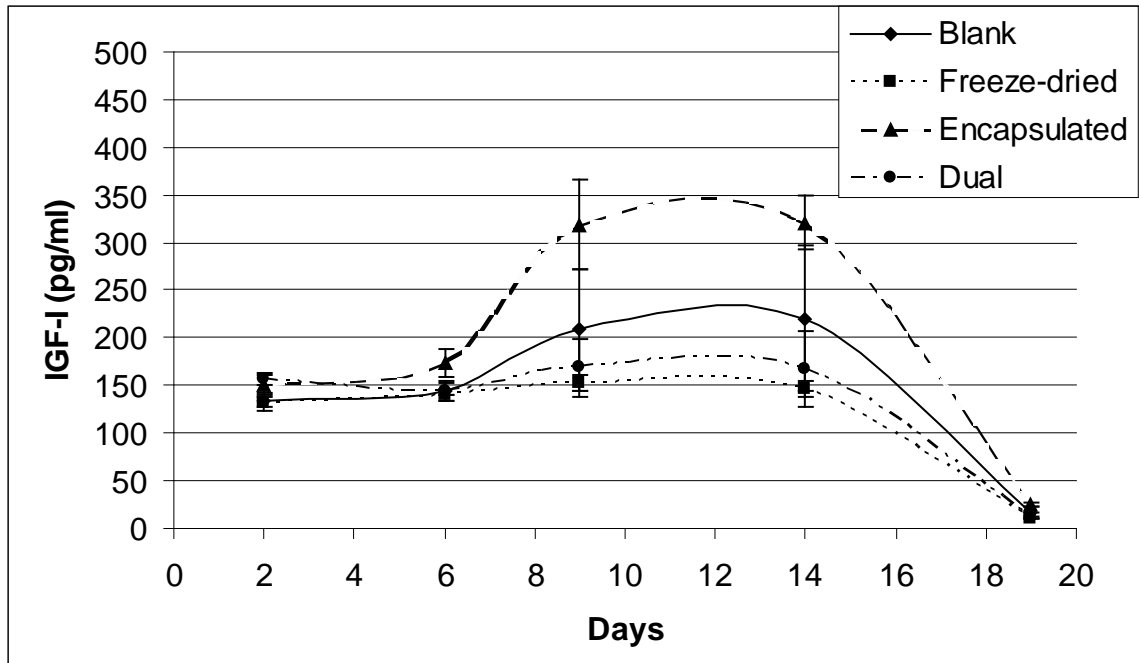
Figure 4.33 rhIGF-I secretion profile from BMC culture on IGF-I plasmid-releasing
PLGA scaffolds

Figure 4.34 shows the DNA content on similar IGF-I plasmid-releasing scaffolds
after culturing rat bone marrow cells for 4 weeks. Blank scaffolds and dual scaffolds had
the lowest amount of DNA content at weeks. Highest DNA content was found on
plasmid encapsulated scaffolds. The difference in DNA content among the different
groups was not statistically significant (p-value > 0.05).

77
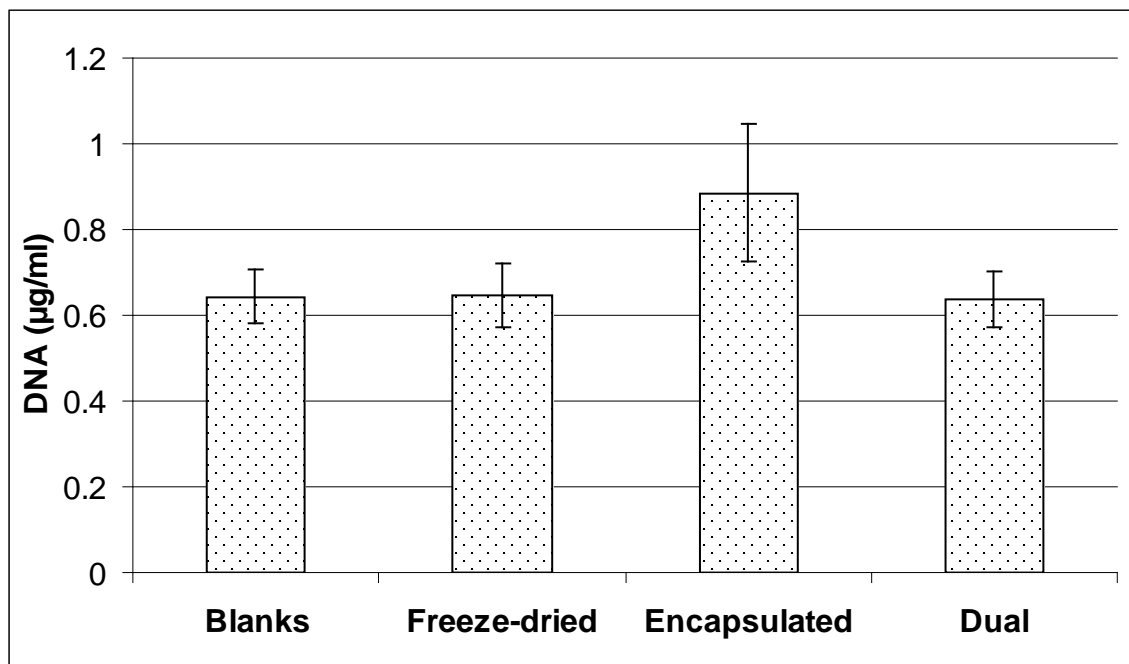
Figure 4.34 DNA content of BMCs growing on IGF-I plasmid-releasing scaffolds for 4 weeks

GAG content on the different scaffolds are shown in Figure 4.35. The lowest amount of GAG was detected in the blank scaffolds. IGF-I plasmid encapsulated scaffolds had 6% higher GAG content compared to blank scaffolds. Scaffolds with IGF-I plasmid freeze-dried on the surface had 15.3% higher GAG content compared to blank scaffolds, and scaffolds that had both encapsulated and freeze-dried plasmid had 20% higher GAG compared to blank scaffolds. None of these differences were statistically significant (p-value > 0.05).
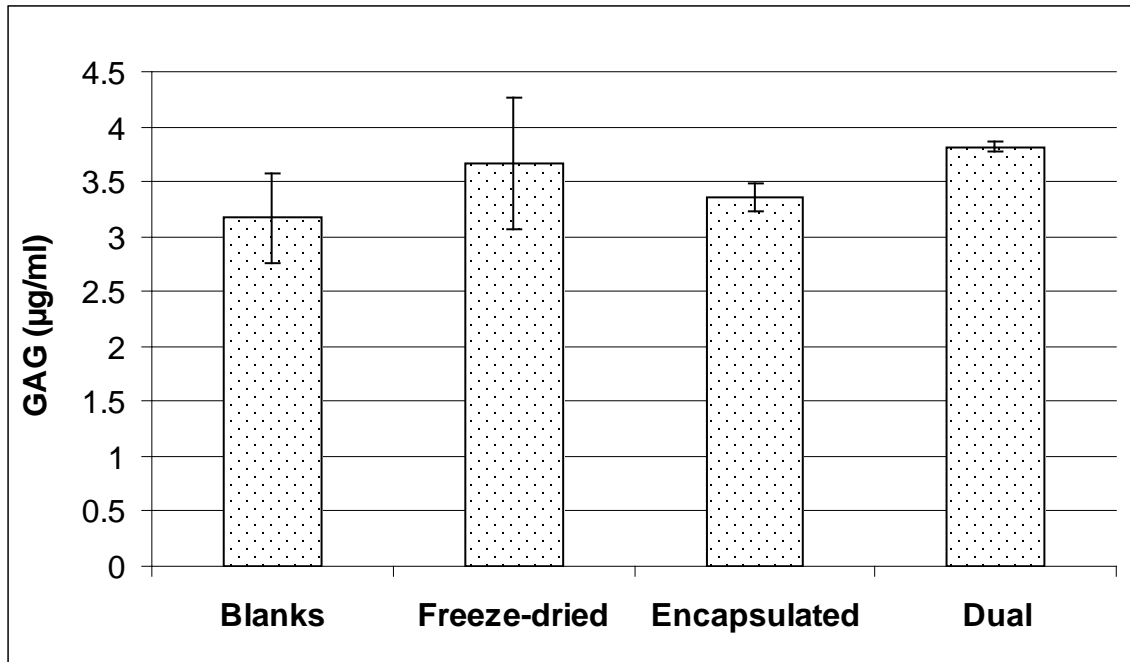
Figure 4.35 GAG content on IGF-I plasmid releasing scaffolds after 4 weeks of culture with BMCs
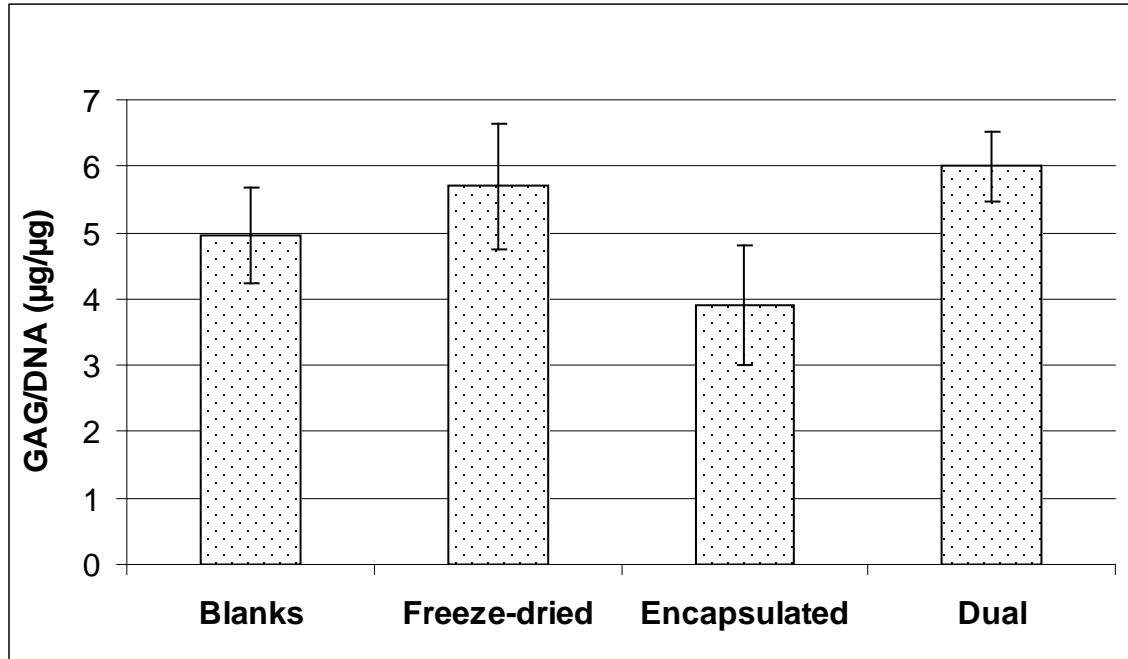
Figure 4.36 Normalized GAG content on IGF-I plasmid-releasing scaffolds after 4 weeks of culture with BMCs

Figure 4.36 shows the normalized GAG content on IGF-I plasmid-releasing scaffolds after 4 weeks of culture with rat BMCs. Plasmid encapsulated scaffolds had the lowest normalized GAG content among all groups. Scaffolds with both encapsulated and freeze-dried plasmid had the highest normalized GAG content. Scaffolds with freeze-dried IGF-I plasmid as well as scaffolds with both freeze-dried and encapsulated IGF-I plasmid had significantly higher normalized GAG content compared to scaffolds with encapsulated IGF-I plasmid. P-value for the ANOVA comparing the normalized GAG content between different groups was greater than 0.05.

4.4 DISCUSSION

4.4.1 D1 cells on tissue culture plate

D1 cells are mesenchymal multipotent cells, originally isolated from mouse bone marrow, and have been shown to have osteogenic and adipogenic potential (Diduch, 1993). After culture on tissue culture plates, DNA content in the control and IGF-I treated groups were similar at both 4 days and 8 days time point. We observed that the cells were detaching from the plate after reaching confluence. The time to reach confluence was hastened when IGF-I was added to the medium. IGF-I treated group had higher GAG and normalized GAG content at 4 days, although this difference was not statistically significant. We expected this difference to increase with time, but on the contrary, GAG content decreased for the IGF-I treated group with time. Limited area for the cells to proliferate on 6 well tissue culture plates was interfering with the experimental design. Comparison of total GAG and normalized GAG content after 8 days of culture showed that IGF-I treated group had lower values than the controls. This was probably due to the sloughing off of cells in the IGF-I treated group around 6 days, removing the newly synthesized GAG with them. Expansion of articular chondrocytes as monolayer culture has been shown to decrease collagen-II and aggrecan production previously (Binette, 1998). This is an indication of dedifferentiation of chondrocytes, as they are cultured on a two-dimensional surface rather than their native three-dimensional matrix.

It has been reported previously that chondrogenic differentiation of adult mesenchymal stem cells on monolayer culture is dependent on seeding density (Takagi, 2007). This was thought to be due to higher amounts of cytokines produced by the cells acting in a paracrine mechanism, and aiding their differentiation (Takagi, 2007). We cultured high density micromass cultures of D1 cells on tissue culture plates to study the effects of high seeding density on chondrogenic differentiation of D1 cells. The amount of DNA in control and IGF-I treated groups were similar at 7 days, and again at 14 days. But the DNA content increased significantly for both the control and IGF-I treated groups from 7 to 14 days, as the cells proliferated on the plate surface. Total GAG and normalized GAG were significantly higher for the IGF-I treated group compared to controls at 7 days, but surprisingly, were lower than the controls at 14 days. This can again be explained by the observation that around days 10-12 IGF-I treated cells reached confluence and sloughed off from the plate surface. Culturing embryonic mesenchymal cells on tissue culture plate at high density has shown a time-dependent increase in cartilaginous matrix production (Mello, 1999). Micromass culture of murine multipotent cells C3H10T1/2 on tissue culture plate with Ham's F12 medium and BMP-2 resulted in chondrocytes-like cells with high collagen-II and sulfate content (Denker, 1999). In our experiment, loss of extracellular matrix resulted in lower GAG content in the IGF-I treated group compared to the controls by 14 days. Differences in cell type and culture conditions might have resulted in different results in our case compared to other high density micromass cultures on TCP.

4.4.2 Agarose gel culture of D1 cells

It has been reported previously that dedifferentiated chondrocytes revert to the differentiated form when cultured in 0.5% agarose gel (Benya, 1982). It was suggested that this reversion was primarily due to the return of chondrocytes to their native round

80

morphology in suspension culture (Benya, 1982). Mesenchymal stem cells embedded in agarose have been used to treat growth plate injury model in rabbits with resultant correction of angular deformity and limb length inequality (Chen, 2003). We cultured D1 cells in 0.5% agarose gel with the addition of IGF-I for 28 days to study the effect of anchorage-independent culture on chondrocytic differentiation of mesenchymal cells. We did not see much difference in DNA content of the cultures from7 to 14 to 28 days. There was an 18% increase in DNA content of the control group from 14 to 28 days, but this was not statistically significant. DNA content of control and IGF-I treated groups were similar at all time points. The lack of increase in DNA content over time could be from the physical constraint of being encapsulated in a 3D matrix, as well as from switching to a differentiation phase from proliferative phase. Both GAG and normalized GAG showed statistically significant increase from 7 to 14 days in both the control group and IGF-I treated group. More importantly, GAG and GAG/DNA values were significantly higher for the IGF-I treated group at all three time points. The difference in GAG and GAG/DNA values between the control group and IGF-I treated group increased with time. All these observations suggest that 0.5% agarose gel culture of D1 cells resulted in cartilage matrix synthesis, and this matrix synthesis was significantly higher when treated with IGF-I. These results are similar to the reported collagen-II and proteoglycan synthesis by dedifferentiated chondrocytes when grown in 0.5% agarose gel (Benya, 1982).

4.4.3 D1 cells on PLGA scaffolds

Mesenchymal stem cells have been cultured on three dimensional scaffolds in order to create cartilaginous matrix (Kafienah, 2007; Farrell, 2006). Adult rat mesenchymal stem cells grown on collagen-glycosaminoglycan scaffolds with the addition of dexamethasone and TGF-1β resulted in increased collagen-II production (Farrell, 2006). Mesenchymal stem cells dispersed in collagen gel have been used to repair full thickness chondral defects (Wakitani, 1994). Mesenchymal stem cells seeded on poly(glycolic acid) scaffold with the addition of retinoic acid inhibitor resulted in cartilage synthesis, as determined histologically (Kafienah, 2007).

Hydrophilic PLGA scaffolds created by us supported the growth and transfection of D1 cells from released PEI complexed plasmids. Cells were seen growing along the entire thickness of the scaffold after 14 days of culture. Culturing D1 cells on blank scaffolds resulted in significant cell proliferation up to 28 days, as shown by significant increases in DNA content from 7 to 28 days for both control and IGF-I treated groups. There was an increase in the amount of GAG produced by D1 cells grown on blank scaffolds from 7 to 28 days with and without IGF-I, although the increase was not statistically significant. Because the DNA content of the scaffolds increased at a faster rate than the GAG content, we saw a decrease in GAG/DNA content from 7 to 14 to 28 days for both the control and IGF-I treated group. It appears that the cells continued to proliferate rather than differentiate after seeding on PLGA scaffolds. Mesenchymal stem cell cultured on PLGA scaffolds with TGF-β1 and dexamethasone showed significant increase in DNA content from 2 to 4 weeks, but the increase in total GAG was not significant (Park, 2009). When mesenchymal stem cells were seeded on PLLA scaffolds and grown for 42 days in spinner culture with the addition of TGF-β1 and IGF-I, significant increase in GAG/DNA content was observed from 14 to 42 days (Janjanin,

2008). But DNA content in the same culture did not increase during the same time period. The physical constraint of growing on PLLA scaffolds that were compressed between two polypropylene discs might have pushed the cells into a differentiation phase instead of a proliferative phase, resulting in the synthesis of cartilaginous matrix.

Culturing mesenchymal stem cells on collagen-PLGA mesh with TGF-β3 resulted in collagen II and aggrecan mRNA upregulation after 4 weeks, but GAG and collagen II was expressed in significant amounts only by 10 weeks of culture (Chen, 2004). When mesenchymal cells were cultured on PLGA scaffolds with the addition of TGF-β3, GAG secretion started to increase after 17 days of culture (Lee, 2004). These studies demonstrate the incubation period needed for mesenchymal cells to differentiate and synthesize cartilaginous matrix on PLGA matrices in chondrogenic media.

It is possible that the duration of our experiment was not sufficient for detecting significant differences in GAG content between the IGF-I treated and control groups, as the cells continued to be in the proliferative phase 4 weeks after culture. But there was a clear pattern of higher GAG content for the IGF-I treated group at every time point, and the difference would have become significant as the mesenchymal stem cells differentiated and synthesized significant amounts of extracellular matrix.

4.4.4 BMCs on PLGA scaffolds

Bone marrow cells have been shown to be particularly useful in tissue engineering because of their superior proliferation and matrix production (Eijk, 2004). Human bone marrow stromal cells cultured in alginate-collagen II capsules showed large regions of cell generated matrix (Pound, 2007). Human bone marrow cells cultured using a rotating wall bioreactor without any growth factors showed significant GAG synthesis at 2 weeks (Sakai, 2009), while human bone marrow stromal cells grown on silk scaffolds with TGF-β1, insulin, and dexamethasone in a rotating bioreactor showed significantly higher GAG/DNA content compared to control scaffolds without chondrogenic growth factors (Marolt, 2006). These studies demonstrate the chondrogenic potential of bone marrow stromal cells in various chondrogenic media and three dimensional matrices.

In our study, rat bone marrow cells seeded on hydrophilic PLGA scaffolds continued to grow until 28 days, when the scaffolds were degraded extensively. When these cells were seeded with the addition of IGF-I to the culture medium, we saw significantly higher DNA and GAG contents in the IGF-I treated scaffolds compared to the untreated controls. Normalized GAG content however, was significantly lower compared to the control group. The lower GAG/DNA content for the IGF-I treated group compared to control was because of the much higher DNA content in the IGF-I treated group compared to the untreated group. It appears that IGF-I acted as a strong mitogen, driving the proliferation of seeded cells in the treated scaffold, along with synthesis of extracellular GAG. Critical factors in chondrogenesis from bone marrow-derived progenitor cells are high cell density and cell-cell interaction (Johnstone, 1998; Yoo, 1998). Mesenchymal stem cells growing on three dimensional scaffolds still involve surface contacts similar to monolayer culture, and are likely to inhibit differentiation (Murdoch, 2007). IGF-I during the initial periods of culture would not have aided in the differentiation of seeded bone marrow cells until they reached the critical density, after which they would have driven differentiation and enhanced synthesis of extracellular matrix proteoglycans such as GAG. This initial lag would have shortened the effective

duration for chondrogenic action of IGF-I in our experiment, and led to lower GAG/DNA content for the treated scaffolds compared to the control group at 4 weeks.

4.4.5 PLGA-fibrin scaffolds

Fibrin is a natural polymer formed as the end result of the blood coagulation cascade, and can be expected to form at the implant site as blood from surrounding bone infiltrates the implanted porous scaffold. Suspending cells in fibrin prior to seeding them on porous scaffolds can minimize cell-loss during the addition of culture medium, as the cells get clotted inside the pores. Fibrin-cell suspension has also been shown to lead to a homogenous distribution of cells in porous scaffolds (Zheng, 2006). Porous PLGA scaffolds have been used previously for chondrogenesis by seeding chondrocytes-fibrin suspension (Munirah, 2008). In that study, significant cartilage tissue was synthesized as early as 2 weeks, and collagen II and aggrecan mRNA were expressed. PLGA-fibrin scaffolds had significantly higher GAG content compared to PLGA scaffolds with chondrocytes alone at 3 weeks (Munirah, 2008). Subcutaneous implantation of PLGA-fibrin scaffolds seeded with chondrocytes in mice resulted in significantly higher GAG content after 2 weeks of implantation (Munirah, 2008b).

We seeded hydrophilic PLGA scaffolds with D1 cells and BMCs suspended in fibrinogen, and then clotted them using thrombin-$CaCl_2$ solution to study the benefit of using PLGA-fibrin scaffolds in chondrogenesis. DNA content of PLGA-fibrin scaffolds seeded with D1 cells increased significantly from 2 to 4 weeks for both the control group and IGF-I treated group. There was no significant difference in DNA content between the control and IGF-I treated group at either 2 or 4 weeks. Total GAG content was significantly higher for IGF-I treated group compared to control group at 2 weeks, but the difference was not significant at 4 weeks, although IGF-I treated group had 16% higher GAG compared to the control group. Interestingly, there was little change in total GAG content from 2 to 4 weeks for the IGF-I treated group, while there was significant increase for the control group. It appears that most of the GAG synthesis in the IGF-I treated group happened in the first 2 weeks of culture. Actions of feedback mechanisms might explain this apparent lack of response to growth factor later in culture. Cytokine production after TGF-β receptor activation has been shown to suppress further cellular response to TGF-β (Fromigue, 1998). In our study, GAG/DNA was significantly higher at both 2 weeks and 4 weeks in the IGF-I treated group compared to the control groups. This indicates that the seeded cells had differentiated to a chondrogenic phenotype, and were synthesizing cartilaginous extracellular matrix. This was in contrast to the D1 cell culture without fibrin when the difference in GAG/DNA content between the IGF-I treated group and control group was not significant at 4 weeks. Similar results were seen when chondrocytes were cultured with and without fibrin on PLGA scaffolds, and was ascribed to the higher seeding efficiency and homogenous cell distribution in fibrin-PLGA cultures compared to non-fibrin PLGA scaffolds (Munirah, 2008). Culturing mesenchymal stem cells on fibrin-polyurethane scaffolds with the addition of TGF-β1 and dexamethasone has shown comparable GAG/DNA to pellet cultures with higher collagen II and aggrecan gene expression (Li, 2009). Suspending chondrogenic cells in fibrin prior to seeding has the advantages of increasing the cell density in scaffolds, ensuring that the cells remain in the scaffold, as well as encapsulating the cells in a true

83

three dimensional matrix, all of which have been previously shown to be beneficial to chondrogenesis.

Seeding BMCs on PLGA scaffolds with fibrin showed the most difference in GAG production between IGF-I treated and control scaffolds among all the cell-scaffold combinations investigated by us. There was no significant difference in DNA content between IGF-I treated and control scaffolds, but IGF-I treated scaffolds had 167% higher GAG content compared to controls after 4 weeks of culture. IGF-I treated scaffolds had 119% higher GAG/DNA content compared to controls after 4 weeks. Similar to the results we saw for D1 cells with and with out fibrin, BMCs seeded with fibrin responded much differently compared to the BMCs that were seeded directly on PLGA scaffolds. All the reasons that we mentioned above for the successful chondrogenesis using D1 cells with fibrin-PLGA scaffolds compared to PLGA alone apply to BMCs also. In addition, the robust response to IGF-I by BMCs might be due to their low passage number compared to D1 cells used in our experiment. Monolayer expansion of chondrocytes after passage 5 has been shown to lead to their dedifferentiation and lack of collagen II and GAG synthesis when cultured on scaffolds in vitro (Kang, 2007). Similarly, it has been shown that mesenchymal stem cells can be expanded in monolayer cultures until passage 5 without losing their undifferentiated phenotype (Cournil-Henrionnet, 2008). D1 cells were originally isolated from mouse bone marrow, and have been shown to have osteogenic and adipogenic potential (Diduch, 1993). D1 cells used in our experiments were from passage 26 or later, and it is possible that these cells had dedifferentiated and become less responsive to IGF-I compared to the BMCs that were from passage 1.

4.4.6 Chondrocytes on PLGA-fibrin scaffolds

Rabbit articular chondrocytes have been seeded with fibrin glue in PLGA scaffolds, with resultant production of a cartilaginous matrix as early as 2 weeks (Munirah, 2008). These scaffolds had significantly higher GAG content compared to PLGA scaffolds that were seeded with articular chondrocytes without fibrin (Munirah, 2008). Implantation of these scaffolds in athymic nude mice also showed significantly higher GAG content after 2 weeks compared to PLGA scaffolds without fibrin (Munirah, 2008b). Fibrin glue with gelatin/hyaluronic acid/chondroitin sulphate copolymer has been used for neocartilage formation using porcine chondrocytes (Chou, 2007). Gelatin/hyaluronic acid/chondtroitin sulfate copolymer was added to fibrin glue to improve the mechanical properties of an otherwise soft fibrin gel, to withstand forces experienced by articular surfaces (Chou, 2007).

We seeded porcine articular chondrocytes into fibrin-PLGA scaffolds, and cultured them for 4 weeks with the addition of IGF-I. Seeded chondrocytes were seen growing along the surface of the scaffold after 7 days. There was no significant difference in the DNA content of IGF-I treated scaffolds and control scaffolds, but both GAG and GAG/DNA contents were significantly higher in the IGF-I treated group after 4 weeks of culture. Not surprisingly, these scaffolds also had the highest GAG and GAG/DNA content among all the cell-fibrin-PLGA scaffolds we tested. Since chondrocytes are already differentiated cells, any added IGF-I to the media can lead to an increase in GAG content, as the cells proliferate and populate the porous scaffolds. An increase in cell number would also have lead to an increase in associated matrix components such as GAG. Chondrocytes grown in fibrin cultures with exogenous IGF-I

84

have been shown to increase cell proliferation and proteoglycan synthesis (Fortier, 1999). The cumulative effect of using well differentiated cells such as chondrocytes with a chondrogenic growth factor, such as IGF-I, might be the reason for high GAG and GAG/DNA content for chondrocyte-fibrin-PLGA cultures.

4.4.7 BMCs on IGF-I plasmid-releasing scaffolds

Rat bone marrow cells were cultured on IGF-I plasmid releasing scaffolds to investigate if the cultured cells would get transfected by the released the PEI complexed plasmid, express IGF-I protein and then differentiate towards a chondrocytic lineage. Previous studies have shown that ex vivo transfer of IGF-I DNA into chondrocytes can enhance chondrogenesis in vitro and in vivo (Madry, 2002; Madry, 2005). Cationized gelatin nanoparticles have been used to deliver IGF-I plasmid to canine articular chondrocytes in vitro, which resulted in transfection and release of IGF-I protein from 3 to 12 days into the culture medium (Xu, 2008). When these transfected cells were seeded on collagen-GAG scaffolds, there was significantly higher GAG/DNA amount compared to control scaffolds with untransfected chondrocytes (Xu, 2008). Mesenchymal cells infected with AdIGF-I, and suspended in fibrin glue has been used for successful repair of articular cartilage (Gelse, 2003).

In our study, significant production of IGF-I was observed only for the PEI:IGF-I plasmid encapsulated scaffolds. These scaffolds produced a peak concentration of 320 pg/ml IGF-I on days 9 and 14. The p-value for the difference in secreted IGF-I between plasmid encapsulated and blank scaffolds was 0.07, suggesting that we narrowly missed statistical significance. Increasing the number of samples per group might be able to bring out the statistical significance in this case. Chondrocytes seeded on collagen-GAG scaffolds that had lipid-complexed IGF-I plasmid crosslinked on the surface showed peak IGF-I production of 2500pg/ml on day 14 (Capito, 2007). The differences in cell type as well as plasmid carrier could account for this difference in secreted IGF-I concentration. The highest concentration of IGF-I produced from our scaffolds were 1000 times lower than the concentration of IGF-I used as a medium supplement for chondrogenesis in our experiments. However, it is possible that the local concentration of IGF-I around transfected cells within the scaffold be much higher than the concentration in the culture medium. Significant chondrogenesis was reported with IGF-I plasmid-transfected chondrocytes on collagen-GAG scaffolds, although these cells produced IGF-I at a concentration of 2000-2500pg/ml in the culture medium (Xu, 2008). Interestingly, scaffolds with freeze-dried PEI:IGF-I plasmid on the surface alone and in combination with encapsulated PEI:IGF-I plasmid failed to produce any significant amounts of IGF-I. It is possible that the high concentration of freeze-dried PEI:DNA particles on the surface of these scaffolds led to their aggregation into larger particles, making it difficult or impossible for the cells to internalize them and get transfected. The surface coating of PEI:DNA particles could also have interfered with the cell adhesion process, effectively decreasing the initial number of cells on the scaffold and IGF-I produced, compared to blank and plasmid encapsulated scaffolds. A decrease in the amount of protein expressed has been noted with very high PEI:DNA loading of PLGA scaffolds, and was speculated to be due to aggregation of PEI:DNA particles and sequestration of DNA, making it less accessible for gene transfer (Huang, 2003). It is also possible that the freeze-dried PEI:DNA particles might be interacting with the PLGA polymer, slowing their release to

the cells for transfection. Only 40% of adsorbed PEI:DNA particles were released at the end of 4 days of release from PLGA scaffolds (Jang, 2006). We saw a small amount of IGF-I produced from blank scaffolds that had BMCs seeded on them. Similar production of small amounts of IGF-I was seen when assaying for IGF-I after canine chondrocytes were seeded on collagen-scaffolds (Capito, 2007). This small amount of IGF-I might be due to the constitutive expression of rat IGF-I from bone marrow cells crossreacting with the human IGF-I antibody in our assay.

We saw increased cell proliferation on IGF-I plasmid encapsulated scaffolds when rat bone marrow cells were cultured on IGF-I plasmid releasing PLGA scaffold with fibrin. DNA content of IGF-I plasmid encapsulated scaffolds were approximately 38% higher than other groups of scaffolds, although this difference was statistically insignificant with a p-value of 0.07. We had seen peak IGF-I release from the IGF-I plasmid encapsulated scaffold around 350pg/ml on days 10-12. The low concentration of IGF-I along with the delay in getting the IGF-I into the culture medium by the transfected cells would have effectively shortened the exposure of seeded cells to IGF-I when the culture was ended at 4 weeks. There were no significant differences in the total GAG content between blank scaffolds and other IGF-I plasmid releasing scaffolds at 4 weeks, although blank scaffolds had the least amount of total GAG among the different groups. The decreased exposure of cells to IGF-I produced by transfected cells might have been the reason for this result. When comparing GAG/DNA content between scaffolds, plasmid encapsulated scaffolds had the lowest value among the groups. This was not surprising because of the high DNA content of these scaffolds, which naturally decreased the GAG/DNA ratio. GAG/DNA contents among the other scaffold groups were statistically similar. To our surprise, scaffolds that had 10µg PEI:DNA complexes freeze-dried on the surface fared poorly in both DNA and GAG contents compared to control and PEI:DNA encapsulated scaffolds. When canine chondrocytes were seeded on collagen-GAG scaffolds with freeze-dried lipid:DNA complexes on the surface, similar decrease in DNA content was observed after 2 weeks of culture (Capito, 2007). It was speculated that the surface coating of lipid:DNA complexes might have inhibited cell attachment and proliferation on these scaffolds, leading to low DNA content. Surface coating of sucrose and PEI:DNA particles on our scaffolds with freeze-dried PEI:DNA complexes could have had the same inhibitory effect.

Scaffolds made of high molecular weight PLGA with encapsulated IGF-I plasmid can increase the exposure of cells to secreted IGF-I by releasing the plasmid longer, and degrading at a slower rate. This increase in exposure might result in significant chondrocytic differentiation of mesenchymal progenitor cells grown on such scaffolds.

4.5 CONCLUSION

Agarose cultures of D1 cells were able to show differentiation to a chondrocytic phenotype as evidenced by increased total GAG and GAG/DNA contents. Our porous PLGA scaffolds supported the growth and differentiation of D1 cells, chondrocytes and bone marrow cells in vitro. Suspension of cells in fibrin prior to seeding resulted in significant differences in total GAG and GAG/DNA contents between IGF-I treated and control groups for mesenchymal stem cells, bone marrow cells and chondrocytes, where as the differences were not significant when cultured on scaffolds without fibrin. This proved that fibrin was critical in the differentiation of the cells into chondrogenic phenotype, probably by retaining seeded cells within the scaffold and thus increasing cell density, as well as encapsulating the cells in a three dimensional environment. Among the three cells types studied, chondrocytes had the highest GAG/DNA content after 4 weeks of culture, where as bone marrow cells showed the largest difference in GAG/DNA between IGF-I treated and control groups. Culturing BMCs on IGF-I plasmid encapsulated scaffolds resulted in elevated expression of rhIGF-I compared to blank and IGF-I plasmid freeze-dried scaffolds. Although the amount of IGF-I produced was not statistically significant compared to controls, the p-value was 0.07, suggesting that increasing the number of samples can make the difference statistically significant. Bone marrow cells cultured on the IGF-I plasmid encapsulated scaffolds showed the highest DNA content among all the groups. Total GAG was higher for all plasmid-releasing scaffolds compared to the blank scaffolds, but these differences were not statistically significant. Low concentration of IGF-I released from transfected cells along with the delay in its production might have been the reason for the inability to observe significant chondrocytic differentiation in bone marrow cells seeded on IGF-I plasmid-releasing scaffolds. Using scaffolds made from higher molecular weight hydrophilic PLGA to culture cells, along with increasing the amount of IGF-I secreted can increase the exposure of cells to IGF-I, and might result in successful chondrogenesis using bone marrow progenitor cells.

5. IGF-I PLASMID-RELEASING PLGA SCAFFOLDS FOR GROWTH PLATE REGENERATION IN VIVO

5.1 INTRODUCTION

Growth plate injuries account for approximately 15% to 30% of all fractures of long bones in children (Mizuta, 1987). About 10% of these will result in significant growth disturbances due to the formation of a boney bar (Salter, 1994). This boney bar can act as a tether, attaching the epiphyseal bone to the diaphyses, and limiting the continued normal growth of the limb. If not treated correctly, this can lead to life lasting consequences of limb length inequalities and angular deformities. Most cases of growth arrest from the formation of boney bars occur during early adolescence because this is when the growth plate is thickest and weakest (Khoshhal, 2005). If the physeal fracture occurs at the periphery of long bones, angular deformity can result, whereas a centrally located physeal fracture can lead to metaphyseal tenting and damage to articular surface (Khoshhal, 2005). It has been postulated that cellular disruption and ischemia resulting from a fracture might be the mechanism of growth plate injury (Khoshhal, 2005). Surgical resection of a boney bar is indicated only if the injury involves less than 50% of the growth plate, and the patient has more than 2 years of growth remaining. The chances of success are greater for younger patients and smaller boney bridges (Khoshhal, 2005).

Use of an interpositional material after resection of the boney bar was first reported by Langenskiöld, who used fat to fill the defect, using an approach now called the Langenskiöld technique (Langenskiöld, 1967). Current treatments for growth plate injuries include removal of boney bar, and insertion of fat, silicone, bone cement etc to replace the growth plate. These treatment modalities are inadequate, leaving almost half of these patients with continued deformities (Hasler, 2002).

Tibiae that received fat as interpositional material in a rabbit growth plate injury model developed severe varus and failed to grow in length (Lee, 1993). But this is in contrast to what was reported by Langenskiöld, whose patients benefited from fat grafts to treat growth plate arrest (Langenskiöld, 1987). Implantation of silastic in a rabbit model of growth plate injury resulted in less angular deformity and length discrepancy during the first few weeks after surgery, but this was lost 12 weeks after surgery (Lee, 1993). Implantation of an iliac physeal transplant showed the least varus and length discrepancy at 12 weeks after surgery (Lee, 1993). But this would necessitate a second surgical site, removal of healthy tissue with its associated risks and scarring at the donor site. Another material that has been used a graft to replace the physis is poly(methyl methacrylate) polymer, which is not biodegradable (Klassen, 1982). Implantation of an atelocollagen gel embedded with autologous chondrocytes resulted in significantly lower varus and length discrepancy 52 weeks after surgery in a rabbit model of physeal injury (Tobita, 2002). This technique would also require harvesting healthy articular chondrocytes, which can lead to other articular cartilage problems. Implantation of mesenchymal stem cells embedded in agarose gel in a rabbit physeal injury model resulted in correction of varus deformity and limb length discrepancy (Chen, 2003). When agarose embedded chondrocytes were implanted in a rabbit model of physeal injury, only mild varus deformity and limb length discrepancies were seen (Lee, 1998).

Although implantation of scaffolds with embedded autologous cells have shown positive results, the technique has the disadvantages of donor site scarring, and the need

for a harvest procedure. When applying this technique to humans, it also requires that the treatment be tailored to individual patients. The stem cells or chondrocytes will have to be harvested and multiplied to sufficient numbers before they can be incorporated into scaffolds and readied for implantation. This can significantly increase the cost of treatment. An interpositional material that can regenerate native growth plate by releasing chondrogenic growth factors, match the mechanical properties of cartilage, and degrade at an appropriate rate will be superior to one that incorporates cells prior to implantation. Previous chapters of this dissertation have presented the development of porous PLGA scaffolds that can release naked and PEI-complexed DNA in a controlled manner, and that culturing chondrocyte-progenitor cells on these scaffolds with IGF-I can lead to significant synthesis of cartilage in vitro. This chapter of my dissertation presents the in vivo trial of IGF-I plasmid-releasing porous PLGA scaffolds in a rabbit model of growth plate injury.

5.2 MATERIALS AND METHODS

5.2.1 Preparation of porous PLGA scaffolds

Blank and PEI:IGF-I-plasmid encapsulated hydrophilic PLGA microspheres were prepared as described in chapter 1. To create PLGA discs for implantation, 120 mg of PLGA microspheres were hand-mixed with 180 mg of salt particles for 2 minutes, and compressed at 7 tons for 2 minutes in a 13 mm die using a Carver press. The discs were then sintered in an oven for 48 hours at 42°C. The sintered discs were then leached in deionized water overnight and dried in vacuum to create porous PLGA scaffolds. These scaffolds were then sterilized using 70% ethanol prior to implantation. To create scaffolds with freeze-dried and encapsulated IGF-I plasmid, 15µg of PEI:DNA complex was freeze-dried on to the surface of IGF-I plasmid encapsulated scaffolds.

5.2.2 Animal Surgery

Six to eight weeks old New-Zealand white rabbits were used in our study. Animals were anesthetized and radiographic images of hind limbs were taken prior to inducing growth plate injury. Incision was made on the anteromedial side of tibia, and medial tibia was exposed. Figure 5.1 shows the intact growth plate as a thin white line. Medial half of the tibial growth plate was removed using a 1 mm burr (Stryker Medical). Incision was closed using sutures after thorough irrigation. This procedure was repeated on the contralateral limb. Animals were allowed to recover in their pens.

Three weeks after the growth plate injury, animals were brought back for the implantation of PLGA scaffolds. Radiographic images of hind limbs were taken to confirm growth plate injury and formation of the boney bar. Figure 5.2 is a radiograph of the lower hind limbs taken 3 weeks after the growth plate was removed. Increased radioopacity, indicating formation of bone, can be seen in the medial halves of tibia bilaterally (arrows), while the lateral growth plate can be seen to be intact. Medial proximal tibia was exposed through an anteromedial incision. Boney bar was removed using a burr. Blank or IGF-1 DNA loaded disk was inserted into the defect. Incision was closed after thorough irrigation. For the control legs, boney bar was resected and nothing was implanted in the defect. Figure 5.3 shows the implantation of a hydrophilic scaffold that has been placed into the defect after removal of the boney bar. The scaffold is then trimmed to the size of the defect to create a good fit and inserted into the defect, as shown in Figure 5.4.

Animals were returned to their pens, and allowed to heal for 8 or 16 weeks. At the end of eight or sixteen weeks, animals were euthanized. Radiographic images of hind limbs were taken, and lower hind limbs harvested for further analysis. Figure 5.5 illustrates the experimental design. Implantation of scaffolds was randomized such that no animal received the same type of scaffold in both legs.

Figure 5.1 Intact tibial growth plate of New Zealand white rabbit

Figure 5.2 Radiograph of rabbit lower hind limbs 3 weeks after surgery to remove medial tibial growth plate. Arrows indicate boney bars
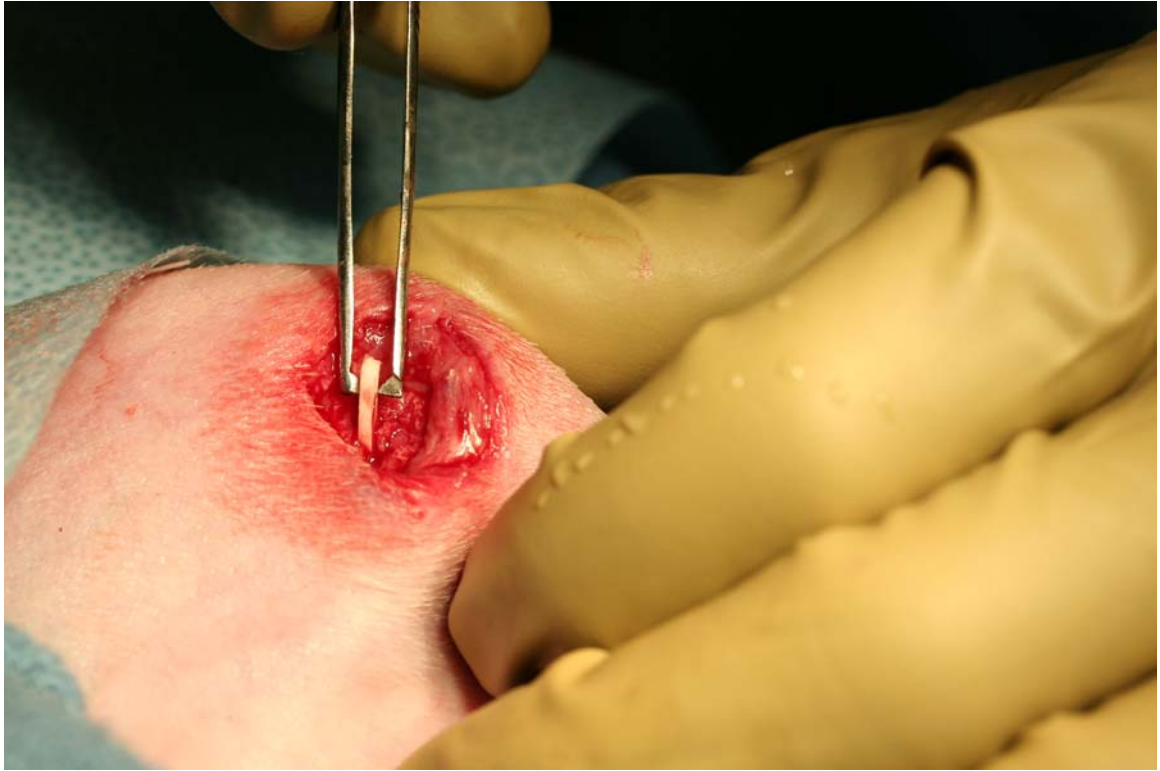
Figure 5.3 Scaffold being inserted into medial tibia

Figure 5.4 Hydrophilic scaffold in medial tibia
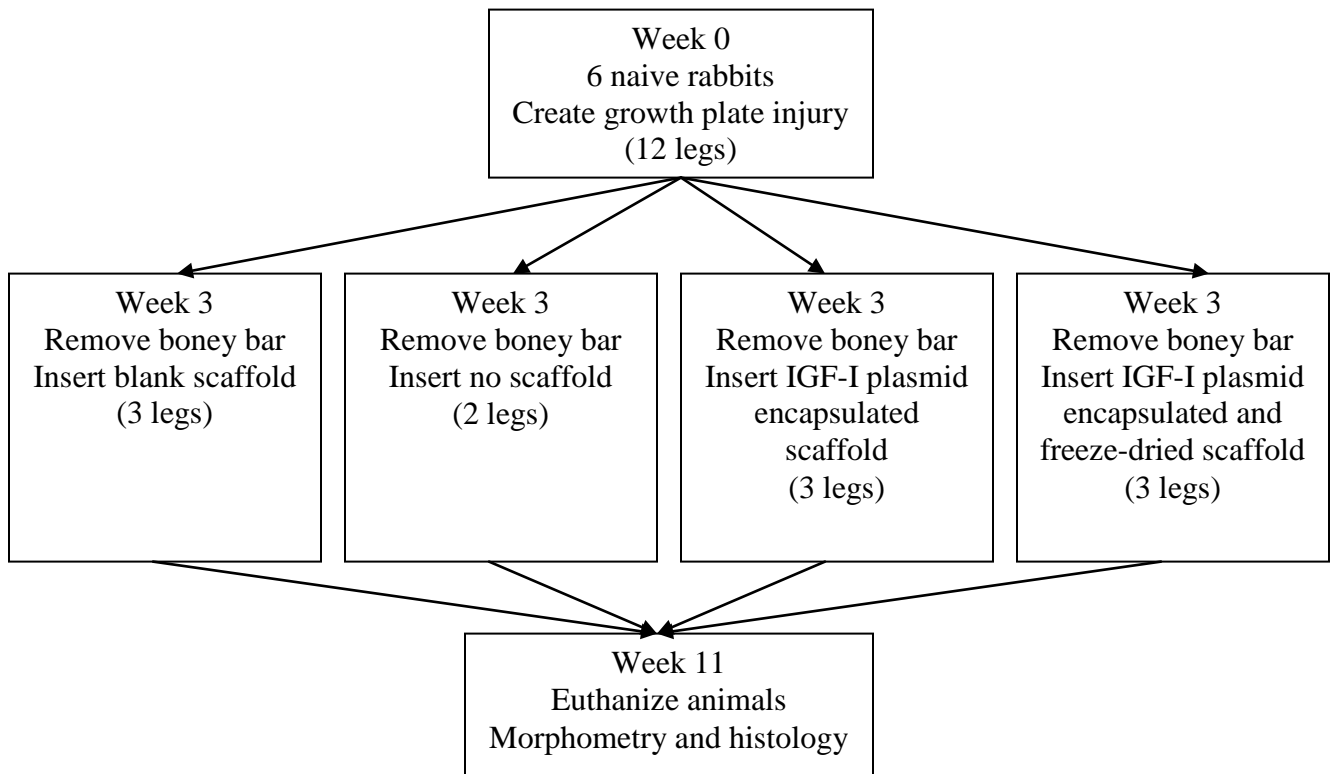
Figure 5.5 Experimental design

5.2.3 Morphometry

Medial and lateral lengths of tibiae were measured using a digital caliper (Fisher scientific Model No. 14-648-17) for each lower hind limb. Widths of fibulae were also measured.

Radiographic images were analyzed using Scion Image software. Medial proximal tibial angle (MPTA) and lateral distal femoral angle (LDFA) were measured for each lower hind limb. Measurements were done twice on each image by a single examiner. Medial proximal tibial angle is the internal angle formed between the shaft of tibia and top of the tibia. Lateral distal femoral angle is the internal angle formed between the bottom plane of femur and hip joint. Figure 5.6 illustrates medial proximal tibial angle and lateral distal femoral angle on a radiograph.

93
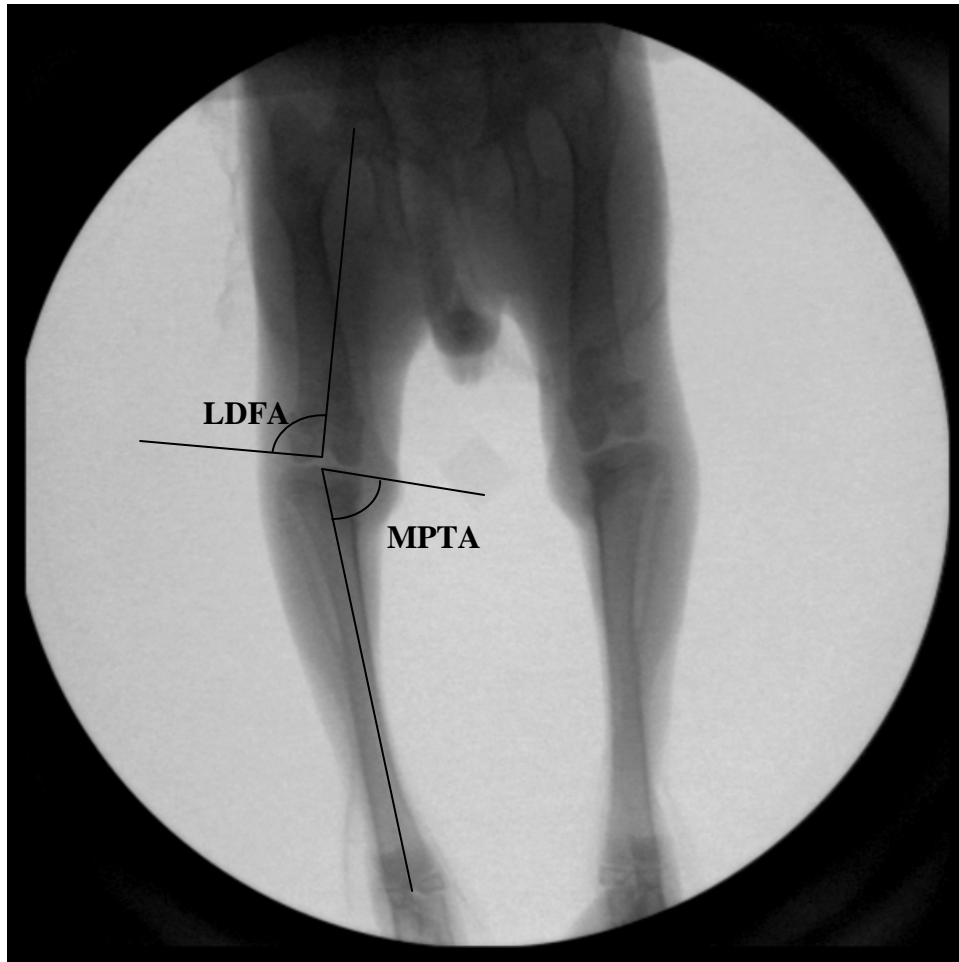
Figure 5.6 Medial proximal tibial angle and lateral distal femoral angle illustrated on a rabbit lower limb radiograph

5.2.4 Histological analysis

After removal of fibulae, upper half of tibiae were cut sagittally or coronally and fixed in 10% buffered formalin for 2 weeks. These samples were then decalcified in 10% nitric acid for 4 days for histological staining. Decalcified samples were cut into two halves in the coronal plane into anterior and posterior proximal tibiae. Each half was embedded in paraffin and cut into 10 micron sagittal or coronal sections using a microtome (Finesse ME+). Sections were stained using hematoxylin and eosin by deparaffinising in xylene, hydrating through graded alcohol series, immersing in hematoxylin for 2 minutes and eosin for 30 seconds, followed by dehydration in alcohol series and xylene. Sections stained with safranin-O and acid-fast green were first deparaffinised in xylene, hydrated in graded alcohol series, and then immersed in acid-fast green for 5 minutes and safranin-O for 5 minutes. These sections were then dehydrated using graded alcohol series and xylene. Slides were coverslipped using Permount SP15-500 (Fisher Scientific). Stained sections were visualized and photographed using a Nikon Eclipse E600 microscope (Nikon) attached to a Nikon DN 100 digital camera (Nikon).

94

5.2.5 Statistical analysis

Statistical analysis was done using SAS 9.1 NC software. ANOVA was used to find statistical difference in morphometric parameters between treatment groups. Tukey-Kramer multiple comparison test was used post-hoc. Sample size calculation was done using nQuery Advisor software with 80% power.

5.3 RESULTS

5.3.1 Angular measurements

Figure 5.7 shows the lower hind limbs of an 8 weeks old rabbit prior to injury to growth plate (naive). Medial proximal tibial angle and distal lateral femoral angle of naive rabbits were measured to calculate how much of varus (inward angulation of limbs) occurred as a result of growth plate arrest, and how much varus was corrected after implantation of various scaffolds. The medial proximal tibial angles in this particular case were 84.64° (right) and 90.58° (left). The lateral distal femoral angles were 96.59° (right) and 100.58° (left).

Figure 5.7 Radiograph of lower hind limbs of an 8 weeks old naive rabbit

Figure 5.8 shows the hind limbs after the growth plate arrest was created by removing the medial growth plate and allowing the boney bar to form. Note the varus created bilaterally. The medial proximal tibial angles decreased to 74.80° (right) and 83.39° (left), confirming varus in both legs. The lateral distal femoral angles were 96.36° (right) and 99.55° (left).

96

Figure 5.8 Radiograph of rabbit lower hind limbs 3 weeks after surgery to remove medial tibial growth plate, with resultant boney bars

The varus was improved after implantation of scaffolds to remove the boney bars, as seen in Figure 5.9. Figure 5.9 shows the hind limbs 8 weeks after a blank hydrophilic scaffold was implanted into the right tibia and IGF-I DNA freeze-dried scaffold was implanted into the left tibia. The medial proximal tibial angles increased to 78.68° (right) and 85.40° (left).

97

Figure 5.9 Radiograph of rabbit lower hind limbs 8 weeks after a blank hydrophilic PLGA scaffold was implanted in the right tibia, and IGF-I plasmid freeze-dried and encapsulated scaffold was implanted in the left tibia to replace boney bars

Medial proximal tibial angle and lateral distal femoral angles were measured from the radiographs for each limb at the start of the study, 3 weeks after the first surgery, and 8 weeks after the second surgery to study the effect of treatment on correction of angular deformity (varus). The results are shown in Figures 5.10 and 5.11. Figure 5.10 shows the medial proximal tibial angle for all 4 treatment groups at the start of the study, 3 weeks and 11 weeks after the physeal injury. This angle decreased for all treatment groups from the start of the study to 3 weeks after physeal injury, confirming formation of boney bar, and the success of the physeal injury model. Eight weeks after implantation surgery, the MPTA decreased further in all treatment groups, including the group that did not receive any implants. The lowest MPTA angle (highest varus) was seen in the no implant group, with an average value of 65.19°. The average MPTA for IGF-I plasmid encapsulated scaffold treated group was 70.2°, IGF-I plasmid freeze dried scaffold treated group was 73.11° and blank scaffold treated group was 76.75°. There was no statistical difference in MPTA between any treatment groups at any particular time point (p-value > 0.05). MPTA for all treatment groups were significantly lower at the 11 weeks time point compared to the corresponding MPTA at start of the study (p-value < 0.05). MPTA for all treatment groups except "no scaffold" group were significantly lower at the 3 weeks time point compared to the corresponding MPTA at the start of the study (p-value < 0.05). A sample size of 92/treatment group is needed for getting p-value <0.05 with a power of 80%.
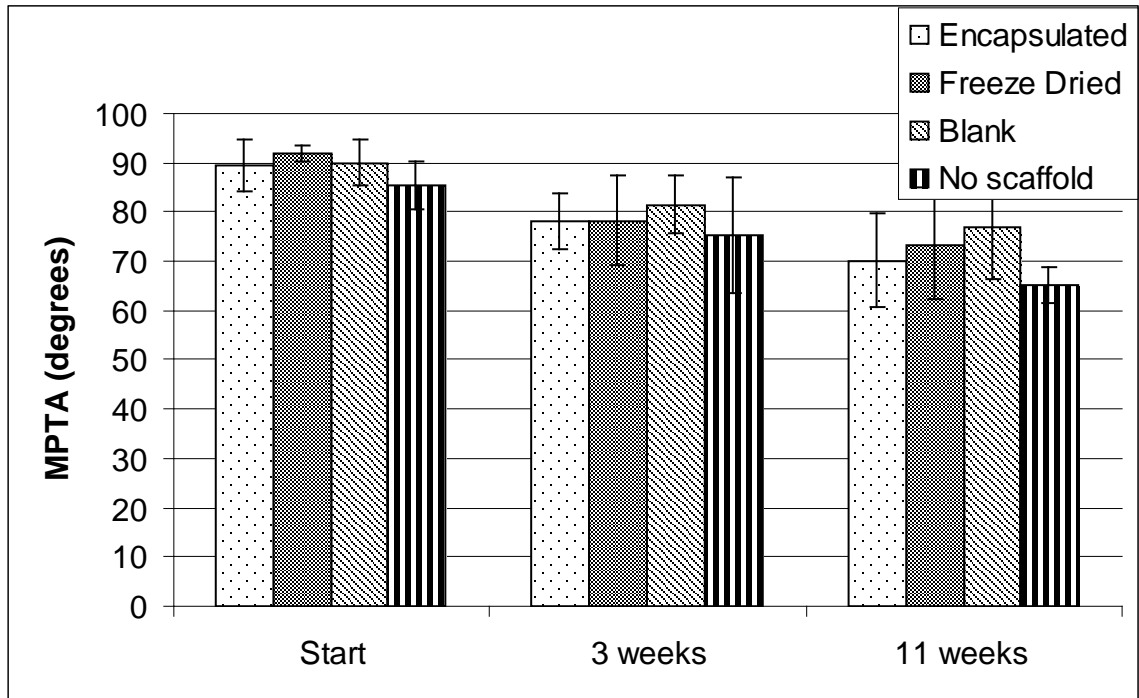
Figure 5.10 Medial proximal tibial angle at start of study, 3 weeks after growth plate injury and 8 weeks after implantation of scaffold

Figure 5.11 shows the lateral distal femoral angle for all 4 treatment groups at the start of the study, 3 weeks and 11 weeks after the physeal injury. There was no statistically significant difference in LDFA between any treatment groups at any particular time point (p-value > 0.05).
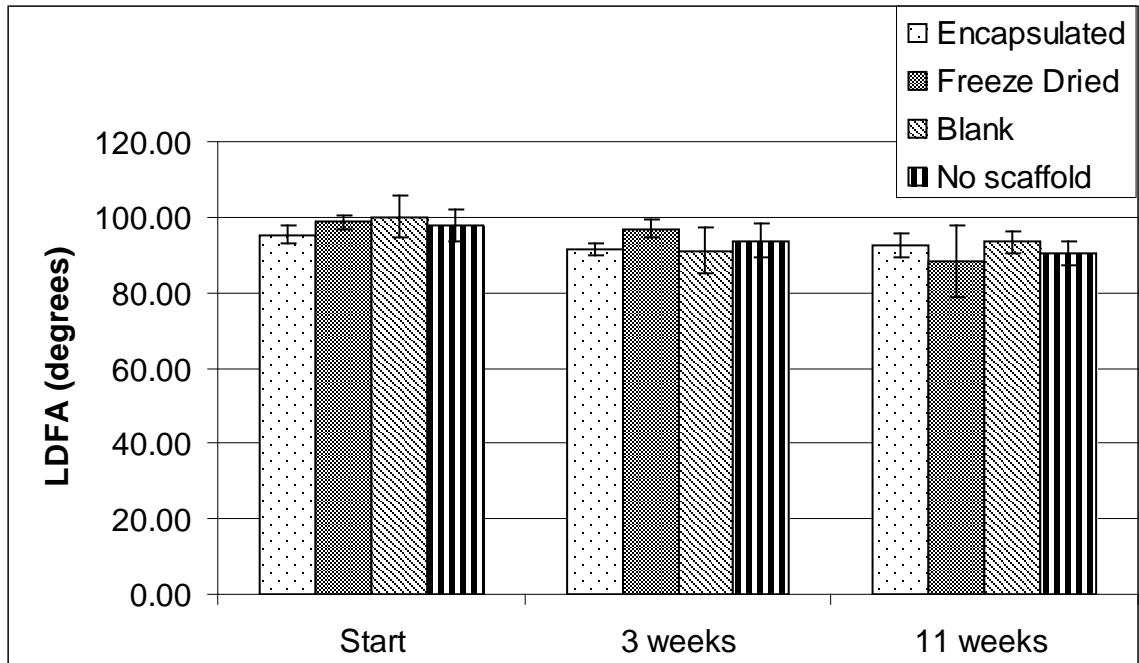
Figure 5.11 Lateral distal femoral angle at start of study, 3 weeks after growth plate injury and 8 weeks after implantation of scaffold

5.3.2 Tibia and fibula length measurements

Medial tibial length was compared across treatment groups to analyze the effect of treatment on restoration of medial tibial growth. The results can be seen in Figure 5.12. The average length of medial tibia was 94.49 mm for legs implanted with IGF-I DNA encapsulated scaffolds. The average medial tibial lengths were 90.87 mm, 91.64 mm and 91.52 mm for legs implanted with IGF-I DNA freeze dried scaffolds, blank scaffolds, and no scaffolds, respectively. Although medial tibial length was highest in the group that received IGF-I DNA encapsulated scaffolds, there was no significant difference in the length of medial tibia between treatment groups (p-value > 0.05). A sample size of 31/group is needed for getting p-value < 0.05 with a power of 80%.

Figure 5.13 shows the difference in length between lateral and medial tibia for each treatment group. This is an indicator of how much growth arrest was present in each limb because of the physeal damage/regeneration on the medial tibia. The mean difference in lateral and medial tibial length was 9.55 mm for IGF-I DNA encapsulated scaffold group, 8.49 mm for IGF-I DNA freeze dried scaffold group, 10.48 mm for blank scaffold group and 8.525 mm for the group that received no implants. There was no statistical difference in intra-tibial length inequality between the treatment groups (p-value > 0.05).

Width of the fibula at mid shaft was measured to look for signs of remodeling in fibula in response to the changes in tibia. The results can be seen in Figure 5.14.

100
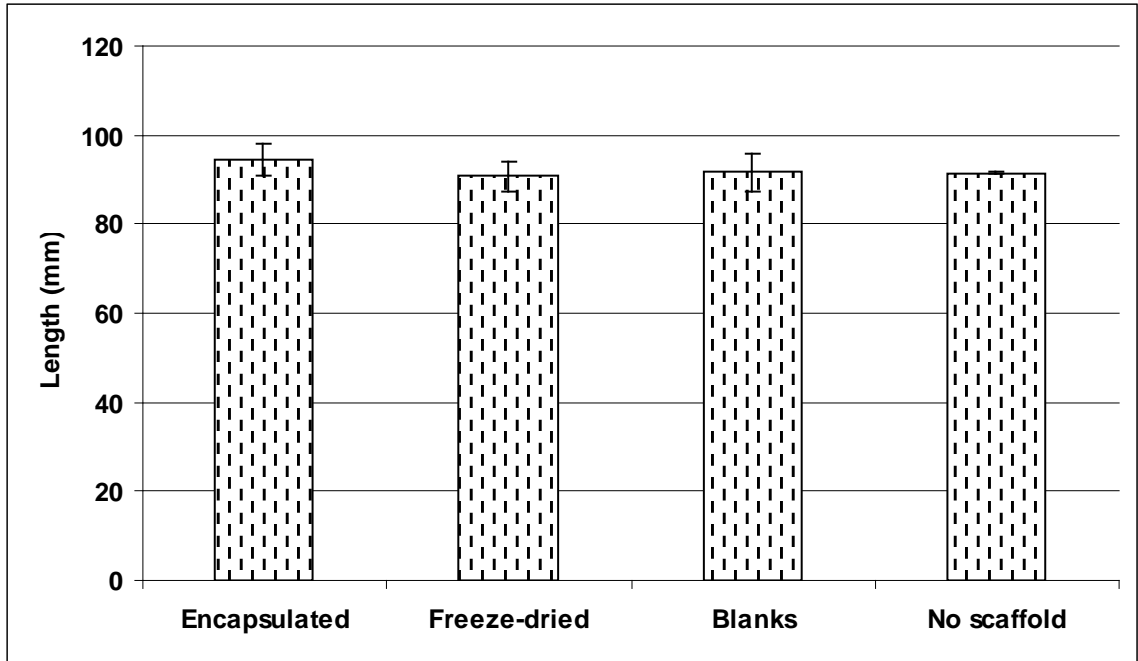
Figure 5.12 Medial tibial length 8 weeks after removal of bony bar and implantation of scaffolds
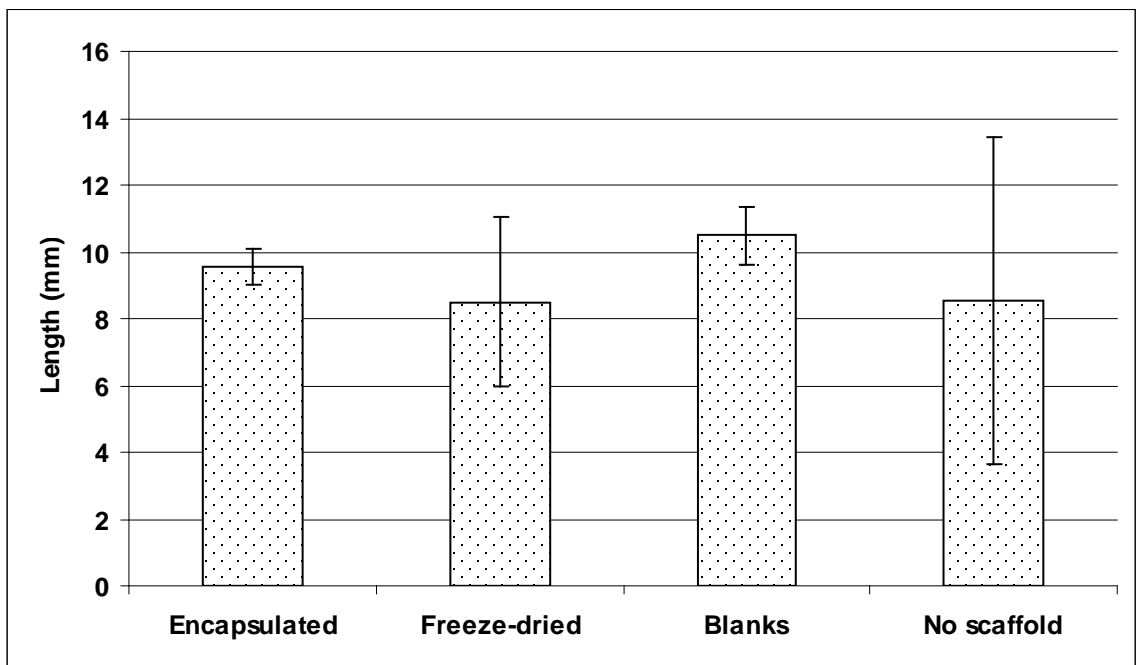
Figure 5.13 Lateral-medial tibial length 8 weeks after removal of boney bar and implantation of scaffolds

101
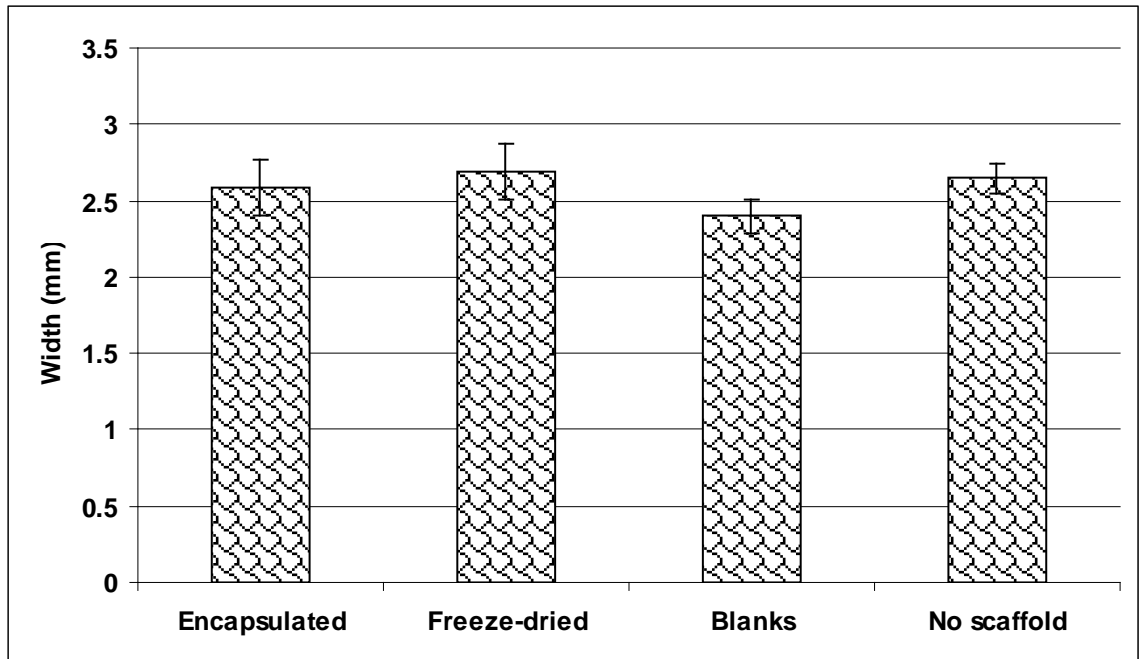
Figure 5.14 Width of fibula at mid-shaft 8 weeks after implantation of scaffolds in tibia

The average width of fibula was 2.58 mm, 2.69 mm, 2.4 mm, and 2.645 mm for IGF-I DNA encapsulated scaffolds, IGF-I DNA freeze dried scaffolds, blank scaffolds and no scaffold implantation, respectively. There was no significant difference in the width of fibula across treatment groups (p-value > 0.05).

5.3.3 Histology

5.3.3.1 No scaffold implantation

Figure 5.15 shows rabbit tibia cut in coronal plane 8 weeks after boney bar was removed and no scaffold was implanted. Remnant of growth plate can be seen in the lateral side, and bone has reformed in the region where the boney bar was removed in the medial side (arrow).
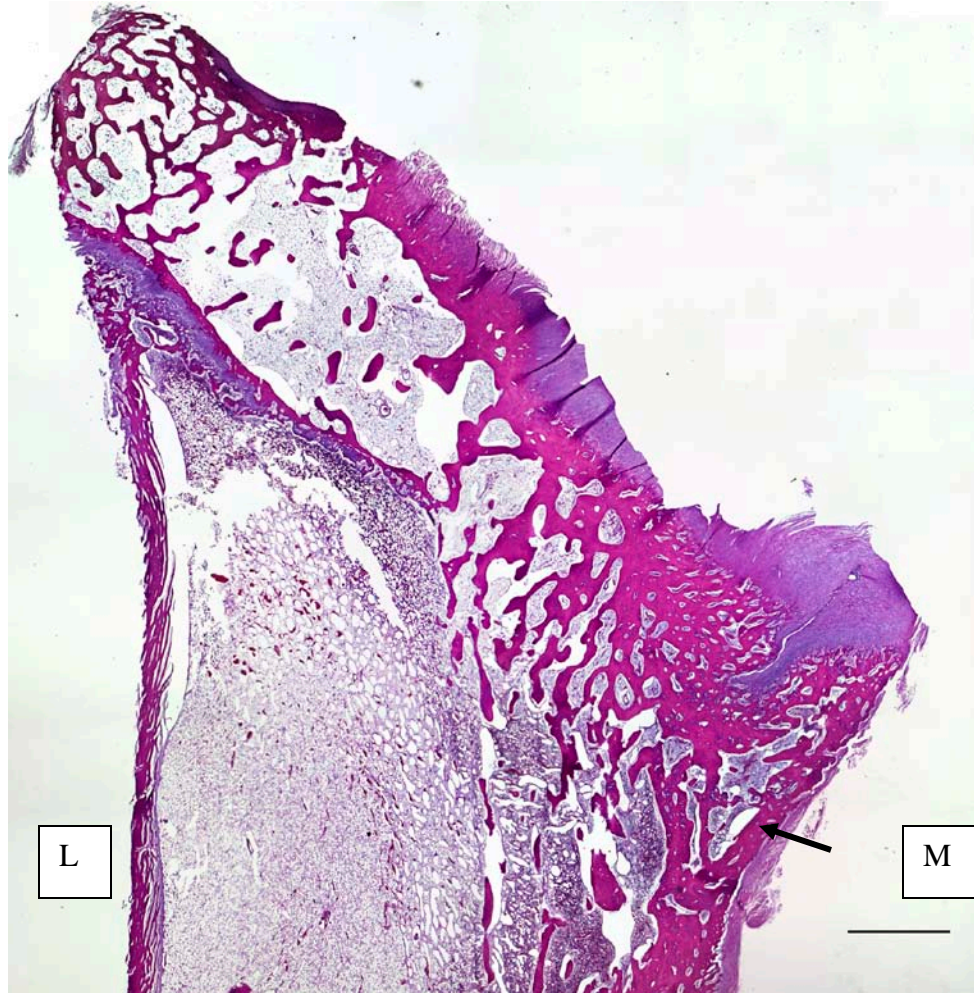
Figure 5.15 H&E stained coronal section of a rabbit medial proximal tibia 8 weeks after removal of boney bar with no scaffold implantation. Scale bar is 2 mm. Arrow indicates reformed bone. M and L denote medial and lateral

5.3.3.2 Blank scaffolds

Figure 5.16 shows an H&E stained proximal tibia, cut in coronal plane, 2 weeks after implantation of blank PLGA scaffold. Note the cartilaginous tissue seen in blue. The bulk of the newly formed tissue is towards the posterior of the section, where the scaffold was implanted. Figures 5.17 and 5.18 are higher magnifications from the same section. Figure 5.17 shows chondrocytes growing out of the growth plate (arrow). Note the nests of chondrocytes seen in Figure 5.18 (arrow).

Figure 5.16 H&E stained coronal section of rabbit proximal tibia 2 weeks after implantation of blank PLGA scaffold. Scale bar is 2 mm. M and L denote medial and lateral

104
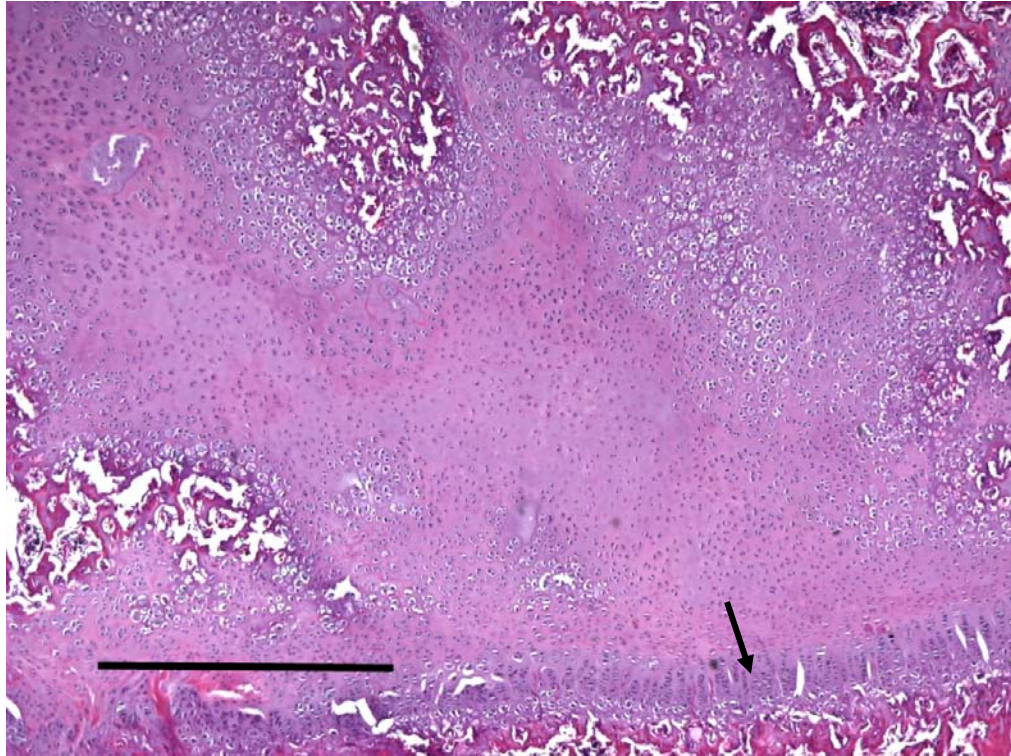
Figure 5.17 H&E stained section of rabbit proximal tibia 2 weeks after implantation of PLGA scaffold. Scale bar is 1mm. Arrow indicates growth plate
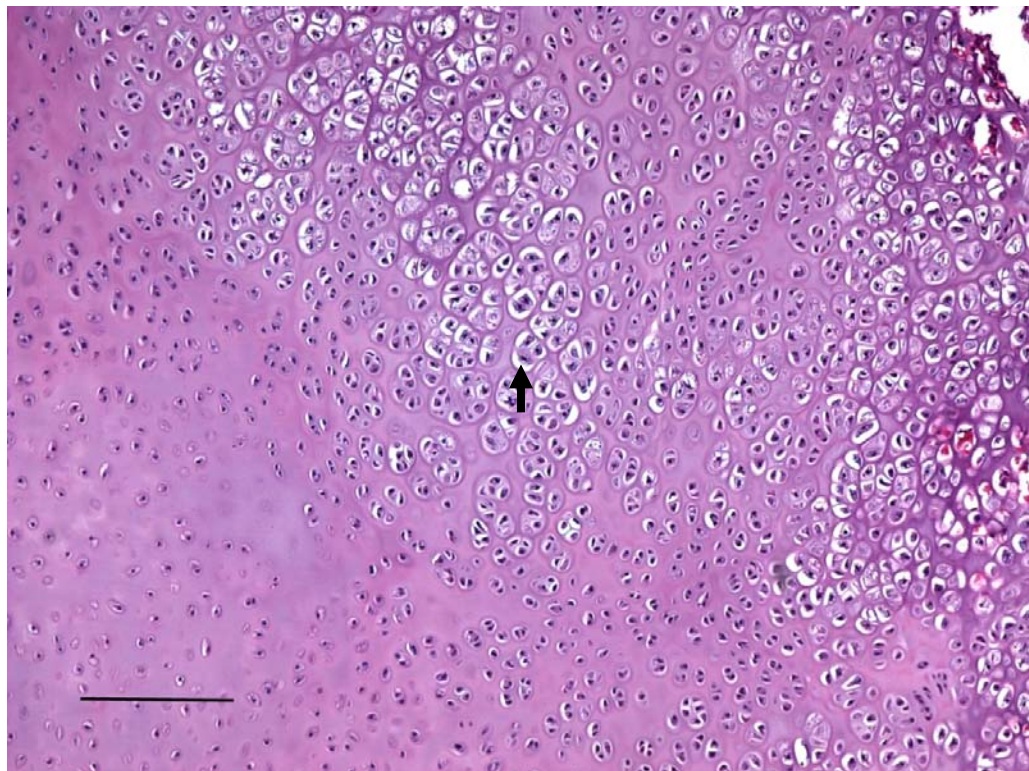
Figure 5.18 H&E stained section of rabbit proximal tibia 2 weeks after implantation of PLGA scaffold. Scale bar is 200 microns. Arrow indicates nest of chondrocyte

Figures 5.19 and 5.20 show sagittal sections of the medial proximal tibia of a rabbit 8 weeks after implantation of a hydrophilic scaffold. Note the cartilaginous region growing out of the remnants of growth plate in Figure 5.19. This cartilaginous region 8 weeks after implantation is significantly smaller compared to the 2 weeks time point seen in Figure 5.16. Figure 5.20 is a higher magnification of the same section that shows hypertrophic chondrocytes and nests of chondrocytes.

Figure 5.19 H&E stained sagittal section of rabbit medial proximal tibia 8 weeks after implantation of PLGA scaffold. Scale bar is 2 mm
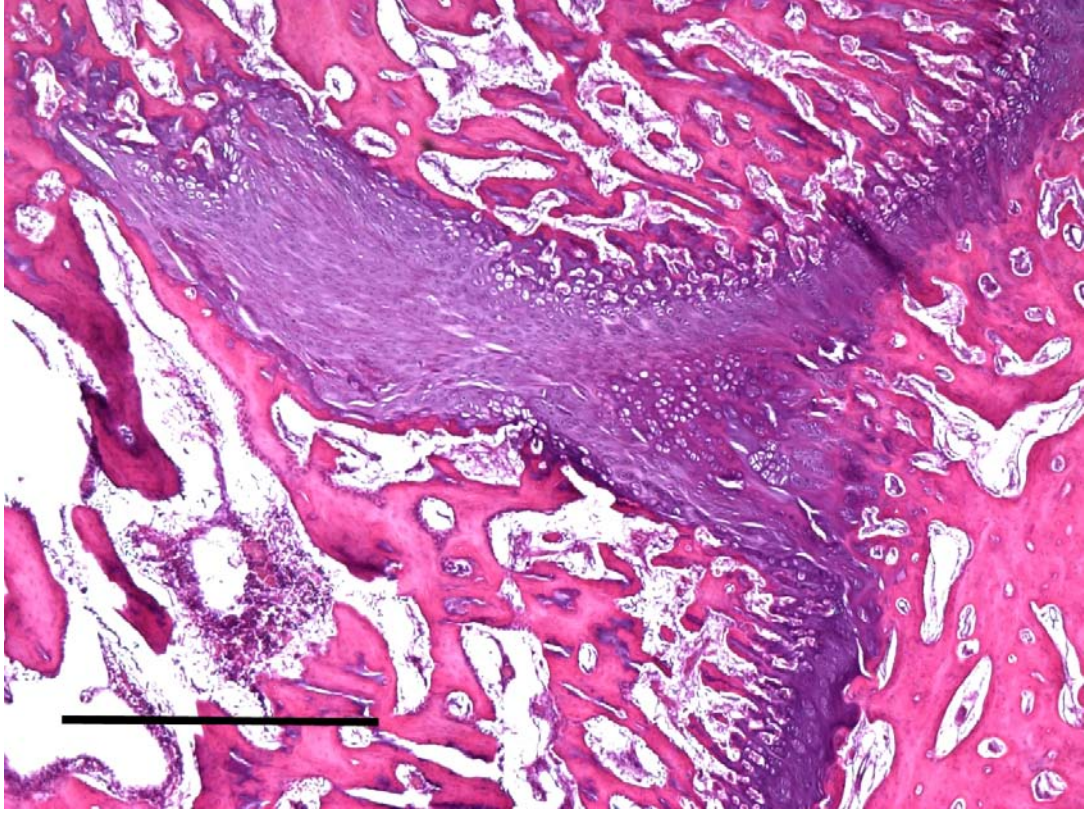
Figure 5.20 H&E stained section of rabbit medial proximal tibia 8 weeks after implantation of PLGA scaffold. Scale bar is 1 mm

Figures 5.21 and 5.22 are sagittal sections of medial proximal tibia from a rabbit 16 weeks after implantation of a hydrophilic PLGA scaffold. Notice the short band of growth plate remnant (arrow). No cartilaginous tissue is seen at the implant site on the other end. Figure 5.22 is a higher magnification of the same section showing the distorted remnant of growth plate. The distortion was caused by a collapse of tibial plateau after creation of growth plate injury.
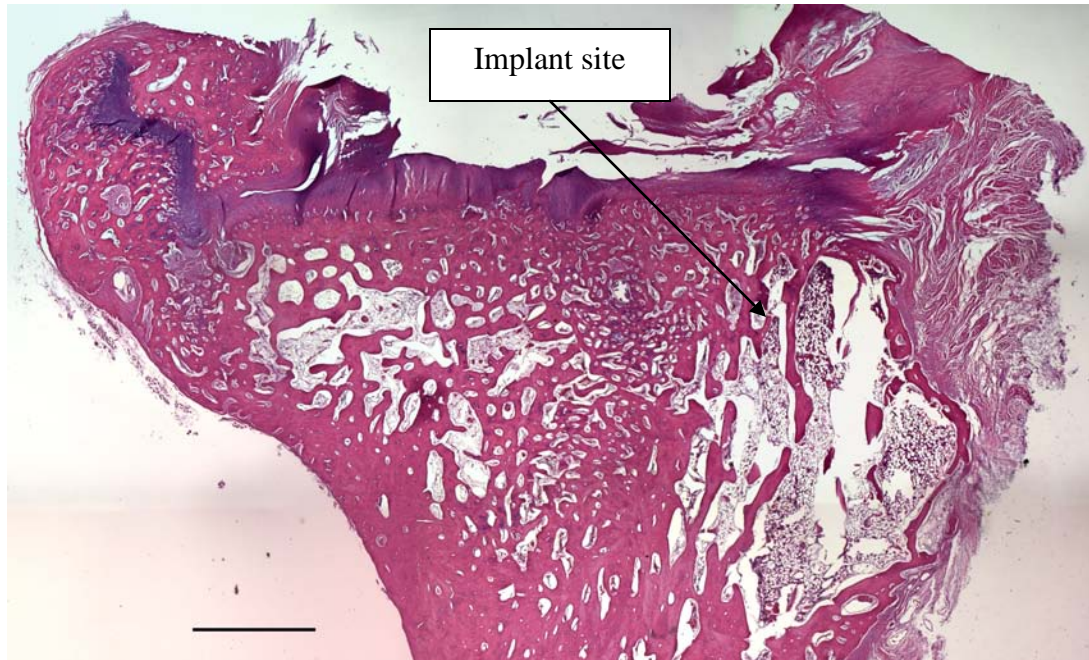
Figure 5.21 H&E stained sagittal section of rabbit medial proximal tibia 16 weeks after implantation of PLGA scaffold. Scale bar is 2 mm
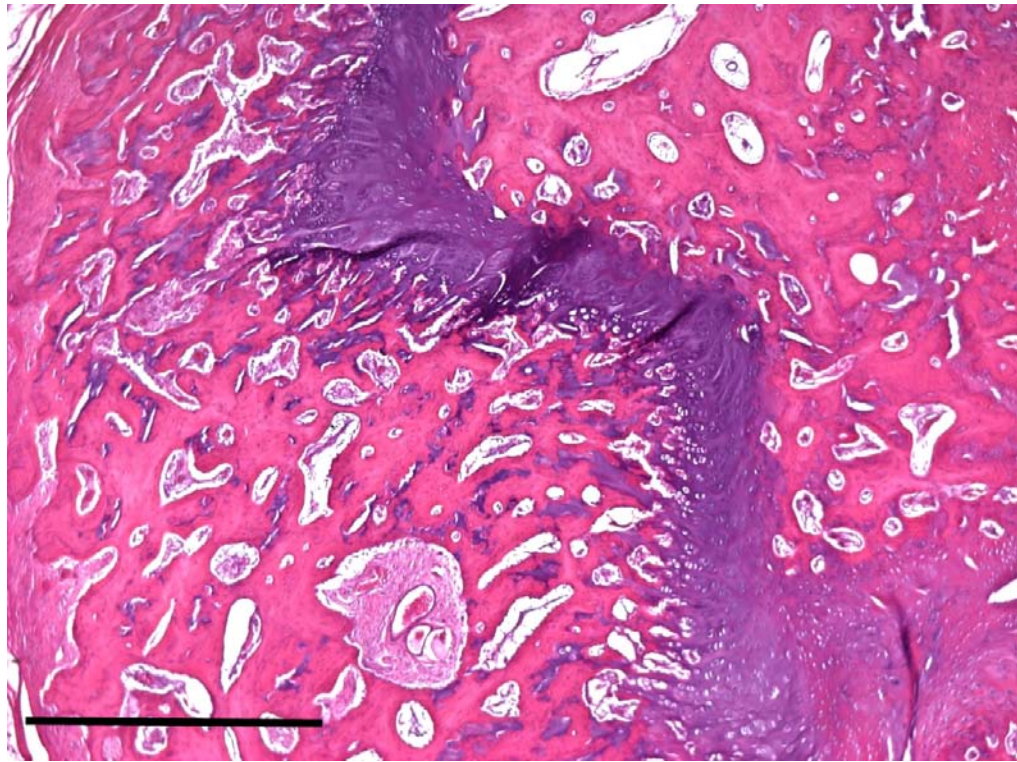
Figure 5.22 H&E stained section of rabbit medial proximal tibia 16 weeks after implantation of PLGA scaffold. Scale bar is 1 mm

108

5.3.3.3 IGF-I plasmid-releasing scaffolds

Figure 5.23 shows rabbit tibia cut in coronal plane 8 weeks after implantation of an IGF-I plasmid encapsulated scaffold. The remnant of growth plate can be seen to the right side of the image, while cartilaginous growth can be seen to the left side, where the scaffold was implanted (arrow). Figure 5.24 is a higher magnification of the cartilaginous region, that shows nests of chondrocytes. Figure 5.25 of the same region shows nests of chondrocytes, as well as growth-plate-like stacks of chondrocytes.
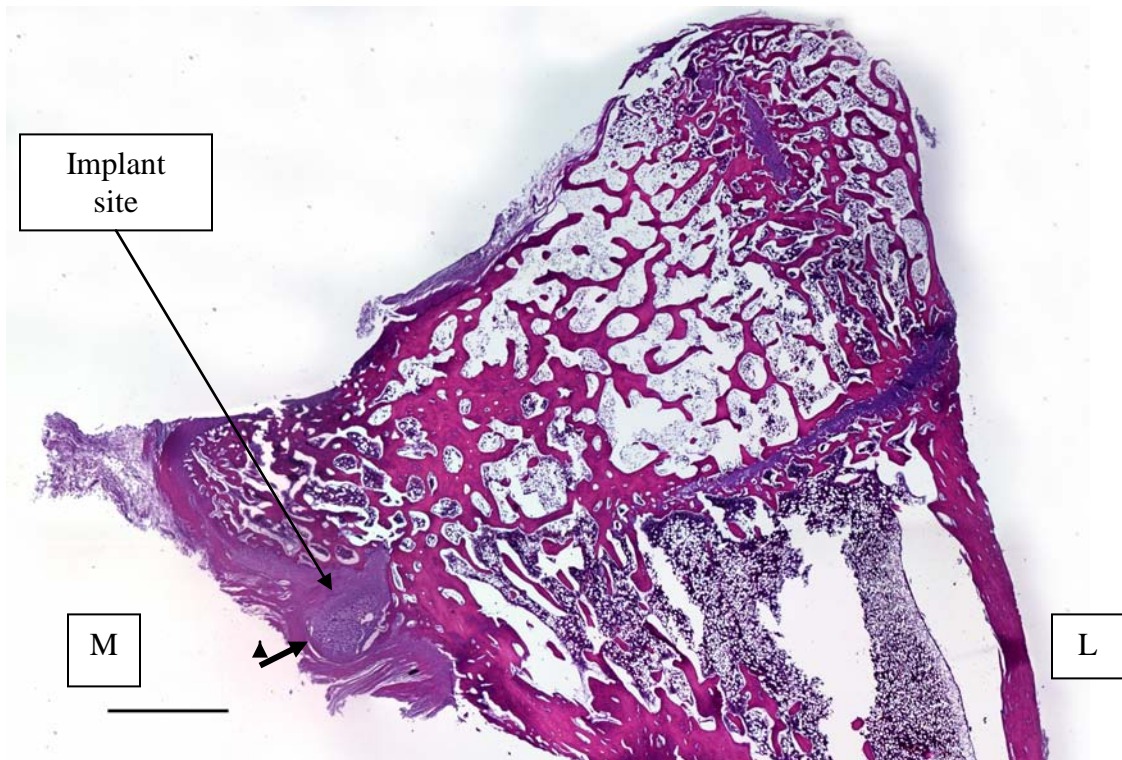
Figure 5.23 H&E stained coronal section of rabbit medial proximal tibia 8 weeks after implantation of an IGF-I plasmid encapsulated scaffold. Scale bar is 2 mm. Arrow indicates new cartilage. M and L denote medial and lateral
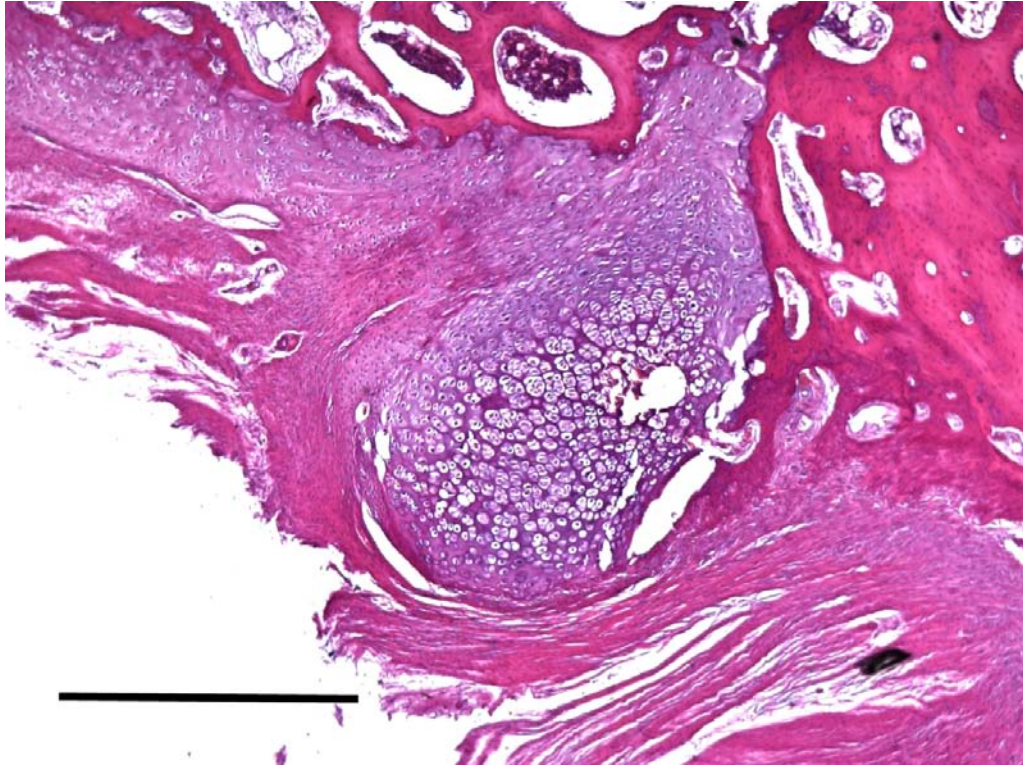
Figure 5.24 H&E stained section of rabbit medial proximal tibia 8 weeks after implantation of an IGF-I plasmid encapsulated scaffold. Scale bar is 1 mm

www.manaraa.com
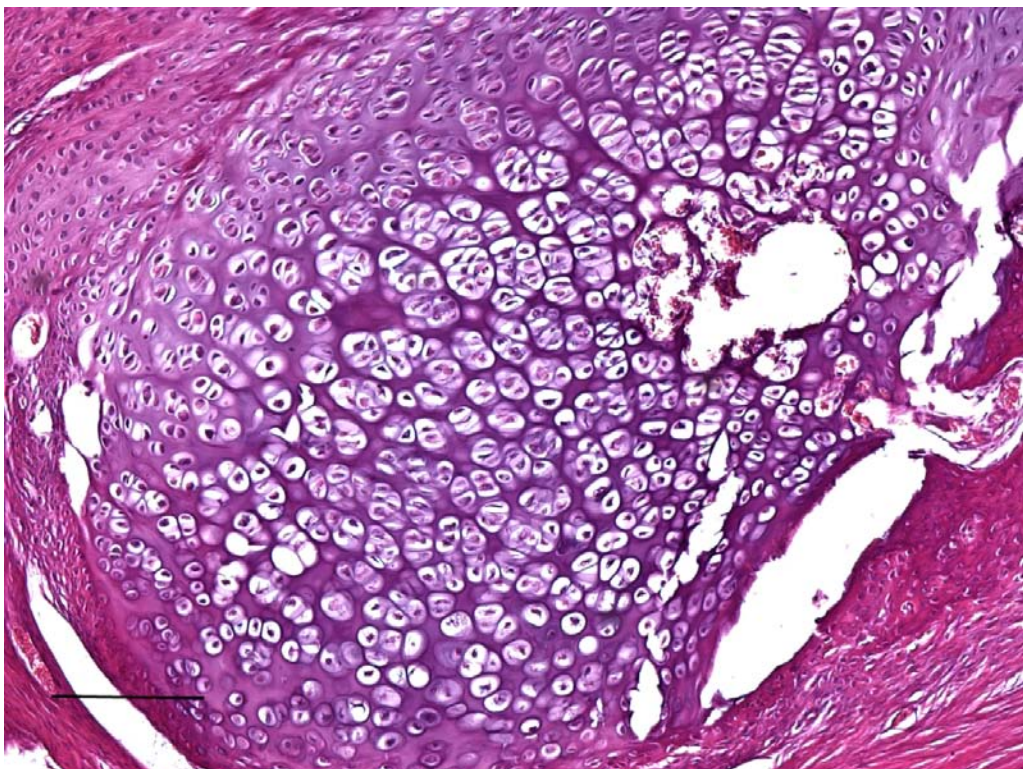
Figure 5.25 H&E stained section of rabbit medial proximal tibia 8 weeks after implantation of an IGF-I plasmid encapsulated scaffold. Scale bar is 200 microns

Figures 5.26 and 5.27 are safranin-O and fast-green stained sections of a rabbit medial proximal tibia 8 weeks after implantation of an IGF-I plasmid encapsulated scaffold. Intense staining is visible in the region where the scaffold was implanted. Nests and stacks of chondrocytes are visible in Figure 5.27 (arrows).
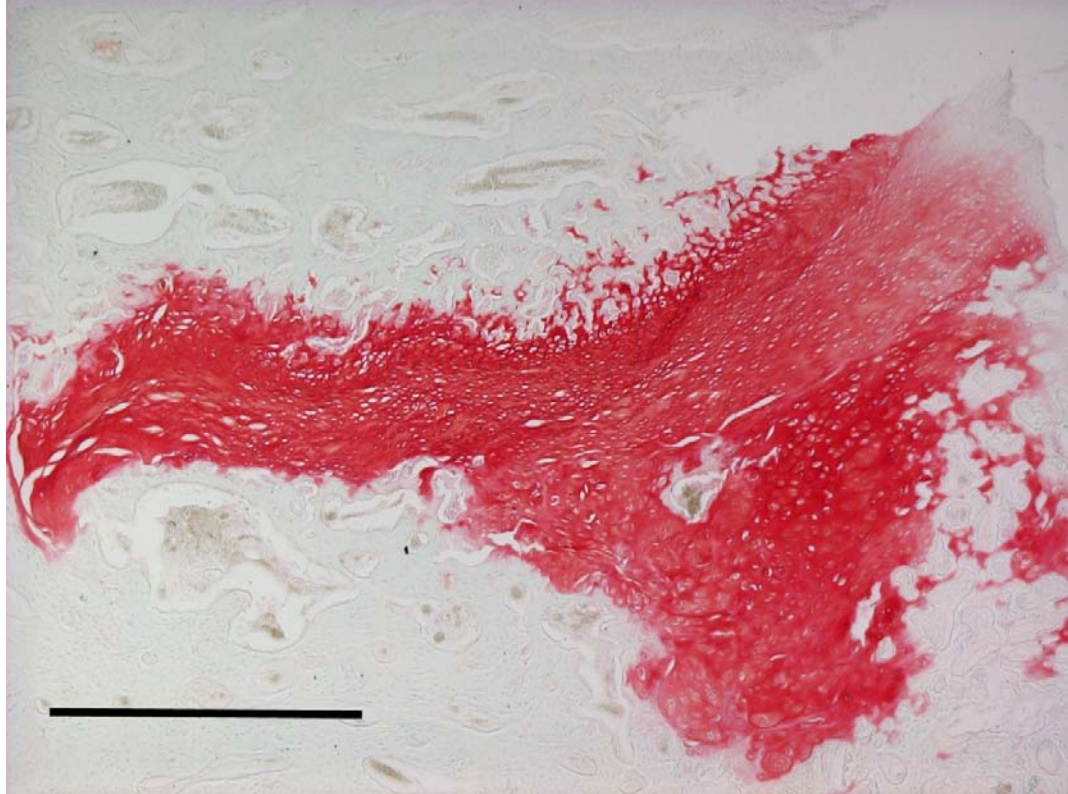
Figure 5.26 Safranin-O stained section of rabbit medial proximal tibia 8 weeks after implantation of an IGF-I plasmid encapsulated scaffold. Scale bar is 1 mm

111
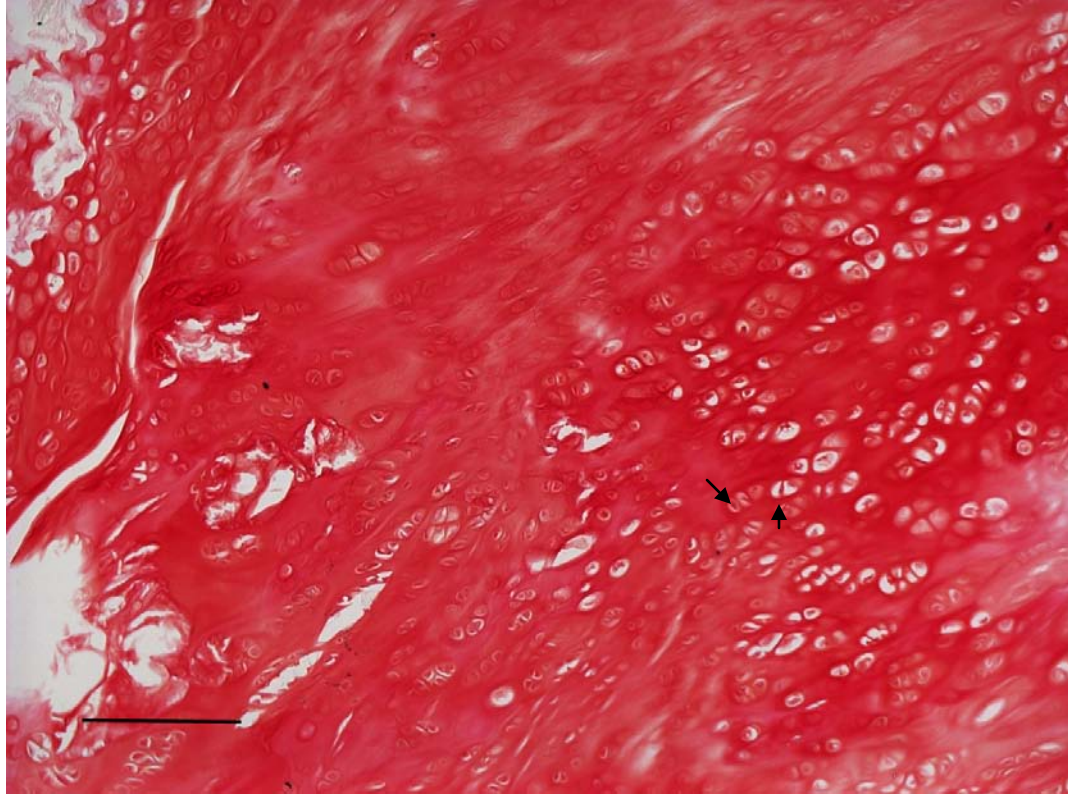
Figure 5.27 Safranin-O stained section of rabbit medial proximal tibia 8 weeks after implantation of an IGF-I plasmid encapsulated scaffold. Scale bar is 200 microns. Arrows indicates stacks of chondrocytes

Figure 5.28 shows rabbit tibia cut in coronal plane 8 weeks after implantation of an IGF-I plasmid freeze-dried scaffold. The remnant of growth plate can be seen to the right side of the image, while cartilaginous growth can be seen to the left side, where the scaffold was implanted. Figures 5.29 and 5.30 are higher magnifications of the same section that show hypertrophic chondrocytes as well as nests of chondrocytes in the implant region. Figure 5.31 is safranin-O and fast green stained section of cartilage formed after implantation of IGF-I plasmid freeze-dried scaffold. Intense staining for GAG is visible.
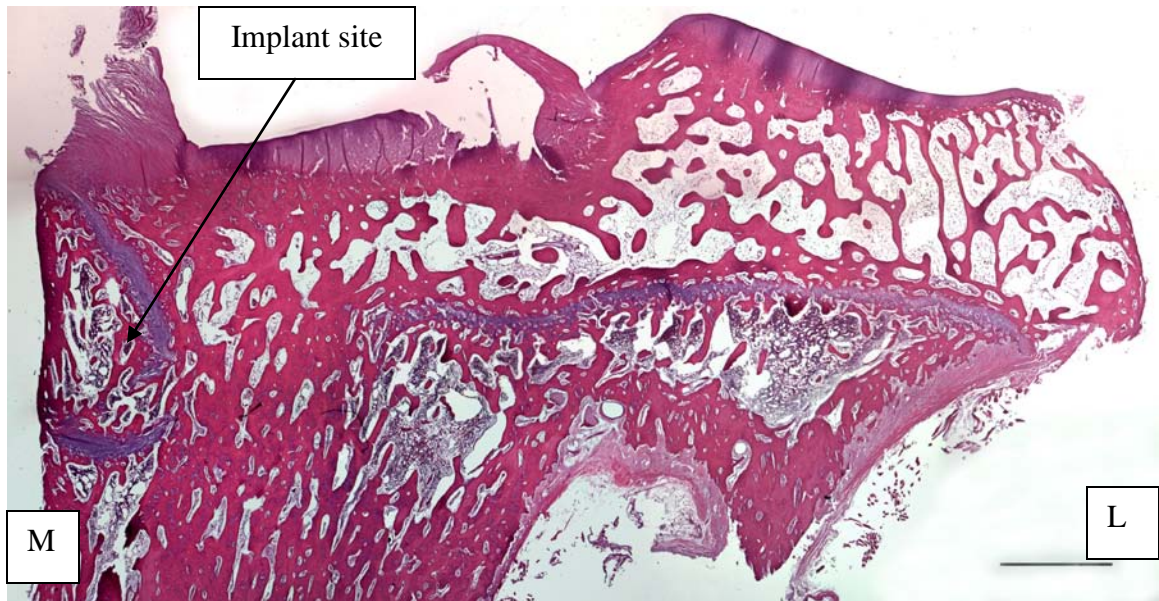
Figure 5.28 H&E stained coronal section of a rabbit medial proximal tibia 8 weeks after implantation of IGF-I plasmid freeze-dried scaffold. Scale bar is 2 mm. M and L denote medial and lateral
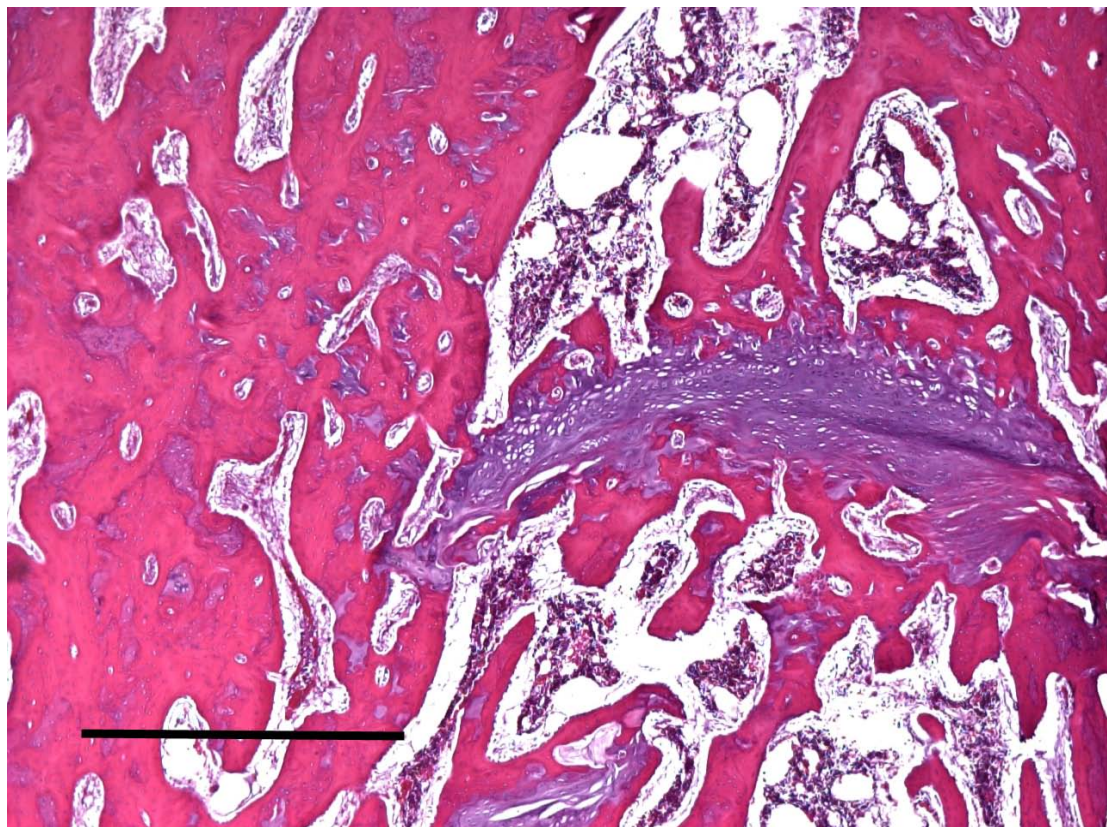
Figure 5.29 H&E stained section of a rabbit medial proximal tibia 8 weeks after implantation of IGF-I plasmid freeze-dried scaffold. Scale bar is 1 mm

113
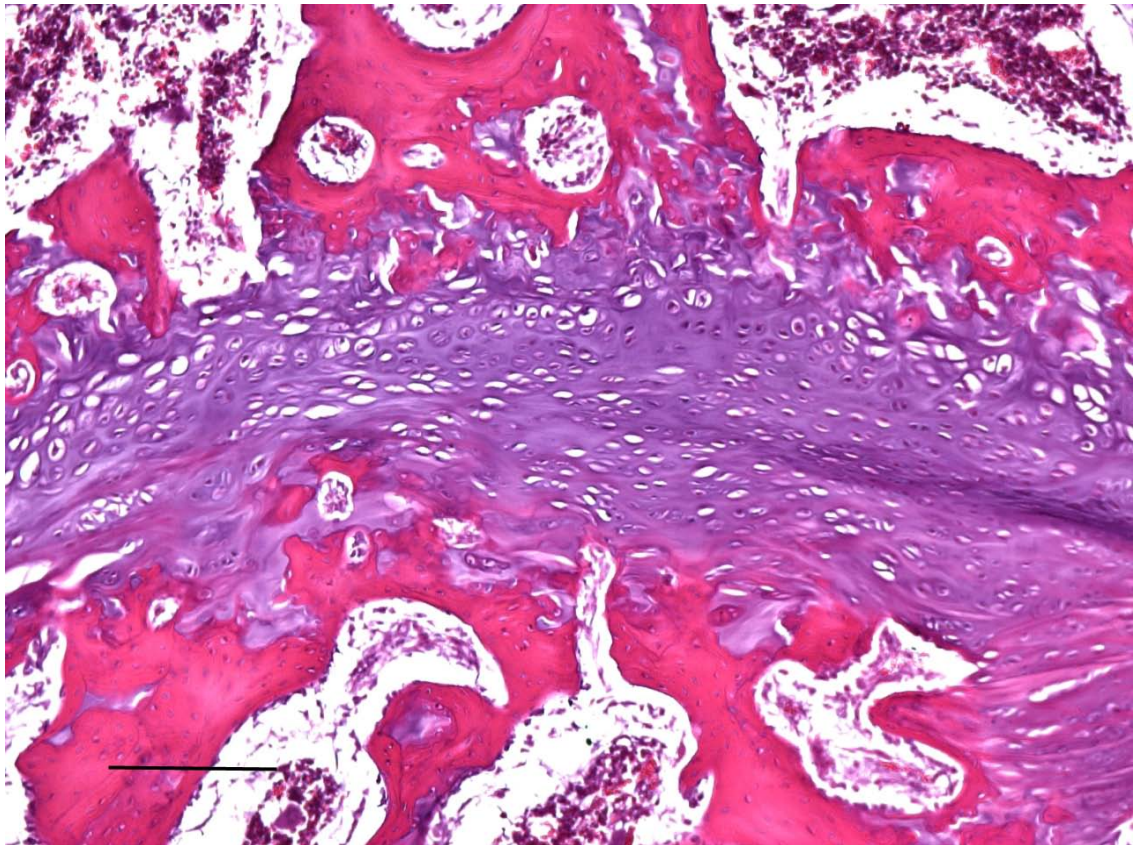
Figure 5.30 H&E stained section of a rabbit medial proximal tibia 8 weeks after implantation of IGF-I plasmid freeze-dried scaffold. Scale bar is 200 microns

114
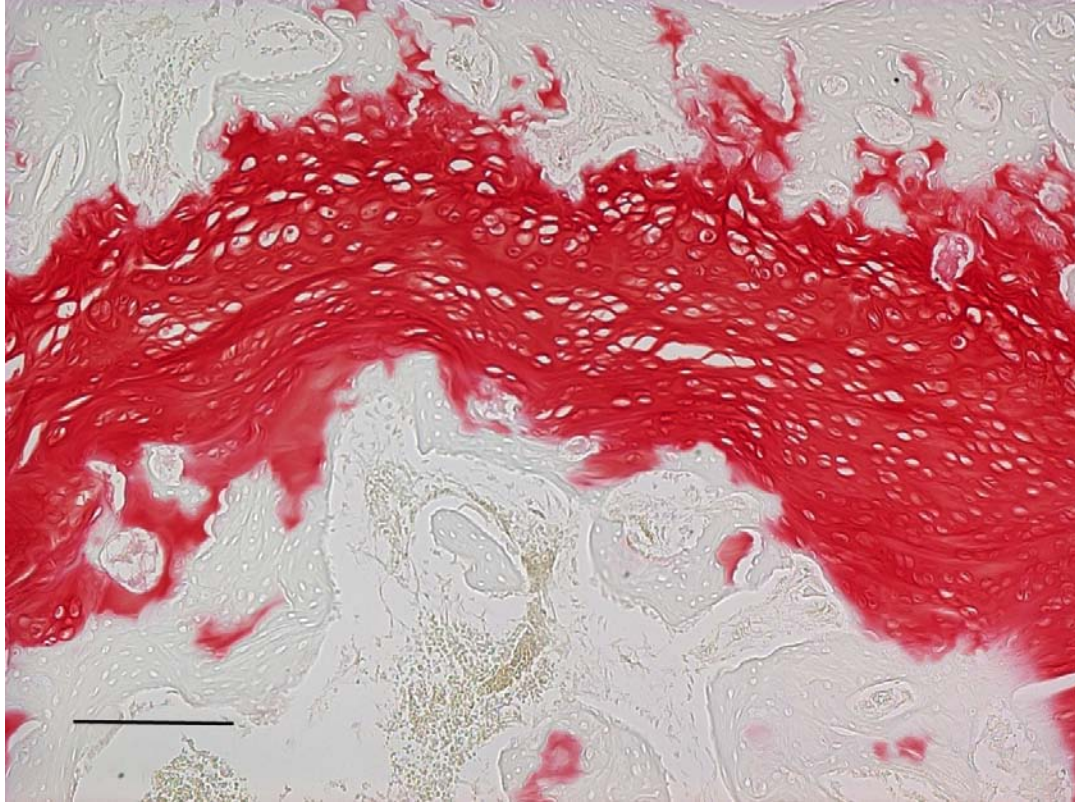
Figure 5.31 Safranin-O stained section of a rabbit medial proximal tibia 8 weeks after implantation of IGF-I plasmid freeze-dried scaffold. Scale bar is 200 microns

Figure 5.32 a shows rabbit tibia cut in coronal plane 8 weeks after implantation of a blank scaffold. The remnant of growth plate can be seen to the right side of the image, while no cartilage is seen to the left side, where the scaffold was implanted.
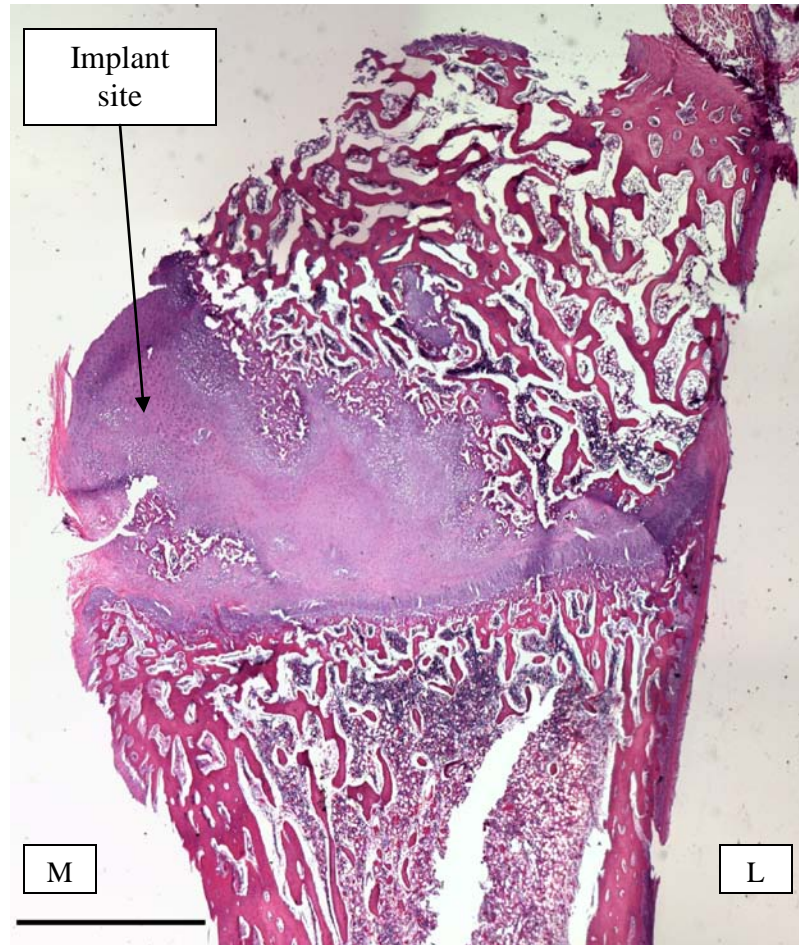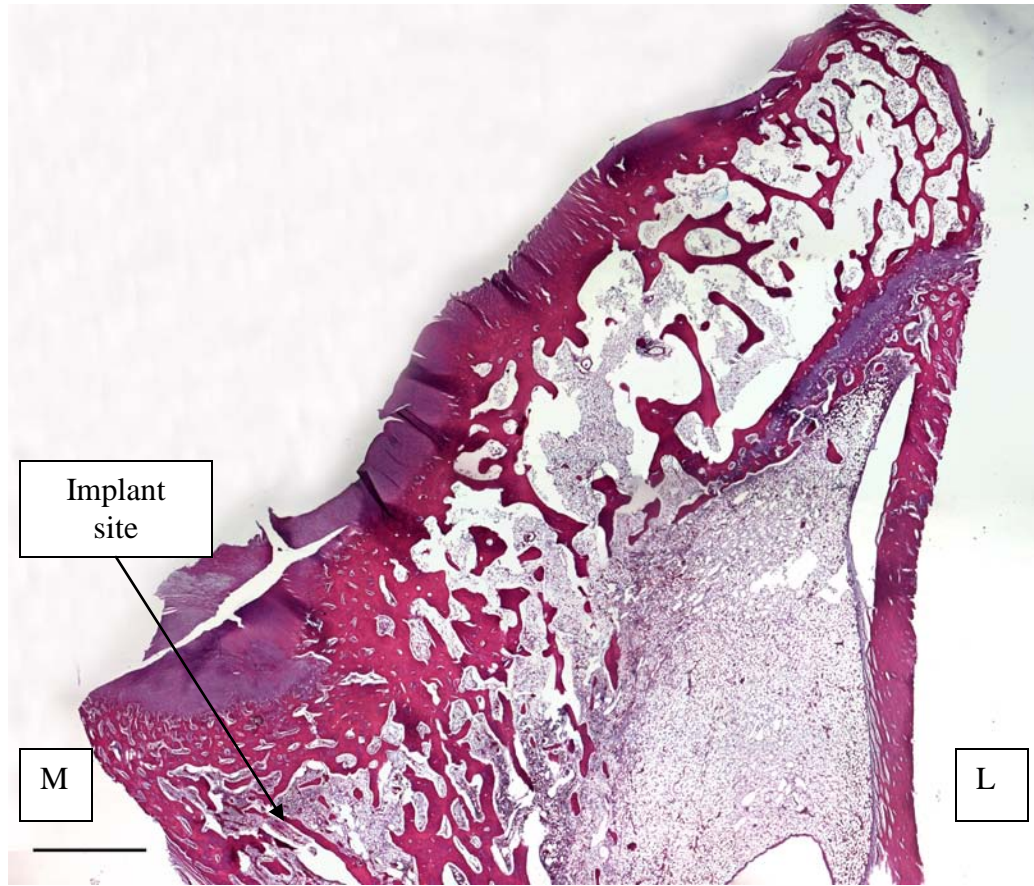
Figure 5.32 H&E stained coronal section of a rabbit medial proximal tibia 8 weeks after implantation of blank scaffold. Scale bar is 2 mm. M and L denote medial and lateral

<center>**5.4 DISCUSSION**</center>

5.4.1 Effect of treatment on correction of varus angular deformity

Growth plate injuries in children often heal with the formation of boney bars, and lead to life lasting consequences of varus deformity and limb length discrepancies unless surgically corrected. Polymer scaffolds have been used for the treatment of physeal injury in different animal models with varying degrees of success by several research groups. Implantation of a chitin fibrin mesh with pre-seeded mesenchymal stem cells in a rabbit model of physeal injury resulted in significantly lower tibiofemoral angle and limb length discrepancy at 16 weeks after implantation (Li, 2004). Implantation of mesenchymal stem cells embedded in agarose gel in a rabbit physeal injury model resulted in some correction of tibiofemoral angle and limb length discrepancy (Chen, 2003). Implantation of atelocollagen scaffolds with autologous chondrocytes into a rabbit physeal injury model resulted in significantly lower angular deformity, as determined by MPTA, compared to untreated defects and defects implanted with fat (Tobita, 2002).

To our knowledge, nobody has succeeded in showing significant morphometric improvements 8 weeks after treatment in an animal model without the use of cell-embedded scaffolds. In our study, implantation of IGF-I DNA freeze-dried PLGA scaffold after removal of boney bar resulted in a medial proximal tibial angle of 85.4º compared to 78.68º when a blank scaffold was inserted. Medial proximal tibial angle for legs with no scaffold implantation were between 69.54º and 62.87º, for IGF-I DNA encapsulated scaffolds between 60.78º and 79.56º, IGF-I DNA freeze-dried scaffolds between 65.60º and 85.40º, and blank scaffolds between 65.6º and 85.98º. It was observed that all treatment groups had at least one animal with significantly lesser residual angular deformity compared to the group that received no scaffold implants. However, as evident in Figures 3.10 and 3.11, when comparing the different treatment groups, no statistical difference was seen in either the medial proximal tibial angle or the lateral distal femoral angle. There are several contributing factors that might have led to this result.

All our angle measurements were done manually using low quality fluorographs, which increases the operator variability of measurements because of speculating the position of anatomical landmarks. We did not have access to a regular X-Ray machine to capture high quality radiographs until the end of this study, which precluded us from making better measurements of medial proximal tibial angles and lateral distal femoral angles.

Close examination of Figure 3.10 will reveal that the mean medial proximal tibial angle for the group that received no scaffolds was lower than the mean medial proximal tibial angle for all the other treatment groups. However this difference was not statistically significant. Our experimental design with three legs in each treatment group might have masked any benefit from treatment because of the low number of samples per group and the high variability between samples. Although variability in our angle measurements is comparable to what other similar studies have shown, the number of samples per group were much higher at 11 legs/treatment group (Lee, 2002; Planka, 2008), and 24 legs/treatment group (Li, 2004). Lateral distal femoral angle, did not show any statistical difference between treatment groups as expected, since no interventions were done on femurs. Absence of any significant differences in lateral distal femoral

<center>117</center>

angle also indicates that the varus was caused solely by the intra-limb length inequality of tibia.

5.4.2 Effect of treatment on correction of limb length inequality

We examined medial tibial lengths and the difference in lateral and medial length for each tibia to see the effect of treatment on correcting intra-limb and inter-limb length inequalities. When fat, silastic spacer, and physeal transplants were used to treat a rabbit model of physeal injury, no significant differences in lateral-medial tibial heights were seen compared to no treatment 8 weeks after resection of boney bars (Lee, 1993). Implantation of 0.3% agarose with autologous chondrocytes in a rabbit physeal injury model resulted in less difference between lateral and medial tibial lengths, compared to groups that received 0.3% agarose alone or no treatment (Lee, 1998). But it is not known if the difference was statistically significant. The results were similar when 0.3% agarose with MSCs were implanted to treat physeal injury, but the difference was still statistically insignificant (Chen, 2003). Hyaluronate-collagen scaffolds seeded with autologous MSCs were implanted into a rabbit femur physeal injury model, resulting in significantly longer femurs at 16 weeks compared to untreated contralateral femurs (Planka, 2008). Lateral-medial tibial length differences were significantly lower compared to untreated defects 52 weeks after implantation of atelocollagen gels with chondrocytes into physeal defects, but the difference was not significant at the 8 week time point after implantation (Tobita, 2002). These studies illustrate the lack of consistent positive results in the treatment of physeal injury animal models using various approaches.

In our study, we saw the highest medial tibial length in the group that was treated with IGF-I DNA encapsulated scaffolds. But, the difference in medial tibial length between treatment groups was not significant. Insufficient number of samples/group might have contributed to this result. Angular and length deformity resulting from an injured growth plate is progressive until the animal reaches skeletal maturity (Salter, 1963). This phenomenon can significantly influence the inference from interventions to treat growth plate injury, depending on the time point at which the morphometric measurements are taken relative to the age of skeletal maturity of the experimental animal. When comparing the results at different time points after implantation of atelocollagen gel with autologous chondrocytes, it was seen that the differences in angular deformity was significant at 24 weeks, but not 8 weeks after implantation of the scaffolds (Tobita, 2002). Similarly, limb length discrepancies for the treated and untreated groups increased at different rates, making the differences significant at 24 weeks, but not 8 weeks after implantation (Tobita, 2002).

New Zealand white rabbits reach skeletal maturity at 28 weeks, and reach adult lengths by 34 weeks of age (Masoud, 1986). Their mean tibial length reach 94% of the adult value by 16 weeks of age, with most tibial growth complete between 26 and 28 weeks (Masoud, 1986). More importantly, the mean age at proxibal tibial growth plate fusion was 25 weeks (Masoud, 1986). Thus, the rabbits used in our study would have had 6 to 11 weeks of tibial growth left after the time point at the experiment was terminated. Continued tibial growth during this time would have amplified the small difference in angular deformity and length difference between treatment groups that we now see at 8 weeks after implantation, and made them significant. This warrants further studies in

118

which morphometric measurements are made at multiple time points without sacrificing the animals, and continuing the study until the animals reach skeletal maturity.

We measured width of fibula to look for signs of remodeling due to alterations in load distribution in the lower limb that can happen because of changes in morphology of tibia. We did not see any patterns in the width of fibula, or any statistically significant differences between treatment groups. This can again be due to insufficient time for any such remodelling to have developed, or because of the quadruped nature of rabbits which reduces the load on hind limbs compared to bipedal animals.

5.4.3 Effect of PLGA scaffold implants on regenerated growth plate

5.4.3.1 No scaffolds and Blank scaffolds
We saw reformation of bone at the surgery site when no scaffold was implanted after removal of the boney bar.

We saw that cartilage had developed just 2 weeks after implantation in the area where a hydrophilic blank scaffold was implanted after resection of boney bar. Nests of chondrocytes were also observed. The newly formed cartilage was disorganized, and appeared to grow out of the remnants of native growth plate. We did not observe any growth plate-like columnar arrangement of chondrocytes in the newly formed cartilage. It is not surprising that we did not see any organized structure to the newly formed cartilage since the implanted scaffold did not have any chondrogenic growth factors to specifically stimulate the formation of a new growth plate. Newly formed cartilage after implantation of hyaluronate-collagen-MSC scaffolds to treat physeal injury in rabbits did not show any growth plate organization (Planka, 2008). But implantation of 0.3% agarose gel with MSC into a physeal defect resulted in physis-like columnar arrangement of chondrocytes in the newly formed physis (Chen, 2003). Growth plate-like columnar arrangement of chondrocytes was also seen when 0.3% agarose with embedded chondrocytes was used to treat physeal defects in rabbits (Lee, 1998).

The interpositional material used after removal of boney bar must remain in its original position, and in contact with metaphysis and epiphysis to prevent the reformation of a boney bar (Khoshhal, 2005). Mass loss studies using our scaffolds have shown previously that about 80% of their mass is lost within 4 weeks of immersion in PBS. The results that we saw from histological analysis of implant site also indicate that the implanted scaffold was quickly replaced by the newly formed tissue. We were unable to see remnants of our scaffold even at 2 weeks after implantation. PLGA has been shown to degrade faster in acidic environments, as would be the case at the implantation site. Decreased pH and cellular activity would have accelerated the degradation rate of our scaffolds after they were implanted in the rabbits. Scaffolds made of PLGA with a molecular weight of 110,000 degraded to half their volumes after implanted subcutaneously in mice for 8 weeks (Jeon, 2007). In contrast, the scaffolds used in our study had a molecular weight of 10,000.

5.4.3.2 IGF-I plasmid-releasing scaffolds
We were able to see several nests of chondrocytes as well as columnar arrangement of chondrocytes in the newly formed cartilage 8 weeks after removal of boney bar and implantation of an IGF-I encapsulated scaffold. The newly formed growth-

plate like structure was thicker than the remnant of the intact growth plate, and covered only a quarter of the area of the boney bar. It also lacked the level of organization seen in native growth plate cartilage. Nevertheless, this is the first time that anyone has shown growth-plate like columnar arrangement in regenerated growth plate without transplanting progenitor cells into the defect.

Implantation of IGF-I plasmid freeze-dried scaffold after removal of boney bar resulted in formation of cartilage with some nests of chondrocytes. The quality of cartilage was inferior to the one seen after implantation of IGF-I plasmid encapsulated scaffolds, as we did not see any growth plate-like stacks of chondrocytes in this case. It is possible that the cells could not be effectively transfected with the released PEI:DNA complexes from the scaffold as PEI:DNA complexes have been shown to aggregate at high concentrations (Huang, 2003).

We saw a decrease in the amount of cartilage at the implant site from 2 to 8 to 16 weeks after blank scaffolds were implanted. The area of newly formed cartilage at 8 weeks was much smaller compared to the cartilaginous area at 2 weeks after implantation. At 16 weeks, almost no cartilaginous region was seen, having been completely replaced by trabecular bone. Even when IGF-I plasmid releasing scaffolds were implanted, very little cartilaginous tissue was seen at the implant site 8 weeks after the scaffold was implanted. This progressive decrease in the amount of cartilage at the implant site might have been because of the normal process of endochondral ossification that progressively replaced newly formed cartilage with trabecular bone. Similar progressive decrease in the amount of newly formed cartilage was seen when atelocollagen gel with chondrocytes were implanted to treat physeal injury (Tobita, 2002). The amount of newly synthesized cartilage on PLGA scaffolds decreased at 12 weeks compared to 8 weeks after subcutaneous implantation in mice, and was almost completely absent at 16 weeks (Jeon, 2007). Even when adIGF-I injected muscle was implanted after removal of boney bar in rabbits, the resultant cartilage lost its columnar appearance by 12 weeks compared to 8 weeks (Lee, 2002).

In order for any intervention to be effective in treating angular and length discrepancies after removal of boney bars, it should be able to maintain the newly formed growth plate/cartilage until such time as the physiological fusion of native growth plate. In fact, reformation of boney bars or secondary tethers after removal of boney bars was the most common mechanism of treatment failure in human subjects (Hasler, 2002).

5.5 CONCLUSION

Removal of boney bar and implantation of IGF-I plasmid-releasing PLGA scaffolds in an animal model of growth plate injury resulted in some improvement of MPTA compared to no scaffold implantation. Medial tibial length was also higher for the scaffold implanted group compared to no scaffold implantation after removal of boney bars. These differences were not statistically significant partly because of insufficient number of animals in each experimental group. Histological analysis of the newly developed cartilage showed growth plate-like columnar arrangement of chondrocytes in an animal that received IGF-I plasmid encapsulated scaffold. Although the newly formed cartilage lacked the level of organization seen in native growth plate, we are the first ones to report the regeneration of growth plate-like structure without the use of stem cells in an animal model of growth plate injury. Histological evaluation suggests that, although we were successful in creating growth plate-like structure using our scaffolds after removal of boney bars, the benefits were quickly lost as the newly formed cartilage was replaced by trabecular bone. Future approaches to regenerate the growth plate might benefit from the sustained presence of IGF-I at the injury site, and scaffolds made of materials that last longer in vivo, and thus sustain the newly formed growth plate until the animals reach skeletal maturity.

6. SUMMARY AND CONCLUSIONS

Controlled release of naked and PEI:DNA complexes was achieved from porous PLGA scaffolds. PEI affected release of complexes from PLGA scaffolds, as PEI:DNA complexes were released at a lower rate compared to naked DNA from low molecular weight and high molecular weight PLGA scaffolds, as well as hydrophilic and hydrophobic PLGA scaffolds. Hydrophilicity and molecular weight of PLGA had effects on the release profiles of both naked DNA and PEI:DNA complexes from the scaffolds, as evidenced by later peak naked DNA and PEI:DNA release with increasing hydrophilicity and molecular weight. Compressive modulus and ultimate strength for high molecular weight PLGA scaffolds were significantly higher than low molecular weight PLGA scaffolds. Porous scaffolds made of PLGA with the right hydrophobicity and molecular weight will allow us to tailor degradation profiles and mechanical properties of these scaffolds for controlled delivery of naked and condensed plasmid DNA in tissue engineering applications.

Low molecular weight hydrophilic PLGA scaffolds supported the growth and differentiation of mesenchymal multipotent D1 cells, chondrocytes and bone marrow cells in vitro. Suspension of cells in fibrin prior to seeding resulted in significant differences in total GAG and GAG/DNA contents between IGF-I treated and control groups for mesenchymal stem cells, bone marrow cells and chondrocytes, whereas the differences were not significant when cultured on scaffolds without fibrin. This proved that fibrin was critical in the differentiation of the cells into chondrogenic phenotype, probably by retaining seeded cells within the scaffold and thus increasing cell density, as well as encapsulating the cells in a three dimensional environment. Culturing BMCs on IGF-I plasmid encapsulated scaffolds resulted in elevated expression of rhIGF-I compared to blank and IGF-I plasmid freeze-dried scaffolds. Although the amount of IGF-I produced was not statistically significant compared to controls, sample size calculations suggested that increasing the number of samples to 4/group can make the difference statistically significant. Bone marrow cells cultured on the IGF-I plasmid encapsulated scaffolds showed the highest DNA content among all the groups. Total GAG was higher for all plasmid-releasing scaffolds compared to the blank scaffolds, but these differences were not statistically significant. Low exposure to IGF-I released from transfected cells might have been the reason for the inability to observe significant chondrocytic differentiation in bone marrow cells seeded on IGF-I plasmid-releasing scaffolds. Using scaffolds made from higher molecular weight hydrophilic PLGA to culture cells, along with increasing the amount of IGF-I secreted can increase the exposure of cells to IGF-I, and might result in successful chondrogenesis using bone marrow progenitor cells.

Removal of boney bar and implantation of IGF-I plasmid-releasing PLGA scaffolds in an animal model of growth plate injury resulted in some improvement of MPTA compared to no scaffold implantation. Medial tibial length was also higher for the scaffold implanted group compared to no scaffold implantation after removal of boney bars. These differences were not statistically significant partly because of insufficient number of animals in each experimental group. Histological analysis of the newly developed cartilage showed growth plate-like columnar arrangement of chondrocytes in an animal that received IGF-I plasmid encapsulated scaffold, even though the level of

122

organization of this newly formed cartilage was inferior to that of native growth plate. We are the first ones to report the regeneration of growth plate-like structure without the use of stem cells in an animal model of growth plate injury. Histological evaluation suggests that although we were successful in creating growth plate-like structure using our scaffolds after removal of boney bars, the benefits were quickly lost as the newly formed cartilage was replaced by trabecular bone. Future approaches to regenerate the growth plate might benefit from the sustained presence of IGF-I at the injury site, and scaffolds made of higher molecular weight PLGA, and thus sustain the newly formed growth plate until the animals reach skeletal maturity.

123

References:

Agrawal, C. M. and R. B. Ray (2001). "Biodegradable polymeric scaffolds for musculoskeletal tissue engineering." J Biomed Mater Res **55**(2): 141-50.

An, Y. H., S. K. Woolf and R. J. Friedman (2000). "Pre-clinical in vivo evaluation of orthopaedic bioabsorbable devices." Biomaterials **21**(24): 2635-52.

Athanasiou, K. A., G. G. Niederauer and C. M. Agrawal (1996). "Sterilization, toxicity, biocompatibility and clinical applications of polylactic acid/polyglycolic acid copolymers." Biomaterials **17**(2): 93-102.

Ballock R. T., O'Keefe R. J., "Growth and development of the skeleton" in Orthopedic Basic Science: Foundations of Clinical Practice. Einhorn T. A., O'Keefe R. J., Buckwalter J. A., Eds. Ed 3, American Academy of Orthopedic Surgeons, Rosemount, IL, 2007.

Beier, F. (2005). "Cell-cycle control and the cartilage growth plate." J Cell Physiol **202**(1): 1-8.

Benya, P. D. and J. D. Shaffer (1982). "Dedifferentiated chondrocytes reexpress the differentiated collagen phenotype when cultured in agarose gels." Cell **30**(1): 215-24.

Bieber, T., W. Meissner, S. Kostin, A. Niemann and H. P. Elsasser (2002). "Intracellular route and transcriptional competence of polyethylenimine-DNA complexes." J Control Release **82**(2-3): 441-54.

Binette, F., D. P. McQuaid, D. R. Haudenschild, P. C. Yaeger, J. M. McPherson and R. Tubo (1998). "Expression of a stable articular cartilage phenotype without evidence of hypertrophy by adult human articular chondrocytes in vitro." J Orthop Res **16**(2): 207-16.

Boussif, O., F. Lezoualc'h, M. A. Zanta, M. D. Mergny, D. Scherman, B. Demeneix and J. P. Behr (1995). "A versatile vector for gene and oligonucleotide transfer into cells in culture and in vivo: polyethylenimine." Proc Natl Acad Sci U S A **92**(16): 7297-301.

Boyan, B. D., Z. Schwartz, D. L. Carnes, Jr. and V. Ramirez (1988). "The effects of vitamin D metabolites on the plasma and matrix vesicle membranes of growth and resting cartilage cells in vitro." Endocrinology **122**(6): 2851-60.

Brannon-Peppas L, Peppas NA et al. (1989). "Solute and penetrant diffusion in swellable polymers IX: the mechanisms of drug release from pH-sensitive swelling controlled systems." J Control Rel **8**:267-74.

Brazel, C. S. and N. A. Peppas (1999). "Dimensionless analysis of swelling of hydrophilic glassy polymers with subsequent drug release from relaxing structures." Biomaterials **20**(8): 721-32.

Buschmann, M. D. and A. J. Grodzinsky (1995). "A molecular model of proteoglycan-associated electrostatic forces in cartilage mechanics." J Biomech Eng **117**(2): 179-92.

Capan, Y., G. Jiang, S. Giovagnoli, K. H. Na and P. P. DeLuca (2003). "Preparation and characterization of poly(D,L-lactide-co-glycolide) microspheres for controlled release of human growth hormone." AAPS PharmSciTech **4**(2): E28.

Capan, Y., B. H. Woo, S. Gebrekidan, S. Ahmed and P. P. DeLuca (1999). "Influence of formulation parameters on the characteristics of poly(D, L-lactide-co-glycolide) microspheres containing poly(L-lysine) complexed plasmid DNA." J Control Release **60**(2-3): 279-86.

Capito, R. M. and M. Spector (2007). "Collagen scaffolds for nonviral IGF-1 gene delivery in articular cartilage tissue engineering." Gene Ther **14**(9): 721-32.

Chen, F., J. H. Hui, W. K. Chan and E. H. Lee (2003). "Cultured mesenchymal stem cell transfers in the treatment of partial growth arrest." J Pediatr Orthop **23**(4): 425-9.

Chen, G., D. Liu, M. Tadokoro, R. Hirochika, H. Ohgushi, J. Tanaka and T. Tateishi (2004). "Chondrogenic differentiation of human mesenchymal stem cells cultured in a cobweb-like biodegradable scaffold." Biochem Biophys Res Commun **322**(1): 50-5.

Choi, S. J., K. Na, S. Kim, D. G. Woo, B. K. Sun, H. M. Chung and K. H. Park (2007). "Combination of ascorbate and growth factor (TGF beta-3) in thermo-reversible hydrogel constructs embedded with rabbit chondrocytes for neocartilage formation." J Biomed Mater Res A **83**(4): 897-905.

Chou, C. H., W. T. Cheng, T. F. Kuo, J. S. Sun, F. H. Lin and J. C. Tsai (2007). "Fibrin glue mixed with gelatin/hyaluronic acid/chondroitin-6-sulfate tri-copolymer for articular cartilage tissue engineering: the results of real-time polymerase chain reaction." J Biomed Mater Res A **82**(3): 757-67.

Chun, K. W., K. C. Cho, S. H. Kim, J. H. Jeong and T. G. Park (2004). "Controlled release of plasmid DNA from biodegradable scaffolds fabricated using a thermally-induced phase-separation method." J Biomater Sci Polym Ed **15**(11): 1341-53.

Chung, R., J. C. Cool, M. A. Scherer, B. K. Foster and C. J. Xian (2006). "Roles of neutrophil-mediated inflammatory response in the bony repair of injured growth plate cartilage in young rats." J Leukoc Biol **80**(6): 1272-80.

Clamme, J. P., G. Krishnamoorthy and Y. Mely (2003). "Intracellular dynamics of the gene delivery vehicle polyethylenimine during transfection: investigation by two-photon fluorescence correlation spectroscopy." Biochim Biophys Acta **1617**(1-2): 52-61.

Clamme, J. P., J. Azoulay and Y. Mely (2003b). "Monitoring of the formation and

dissociation of polyethylenimine/DNA complexes by two photon fluorescence correlation spectroscopy." <u>Biophys J</u> **84**(3): 1960-8.

Colnot, C. (2005). "Cellular and molecular interactions regulating skeletogenesis." <u>J Cell Biochem</u> **95**(4): 688-97.

Colnot, C. I. and J. A. Helms (2001). "A molecular analysis of matrix remodeling and angiogenesis during long bone development." <u>Mech Dev</u> **100**(2): 245-50.

Cournil-Henrionnet, C., C. Huselstein, Y. Wang, L. Galois, D. Mainard, V. Decot, P. Netter, J. F. Stoltz, S. Muller, P. Gillet and A. Watrin-Pinzano (2008). "Phenotypic analysis of cell surface markers and gene expression of human mesenchymal stem cells and chondrocytes during monolayer expansion." <u>Biorheology</u> **45**(3-4): 513-26.

Crank J, Park GS. "Diffusion in polymers." Academic Press, New York, 1968.

Dahiyat, B. I., E. Hostin, E. M. Posadas and K. W. Leong (1993). "Synthesis and characterization of putrescine-based poly(phosphoester-urethanes)." <u>J Biomater Sci Polym Ed</u> **4**(5): 529-43.

Dealy, C. N. and R. A. Kosher (1996). "IGF-I and insulin in the acquisition of limb-forming ability by the embryonic lateral plate." <u>Dev Biol</u> **177**(1): 291-9.

DeLise, A. M., L. Fischer and R. S. Tuan (2000). "Cellular interactions and signaling in cartilage development." <u>Osteoarthritis Cartilage</u> **8**(5): 309-34.

Denker, A. E., A. R. Haas, S. B. Nicoll and R. S. Tuan (1999). "Chondrogenic differentiation of murine C3H10T1/2 multipotential mesenchymal cells: I. Stimulation by bone morphogenetic protein-2 in high-density micromass cultures." <u>Differentiation</u> **64**(2): 67-76.

Diduch, D. R., M. R. Coe, C. Joyner, M. E. Owen and G. Balian (1993). "Two cell lines from bone marrow that differ in terms of collagen synthesis, osteogenic characteristics, and matrix mineralization." <u>J Bone Joint Surg Am</u> **75**(1): 92-105.

Erickson, D. M., S. E. Harris, D. D. Dean, M. A. Harris, J. M. Wozney, B. D. Boyan and Z. Schwartz (1997). "Recombinant bone morphogenetic protein (BMP)-2 regulates costochondral growth plate chondrocytes and induces expression of BMP-2 and BMP-4 in a cell maturation-dependent manner." <u>J Orthop Res</u> **15**(3): 371-80.

Farrell, E., F. J. O'Brien, P. Doyle, J. Fischer, I. Yannas, B. A. Harley, B. O'Connell, P. J. Prendergast and V. A. Campbell (2006). "A collagen-glycosaminoglycan scaffold supports adult rat mesenchymal stem cell differentiation along osteogenic and chondrogenic routes." <u>Tissue Eng</u> **12**(3): 459-68.

Fortier, L. A., G. Lust, H. O. Mohammed and A. J. Nixon (1999). "Coordinate

126

upregulation of cartilage matrix synthesis in fibrin cultures supplemented with exogenous insulin-like growth factor-I." J Orthop Res **17**(4): 467-74.

Fortier, L. A., H. O. Mohammed, G. Lust and A. J. Nixon (2002). "Insulin-like growth factor-I enhances cell-based repair of articular cartilage." J Bone Joint Surg Br **84**(2): 276-88.

Francis-West, P. H., A. Abdelfattah, P. Chen, C. Allen, J. Parish, R. Ladher, S. Allen, S. MacPherson, F. P. Luyten and C. W. Archer (1999). "Mechanisms of GDF-5 action during skeletal development." Development **126**(6): 1305-15.

Fromigue, O., P. J. Marie and A. Lomri (1998). "Bone morphogenetic protein-2 and transforming growth factor-beta2 interact to modulate human bone marrow stromal cell proliferation and differentiation." J Cell Biochem **68**(4): 411-26.

Fujimoto, R., T. Tanizawa, S. Nishida, N. Yamamoto, S. Soshi, N. Endo and H. E. Takahashi (1999). "Local effects of transforming growth factor-beta1 on rat calvaria: changes depending on the dose and the injection site." J Bone Miner Metab **17**(1): 11-7.

Fujisawa, T., T. Hattori, M. Ono, J. Uehara, S. Kubota, T. Kuboki and M. Takigawa (2008). "CCN family 2/connective tissue growth factor (CCN2/CTGF) stimulates proliferation and differentiation of auricular chondrocytes." Osteoarthritis Cartilage **16**(7): 787-95.

Gebrekidan, S., B. H. Woo and P. P. DeLuca (2000). "Formulation and in vitro transfection efficiency of poly (D, L-lactide-co-glycolide) microspheres containing plasmid DNA for gene delivery." AAPS PharmSciTech **1**(4): E28.

Goldring, M. B., K. Tsuchimochi and K. Ijiri (2006). "The control of chondrogenesis." J Cell Biochem **97**(1): 33-44.

Goodrich, L. R., C. Hidaka, P. D. Robbins, C. H. Evans and A. J. Nixon (2007). "Genetic modification of chondrocytes with insulin-like growth factor-1 enhances cartilage healing in an equine model." J Bone Joint Surg Br **89**(5): 672-85.

Granjeiro, J. M., R. C. Oliveira, J. C. Bustos-Valenzuela, M. C. Sogayar and R. Taga (2005). "Bone morphogenetic proteins: from structure to clinical use." Braz J Med Biol Res **38**(10): 1463-73.

Grizzi, I., H. Garreau, S. Li and M. Vert (1995). "Hydrolytic degradation of devices based on poly(DL-lactic acid) size-dependence." Biomaterials **16**(4): 305-11.

Grodzinsky AJ, Frank EH 1990: Electromechanical and physicochemical regulation of cartilage strength and metabolism. In:Connective tissue matrix:Volume II. Topics in Molecular and Structural Biology, pp 91-126. Ed by DWL Hukins. Boca Raton, CRC Press.

Hall, B. K. and T. Miyake (2000). "All for one and one for all: condensations and the initiation of skeletal development." Bioessays **22**(2): 138-47.

Hasler, C. C. and B. K. Foster (2002). "Secondary tethers after physeal bar resection: a common source of failure?" Clin Orthop Relat Res(405): 242-9.

Hatakeyama, Y., R. S. Tuan and L. Shum (2004). "Distinct functions of BMP4 and GDF5 in the regulation of chondrogenesis." J Cell Biochem **91**(6): 1204-17.

Holland, T. A., E. W. Bodde, V. M. Cuijpers, L. S. Baggett, Y. Tabata, A. G. Mikos and J. A. Jansen (2007). "Degradable hydrogel scaffolds for in vivo delivery of single and dual growth factors in cartilage repair." Osteoarthritis Cartilage **15**(2): 187-97.

Hopfenburg HB, Frisch HL et al. (1969). "Transport of organic molecules in amorphous polymers." Polymer Letters **7**:405-9.

Hora, M. S., R. K. Rana, J. H. Nunberg, T. R. Tice, R. M. Gilley and M. E. Hudson (1990). "Release of human serum albumin from poly(lactide-co-glycolide) microspheres." Pharm Res **7**(11): 1190-4.

Huang, Y. C., M. Connell, Y. Park, D. J. Mooney and K. G. Rice (2003). "Fabrication and in vitro testing of polymeric delivery system for condensed DNA." J Biomed Mater Res A **67**(4): 1384-92.

Huang, Y. C., K. Riddle, K. G. Rice and D. J. Mooney (2005). "Long-term in vivo gene expression via delivery of PEI-DNA condensates from porous polymer scaffolds." Hum Gene Ther **16**(5): 609-17.

Huang, Y. C., C. Simmons, D. Kaigler, K. G. Rice and D. J. Mooney (2005b). "Bone regeneration in a rat cranial defect with delivery of PEI-condensed plasmid DNA encoding for bone morphogenetic protein-4 (BMP-4)." Gene Ther **12**(5): 418-26.

Hung, C. T., R. L. Mauck, C. C. Wang, E. G. Lima and G. A. Ateshian (2004). "A paradigm for functional tissue engineering of articular cartilage via applied physiologic deformational loading." Ann Biomed Eng **32**(1): 35-49.

Isaksson, O. G., A. Lindahl, A. Nilsson and J. Isgaard (1987). "Mechanism of the stimulatory effect of growth hormone on longitudinal bone growth." Endocr Rev **8**(4): 426-38.

Iwasaki, M., H. Nakahara, T. Nakase, T. Kimura, K. Takaoka, A. I. Caplan and K. Ono (1994). "Bone morphogenetic protein 2 stimulates osteogenesis but does not affect chondrogenesis in osteochondrogenic differentiation of periosteum-derived cells." J Bone Miner Res **9**(8): 1195-204.

Jaklenec, A., A. Hinckfuss, B. Bilgen, D. M. Ciombor, R. Aaron and E. Mathiowitz (2008). "Sequential release of bioactive IGF-I and TGF-beta 1 from PLGA microsphere-based scaffolds." Biomaterials **29**(10): 1518-25.

Jang, J. H., Z. Bengali, T. L. Houchin and L. D. Shea (2006). "Surface adsorption of DNA to tissue engineering scaffolds for efficient gene delivery." J Biomed Mater Res A **77**(1): 50-8.

Jang, J. H. and L. D. Shea (2003). "Controllable delivery of non-viral DNA from porous scaffolds." J Control Release **86**(1): 157-68.

Jang, J. H. and L. D. Shea (2006b). "Intramuscular delivery of DNA releasing microspheres: microsphere properties and transgene expression." J Control Release **112**(1): 120-8.

Janjanin, S., W. J. Li, M. T. Morgan, R. M. Shanti and R. S. Tuan (2008). "Mold-shaped, nanofiber scaffold-based cartilage engineering using human mesenchymal stem cells and bioreactor." J Surg Res **149**(1): 47-56.

Jenner, J. M., F. van Eijk, D. B. Saris, W. J. Willems, W. J. Dhert and L. B. Creemers (2007). "Effect of transforming growth factor-beta and growth differentiation factor-5 on proliferation and matrix production by human bone marrow stromal cells cultured on braided poly lactic-co-glycolic acid scaffolds for ligament tissue engineering." Tissue Eng **13**(7): 1573-82.

Jeon, Y. H., J. H. Choi, J. K. Sung, T. K. Kim, B. C. Cho and H. Y. Chung (2007). "Different effects of PLGA and chitosan scaffolds on human cartilage tissue engineering." J Craniofac Surg **18**(6): 1249-58.

Johnstone, B., T. M. Hering, A. I. Caplan, V. M. Goldberg and J. U. Yoo (1998). "In vitro chondrogenesis of bone marrow-derived mesenchymal progenitor cells." Exp Cell Res **238**(1): 265-72.

Jones, J. I. and D. R. Clemmons (1995). "Insulin-like growth factors and their binding proteins: biological actions." Endocr Rev **16**(1): 3-34.

Kafienah, W., S. Mistry, M. J. Perry, G. Politopoulou and A. P. Hollander (2007). "Pharmacological regulation of adult stem cells: chondrogenesis can be induced using a synthetic inhibitor of the retinoic acid receptor." Stem Cells **25**(10): 2460-8.

Kang, S. W., S. P. Yoo and B. S. Kim (2007). "Effect of chondrocyte passage number on histological aspects of tissue-engineered cartilage." Biomed Mater Eng **17**(5): 269-76.
Kawabata, K., Y. Takakura and M. Hashida (1995). "The fate of plasmid DNA after intravenous injection in mice: involvement of scavenger receptors in its hepatic uptake." Pharm Res **12**(6): 825-30.

Khoshhal, K. I. and G. N. Kiefer (2005). "Physeal bridge resection." J Am Acad Orthop Surg **13**(1): 47-58.

Klassen RA, Peterson MA, et al. (1982). "Excision of physeal bars: the Mayo clinic experience 1968-1978." Orthop Trans **2**:65.

Knudson, C. B. and W. Knudson (2001). "Cartilage proteoglycans." Semin Cell Dev Biol **12**(2): 69-78.

Kronenberg, H. M. (2003). "Developmental regulation of the growth plate." Nature **423**(6937): 332-6.

Kupfer, Joel. "DNA Delivery Vectors for Somatic Cell Gene Therapy" in Controlled Drug Delivery, Challenges and Strategies. Park K, Ed. American Chemical Society, Washington, DC, 1997.

Langenskiold A. (1967). "The possibilities of eliminating premature closure of an epiphyseal plate caused by trauma or disease." Acta Orthop Scand **38**: 267-79.

Langenskiold, A., K. Osterman and M. Valle (1987). "Growth of fat grafts after operation for partial bone growth arrest: demonstration by computed tomography scanning." J Pediatr Orthop **7**(4): 389-94.

Langer, R. (1998). "Drug delivery and targeting." Nature **392**(6679 Suppl): 5-10.
Lee, C. W., V. Martinek, A. Usas, D. Musgrave, E. A. Pickvance, P. Robbins, M. S. Moreland, F. H. Fu and J. Huard (2002). "Muscle-based gene therapy and tissue engineering for treatment of growth plate injuries." J Pediatr Orthop **22**(5): 565-72.

Lee, E. H., F. Chen, J. Chan and K. Bose (1998). "Treatment of growth arrest by transfer of cultured chondrocytes into physeal defects." J Pediatr Orthop **18**(2): 155-60.

Lee, E. H., G. X. Gao and K. Bose (1993). "Management of partial growth arrest: physis, fat, or silastic?" J Pediatr Orthop **13**(3): 368-72.

Lee, J. W., Y. H. Kim, S. H. Kim, S. H. Han and S. B. Hahn (2004). "Chondrogenic differentiation of mesenchymal stem cells and its clinical applications." Yonsei Med J **45 Suppl**: 41-7.

Lee, M., T. T. Chen, M. L. Iruela-Arispe, B. M. Wu and J. C. Dunn (2007). "Modulation of protein delivery from modular polymer scaffolds." Biomaterials **28**(10): 1862-70.

Li, L., J. H. Hui, J. C. Goh, F. Chen and E. H. Lee (2004). "Chitin as a scaffold for mesenchymal stem cells transfers in the treatment of partial growth arrest." J Pediatr Orthop **24**(2): 205-10.

Leung, L., Chan, C., Baek, S., Naguib, H (2008). "Comparison of morphology and

130

mechanical properties of PLGA bioscaffolds." <u>Biomed Mater</u> **3**: 1-9.

Lewis DH. Controlled release of bioactive agents from lactide/glycolide polymers. In: Chasin M, Langer R, Eds. Biodegradable polymers as drug delivery systems. New York: Marcel Dekker; 1990. p 1–41.

Li, Z., L. Kupcsik, S. J. Yao, M. Alini and M. J. Stoddart (2008). "Chondrogenesis of Human Bone Marrow Mesenchymal Stem Cells in Fibrin-Polyurethane Composites." <u>Tissue Eng Part A</u>.

Liang, D., Y. K. Luu, K. Kim, B. S. Hsiao, M. Hadjiargyrou and B. Chu (2005). "In vitro non-viral gene delivery with nanofibrous scaffolds." <u>Nucleic Acids Res</u> **33**(19): e170.

Lin, Z., C. Willers, J. Xu and M. H. Zheng (2006). "The chondrocyte: biology and clinical application." <u>Tissue Eng</u> **12**(7): 1971-84.

Loeser, R. F., S. Chubinskaya, C. Pacione and H. J. Im (2005). "Basic fibroblast growth factor inhibits the anabolic activity of insulin-like growth factor 1 and osteogenic protein 1 in adult human articular chondrocytes." <u>Arthritis Rheum</u> **52**(12): 3910-7.

Loeser, R. F., C. A. Pacione and S. Chubinskaya (2003). "The combination of insulin-like growth factor 1 and osteogenic protein 1 promotes increased survival of and matrix synthesis by normal and osteoarthritic human articular chondrocytes." <u>Arthritis Rheum</u> **48**(8): 2188-96.

Lu, S., W. F. Ramirez and K. S. Anseth (2000). "Photopolymerized, multilaminated matrix devices with optimized nonuniform initial concentration profiles to control drug release." <u>J Pharm Sci</u> **89**(1): 45-51.

Madry, H., G. Kaul, M. Cucchiarini, U. Stein, D. Zurakowski, K. Remberger, M. D. Menger, D. Kohn and S. B. Trippel (2005). "Enhanced repair of articular cartilage defects in vivo by transplanted chondrocytes overexpressing insulin-like growth factor I (IGF-I)." <u>Gene Ther</u> **12**(15): 1171-9.

Madry, H., R. Padera, J. Seidel, R. Langer, L. E. Freed, S. B. Trippel and G. Vunjak-Novakovic (2002). "Gene transfer of a human insulin-like growth factor I cDNA enhances tissue engineering of cartilage." <u>Hum Gene Ther</u> **13**(13): 1621-30.

Mahato, R. I. (1999). "Non-viral peptide-based approaches to gene delivery." <u>J Drug Target</u> **7**(4): 249-68.

Marolt, D., A. Augst, L. E. Freed, C. Vepari, R. Fajardo, N. Patel, M. Gray, M. Farley, D. Kaplan and G. Vunjak-Novakovic (2006). "Bone and cartilage tissue constructs grown using human bone marrow stromal cells, silk scaffolds and rotating bioreactors." <u>Biomaterials</u> **27**(36): 6138-49.

131

Maroudas A 1979: Physicochemical properties of articular cartilage. In:Adult Articular Cartilage, ed 2. pp 215-290. Ed by MAR Freeman. Tunbridge Wells, England, Pitman Medical.

Masoud, I., F. Shapiro, R. Kent and A. Moses (1986). "A longitudinal study of the growth of the New Zealand white rabbit: cumulative and biweekly incremental growth rates for body length, body weight, femoral length, and tibial length." J Orthop Res **4**(2): 221-31.

Matsusaki, T., T. Aoyama, K. Nishijo, T. Okamoto, T. Nakayama, T. Nakamura and J. Toguchida (2006). "Expression of the cadherin-11 gene is a discriminative factor between articular and growth plate chondrocytes." Osteoarthritis Cartilage **14**(4): 353-66.

Mehlhorn, A. T., P. Niemeyer, K. Kaschte, L. Muller, G. Finkenzeller, D. Hartl, N. P. Sudkamp and H. Schmal (2007). "Differential effects of BMP-2 and TGF-beta1 on chondrogenic differentiation of adipose derived stem cells." Cell Prolif **40**(6): 809-23.

Mello, M. A. and R. S. Tuan (1999). "High density micromass cultures of embryonic limb bud mesenchymal cells: an in vitro model of endochondral skeletal development." In Vitro Cell Dev Biol Anim **35**(5): 262-9.

Minina, E., C. Kreschel, M. C. Naski, D. M. Ornitz and A. Vortkamp (2002). "Interaction of FGF, Ihh/Pthlh, and BMP signaling integrates chondrocyte proliferation and hypertrophic differentiation." Dev Cell **3**(3): 439-49.

Miura, M., K. Tanaka, Y. Komatsu, M. Suda, A. Yasoda, Y. Sakuma, A. Ozasa and K. Nakao (2002). "Thyroid hormones promote chondrocyte differentiation in mouse ATDC5 cells and stimulate endochondral ossification in fetal mouse tibias through iodothyronine deiodinases in the growth plate." J Bone Miner Res **17**(3): 443-54.

Mizuta, T., W. M. Benson, B. K. Foster, D. C. Paterson and L. L. Morris (1987). "Statistical analysis of the incidence of physeal injuries." J Pediatr Orthop **7**(5): 518-23.

Morisset, S., D. D. Frisbie, P. D. Robbins, A. J. Nixon and C. W. McIlwraith (2007). "IL-1ra/IGF-1 gene therapy modulates repair of microfractured chondral defects." Clin Orthop Relat Res **462**: 221-8.

Moussad, E. E. and D. R. Brigstock (2000). "Connective tissue growth factor: what's in a name?" Mol Genet Metab **71**(1-2): 276-92.

Munirah, S., S. H. Kim, B. H. Ruszymah and G. Khang (2008). "The use of fibrin and poly(lactic-co-glycolic acid) hybrid scaffold for articular cartilage tissue engineering: an in vivo analysis." Eur Cell Mater **15**: 41-52.

Murdoch, A. D., L. M. Grady, M. P. Ablett, T. Katopodi, R. S. Meadows and T. E. Hardingham (2007). "Chondrogenic differentiation of human bone marrow stem cells in

transwell cultures: generation of scaffold-free cartilage." <u>Stem Cells</u> **25**(11): 2786-96.

Nagase, H. and M. Kashiwagi (2003). "Aggrecanases and cartilage matrix degradation." <u>Arthritis Res Ther</u> **5**(2): 94-103.

Nakanishi, T., T. Nishida, T. Shimo, K. Kobayashi, T. Kubo, T. Tamatani, K. Tezuka and M. Takigawa (2000). "Effects of CTGF/Hcs24, a product of a hypertrophic chondrocyte-specific gene, on the proliferation and differentiation of chondrocytes in culture." <u>Endocrinology</u> **141**(1): 264-73.

Nilsson, O., R. Marino, F. De Luca, M. Phillip and J. Baron (2005). "Endocrine regulation of the growth plate." <u>Horm Res</u> **64**(4): 157-65.

Nilsson, O., E. A. Parker, A. Hegde, M. Chau, K. M. Barnes and J. Baron (2007). "Gradients in bone morphogenetic protein-related gene expression across the growth plate." <u>J Endocrinol</u> **193**(1): 75-84.

Nixon, A. J., L. A. Fortier, J. Williams and H. Mohammed (1999). "Enhanced repair of extensive articular defects by insulin-like growth factor-I-laden fibrin composites." <u>J Orthop Res</u> **17**(4): 475-87.

Nof, M. and L. D. Shea (2002). "Drug-releasing scaffolds fabricated from drug-loaded microspheres." <u>J Biomed Mater Res</u> **59**(2): 349-56.

Ohlsson, C., A. Nilsson, O. Isaksson and A. Lindahl (1992). "Growth hormone induces multiplication of the slowly cycling germinal cells of the rat tibial growth plate." <u>Proc Natl Acad Sci U S A</u> **89**(20): 9826-30.

Ortega, N., D. J. Behonick and Z. Werb (2004). "Matrix remodeling during endochondral ossification." <u>Trends Cell Biol</u> **14**(2): 86-93.

Oz, O. K., R. Millsaps, R. Welch, J. Birch and J. E. Zerwekh (2001). "Expression of aromatase in the human growth plate." <u>J Mol Endocrinol</u> **27**(2): 249-53.

Park, J. S., K. Park, D. G. Woo, H. N. Yang, H. M. Chung and K. H. Park (2008). "PLGA microsphere construct coated with TGF-beta 3 loaded nanoparticles for neocartilage formation." <u>Biomacromolecules</u> **9**(8): 2162-9.

Park, K., K. J. Cho, J. J. Kim, I. H. Kim and D. K. Han (2009). "Functional PLGA scaffolds for chondrogenesis of bone-marrow-derived mesenchymal stem cells." <u>Macromol Biosci</u> **9**(3): 221-9.

Park, T. G., H. Yong Lee and Y. Sung Nam (1998). "A new preparation method for protein loaded poly(D, L-lactic-co-glycolic acid) microspheres and protein release mechanism study." <u>J Control Release</u> **55**(2-3): 181-91.

133

Pittenger, M. F., A. M. Mackay, S. C. Beck, R. K. Jaiswal, R. Douglas, J. D. Mosca, M. A. Moorman, D. W. Simonetti, S. Craig and D. R. Marshak (1999). "Multilineage potential of adult human mesenchymal stem cells." <u>Science</u> **284**(5411): 143-7.

Planka, L., P. Gal, H. Kecova, J. Klima, J. Hlucilova, E. Filova, E. Amler, P. Krupa, L. Kren, R. Srnec, L. Urbanova, J. Lorenzova and A. Necas (2008). "Allogeneic and autogenous transplantations of MSCs in treatment of the physeal bone bridge in rabbits." <u>BMC Biotechnol</u> **8**: 70.

Pound, J. C., D. W. Green, H. I. Roach, S. Mann and R. O. Oreffo (2007). "An ex vivo model for chondrogenesis and osteogenesis." <u>Biomaterials</u> **28**(18): 2839-49.

Price, J. S., A. F. Tencer, D. M. Arm and G. A. Bohach (1996). "Controlled release of antibiotics from coated orthopedic implants." <u>J Biomed Mater Res</u> **30**(3): 281-6.

Quereshy, F. A., J. A. Goldstein, J. S. Goldberg and Z. Beg (2000). "The efficacy of bioresorbable fixation in the repair of mandibular fractures: an animal study." <u>J Oral Maxillofac Surg</u> **58**(11): 1263-9.

Radhakrishnan, P., N. T. Lewis and J. J. Mao (2004). "Zone-specific micromechanical properties of the extracellular matrices of growth plate cartilage." <u>Ann Biomed Eng</u> **32**(2): 284-91.

Raiche AT. Strategies to improve periprosthetic bone formation by creating biologically inspired time-dependent growth factor profiles. *Diss*. University of Kentucky, 2002.

Richmon, J. D., A. B. Sage, E. Shelton, B. L. Schumacher, R. L. Sah and D. Watson (2005). "Effect of growth factors on cell proliferation, matrix deposition, and morphology of human nasal septal chondrocytes cultured in monolayer." <u>Laryngoscope</u> **115**(9): 1553-60.

Sakai, S., H. Mishima, T. Ishii, H. Akaogi, T. Yoshioka, Y. Ohyabu, F. Chang, N. Ochiai and T. Uemura (2009). "Rotating three-dimensional dynamic culture of adult human bone marrow-derived cells for tissue engineering of hyaline cartilage." <u>J Orthop Res</u> **27**(4): 517-21.

Salter RB, Harris WR, et al. (1963). "Injuries involving the epiphyseal plate." <u>J Bone Joint Surg</u> **45**: 587-622.

Salter BB: Epiphyseal plate injuries, in Letts RM (ed). Management of pediatric fractures. New York, NY:Churchill Livingstone, 1994, pp 11-26.

Schinagl, R. M., D. Gurskis, A. C. Chen and R. L. Sah (1997). "Depth-dependent confined compression modulus of full-thickness bovine articular cartilage." <u>J Orthop Res</u> **15**(4): 499-506.

Schmitt, B., J. Ringe, T. Haupl, M. Notter, R. Manz, G. R. Burmester, M. Sittinger and C. Kaps (2003). "BMP2 initiates chondrogenic lineage development of adult human mesenchymal stem cells in high-density culture." Differentiation **71**(9-10): 567-77.

Schrier, J. A. and P. P. DeLuca (1999). "Recombinant human bone morphogenetic protein-2 binding and incorporation in PLGA microsphere delivery systems." Pharm Dev Technol **4**(4): 611-21.

Sekiya, I., B. L. Larson, J. T. Vuoristo, R. L. Reger and D. J. Prockop (2005). "Comparison of effect of BMP-2, -4, and -6 on in vitro cartilage formation of human adult stem cells from bone marrow stroma." Cell Tissue Res **320**(2): 269-76.

Sendil, D., D. L. Wise and V. Hasirci (2002). "Assessment of biodegradable controlled release rod systems for pain relief applications." J Biomater Sci Polym Ed **13**(1): 1-15.

Shea, L. D., E. Smiley, J. Bonadio and D. J. Mooney (1999). "DNA delivery from polymer matrices for tissue engineering." Nat Biotechnol **17**(6): 551-4.

Shimo, T., M. Kanyama, C. Wu, H. Sugito, P. C. Billings, W. R. Abrams, J. Rosenbloom, M. Iwamoto, M. Pacifici and E. Koyama (2004). "Expression and roles of connective tissue growth factor in Meckel's cartilage development." Dev Dyn **231**(1): 136-47.

Silvestrini, G., P. Ballanti, F. R. Patacchioli, P. Mocetti, R. Di Grezia, B. M. Wedard, L. Angelucci and E. Bonucci (2000). "Evaluation of apoptosis and the glucocorticoid receptor in the cartilage growth plate and metaphyseal bone cells of rats after high-dose treatment with corticosterone." Bone **26**(1): 33-42.

Takagi, M., Y. Umetsu, M. Fujiwara and S. Wakitani (2007). "High inoculation cell density could accelerate the differentiation of human bone marrow mesenchymal stem cells to chondrocyte cells." J Biosci Bioeng **103**(1): 98-100.

Tickle, C. (2003). "Patterning systems--from one end of the limb to the other." Dev Cell **4**(4): 449-58.

Tickle, C. and A. Munsterberg (2001). "Vertebrate limb development--the early stages in chick and mouse." Curr Opin Genet Dev **11**(4): 476-81.

Tobita, M., M. Ochi, Y. Uchio, R. Mori, J. Iwasa, K. Katsube and T. Motomura (2002). "Treatment of growth plate injury with autogenous chondrocytes: a study in rabbits." Acta Orthop Scand **73**(3): 352-8.

Tuan, R. S. (2004). "Biology of developmental and regenerative skeletogenesis." Clin Orthop Relat Res(427 Suppl): S105-17.

Urist, M. R. (1965). "Bone: formation by autoinduction." Science **150**(698): 893-9.

van der Eerden, B. C., M. Karperien and J. M. Wit (2003). "Systemic and local regulation of the growth plate." Endocr Rev **24**(6): 782-801.

Van Eijk, F., D. B. Saris, J. Riesle, W. J. Willems, C. A. Van Blitterswijk, A. J. Verbout and W. J. Dhert (2004). "Tissue engineering of ligaments: a comparison of bone marrow stromal cells, anterior cruciate ligament, and skin fibroblasts as cell source." Tissue Eng **10**(5-6): 893-903.

van Kleffens, M., C. Groffen, R. R. Rosato, S. M. van den Eijnde, J. W. van Neck, D. J. Lindenbergh-Kortleve, E. C. Zwarthoff and S. L. Drop (1998). "mRNA expression patterns of the IGF system during mouse limb bud development, determined by whole mount in situ hybridization." Mol Cell Endocrinol **138**(1-2): 151-61.

Veilleux, N. and M. Spector (2005). "Effects of FGF-2 and IGF-1 on adult canine articular chondrocytes in type II collagen-glycosaminoglycan scaffolds in vitro." Osteoarthritis Cartilage **13**(4): 278-86.

Wakitani, S., T. Goto, S. J. Pineda, R. G. Young, J. M. Mansour, A. I. Caplan and V. M. Goldberg (1994). "Mesenchymal cell-based repair of large, full-thickness defects of articular cartilage." J Bone Joint Surg Am **76**(4): 579-92.

Wang, Y., F. Middleton, J. A. Horton, L. Reichel, C. E. Farnum and T. A. Damron (2004). "Microarray analysis of proliferative and hypertrophic growth plate zones identifies differentiation markers and signal pathways." Bone **35**(6): 1273-93.

Wei, G., G. J. Pettway, L. K. McCauley and P. X. Ma (2004). "The release profiles and bioactivity of parathyroid hormone from poly(lactic-co-glycolic acid) microspheres." Biomaterials **25**(2): 345-52.

Weise, M., S. De-Levi, K. M. Barnes, R. I. Gafni, V. Abad and J. Baron (2001). "Effects of estrogen on growth plate senescence and epiphyseal fusion." Proc Natl Acad Sci U S A **98**(12): 6871-6.

Wightman L, Kircheis R, Wagner E. 'Polymer-based gene delivery systems' in Pharmaceutical Gene Delivery Systems. Rolland A, Sullivan SM Eds. Vol 131, Marcel Dekker Inc, New York, 2003.

Williams, C. G., T. K. Kim, A. Taboas, A. Malik, P. Manson and J. Elisseeff (2003). "In vitro chondrogenesis of bone marrow-derived mesenchymal stem cells in a photopolymerizing hydrogel." Tissue Eng **9**(4): 679-88.

Winn, S. R., Y. Hu, C. Sfeir and J. O. Hollinger (2000). "Gene therapy approaches for modulating bone regeneration." Adv Drug Deliv Rev **42**(1-2): 121-38.

Witt, C. and T. Kissel (2001). "Morphological characterization of microspheres, films and implants prepared from poly(lactide-co-glycolide) and ABA triblock copolymers: is

136

the erosion controlled by degradation, swelling or diffusion?" Eur J Pharm Biopharm **51**(3): 171-81.

Woo, B. H., B. F. Fink, R. Page, J. A. Schrier, Y. W. Jo, G. Jiang, M. DeLuca, H. C. Vasconez and P. P. DeLuca (2001). "Enhancement of bone growth by sustained delivery of recombinant human bone morphogenetic protein-2 in a polymeric matrix." Pharm Res **18**(12): 1747-53.

Xu, X., R. M. Capito and M. Spector (2008). "Delivery of plasmid IGF-1 to chondrocytes via cationized gelatin nanoparticles." J Biomed Mater Res A **84**(1): 73-83.

Yoo, J. U., T. S. Barthel, K. Nishimura, L. Solchaga, A. I. Caplan, V. M. Goldberg and B. Johnstone (1998). "The chondrogenic potential of human bone-marrow-derived mesenchymal progenitor cells." J Bone Joint Surg Am **80**(12): 1745-57.

Yoshida, M., R. I. Mahato, K. Kawabata, Y. Takakura and M. Hashida (1996). "Disposition characteristics of plasmid DNA in the single-pass rat liver perfusion system." Pharm Res **13**(4): 599-603.

Zapf, J., C. Hauri, M. Waldvogel and E. R. Froesch (1986). "Acute metabolic effects and half-lives of intravenously administered insulinlike growth factors I and II in normal and hypophysectomized rats." J Clin Invest **77**(6): 1768-75.

Zheng, Y. X., J. Ringe, Z. Liang, A. Loch, L. Chen and M. Sittinger (2006). "Osteogenic potential of human periosteum-derived progenitor cells in PLGA scaffold using allogeneic serum." J Zhejiang Univ Sci B **7**(10): 817-24.

Zioncheck, T. F., S. A. Chen, L. Richardson, M. Mora-Worms, C. Lucas, D. Lewis, J. D. Green and J. Mordenti (1994). "Pharmacokinetics and tissue distribution of recombinant human transforming growth factor beta 1 after topical and intravenous administration in male rats." Pharm Res **11**(2): 213-20.

VITA

Date and place of birth:

- o May, 08, 1979, Kerala, INDIA

Educational institutions attended and degrees already awarded:

- o B. Tech., Bachelors in Biomedical Engineering, Cochin University of Science and Technology, Kochi, India
- o M.S., Biomedical Engineering University of Kentucky, Lexington, KY, USA

Professional positions held:

- o Biomedical Engineer, Wipro Technologies, India
- o Research Assistant, Bone Biomaterials Laboratory, U of KY

Typed name of student on final copy

- o Nirmal Ravi